Exploiting the versatility of the layer-by-layer approach to fabricate antioxidant polymer microreactors: towards multifunctional systems for therapeutic applications

Edurne Marin Ameztoy

PhD Thesis

2022

Thesis supervisors: Dr. Aitor Larrañaga Espartero, Prof. Jose-Ramon Sarasua Oiz

Doctorate program: Engineering of Materials and Sustainable Processes

eman ta zabal zazu

Universidad del País Vasco Euskal Herriko Unibertsitatea

Acknowledgements

[ENG]

After three years, this thesis work is eventually completed. Three years of a lot of work, a lot of tears, but also full of many joys. During all this process I had the luck of having the help of many people and I don't want to finish this chapter of my life without thanking all of them.

First of all, I would like to thank my thesis directors Dr. Aitor Larrañaga Espartero and Prof. Jose-Ramon Sarasua Oiz for giving me the opportunity to do this thesis. Thank you, Joserra for all your supportive words, all the times you see me working in the lab, they have been so helpful. Thank you Aitor, for your implication, patience and perseverance in my work and formation. Maybe the things won't work this way without them and I would be eternally grateful for all the things I learn working with you.

I don't want to forget all the collaborators that help me to complete and give more consistence to this thesis. I want to thank, Dr. Christos Tapeinos for his collaboration fabricating and characterizing MnO_2 nanoparticles in the 3rd Chapter. I also want to thank to Dr. Neha Tiwari for the synthesis and characterization of the drug conjugated dendritic polyglycerol (dPG-DOX) used in the 4th Chapter. And finally, I would like to thank Dr. Juan Fernando Cadavid-Vargas for the help in the optimization in the glucose concentration measurement, Dr. Daniel Sanchez for the fabrication of the Single Enzyme Nanogels and Manuela Garay-Sarmiento and Dominik Söder for their support with the confocal microscope and FACS employed in the 5th Chapter.

I also want to thank all my department and laboratory mates. Thank you for offering me all your help and support when the things went wrong, and especially thank you for all the funny moments, they were so helpful in the long lab days.

I would like to thank to my family for their constant support. Dad, Mum, Maite, thank you for hearing all my problems and for removing all my tears and why not, thank you for hearing all my advances without having any idea of what I was talking about. You are my home and during these three years I always feel it.

And finally, I want to thank to my friends their support. Arri, Olaia, Amaia, Jone and Irati thank you for being my Drama Queens and hear all my dramas. I know that we couldn't be us without them. Thank you for all the funny moments and why not, for all the beers. You don't know how they help me to maintain my motivation all these three years.

[CAST]

Finalmente, después de tres años esta tesis llega a su fin. Tres años de mucho trabajo, de muchas lágrimas, pero también llenos de muchos momentos de felicidad. En todo este proceso he tenido la suerte de poder disfrutar de la ayuda de mucha gente, y no me gustaría cerrar este capítulo de mi vida sin agradecérselo.

En primer lugar, me gustaría agradecerles a mis directores Dr. Aitor Larrañaga Espartero y al profesor Jose-Ramon Sarasua Oiz la oportunidad de poder hacer esta tesis. Gracias Joserra por tus palabras de aliento todas las veces que me encontraba contigo en el laboratorio, en muchos momentos han sido de gran ayuda. Gracias Aitor, por tu implicación, paciencia y perseverancia en mi trabajo y formación. Seguramente las cosas no hubiesen funcionado de la misma manera sin ellos y estaré eternamente agradecida de todas las cosas que he aprendido trabajando con vosotros.

No me gustaría olvidarme de dar las gracias a todos los colaboradores que me han ayudado y han conseguido darle más consistencia a mi trabajo. Quiero agradecer al Dr. Christos Tapeinos por su colaboración en la fabricación y caracterización de las nanopartículas de MnO_2 utilizadas en el capítulo 3. Querría dar las gracias también, a la Dra. Neha Tiwari por la síntesis y caracterización del poliglicerol dendrítico conjudado a una droga (dPG-DOX) utilizado en el capítulo 4. Por último, quisiera agradecerle al Dr. Juan Fernando Cadavid-Vargas por la optimización de las medidas de glucosa, al Dr. Daniel Sanchez por la fabricación de las Single Enzyme Nanogels y a Manuela Garay-Sarmiento y Dominik Söder por su ayuda con el microscopio confocal y con el FACS empleados en el capítulo 5.

Me gustaría también dar las gracias a los compañeros de departamento y laboratorio. Gracias por ofrecerme siempre vuestra ayuda y apoyo cuando las cosas no iban bien y especialmente gracias por todos los buenos momentos y las risas, han sido de gran ayuda en los largos días de laboratorio.

Quiero también agradecerle a mi familia su continuo apoyo. Aita, ama, Maite, gracias por escuchar mis problemas y secar todas mis lágrimas y por qué no, gracias por escuchar todos mis avances a pesar de no tener ninguna idea de lo que estaba hablando. Vosotros sois hogar y durante estos tres años lo he podido sentir más que nunca.

Por último, quisiera agradecerles a mis amigas su apoyo. Arri, Olaia, Amaia, Jone e Irati, gracias por ser mis Drama Queens y escuchar todos mis dramas. Sé que no podríamos ser nosotras sin ellos. Gracias por todas las risas y por qué no, por todas las cervezas. No sabéis como esos momentos han hecho que mantuviese mi motivación durante estos tres años.

[EUSK]

Hiru urteren ondoren, azkenik ailegatu da tesi hau bukatzeko garaia. Lan anitzeko hiru urte, malko anitzeko hiru urte baina zoriontasunez beteriko hiru urte ere. Prozesu luze honetan, pertsona anitzen laguntza izateko aukera izan dut eta ez nuke nire bizitzako aro hau itxi nahi, guzti hauei eskerrak eman gabe.

Lehenik eta behin, nire zuzendari diren Aitor Larrañaga Espartero doktoreari eta Jose-Ramon Sarasua Oizeri irakasleari eskerrak eman nahi nizkieke tesi hau egiteko aukera emateagatik. Mila esker Joserra zure animo hitzengatik laborategian elkar ikusten genuenean, laguntza anitzekoak izan dira zenbait momentutan. Mila esker Aitor, nire lanean eta formazioan izan duzun inplikazio eta pazientziagatik. Ziurrenik gauzak ez lirateke berdin atera izanen hauek gabe eta beti eskertuko dut zuekin lan eginez ikasitako guztia.

Ez nuke ahantzi nahi tesi hau beteago egiten lagundu didaten kolaboratzaile guztiei eskerrak ematea. Lehenik, Christos Tapeinos doktoreari 3. Kapituluan erabilitako MnO_2 nanopartikulen fabrikazioan eta karaketerizazioan egindako lana eskertu nahiko nioke. Neha Tiwari doktoreari ere eskerrak eman nahi nizkioke 4. Kapituluan erabilitako droga atxikita daramaten poliglizerol dendritikoen (dPG-DOX) sintesi eta karakterizazioagatik. Azkenik, Juan Fernando Cadavid-Vargas doktoteari eskerrak eman nahi nizkioke glukosa neurketaren optimizazioagatik, Daniel Sanchez doktoreari Single Enzyme Nanogelen fabrikazioagatik eta Manuela Garay-Sarmientori eta Dominik Söderri beraien

laguntzagatik mikroskopio fokukidearen eta FACS-aren erabileran, 5. Kapitulurako hagitz erabilgarriak izan direnak.

Departamentu eta laborategi kideei ere, eskerrak eman nahi nizkieke. Mila esker zuen laguntza eta babesa eskaintzeagatik gauzak ongi joan ez direnean eta batez ere, mila esker momentu on eta dibertigarriengatik, laguntza handikoak izan dira laborategi egun luzeetan.

Nire familiari ere eskerrak eman nahi nizkioke beraien babes konstanteagatik. Aita, ama, Maite, mila esker nire arazoak aditzeagatik eta nire malkoak idortzeagatik eta zergatik ez, nire aurrerapen guztiak aditzeagatik nahiz eta ez ulertu zertaz solasten ari nintzen. Zuek nire etxea zarete eta hiru urte hauetan inoiz baino gehiago sentitu ahal izan dut.

Azkenik, nire lagunei eskertu nahi nieke beraien babesa. Arri, Olaia, Amaia, Jone eta Irati, mila esker nire Drama Queenak izateagatik eta nire drama guztiak aditzeagatik. Ez ginen gu izanen hauek gabe. Mila esker botatako irriengatik eta zergatik ez, hartutako garagardo guztiengatik. Ez dakizue astebururoko momentu horiek nola lagundu duten hiru urte hauetan nire motibazioa mantentzen.

Abstract

The fabrication of polymer capsules *via* the layer-by-layer (LbL) approach has attracted a great deal of attention for biomedical applications, thanks to the versatility that this method offers, allowing the functionalization of all the constituent parts of the capsules. Initially, this fabrication method relied on the alternate deposition of oppositely charged polyelectrolytes onto planar substrates. However, thanks to the above-mentioned versatility and simplicity, this method was rapidly translated to another type of geometries (e.g., colloidal particles) together with the introduction of emerging alternative building blocks (e.g., natural polymers, inorganic nanoparticles, drugs, enzymes, etc.). Consequently, the fabrication of polymer micro- /nanocapsules with *ad hoc* physical, chemical, morphological and mechanical properties has been extensively explored during the last decades. Thanks to this extensive work, a plethora of systems has been presented for their use in different biomedical applications, such as drug delivery vehicles, imaging or as micro- and nanoreactors.

However, in most of the cases, these systems are endowed with a single functionality, which may limit their potential use in the biomedical industry and their translation to the clinical use. To overcome those challenges, a translation from monofunctional to multifunctional systems is required, capable of simultaneously treating aberrant mechanisms and/or cellular pathways while being tracked by imaging proves present in the capsules. Hence, the fabrication of multifunctional polymer capsules for the treatment of complex pathologies like cancer, neurodegeneration or heart diseases is an actual challenge which has been placed in the spotlight of many investigations.

Those aforementioned pathologies present complex scenarios in which dysregulated inflammatory responses, pH reduction and/or oxidative stress among others are implicated. The last one is caused by an overproduction of reactive oxygen species (ROS), such as hydrogen peroxide (H_2O_2) and hydroxyl (·OH) and superoxide anion radicals (O_2^-). These ROS play a pivotal role in numerous cell signalling processes, and in normal cellular activity conditions are efficiently regulated by several antioxidant enzymes and molecules present in the cells. On the contrary, when this native

antioxidant capacity is overwhelmed, oxidative stress occurs leading to cellular apoptosis and senescence by damaging important cell structures.

Hence, taking advantage of the versatility of LbL method, this thesis has been focused on the fabrication of LbL antioxidant microreactors for the treatment of oxidative stress. Three different models have been analysed starting with one monofunctional system and following with two multifunctional, in which different parts of the polymer capsules were functionalized. In the third chapter of this thesis, the core of the capsules has been modified using antioxidant inorganic nanoparticles (i.e., MnO_2 nanozymes) for the reduction of H_2O_2 from the cellular microenvironment. To impart multifunctional attributes, in the following chapter the core of the capsule has been functionalized with an antioxidant enzyme (e. g., catalase) and the membrane was fabricated with a dendritic polyglycerol with a pH cleavable linker, capable of simultaneously releasing a model drug under acidic conditions and protecting cells from multiple H_2O_2 insults. Finally, following with the fabrication of multifunctional antioxidant microreactors, microcapsules capable of performing a cascade reaction were fabricated, which were constituted with a model enzyme (e.g., glucose oxidase) within their core and an outer inorganic (i.e., *in situ* MnO_2 fabrication) or organic (single enzyme nanogels with catalase) antioxidant layer.

This way, with this thesis work, we propose three model systems capable of efficiently reducing H_2O_2 from the cellular microenvironment, thus protecting cells from apoptosis. Furthermore, we demonstrate the versatility of the LbL approach, functionalizing different parts of the polymer capsules toward the fabrication of multifunctional microplatforms obtaining thus promising results for a simultaneous treatment of various mechanisms, required in the current biomedical industry.

Resumen

La fabricación de cápsulas poliméricas mediante el método *layer-by-layer* (LbL) ha adquirido gran protagonismo en el ámbito de las aplicaciones biomédicas, gracias a la versatilidad que presenta, ya que permite la funcionalización de todos los elementos constituyentes de la cápsula. En sus orígenes, este método de fabricación se basaba en la deposición alternante de polielectrolitos de carga opuesta sobre sustratos planos. Sin embargo, gracias a la versatilidad y simplicidad arriba mencionadas, este método fue rápidamente trasladado a otro tipo de geometrías (p.ej.: partículas coloidales) junto con la introducción de materiales y agentes terapéuticos alternativos para la formación de la membrana polimérica (p.ej.: polímeros naturales, partículas inorgánicas, fármacos, enzimas, etc.). Consecuencia de ello, en las últimas décadas se ha explorado de forma extensa la fabricación de micro-/nanocápsulas poliméricas con propiedades físicas, químicas, morfológicas y mecánicas *ad hoc*. Gracias a este extenso trabajo, se han propuesto una gran variedad de sistemas para aplicaciones biomédicas como, sistemas de liberación de fármacos, adquisición de imágenes o micro- y nanoreactores.

Sin embargo, en la mayoría de los casos, estos sistemas suelen estar dotados de una única funcionalidad, limitando así su potencial uso en la industria biomédica y su traslado al uso clínico. Para poder superar estos retos, es evidente la necesidad de cambiar la configuración de estos sistemas de monofuncionales a multifuncionales, para así simultáneamente tratar mecanismos y/o vías celulares anómalas mientras se hace un seguimiento de ello mediante agentes de imagen presentes en las propias cápsulas. Actualmente, la fabricación de cápsulas poliméricas multifuncionales para el tratamiento de patologías complejas como el cáncer, enfermedades neurodegenerativas o del corazón es un reto en continua investigación.

Estas patologías arriba mencionadas presentan escenarios complejos en los que suelen estar implicadas entre otros, respuestas infamatorias, reducción de pH y/o el estrés oxidativo. Este último suele ser causa de una superproducción de especies reactivas de oxigeno (*Reactive Oxigen Species*, ROS) como peróxido de hidrogeno (H_2O_2) y radicales hidroxilos (·OH) y anión superóxido (O_2^-). Estas ROS, tienen un papel importante en procesos de señalización celular y en condiciones normales de actividad suelen ser

reducidas de una forma eficaz mediante enzimas y moléculas antioxidantes presentes en la célula. Por el contrario, cuando esta capacidad antioxidante innata se sobrepasa se produce el ya mencionado estrés oxidativo que conduce a una apoptosis y senescencia celular mediante el daño sobre estructuras celulares vitales.

Por ello, haciendo uso de la versatilidad que presenta el método LbL, esta tesis se ha enfocado en la fabricación de microreactores antioxidantes para el tratamiento del estrés oxidativo. Se han analizado tres modelos diferentes, empezando con un sistema monofuncional para posteriormente analizar dos sistemas multifuncionales, en los que se han funcionalizado diferentes constituyentes de las cápsulas poliméricas. Así, en el tercer capítulo de esta tesis, se ha modificado el núcleo de las cápsulas utilizando nanopartículas inorgánicas antioxidantes (nanozimas de MnO_2) para la reducción del H_2O_2 del microambiente celular. Para dotar a las cápsulas con cualidades multifuncionales, en el siguiente capítulo el núcleo se ha funcionalizado con una enzima antioxidante (p. ej.: catalasa) y la membrana se ha formado utilizando un poliglicerol dendrítico con un enlace sensible al pH, para así obtener cápsulas poliméricas en las que simultáneamente se libera un fármaco modelo en pH ácidos mientras se protege a las células de varios estímulos de H_2O_2. Por último, siguiendo con el objetivo de fabricar microreactores antioxidantes multifuncionales, se han fabricado microcápsulas para llevar a cabo reacciones en cascada. Estas han sido formadas por una enzima modelo (p. ej.: glucosa oxidasa) en su núcleo y con una capa externa inorgánica (fabricación *in situ* de MnO_2) u orgánica (*single enzyme nanogels* de catalasa) con propiedades antioxidantes.

De esta manera, mediante este trabajo de tesis, hemos propuesto tres sistemas modelo capaces de reducir de forma eficaz H_2O_2 del microambiente celular, protegiendo así a las células de la apoptosis. Además, hemos demostrado la versatilidad del método LbL mediante la funcionalización de diferentes partes de las cápsulas poliméricas, con el objetivo de fabricar microplataformas multifuncionales, obteniendo así, resultados prometedores para el tratamiento simultaneo de varios mecanismos y así poder cumplir con los requisitos actuales de la industria biomédica.

Laburpena

Aurkezten duen moldakurtasunari esker, *layer-by-layer* (LbL) metodo bidezko kapsula polimerikoen fabrikazioak garrantzi handia hartu du aplikazio biomedikoen sektorean, izan ere, metodo honek kapsula osatzen duten atal guztien egokitzapena eta aldaketa ahalbidetzen baitu. Hasieran, fabrikazio metodo hau geruza lauen gainean kontrako kargako polielektrolito ezberdinen jalkitzean oinarriturik zegoen. Hala ere, aipaturiko moldakortasun eta sinpletasunari esker, metodo hau azkar egokitu ahal izan zen beste geometria mota batzuetara (adb., partikula koloidalak), geruza polimerikoa osatzeko beste material eta agente terapeutiko desberdinen erabilerarekin batera (adb., polimero naturalak, partikula inorganikoak, drogak, entzimak, etab.). Honen ondorioz, azken hamarkadetan, bereziki aukeratutako propietate fisiko, kimiko, morfologiko eta mekanikoak dituzten mikro-/nanokapsulen fabrikazioa modu konstantean aztertu da. Honi esker, aplikazio biomedikoetara zuzenduriko sistema desberdin asko proposatu dira, hala nola, droga liberaziorako sistemak, irudiak lortzekoak eta mikro- eta nanoerreaktoreak.

Hala ere, kasu gehienetan, sistema hauek funtzio bakarrekoak izan ohi dira, honela beraien erabilgarritasuna industria biomedikoan eta kliniketan mugatuz. Erronka hauek gainditu ahal izateko, argi dago sistema hauen egitura aldatu behar dela funtzio bakarreko kapsuletatik funtzio anitzekoetara, honela, ezohiko jokabidea duten mekanismo edota bide zelularrak tratatzen dituzten eta aldi berean kapsuletan dauden irudi agenteei esker jarraipen bat egiteko gai diren kapsula polimerikoak sortuz. Horregatik, gaur egun, minbizia, gaixotasun neuronalak edo bihotzeko gaixotasunak bezalako patologia konplexuak tratatzeko, funtzio anitzeko kapsula polimerikoen fabrikazioa etengabeko ikerketan dagoen erronka da.

Gorago aipaturiko patologiek, ezaugarri konplexuko inguruneak izan ohi dituzte, non inflamazio irregularra, pH jaitsiera edota oxidazio estresa bezalako egoerak aurkitu daitezkeen. Azken hau, ur oxigenatua (H_2O_2), eta hidroxilo (·OH) eta anioi superoxido (O_2^-) erradikalak bezalako oxigeno espezie erreaktiboen (*Reactive Oxigen Species*, ROS) gainprodukzioaren ondorioz ematen da. ROS hauek, garrantzi handia dute zelulen seinalizazio prozesuetan, eta baldintza normaletan zelulan bertan dauden entzima eta

molekula antioxidatzaileen bidez erreduzituak izan ohi dira. Bestalde, zelulek berezkoa duten gaitasun antioxidatzaile hau gainditzen denean, aipaturiko oxidazio estres egoera ematen da eta honek zelulen egitura garrantzitsuen hondaketaren bidez, hauen apoptosi edota zahartzea eragin dezake.

Hori dela eta, fabrikazio metodo honek eskainitako moldakortasunaz baliatuz, tesi hau oxidazio estresa tratatzeko mikroerreaktore antioxidatzaileen fabrikazioan oinarritu da. Hiru modelo ezberdin aztertu dira, funtzio bakarreko batekin hasiz eta ondoren funtzio anitzeko bi sistema aztertuz, non kapsula polimerikoa osatzen duten atal desberdinak eraldatu diren. Honela, tesi honetako 3. Kapituluan kapsularen nukleoa nanopartikula inorganiko antioxidatzaileak (MnO_2 nanozimak) erabiliz aldatu da H_2O_2-aren murrizketa lortu ahal izateko. Funtzio anitzeko kapsulak sortzeko, ondorengo kapituluan nukleoa entzima antioxidatzaile (adb.: katalasa) batekin bete da eta geruza polimerikoa pH-arekiko hauskorra den lotura batez osaturiko poliglizeroi dendritiko batez osatu da, honela aldi berean pH baxuko egoeretan eredu droga bat liberatuz, zelulak H_2O_2 estimulu desberdinez babesten diren bitartean. Azkenik, funtzio anitzeko mikroerreaktore antioxidatzaileak sortzeko helburuarekin jarraituz, kate erreakzioak egiteko gai diren mikrokapsulak sortu dira. Hauei, bere nukleoan eredu entzima bat sartu zaie (adb.: glukosa oxidasa) eta kanpo geruza inorganiko (*in situ* sortutako MnO_2 geruza) edo organiko (katalasa barne duten *single enzyme nanogelak*) antioxidatzaile batekin eraldatu dira.

Honela, tesi lan honen bidez, hiru sistema proposatu ditugu inguruneko H_2O_2 modu eraginkorrean gutxitzeko gai direnak, modu honetan, zelulak apoptositik babestuz. Gainera, funtzio anitzeko mikroplataformak sortzeko helburuarekin, LbL metodoaren moldakortasuna frogatu dugu kapsula polimerikoak osatzen dituzten atal desberdinak eraldatuz, eta hauekin, emaitza erakargarriak lortu ditugu mekanismo eta egoera ezberdinenak aldi berean tratatzeko gai diren kapsulen sorkuntzan, horrela gaur egungo industria biomedikoaren eskaeretara egokituz.

Publications related to this thesis

- Marin E, Tapeinos C, Lauciello S, Ciofani G, Sarasua JR, Larrañaga A. Encapsulation of manganese dioxide nanoparticles into layer-by-layer polymer capsules for the fabrication of antioxidant microreactors. *Materials Science & Engineering C* **117** (2020) 111349.
- Marin E, Tiwari N, Calderón M, Sarasua JR, Larrañaga A. Smart layer-by-layer polymeric microreactors: pH- triggered drug release and attenuation of cellular oxidative stress as prospective combination therapy. *ACS Applied Materials & Interfaces* **13** (2021) 18511-18524.
- Marin E, Tapeinos C, Sarasua JR, Larrañaga A. Exploiting the versatility of the layer-by-layer approach for the fabrication of polymer capsules: a toolbox to provide multifunctional properties to target complex pathologies. (Under review in *Advances in Colloid and Interface Science*)

Other publications

- Fanjul-Mosteirín N, Aguirresarobe R, Sadaba N, Larrañaga A, Marin E, Martin J, Ramos-Gomez N, Arno MC, Sardon H, Dove AP. Crystallization-induced gelling as a method to 4D print low-water-content non-isocyanate polyurethane hydrogels. *Chemistry of Materials* **33** (2021) 7194-7202.

Congress participations

- Marin E, Tapeinos C, Lauciello S, Ciofani G, Sarasua JR, Larrañaga A. Fabrication of manganese dioxide (MnO_2)-loaded polymer capsules to prevent oxidative stress. *TERMIS EU 2019. Tissue Engineering Therapies: From Concenpt to Clinical Translation & Commercialisation.* Oral communication; Rhodes, Greece; May 2019.
- Marin E, Tapeinos C, Lauciello S, Ciofani G, Sarasua JR, Larrañaga A. Fabrication of manganese dioxide (MnO_2)-loaded polymer capsules to prevent oxidative stress. *X Congreso de Jóvenes Investigadores den Polímeros.* Oral communication; Burgos, Spain; May 2019.
- Marin E, Tiwari N, Calderón M, Sarasua JR, Larrañaga A. Fabrication of multifunctional capsules with antioxidant capacity for the release of a model drug. *Controlled Resealed Society. Virtual Annual Meeting: 2020 Vision for Global Impact.* Poster communication; Virtual; June 2020.
- Marin E, Cadavid-Vargas J, Sarasua JR, Larrañaga A. In situ mineralization of MnO2 on layer-by-layer polymer capsules to limit the accumulation of cytotoxic by-products resulting from enzymatic reactions. *ESB 2021. 31st Conference of the European Society for Biomaterials.* Oral communication; Virtual; September 2021.

Table of content

CHAPTER 1.

Hypothesis and Aims

CHAPTER 1. Hypothesis and Aims

HYPOTHESIS

The layer-by-layer approach can be exploited for the fabrication of polymer capsules with antioxidant activity and additional functionalities to create multifunctional microreactors capable of treating oxidative stress in the cellular microenvironment.

AIMS

The main aim of this thesis is the fabrication and functionalization of polymeric microreactors with antioxidant capacity for the treatment of oxidative stress. For this, three specific objectives were established:

1. To fabricate polymer microcapsules *via* de layer-by-layer approach with encapsulated inorganic antioxidant nanoparticles (*nanozymes*).
2. To fabricate multifunctional polymer microcapsules for the simultaneous release of a therapeutic agent and oxidative stress reduction.
3. To develop polymer capsules with an antioxidant outer layer capable of performing cascade reaction.

These objectives were divided into several sub-objectives:

1. To fabricate polymer microcapsules *via* de layer-by-layer approach with encapsulated inorganic antioxidant nanoparticles (*nanozymes*) (Chapter 3).

- 1.1. Optimization of the encapsulation of the antioxidant nanoparticles and characterization of the fabrication process of inorganic multilayer capsules.
  - 1.1.1. Setting of the encapsulated nanozyme (MnO_2) quantity to obtain antioxidant capsules.
  - 1.1.2. Physico-chemical and morphological analysis of the polymer capsules.
  - 1.1.3. Antioxidant capacity assessment of the capsules.
- 1.2. Internalization and cytotoxicity analysis of the polymer capsules.

1.2.1. Characterization of the effect of surface charge and capsule quantity in the metabolic activity of the cells.

1.2.2. Analysis of the internalization and distribution of the capsules in the cellular microenvironment.

1.3. Therapeutic potential assessment of the fabricated systems.

1.3.1. Setting of the detrimental H_2O_2 concentration.

1.3.2. Analysis of the cell survival using antioxidant capsules against H_2O_2 stimuli.

2. To fabricate multifunctional polymer microcapsules for the simultaneous release of a therapeutic agent and oxidative stress reduction (Chapter 4).

2.1. Optimization and subsequent characterization of the fabrication of polymer capsules using a pH cleavable conjugate of a dendritic polyglycerol with a model drug (dPG-DOX) as active layer.

2.1.1. Encapsulation of an antioxidant enzyme (catalase) into the polymer capsule.

2.1.2. Physico-chemical and morphological analysis of the polymer capsules.

2.2. Assessment of the multifunctional capacity of the fabricated capsules.

2.2.1. Antioxidant capacity assessment of the capsules and setting of the proper capsule quantity.

2.2.2. pH dependent release analysis of the capsules using different pH values.

2.3. Internalization and cytocompatibility analysis of the polymer capsules.

2.3.1. Characterization of the effect of the capsules and their quantity in the metabolic activity of the cells.

2.3.2. Analysis of the internalization and distribution of the capsules in the cellular microenvironment.

2.4. Analysis of the protective effect of the capsules against different H_2O_2 stimuli.

3. To develop polymer capsules with an antioxidant outer layer capable of performing a cascade reaction (Chapter 5).

3.1. Optimization of the encapsulated enzyme quantity and of the addition of antioxidant outer layer, and subsequent characterization of the fabricated polymer capsules.

3.1.1. Setting of the proper encapsulated enzyme (glucose oxidase (GOx)) quantity.

3.1.2. Setting of the proper $KMnO_4$ quantity for the fabrication of the inorganic antioxidant outer layer of MnO_2.

3.1.3. Setting of the proper quantity of single enzyme nanogels (SENs), encapsulating catalase, for the fabrication of the organic antioxidant outer layer.

3.1.4. Physico-chemical and morphological analysis of the polymer capsules.

3.2. Characterization of the cascade reaction between GOx and the inorganic and organic antioxidant layers.

3.2.1. Antioxidant capacity assessment of the fabricated capsules with inorganic and organic outer layer.

3.2.2. Glucose reduction capacity assessment of the polymer capsules.

3.2.3. Analysis of the simultaneous glucose reduction and subsequent H_2O_2 scavenging of the fabricated capsules.

3.3. Cytocompatibility analysis of the fabricated polymer capsules

CHAPTER 2.

Introduction

CHAPTER 2. Introduction

Abstract

Polymer capsules fabricated *via* the layer-by-layer (LbL) approach have attracted a great deal of attention for biomedical applications thanks to their tunable architecture. Compared to alternative methods, in which the precise control over the final properties of the systems is usually limited, the intrinsic versatility of the LbL approach allows the functionalization of all the constituents of the polymeric capsules following relatively simple protocols. In fact, the final properties of the capsules can be adjusted from the inner cavity to the outer layer through the polymeric shell, resulting in theranostic agents that can be adapted to the particular characteristic of the patient and face the challenges encountered in complex pathologies. The biomedical industry demands novel biomaterials capable of targeting several mechanisms and/or cellular pathways simultaneously while being tracked by minimally invasive techniques, thus highlighting the need to shift from monofunctional to multifunctional polymer capsules. In the present chapter, those strategies that permit the advanced functionalization of polymer capsules are accordingly introduced. Each of the constituents of the capsule (i.e., core, multilayer membrane and outer layer) is thoroughly analyzed and a final overview of the combination of all the strategies toward the fabrication of multifunctional capsules is presented. Special emphasis is given to the potential biomedical applications of these multifunctional capsules, including particular examples of the performed *in vitro* and *in vivo* validation studies.

2.1 Introduction

Biomaterials are in constant evolution to face the challenges of our current aging population. The definition of biomaterial has been accordingly adjusted to reflect this dynamic situation. According to a contextual dictionary published in 1999, a biomaterial can be considered as a "material intended to interface with biological systems to evaluate, treat, augment or replace any tissue, organ or function of the body".[1] This definition was further reformulated by the same author to be in line with the new biomaterials paradigm, stating that "A biomaterial is a substance that has been engineered to take a form which, alone or as part of a complex system, is used to direct,

through the control of the interactions with components of living systems, the course of any therapeutic or diagnostic procedure, in human or veterinary medicine".[2]

Within the frame of biomaterials for therapeutic and diagnostic applications, future biomaterials are expected to achieve several biological responses simultaneously, being multifunctional in nature and showing optimized performance to treat and track complex pathologies. These complex pathologies, led, among others, by cancer, cardiovascular diseases and central nervous system disorders, demand customized micro- and nanomaterials capable of crossing biological barriers and interacting with the peculiarities of the tissue microenvironment opening new avenues in personalized medicine.[3] For example, central nervous system diseases, which show a rapidly increasing incidence, would be clearly benefited by the combination of multiple functionalities in a single micro- or nanoplatform for their diagnosis and treatment. The ideal future formulations in this field should actively target the disease-associated markers to allow a more precise and efficient drug delivery, thus minimizing off-target side effects. At the same time, the formulation should be equipped with several contrast agents, favouring the multimodality imaging for early detection. This combination will result in theranostic tools that will have to cross the blood-brain barrier in a non-invasive manner.[4] It is concluded from the previous example that, all in all, biomaterials displaying a single functionality will be clearly inappropriate to meet the requirements demanded by complex pathologies. Diagnosis and/or treatment of cancer represents another clear example where multifunctional biomaterials will be of vital importance. The combination of multiple therapy modalities (e.g., chemotherapy, photodynamic and photothermal therapy) in a nano- or micro-formulation capable of simultaneously acting as an imaging agent could overcome in the near future the limited clinical efficacy observed for monotherapy approaches.[5,6]

In this work, the layer-by-layer (LbL) approach is presented as a potent tool to fabricate polymeric and hybrid micro- and nanoplatforms displaying multifunctional properties, placing particular emphasis on their potential application as diagnostic and therapeutic tools (**Fig. 2.1**). Originally, the LbL approach was based on the alternate deposition of charged synthetic polyelectrolytes onto planar substrates to create self-assembled multilayer films through electrostatic interactions.[7] The versatility of the process was

rapidly exploited to consider alternative building blocks or elementary units (e.g., natural polymers, inorganic nanoparticles, enzymes, growth factors, genetic material, drugs, etc.) to create multicomponent films not only in planar substrates but also in micro- and nano-colloidal (sacrificial) templates. As a result, polymer micro-/nanocapsules and micro-/nanoparticles of both scientific and technological interest were developed.[8] These systems are now regularly considered in a plethora of biomedical applications as drug/protein/gene delivery vehicles. Furthermore, the precise control over the permeability of the multilayer membrane that results in a selective diffusion of reagents and by-products through it has allowed their use as micro- and nanoreactors where the reactions of interest are performed in a time- and spatial-controlled manner.[9] The shift from monofunctional to multifunctional platforms, together with validation experiments to test their suitability in real *in vivo* scenarios, could pave the way for polymer capsules towards representing a real alternative in the clinical practice.

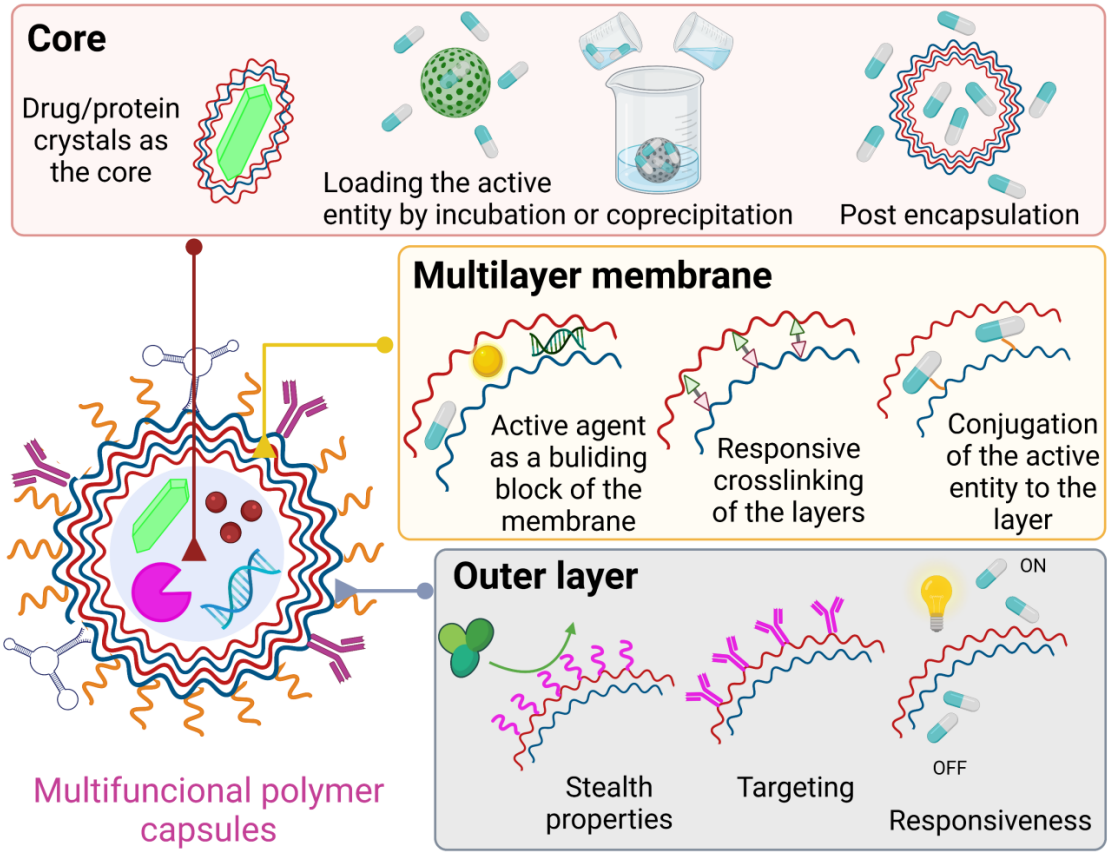

Fig. 2.1. *Schematic representation of the strategies available for the fabrication of multifunctional/multicomponent polymer capsules via the LbL approach.*

2.2. Core

The fabrication of polymer micro- and nanocapsules relies on the alternate deposition of building blocks onto a (sacrificial) template. The choice of the template must be carefully considered accordingly because it will determine the shape and the size of the resulting capsules and their subsequent interaction with cells, tissues, and organs. The stability of the template must be preserved during the LbL process to ensure the proper deposition of the multiple layers. At the same time, the removal of the template should be carried out in mild conditions, avoiding any damage to the multilayer assembly and their sensitive components. A thorough consideration of the selected template is thus a must in any protocol intended to be used in the fabrication of polymer capsules for therapeutic and diagnostic applications.

2.2.1. The core as the active agent

The LbL method allows the deposition of nanometer-thick films on virtually any substrate through either physical or chemical interactions. Using drug crystals as a template for the LbL approach results in high loading capacities (i.e., usually in the range of 80-90%), thus representing an important advantage with respect to alternative carriers (e.g., liposomes, micelles, polymer-drug conjugates), particularly for drugs showing poor solubility in water. The precise control over the wall thickness and the versatility of the process in terms of available natural and synthetic polymers allows the design of a plethora of configurations with tuneable features and controlled drug release. The pioneering studies in this field were focused on the encapsulation of drug microcrystals and subsequent modulation of their release by controlling the permeability of the polymeric membrane.[10-13] Increasing the number of deposited layers (i.e., increasing the thickness of the membrane),[10] using polymers with a loopy conformation (e.g., gelatine),[10,13] or annealing the multilayer capsules[12] were some of the strategies that were explored to control the release kinetics. The shift from micron-sized to nano-sized drug crystals further expanded the applicability of these systems by developing novel nanoformulations that could be intravenously administered and boost their capacity to reach target areas passively (e.g., *via* enhanced permeability and

retention effect). Besides, the modification of the surface of the particles with targeting moieties (e.g., antibodies,[14] lectins,[15] etc.) could also exploit active targeting and deliver the drug at the site of action. For the fabrication of nanocrystals, top-down approaches rely on particle size reduction, usually by ultrasonication and subsequent LbL coating, to stabilize the resulting suspension.[16] Contrarily, in bottom-up approaches, a sonication-assisted crystallization of the drug is favoured by the progressive addition of a non-solvent to a drug solution (**Fig. 2.2a**).[17,18] Alternative approaches for the synthesis of drug nanocrystals such as solvent evaporation emulsification method,[19] nanoprecipitation[20] or spray drying[21] have also been explored. The modification of the outermost layer with poly(ethylene glycol) (PEG) (i.e., PEGylation) is regularly acquired as an effective strategy to improve the colloidal stability of the nanoparticles, reduce protein fouling and consequently increase the circulation time *in vivo*.[22,23] The therapeutic efficacy of this approach was, however, questioned when PEGylated nanoparticles were challenged in an *in vivo* context.[24] PEGylated nanoparticles were rapidly cleared from the blood circulation and did not reach the target tissue, probably due to the displacement of the last layer by serum components and subsequent adsorption of opsonins. This clearly demonstrates the need for more studies about the behaviour of LbL particles in the complex environment of the body. The encapsulation of drug nanocrystals *via* the LbL approach has also been recently proposed to overcome the physiological and anatomical barriers of the gastrointestinal tract after oral administration.[25] In an experimental model of colitis in mice, the multilayer nanoparticles were able to reduce the leakage of the encapsulated cargo (i.e., curcumin) in the stomach (pH = 1.2) and small intestine (pH = 5-7). However, the nanoparticles were accumulated in the inflamed colon (pH > 7) thanks to the charge-reversal of the particles resulting from the dissolution of the negatively-charged outermost layer of cellulose acetate phthalate. Consequently, curcumin was released at the diseased tissue and reduced the symptoms of colitis (**Fig. 2.2b**).

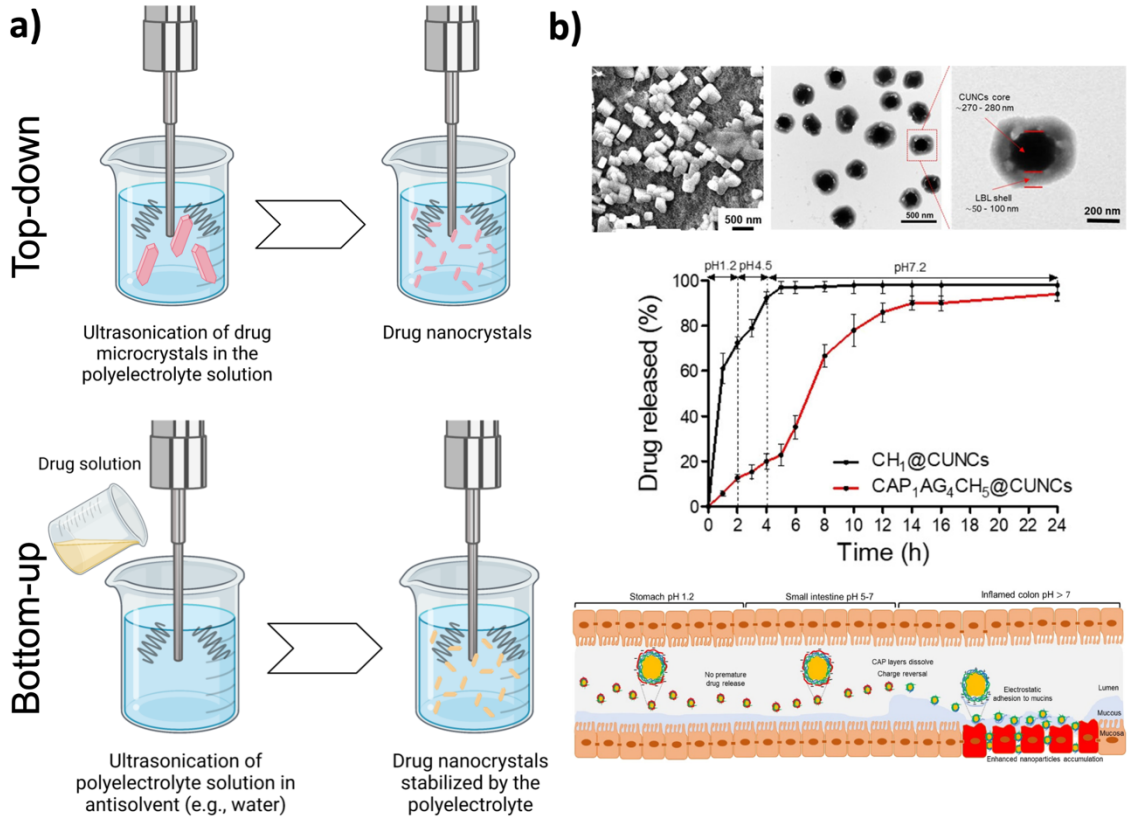

Fig. 2.2. *a) Top-down vs. bottom-up approaches for the fabrication of drug nanocrystals. In this particular example, the figure below describes ultrasound-assisted antisolvent crystallization of the drug. b) Above, SEM and TEM micrographs of curcumin nanocrystals coated with chitosan (CH) and sodium alginate (AG) and surface-coated with cellulose acetate phthalate (CAP). Increasing the number of multilayers limited the release of curcumin at pH 1.2 (stomach) and pH 5-7 (small intestine), whereas the release was accelerated at pH > 7 (inflamed colon). The dissolution of the outer layer (i.e., CAP) at pH > 7 exposed the positively charged CH and benefitted their electrostatic adhesion to mucins in the inflamed colon. Reprinted (adapted) with permission from Biomacromolecules 2020, 21, 9, 3571-3581. Copyright 2021 American Chemical Society.*

Most of the studies mentioned above describe the use of poorly soluble drugs of small molecular weight as the active core. However, the LbL approach has also been proposed for the encapsulation and delivery of (bio)macromolecules (e.g., enzymes, peptides), thus overcoming the limitations of these therapeutics such as poor permeability across biological barriers, short half-life in the bloodstream and susceptibility to undergo

proteolytic degradation. The encapsulation and sustained delivery of insulin, which is an essential protein hormone for the treatment of diabetes, has attracted particular attention.[26] Insulin micro- and nano-aggregates can be synthesized *via* precipitation[27] or salting-out method and subsequently used as the template for the LbL deposition of polymers. The salting-out method is directly influenced by the ionic strength and pH of the solution and determines both the yield of the process and the size of the resulting aggregates.[28] The LbL approach opens the possibility to explore alternative delivery routes for insulin, including oral[29] or pulmonary[30] administration and could overcome the drawbacks associated with subcutaneous injections such as discomfort and poor compliance. The reported *in vivo* studies[27] showed that encapsulated insulin decreased blood glucose levels more efficiently and in a more sustained manner than the non-encapsulated counterpart after oral administration, thanks to a preserved stability of the insulin under acidic gastric conditions.

Encapsulation of active enzyme biocrystals allows the use of LbL micro- and nano-entities as micro- and nanoreactors. Contrarily to the aforementioned examples, where the encapsulated cargo is released by diffusion or triggered by a relevant stimulus, in micro- and nanoreactors, the confined enzyme is protected from the outer environment while the substrates and reaction (by)products diffuse across the polymeric membrane.[9,31] The LbL deposition can be performed without causing any detrimental effect on the encapsulated enzyme and can further protect the activity of the enzyme against proteolysis.[32] In comparison to the conventional LbL deposition of enzymes in solution, the use of encapsulated enzymes results in films displaying up to 50 times higher biocatalytic activities.[33] This allows the development of more stable, robust and sensitive biosensors.[34,35]

Recently, an alternative method that allows the encapsulation of virtually any active cargo at high loading capacity (> 80%) has been presented for the fabrication of capsules with controllable geometry.[36,37] This method represents a shift from traditional to reversed production processes, in which defined-shape open microchambers are first created by imprinting and subsequently covered with a polymeric film *via* the LbL approach. Then, the cargo is placed inside each microchamber through either powder deposition or crystallization from saturated solutions. Finally, the microchambers are

sealed with the polymeric film and the template removed to yield a core-shell microstructure. Although this method presents important advantages with respect to more traditional approaches in terms of versatility in the choice of active substances and controllable geometry of the resulting microcapsules, the transition from micro- to nanoscale is currently a limitation.

2.2.2. Modification of the (sacrificial) template

As outlined in the previous section, using drug crystals as a template in the LbL approach is a valid strategy to improve the stability and availability of drugs, particularly in the case of highly hydrophobic and poorly water-soluble compounds. However, controlling the shape, the polydispersity and the size at the nanometer scale of the resulting formulations still represents a limitation in this approach. The use of pre-synthesized templates as drug carriers and their subsequent coating *via* the LbL approach may overcome the aforementioned limitations. The use of highly porous templates such as mesoporous silica or calcium carbonate nano- and microparticles are of great value in this context thanks to their high surface area and controllable pore size that results in high loading capacities. Dissolving the drug of interest in an adequate solvent (e.g., chloroform, ethanol) and incubating with the porous template has become a routine protocol to encapsulate high payloads of water-insoluble drugs within polymer capsules made by LbL.[38] The template can be finally eliminated or not, leaving behind polymer capsules or core-shell structures, respectively. This strategy has been used for the encapsulation of doxorubicin (DOX) within polymer capsules made out of tannic acid (TA) and poly(N-vinylpyrrolidone) (PVPON) that respond to ultrasound irradiation and allow a triggered release of the encapsulated cargo under both low-power and high-power irradiation.[39] For that purpose, DOX was dissolved in chloroform and incubated with 5 µm porous silica templates overnight. Then, the template was coated with TA/PVPON multilayers and finally eliminated with hydrofluoric acid. Co-incubation of porous templates with other small molecules permits the encapsulation of alternative entities including contrast agents, which are of high interest for imaging applications.[40] In this particular example, the mesoporous silica nanoparticles were functionalized with either amine or phosphonate terminal groups, which greatly improves the loading

capacity of indocyanine green (1.96 wt% for pristine mesoporous silica nanoparticles *vs.* 16.5 wt% for the amine-functionalized counterparts). Thanks to this high loading capacity and the LbL coating, the resulting nanoparticles presented increased photoacoustic signal intensity both *in vitro* and *in vivo*. Even if the use of porous templates has been the preferred method to encapsulate water-insoluble drugs into LbL structures, alternative approaches are also being explored. These include, among others, the use of zein nanoparticles as colloidal delivery systems for hydrophobic compounds with a reported loading capacity for curcumin loaded by antisolvent precipitation of 5.7%.[41,42]

Apart from the incorporation of small molecules into solid templates, their modification with biomacromolecules has been also widely reported. Adsorption of single-stranded (ss), double-stranded (ds) and plasmid DNA on amine-functionalized silica microparticles, followed by the LbL deposition of thiolated poly(methacrylic acid) (PMASH)/PVPON multilayers and elimination of the sacrificial template, resulted in polymer capsules applicable in gene therapy and diagnostic applications.[43] The encapsulated DNA is protected from external insults (e.g., chemical degradation by nucleases) by the polymeric membrane and remains active after the encapsulation process, as demonstrated by PCR using encapsulated ss- and dsDNA as primers and templates. This approach requires fine control over the adsorbed DNA on the sacrificial template: a complete surface coverage of the template with DNA hinders the formation of the capsules because of the poor interaction between PVPON and DNA. Mesoporous silica particles were used by the same group to co-encapsulate both dsDNA and DNase I enzyme in LbL polymer capsules.[44] The permeability of the polymer membrane to Mg^{2+} and Ca^{2+} ions allowed the activation of the enzyme that resulted in the degradation of the dsDNA and demonstrated the potential of this system to work as a microreactor. In a different example, polystyrene microparticles functionalized with branched poly(ethylene imine) (bPEI) were incubated with plasmid DNA and subsequently coated with silk fibroin *via* the LbL approach prior to template elimination with tetrahydrofuran (THF).[45] In comparison to bPEI/DNA complexes, which were used as a control, the incorporation of bPEI/DNA in the interior of the capsules and the protection with silk fibroin resulted in less cytotoxic gene delivery vehicles. However, the transfection

efficiency was very limited. As an alternative, bPEI/DNA was adsorbed on the capsule surface, reaching a good balance between cytotoxicity and transfection efficiency. Enzymes or nanoparticles are also prone to be incorporated in solid templates by simple coincubation.[46] In the case of enzymes, a high loading capacity must be accompanied by the preservation of the enzyme activity to ensure the viability of the process. In this sense, the shape of vaterite (i.e., a polymorph of calcium carbonate) microparticles determined the activity of the adsorbed enzyme, being the star-like vaterite particles preferable over other shapes (e.g., spherical, elliptical and rhomboidal).

The coprecipitation process, which relies on the *in situ* incorporation of the active agent during the formation of calcium carbonate micro- and nanoparticles, has been widely reported as an alternative strategy to the coincubation process described above. This process allows the incorporation of a wide variety of theranostic agents (e.g., nanoparticles, growth factors, enzymes, DNA) in a simple way, displaying extraordinarily good encapsulation efficiencies. Besides, since the subsequent elimination of the template occurs in mild conditions *via* the incubation with a calcium-chelating agent, the process to obtain polymer capsules does not have any detrimental effect on the activity of the encapsulated entity. Following this approach, iron oxide nanocubes were incorporated into calcium carbonate particles that were used as a sacrificial template for the fabrication of polymer capsules.[47] In comparison to free nanocubes which tend to agglomerate in the cellular microenvironment, encapsulated counterparts maintained higher specific absorption rate values and preserved the magnetic losses. This is of great importance for hyperthermia applications since the dynamic magnetic response is almost unaffected in a real biological environment. Following similar strategies, other inorganic nanoparticles (e.g., gold nanorods, superparamagnetic iron oxide nanoparticles) have been coprecipitated within the calcium carbonate templates for the fabrication of polymer capsules displaying multifunctional properties (e.g., cancer chemo-photothermal therapy[48]), or for tracking stem cells after *in vivo* administration.[49]

The encapsulation of proteins, including growth factors and enzymes, has clearly benefited from the coprecipitation process. Moreover, the coprecipitation process allows the incorporation of a cocktail of proteins in the calcium carbonate template,

which may be essential to preserve the activity of the encapsulated entity.[50,51] In this context, basic fibroblast growth factor, heparin and bovine serum albumin (BSA) were all incorporated in vaterite microparticles *via* the coprecipitation approach. In the absence of heparin and BSA, the growth factor completely lost its activity during the encapsulation process. Contrarily, in the presence of these two components, it remained active and promoted the proliferation of L929 fibroblasts. Therapeutic enzymes, such as catalase (CAT)[52] and asparaginase,[53] have also been successfully incorporated into calcium carbonate microparticles for the fabrication of polymer capsules with potential biomedical applications (**Fig. 2.3a**). As demonstrated by stopped-flow measurements and hydrogen peroxide detection kits, CAT remained active after the coprecipitation process and subsequent formation of polymer capsules (**Fig. 2.3b**). These capsules were able to scavenge hydrogen peroxide in an inflammation model of nucleus pulposus cells and consequently attenuated the expression of major proteolytic enzymes (**Fig. 2.3c**). In the case of asparaginase, direct incubation with standard concentrations of the calcium chelating agent (i.e., 0.1 M) inhibited the activity of the enzyme. Thus, a dialysis process with a lower concentration of ethylenediaminetetraacetic acid (EDTA) (i.e., 20 mM) was adopted as a protocol to maintain the activity of the enzyme within the polymer capsules. The encapsulated enzyme was accordingly protected from proteases by the polymeric membrane and showed potential application for the treatment of leukaemia.

Finally, within the process of coprecipitation to functionalize the template, recent advances about the incorporation of genetic material must be highlighted. In a recently reported systematic study,[54] plasmid DNA was co-precipitated in calcium carbonate submicron particles, together with organic additives (e.g., human serum albumin, dextran sulfate, glutathione, poly-L-arginine, protamine sulfate, tannic acid, inhibitors of DNase II). In the absence of organic additives, very low transfection efficiencies were obtained (<6%) for the resulting polymer capsules. In contrast, the combination of poly-L-arginine and DNase II inhibitor resulted in a transfection efficiency as high as 72% due to the synergistic effect of these organic additives that target different cellular mechanisms. In a different example,[55] messenger RNA (mRNA) and RNase inhibitors were simultaneously coprecipitated in calcium carbonate templates. RNase inhibitors

protected the encapsulated mRNA from exogenous RNases, which are abundant in ambient space. As a result, the transfection efficiency of the developed capsules was much higher in the presence of co-encapsulated RNase inhibitors.

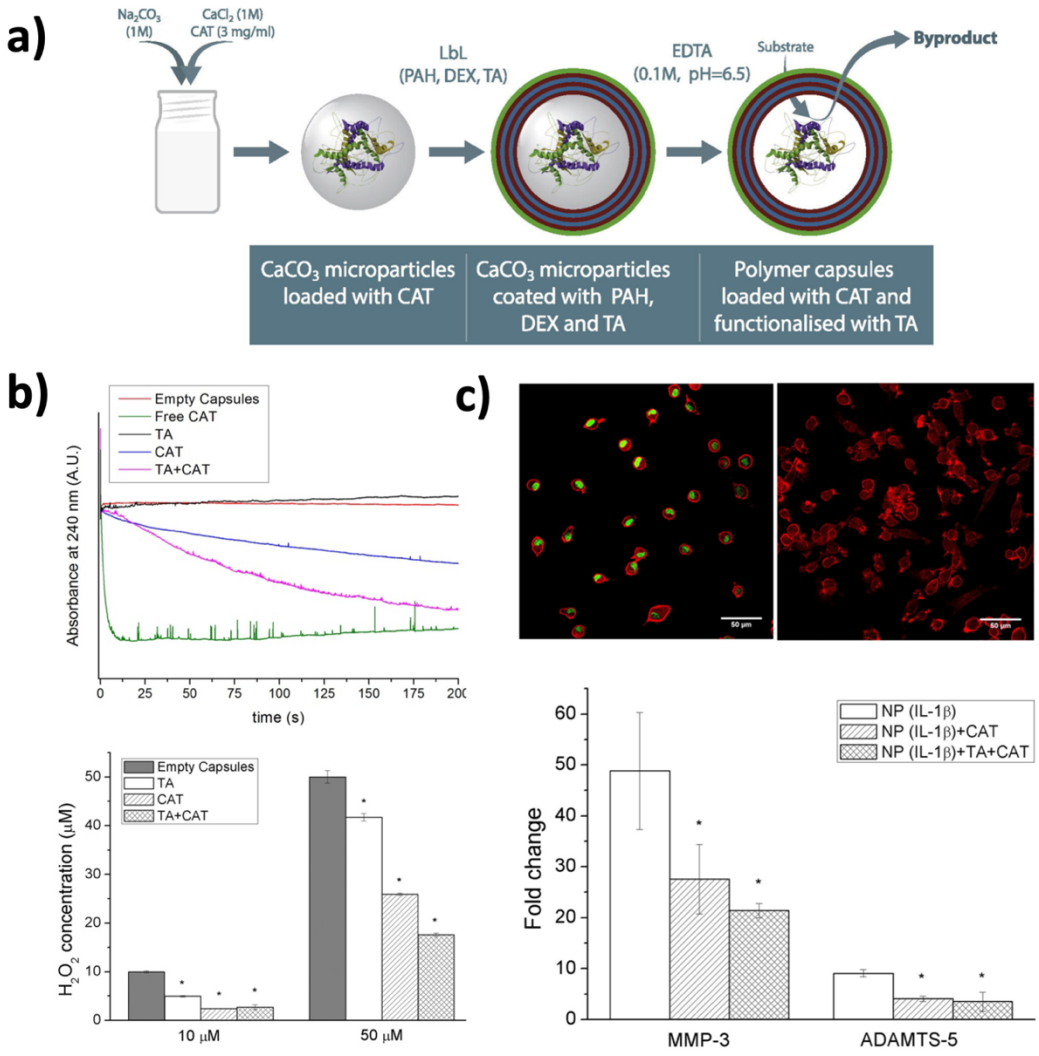

Fig. 2.3. *a) Schematic representation of the fabrication of CAT-loaded capsules. The template is fabricated via the coprecipitation process in the presence of catalase. b) Stopped-flow (above) and hydrogen peroxide detection kit (below) measurements showing the capacity of CAT-loaded capsules (CAT) to scavenge H_2O_2 from solution. c) Cellular oxidative stress staining (green) of nucleus pulposus cells stimulated with a pro-inflammatory cytokine (IL-1β) (left) and further incubated with CAT-loaded capsules (right). Below, the expression of major proteolytic enzymes (i.e., MMP-3 and ADAMTS-5) by cells stimulated with IL-1β (NP (IL-1β)) and further treated with CAT-loaded capsules (NP (IL-1β) + CAT)). Reprinted from Acta Biomaterialia, 67, A. Larrañaga et al., Antioxidant functionalized polymer capsules to prevent oxidative stress, 21-31, 2018, with permission from Elsevier.*

The versatility and simplicity of the coprecipitation process in terms of the possibility to co-encapsulate a wide variety of entities within calcium carbonate particles could pave the way for the development of theranostic systems with multifunctional properties. Recently, positron emitters were incorporated in calcium carbonate core-shell particles *via* the coprecipitation approach, allowing to determine the biodistribution of the particles by both positron emission tomography (PET) and computerized tomography (CT).[56] Among the studied strategies to incorporate the positron emitter into the core-shell particles, the coprecipitation technique was the most efficient in terms of radiolabelling stability. Alternatives to the most generally employed approaches for the modification of the template discussed herein (i.e., coincubation of the template with the active agent and coprecipitation) are regularly being reported. Among them, freezing-induced loading appears as a promising strategy, considering that it can be used for the incorporation of proteins and inorganic nanoparticles into calcium carbonate nanoparticles and also due to the reported high loading efficiencies (four times larger encapsulated amount in comparison to coincubation and coprecipitation).[57,58] However, the freezing/thawing cycles could have detrimental effects on the activity of more sensitive entities (e.g., enzymes) that could limit the universal application of this approach.

2.2.3. Post-encapsulation

The controllable permeability of the polymeric shell allows the loading of therapeutic agents after the fabrication of the capsules. Although post encapsulation has also been applied for the loading of macromolecules, encapsulation of high-molecular weight entities requires the "opening" of the capsules, usually by reducing the interaction of its shell constituents. The conditions to promote the transition from the "closed" to the "opened" state should be carefully controlled to avoid the complete disassembly of the capsule and the degradation/denaturation of the encapsulated entity, which cannot always be guaranteed. Therefore, several authors studying the encapsulation of a library of entities have preferred the preloading process (described in the previous section) for molecular cargos with molecular weight above 10 kDa, while the post encapsulation process followed by a heat shrinking was used for cargos of small-molecular weight.[59]

The incubation of hollow polymer capsules with water-soluble drugs (e.g., doxorubicin hydrochloride) in aqueous solutions is a simple method to load the drug of interest in the cavity of the capsules. However, since the process relies simply upon a diffusion mechanism, the release profile usually resembles the loading profile and results in a very rapid release rate. Crosslinking of the polymeric shell constituents[60] or temperature-induced shrinking of the capsules[61] are commonly followed to ensure a more controlled release of the encapsulated cargo. The latest was recently used for the encapsulation of small-molecular weight water-soluble drugs (i.e., gemcitabine and clodronate) into poly-L-arginine/dextran sulfate (Parg/Dex) capsules.[62] After the fabrication and loading of the capsules, they were subjected to a heat treatment (i.e., 90 ^{o}C, 60 min) that resulted in the tightening of the polymeric multilayer network, thus avoiding the leakage of the encapsulated compound (**Fig. 2.4a**). The resulting polymer capsules, with sizes below 300 nm, were preferentially accumulated in the tumour lungs in comparison to healthy organs thanks to the enhanced permeability and retention (EPR) effect, demonstrating their potential accordingly to treat lung cancer (**Fig. 2.4b**).

Although the incubation of water-soluble drugs with hollow polymer capsules may seem a trivial approach, there are several parameters (e.g., incubation time, solute concentration, pH, ionic strength) that need to be finely adjusted to achieve high loading efficiencies and capacities.[63] Drug molecules will not only fill the inner cavity of the capsule but will also be adsorbed by the constituents of the polymeric shell through molecular interactions. Considering the varying charge of the drugs and the polymeric constituents at different pHs and the influence of ionic strength on their conformation, small alterations in these parameters can result in dramatic changes in the loading efficiency and capacity. For the encapsulation of lipophilic drugs (e.g., doxorubicin and 5-fluorouracil), an alternative incubation approach has been proposed. For example, capsules made out of poly(methacrylic acid) (PMA) were incubated in a drug/oleic acid mixture, allowing its infiltration through the polymeric walls and filling of the capsules.[64] The release of the drug occurred only in the presence of reducing conditions (e.g., intracellularly) thanks to the disulfide bonds between the layers, thus limiting any systemic toxicity resulting from the release of the drug in the oxidative bloodstream.

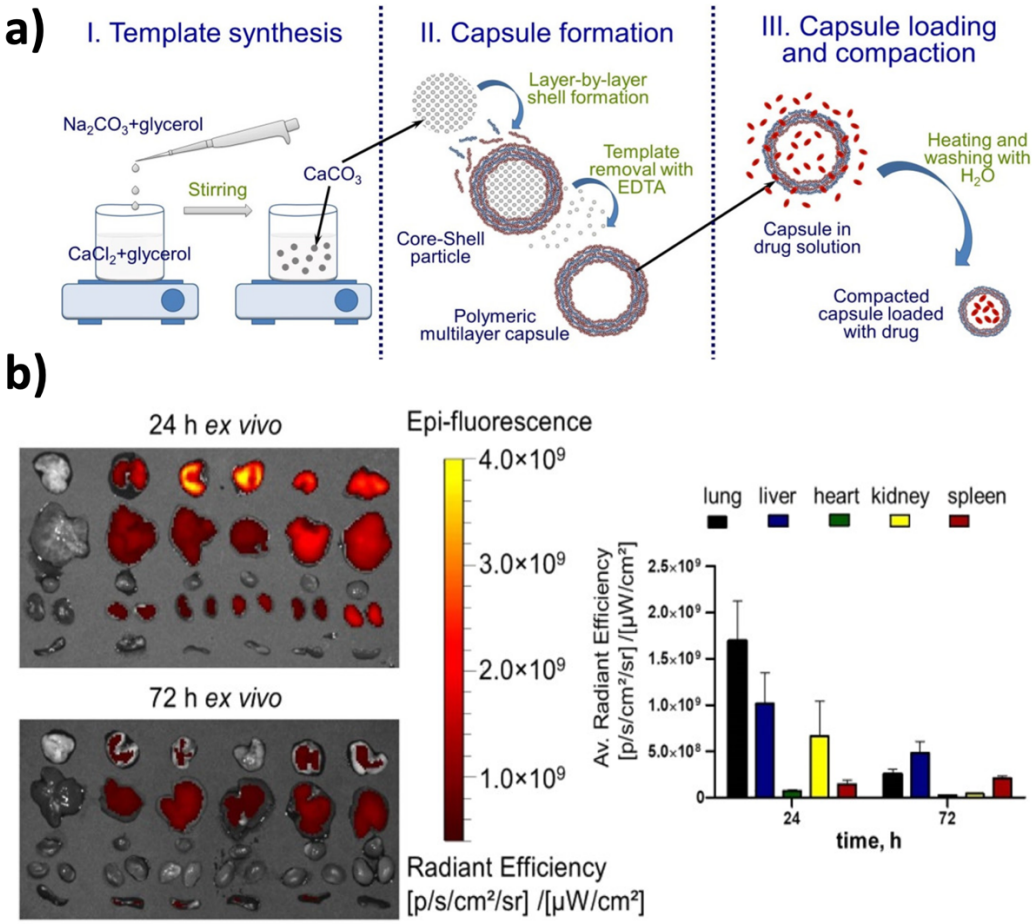

Fig 2.4. *a) Schematic representation of the capsule fabrication and drug loading by incubation and subsequent shrinking by heat treatment. b) Imaging of isolated organs after the administration of fluorescent capsules and its quantification, highlighting the preferential accumulation in lung and liver. Reprinted (adapted) with permission from ACS Appl. Mater. Interfaces 2020, 12, 5, 5610-5623. Copyright 2021 American Chemical Society.*

The so-called spontaneous deposition has been widely reported as a strategy to load a plethora of active entities in the interior of polymer capsules under ordinary conditions (i.e., room temperature, neutral pH, in pure water).[65,66] In this approach, a positively-charged drug can spontaneously diffuse from a low- (e.g., the bulk) to a high-concentration region (e.g., the interior of the capsule) thanks to the presence of negatively charged species in the interior of the capsule. This phenomenon was first reported for capsules fabricated with melamine formaldehyde (MF) as a core and poly(sodium 4-styrene sulfonate)/poly(allylamine hydrochloride) (PSS/PAH) as polyelectrolytes. During template removal at low pH, a complex between PSS and MF is formed, which remains inside the capsule due to its large size and provides the driving

force to induce positively-charged molecules to penetrate through the capsule wall. The loading and subsequent release of the drug can be further adjusted by controlling several factors, including feeding concentrations, temperature, and salt concentrations.[65] Apart from small drugs, biomacromolecules (e.g., enzymes) have also benefited from the spontaneous deposition.[67] By adjusting the pH of the enzymatic solution below its isoelectric point, the charge of the enzymes becomes positive, thus favouring the spontaneous diffusion towards the interior of the capsule. Moreover, the encapsulated enzyme preserved its activity better than the non-encapsulated counterpart when exposed to high temperatures. However, this process may not be valid for more sensitive enzymes, in which a slight change in the pH of the solution may result in conformational changes and a detrimental effect on their activity. Inspired by the spontaneous deposition first described for MF cores, other templates have been modified to facilitate the encapsulation of therapeutic agents. For example, Zhao *et al.* fabricated polymer capsules made out of PAH/PSS using PSS-doped $CaCO_3$ microparticles for the subsequent loading of daunorubicin (DNR) and DOX.[68] The charge-controlled permeability (Donnan equilibrium) favours the diffusion of positively-charged drugs, which can be further optimized by controlling important loading parameters (e.g., drug feeding and salt concentration) and multilayer configuration (i.e., a positive outmost layer limits the loading of the drug due to charge repulsion). The modification of the $CaCO_3$ template by coprecipitation with heparin[69] or cyclodextrin[70] are alternative examples that have been reported to facilitate the post encapsulation of growth factors (e.g., TGF-β1) and hydrophobic entities (e.g., coumarin, Nile red) respectively by electrostatic and host-guest interactions. An encapsulation efficiency of 35% was achieved in the case of TGF-β1 loaded into strongly anionic polymer capsules due to the presence of heparin. The growth factor remained active after the encapsulation and release process, as demonstrated by its capacity to transdifferentiate fibroblast into myofibroblasts. The modification of nanoporous silica particles with polylysine has been similarly used to post encapsulate small interfering RNA (siRNA) into PMA polymer capsules.[71] By limiting the number of bilayers to five, siRNA could cross the polymeric membrane and be sequestered by polylysine, forming a polylysine-siRNA complex that is retained in the capsule interior. In this particular study, the expression of the target gene was downregulated even when scrambled siRNA or empty capsules were used,

suggesting a capsule-dependent off-target effect due to a cellular macroautophagy response.

As mentioned at the beginning of this section, biomacromolecules (e.g., enzymes, growth factors) can also be post encapsulated in prefabricated microcapsules by reversibly switching the state of the capsules from a "closed" (impermeable) to an "opened" (permeable) state. The permeability of PAH/PSS multilayer microcapsules was reversibly switched when the NaCl concentration was varied between $0.5 \cdot 10^{-2}$ to $2 \cdot 10^{-2}$ M.[72] At increasing salt concentration, the ionic strength may weaken the electrostatic interaction between polyelectrolytes, thus favouring the swelling of the capsules and the corresponding diffusion of the macromolecules that were used as a control model. Raising the pH of the solution also resulted in increased permeability of chitosan/dextran sulfate (CHI/Dex) and protamine/dextran sulfate (Pro/Dex) based capsules, presumably because of the electrostatic repulsion caused by the gradual deprotonation of the amine groups in the cationic polyelectrolyte.[73,74] This allowed the encapsulation of basic fibroblast growth factor (bFGF) and peroxidase (POD), respectively, with reported loading capacities of 34 μg/mg of capsules in the case of bFGF and $2.2 \cdot 10^8$ molecules/capsule in the case of peroxidase. Alternative approaches to reversibly switch the permeability of the capsule and allow the encapsulation of biomacromolecules, including the incubation of multilayer polymer capsules in water/ethanol mixtures, have also been reported.[75] The amount of post encapsulated biomacromolecules will be strongly affected by the multilayer shell composition. In this respect, the amount of encapsulated BSA in alginate/dextran sulfate (Alg/Dex) capsules was 2.5 times higher than in dextran/poly(L-arginine) (Dex/Parg) counterparts.[76] During their post encapsulation, the diffusion of the biomacromolecule is directed toward the centre of the capsule and can be accumulated in the polymeric shell, which will, in turn, also affect the subsequent release rate. Therefore, several aspects need to be carefully considered when trying to post-encapsulate biomacromolecules in multilayer polymer capsules to ensure an efficient loading process and a sustained release. Above all, preserving the activity of pH-, salt-, solvent-sensitive biomacromolecules (i.e., enzymes) is of vital importance and this cannot always be guaranteed with the aforementioned strategies.

Table 1. *Strategies to incorporate functionalities into the core of LbL capsules intended to be used in biomedical applications.*

Strategy	Encapsulated entity	Approach	Biomedical application	Outcomes	Ref.
Core as the active agent	Curcumin	Ultrasound-assisted antisolvent crystallization (core of c.a. 300 nm).	Ulcerative colitis (*in vitro* and *in vivo*)	• Preferential accumulation in inflamed colon. • Enhanced efficacy in controlling inflammation.	25
	Paclitaxel	Solvent emulsification evaporation method (core of c.a. 100 nm)	Cancer (*in vitro* with Caco-2 cells)	• More targeted binding of the lectin-functionalized particles.	15
		Ultrasonication (Core of c.a. 100 nm)	Cancer (*in vitro* with MCF-7 and BT-20 cells)	• Enhanced cytotoxic effect on antibody-functionalized nanoparticles.	14
		Wet milling (Core of c.a. 200 nm)	Cancer (*in vitro* and *in vivo*)	• Improved colloidal stability *in vitro* after PEGylation. • Rapid clearance from the bloodstream *in vivo*.	24
		Nanoprecipitation (Core of c.a. 150 nm)	Cancer (*in vitro* with MCF-7)	• The encapsulation of the drug did not weaken its mechanism of action.	20
	Campotothecin	Nanoprecipitation (Core of c.a. 160 nm)	Cancer (*in vitro* with a glioblastoma cell line)	• Improved colloidal stability *in vitro* after PEGylation. • Prolonged activity of the drug.	23

Table 1. *Continuation*

Strategy	Encapsulated entity	Approach	Biomedical application	Outcomes	Ref.
Core as the active agent	Ibuprofen	Ultrasonication (Core of c.a. 100 nm)	Oral delivery of therapeutics (*in vitro* with Caco-2 cells)	• Good cytocompatibility of the capsules.	16
	Insulin	Core of c.a. 5-20 µm	Diabetes, pulmonary delivery (*in vivo*)	• Controlled delivery of insulin *via* intrapulmonary administration depending on the number of layers.	30
		Precipitation (Core of c.a. 1 µm)	Diabetes, oral delivery (*in vivo*)	• Enhanced stability of the encapsulated insulin at acidic pH. • Sustained and dose-dependent reduction of blood glucose after oral administration.	27
		Salting out (Core of c.a. 100-230 nm)	Diabetes (Neither *in vitro*, nor *in vivo*)	• Low release of insulin at acidic pH but sustained release at neutral pH.	28
	Catalase	Catalase crystals (Core of c.a. 10 µm)	Hydrogen peroxide biosensor	• Higher biocatalytic activities with respect to non-encapsulated counterpart.	32-34
	Glucose oxidase	Glucose oxidase crystals (Core of c.a. 30 µm)	Glucose biosensor	• Faster response of the biosensor with respect to non-encapsulated counterpart.	35

Table 1. *Continuation*

Strategy	Encapsulated entity	Approach	Biomedical application	Outcomes	Ref.
Modification of the (sacrificial) template	Paclitaxel	Coincubation with mesoporous silica nanoparticles (core of c.a. 400 nm)	Cancer (*in vitro* with LIM1899 colorectal cancer cells)	• Encapsulated drugs show similar efficacy to the free drugs.	38
	Doxorubicin	Coincubation with porous silica microparticles (core of c.a. 3-5 μm)	Cancer (*in vitro* with MCF-7)	• Ultrasound triggered release of the encapsulated cargo. • Ultrasound imaging contrast depend on capsule´s rigidity, thickness and molecular weight.	39
	Indocyanine green	Coincubation with surface-functionalized mesoporous silica nanoparticles (core of c.a. 65 nm)	Photoacoustic imaging (*in vitro* and subcutaneously with mouse cadavers)	• Increasing photostability and photoacoustic signal for the LbL encapsulated formulations.	40
	Curcumin	Antisolvent precipitation with zein nanoparticles (core of c.a. 150 nm)	Oral delivery of therapeutics (neither *in vitro*, nor *in vivo*)	• Increased light, thermal and storage stability of the encapsulated drug. • Controlled release of the encapsulated drug.	41,42

Table 1. *Continuation*

Strategy	Encapsulated entity	Approach	Biomedical application	Outcomes	Ref.
Modification of the (sacrificial) template	Iron oxide nanocubes	Coprecipitation in calcium carbonate particles (core of c.a. 1 µm)	Hyperthermia-Cancer (*in vitro* with SKOV-3 ovarian carcinoma cells)	• Higher specific absorption rate values for the encapsulated nanocubes. • More predictable heating dose inside biological matrices for encapsulated nanocubes.	47
	Gold nanorods	Coprecipitation in calcium carbonate particles (core of c.a. 4.5 µm)	Chemo-photothermal therapy-Cancer (*in vitro* with THP-1 cells)	• NIR triggered drug release. • Increased cell death under combination of drugs + NIR stimulation.	48
	Nerve growth factor	Coprecipitation in calcium carbonate particles (core of c.a. 2-3 µm)	Treatment of neuropathologies (*in vitro* with hippocampal neurons)	• The presence of capsules accelerated neurite growth and promote the development of primary and secondary-order branches.	51
	Catalase	Coprecipitation in calcium carbonate particles (core of c.a. 2-3 µm)	Intervertebral disc degeneration (*in vitro* with nucleus pulposus cells)	• Encapsulated catalase preserves its activity. • Capsules scavenge hydrogen peroxide from solution and attenuate oxidative stress in cells.	52

Table 1. *Continuation*

Strategy	Encapsulated entity	Approach	Biomedical application	Outcomes	Ref.
Modification of the (sacrificial) template	Asparaginase	Coprecipitation in calcium carbonate particles (core of c.a. 1-2 µm)	Leukaemia (*in vitro* with SD1 and MOLT-4 cancerous lymphocytes)	• Template removal under dialysis preserve the activity of the enzyme. • Encapsulated enzyme promotes cell death in the presence of proteases, which inhibited the activity of the free enzyme.	53
	siRNA	Coprecipitation in calcium carbonate particles (core of c.a. 2-3 µm)	Treatment of influenza virus infection (*in vitro* with MDCK kidney and A549 epithelial cells)	• Reduction of viral nucleoprotein level and inhibition of influenza virus production in infected cells.	77
Post-encapsulation	Doxorubicin	Incubation with prefabricated capsules followed by crosslinking of the polyelectrolytes (core of c.a. 220 nm)	Combination cancer therapy (*in vitro* with HeLa cells)	• The release of the encapsulated cargo occurs too fast if the polymeric shell is not crosslinked.	60
		Incubation with prefabricated capsules followed by temperature induced shrinking (core of c.a. 490 nm)	Cancer (*in vitro* with MCF-7 and MCF7-ADR cells)	• Shrunken capsules allow a more sustained release of the encapsulated drug.	61

Table 1. *Continuation*

Strategy	Encapsulated entity	Approach	Biomedical application	Outcomes	Ref.
Post-encapsulation	Gemcitabine and clodronate	Incubation with prefabricated capsules followed by temperature induced shrinking (core of c.a. 500 nm)	Lung cancer (*in vitro* with mouse lung cancer spheroids and bone marrow-derived macrophages; *in vivo* in a lung cancer model with mice)	• Preferential accumulation of capsules in tumour lungs with respect to healthy tissue. • The tumour-promoting function of macrophages is suppressed after the pretreatment with capsules.	62
	5-fluorouracil	Filling hollow polymer capsules with an oil phase containing the drug (core of c.a. 500 nm)	Cancer (*in vitro* with LIM1215 human colorectal cancer cell line)	• Release of the encapsulated cargo under reducing conditions. • Encapsulated drugs are more effective in killing cancer cells than free drugs.	64
	Daunorubicin	Spontaneous deposition using melamine formaldehyde as a sacrificial core (core of c.a. 5 μm)	Leukaemia (*in vitro* with HL-60 cells)	• Gradual cytotoxic effect was observed for encapsulated drugs in comparison to “just at one time” effect for free drugs.	65

Table 1. *Continuation*

Strategy	Encapsulated entity	Approach	Biomedical application	Outcomes	Ref.
Post-encapsulation	TGF-β1	Spontaneous deposition into heparin loaded prefabricated capsules (core of c.a. 5 µm)	Wound healing (*in vitro* with human dermal fibroblast)	• The growth factor remains active after the encapsulation process and is able to induce transdifferentiation to myofibroblast in a similar way to the growth factor in solution.	69
	bFGF	Loading the growth factor at high pH to increase the permeability of the polymeric shell (core of c.a. 3 µm)	Proof of concept work for the delivery of biomacromolecules (*in vitro* with L929 fibroblasts)	• Steady state growth of cells cultured with encapsulated growth factor thanks to the sustained release.	73
	siRNA	Complexation with preinfiltrated polylysine (core of c.a. 1 µm)	Prostate cancer (*in vitro* with PC-3 cells)	• Down-regulation of the target gene also occurs in the presence of empty capsules, suggesting a capsule-dependent off-target effect.	78

2.3. Multilayer Membrane

A rational design of the polymeric membrane architecture and its subsequent assembly onto the colloidal template may affect both the mechanical integrity of the resulting capsule and its performance during a required application. Apart from shielding the encapsulated cargo from the surrounding harsh environment, the polymeric shell endows the capsules with responsiveness towards relevant stimuli and structural stability to avoid their disassembly along their journey to the target site. The functionalization of the membrane can be achieved by using a wide variety of inorganic particles and/or therapeutic agents as building blocks in the assembly process. Alternatively, building blocks can be functionalized prior to or after their deposition on the template. This enables adaptation of the features and performance of the membrane to meet the requirements of a specific biomedical application.

2.3.1. The layer as the active agent

The use of an active agent as a constituent of the polymeric membrane is one of the most employed strategies to provide functional properties to the multilayered capsules. The incorporation of inorganic nanoparticles between the layers endows polymeric capsules with functionalities such as the capability to be guided, activated with an external stimulus or monitored/tracked. Incorporation of iron oxide nanoparticles, especially magnetite (Fe_3O_4) nanoparticles, is a common approach in those scenarios in which an external *in vivo* monitoring and visualization of the capsules is needed,[49,79-81] or when the guiding and controlled release are a must to obtain an efficient treatment (**Fig. 2.5a**).[82-87] In stem cell regenerative medicine therapies, the monitoring and tracking of the implanted cells is a prerequisite to determining the safety and efficacy of the treatment.[49] For this, the use of inorganic nanoparticles in combination with other genetic reporters is a useful tool to track those cells after their implantation.[49] Furthermore, in drug release applications, the possibility to track the *in vivo* fate of the administered particles could provide useful information about the biodistribution, which is directly associated with the release of the bioactive substance and its effect on the treatment.[79-81] Introducing magnetite, especially superparamagnetic nanoparticles

(i.e., SPIONs) as contrast agents, allows monitoring the polymer capsules *via* magnetic resonance imaging (MRI) analysis, which shows high resolution and penetrations with a high safety level.[49,80,81] The obtained contrast depends on size, shape and aggregation level of the nanoparticles.[81] When the nanoparticle concentration in the capsules increases, the surface density of the capsule proportionally increases and the signal intensity change does not exceed 25%. With lower magnetite concentration, the reported signal intensity change is around 100%.[81] Another benefit of using magnetite nanoparticles as an element of the polymeric membrane is the possibility to fabricate LbL capsules that can be remotely navigated to the target site, as well as capsules that deliver the encapsulated cargo in response to an external trigger.[82,84-86] Under the effect of an alternating magnetic field (AMF) or near-infrared light (NIR), the permeability of the polymeric membrane increased due to the mechanical vibration produced on the magnetite nanoparticles, thus allowing the release of the encapsulated cargo.[82,84-87] As an illustration, Deng *et al.* fabricated doxorubicin-loaded multifunctional capsules containing an iron oxide-decorated graphene oxide sheet, which were activated by NIR and a magnetic hyperthermia system (MHS), thus allowing the release of the chemotherapeutic drug. As a result, a higher hyperthermia effect and an efficient tumour reduction were achieved (**Fig. 2.5b**).[87] Furthermore, the outer hyaluronic acid (HA) layer, with the help of iron oxide nanoparticles excited by a low magnet intensity or NIR light, enhanced the internalization of the capsules obtaining thus an efficient tumour targeting (**Fig. 2.5b**). Another way to induce the loosening/rupture of the polymeric membrane is the use of high-intensity focused ultrasound (HIFU).[83,88] These individual harmless beams focused on a small area can create a collective energy that will lead to the rupture of the carrier walls in the presence of magnetite nanoparticles. The position of the layer, including the magnetic nanoparticles, is a key parameter in this case since it will affect the stability of the capsule before and during the sonication process. For example, as reported by Stavarache *et al*., capsules comprising magnetite nanoparticles in the fourth or tenth layer were more likely to be disassembled than capsules with magnetite nanoparticles in the sixth layer. Consequently, the latest displayed greater stability in terms of capsule rupture, cargo release and nanoparticle leakage.[83]

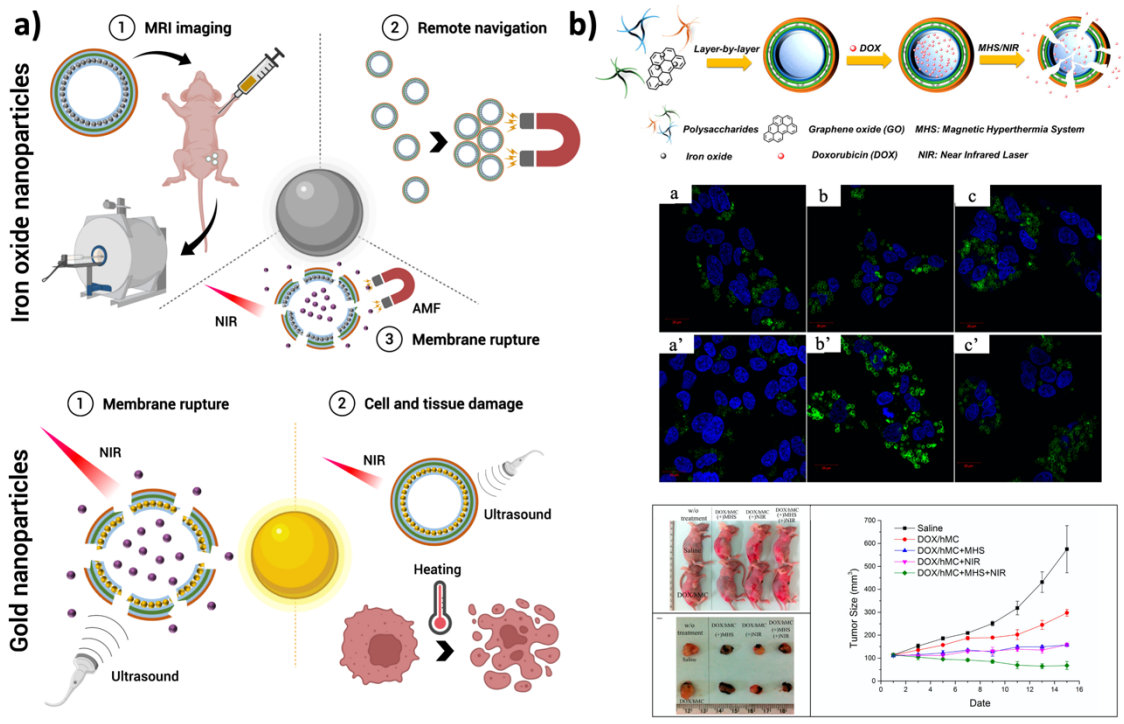

Fig. 2.5. *a) Iron oxide vs. gold nanoparticle incorporation in LbL polymer membranes. The figure shows the characteristics and the possible applications of the incorporated nanoparticles. b) Above, schematic representation of the fabrication process of DOX loaded microcapsules. The iron oxide decorated graphene oxide (GO) nanosheets were incorporated between the polysaccharide layers used for the formation of the polymeric membrane. To enhance the targetability, an outer hyaluronic acid (HA) layer was added. The outer layer of HA, together with a low magnetic field (middle, b') or NIR light (middle, c') improved the internalization and the adhesion of the fabricated capsules comparing to the control (i.e., capsules without iron oxide, GO) (middle, b,c). Below, images of mice and extracted tumours after the administration of capsules and the quantification of the tumour size, highlighting that the synergistic effect of magnetic hyperthermia and NIR light promoted tumour reduction. Reprinted (adapted) with permission from ACS Appl. Mat. Interfaces 2016, 8, 11, 6859-6868. Copyright 2021 American Chemical Society.*

Remote control on the fabricated capsules and controlled release can also be achieved by using gold nanoparticles and nanorods (**Fig. 2.5a**).[89-93] In the presence of near-infrared light (NIR), gold nanoparticles exhibit strong surface plasmon resonance (SPR) and, consequently, are capable of converting this NIR into heat, which is useful in drug release applications.[89] This strategy is helpful in cancer treatments, where a specific and controlled release of the encapsulated cargo is required only at the site of action, with

the aim of reducing side effects associated with the cytotoxic drugs and avoiding cellular drug resistance.[94,95] Irradiating the gold nanoparticles that are present in the polymeric membrane results in a local temperature increase and subsequent disintegration of the capsule, thus leading to the release of the encapsulated cargo.[93] Furthermore, these nanoparticles hinder the leakage of the encapsulated agent and mitigate the so common initial burst release observed on similar release platforms.[91] By using ultrasound instead of NIR, increased permeability of the polymeric membrane can also be achieved, with an increase in the release efficiency by up to 4-fold.[92] The local increase of the temperature associated with the response of gold nanoparticles to NIR or high-frequency ultrasound can also be used to damage the surrounding tissues and cells (**Fig. 2.5a**).[92,93] Accordingly, a plethora of works has focused on the use of free gold nanoparticles to cancer cell ablation, obtaining high tumour volume reductions.[96-99] However, these free nanoparticles may usually need their functionalization to promote their accumulation in the tumour and avoid the aggregation and systemic clearance.[97-99] Within this context, the incorporation of gold nanoparticles in the membrane of LbL capsules could be a useful tool to simultaneously protect them and provide additional functionalities, improving the outcomes of the treatment accordingly.

Less common alternatives to the use of iron- or gold-based nanoparticles mentioned above are titania (TiO_2),[100] silica (SiO_2),[101] quantum dots[102] and cerium oxide (CeO_2)[103,104] nanoparticles. These nanoparticles are useful for imaging and as protective barriers of the encapsulated active entity, thus maintaining its activity during their *in vitro* or *in vivo* application. In the specific case of cerium oxide nanoparticles, their remarkable redox potential inactivates a wide variety of reactive oxygen species (ROS) and protects the activity of the encapsulated agents (e.g., enzymes) from surrounding insults.[103,104] As an example, Popov and co-workers demonstrated that adding CeO_2 nanoparticles in the shell of the fabricated capsules preserved the activity of the encapsulated enzyme in the presence of H_2O_2. In contrast, the enzyme lost its activity in the absence of protecting CeO_2 nanoparticles.[103]

Graphene oxide (GO) or reduced graphene oxide (rGO) as constituents of the multilayer membranes are commonly used as structural elements and also for the remote-controlled release. Using low doses and a low laser power, a controlled drug release can

be achieved, especially with rGO.[105-107] GO presents unique properties, including dispersibility in water and physiological components, excellent biocompatibility and prolonged blood circulation. Thanks to these characteristics and its good permeability for drug encapsulation, GO-based LbL capsules with simultaneous structural stability and capability to release a drug have been reported.[106,107]

The incorporation of enzymes like glucose oxidase (GOx),[108-112] catalase (CAT),[111,112] peroxidase (POD),[109,113] or urease[114,115] in the membrane of polymer capsules fabricated *via* the LbL approach is a facile way to obtain micro- and nanoreactors. In the case of some enzymes, their immobilization between the membrane layers enhances their stability against fluctuations in temperature and pH and also prolongs their storage time.[109,114] In this way, GOx entrapped between layers is capable of achieving its maximum activity at 25 ^{o}C while the free enzyme achieves it at 35 ^{o}C. The enzyme suffers a sharp reduction in its activity with temperature in both cases, being sharper in the case of the free enzyme.[109] Furthermore, the immobilized enzyme presents higher resistance to pH changes.[109] Taking advantage of the stability obtained by trapping GOx between layers, these polymer capsules can be potentially used as glucose sensors and as micro-platforms for diabetes treatment.[108,110-112] The by-products resulting from the reaction between GOx and glucose can react with a fluorescence substrate in the presence of a catalyzer, thus resulting in an increase in the fluorescence intensity, which enables their use as glucose sensors.[108,110] One way to obtain the fluorescence signal is to incorporate fluorescent layers that are activated when the O_2 level decreases. For example, Fang and collaborators incorporated oxygen quenchable ruthenium-based complexes as layers.[108] Another way is to include within the membrane H_2O_2 consuming agents such as Hemoglobin, which will react with Amplex red to yield Resorufin as a fluorescent product.[110] These O_2 consuming sensors are a useful platform to study physiological processes inside cells and monitor a disease for the subsequent treatment.[108] For the treatment of diabetes, the main requisite is to have a system that is switched on when the glucose level is above the established value and switched off when it drops, thus mimicking normal physiological processes.[112] As an example, Xu *et al.* fabricated multilayer capsules that were capable of being repeatedly activated during four cycles obtaining a total insulin release of 30% under normal glucose levels and of 70% release

under hyperglycaemia conditions.[112] This phenomenon was achieved thanks to the increase in the permeability of the layers as a consequence of pH drop resulting from the reaction of GOx with glucose.[110,111]

The use of small interfering RNA (siRNA) is a promising tool to improve the therapeutic efficacy of some treatments towards more personalized medicine, particularly for cancer.[116,117] siRNA is capable of targeting oncogenes and genes implicated in cancer cell growth and metabolism.[116,118] However, the efficiency of free siRNA has limitations such as immunogenicity, nuclease degradation, low cellular uptake, fragile stability and systemic side effects as a consequence of uncontrolled distribution and limited transfection. Consequently, encapsulation or protection of siRNA is a must to ensure safe use of this technology.[119-122] The fabrication of multilayer LbL micro- and nanocapsules containing siRNA between their layers is a promising strategy to prolong the circulation time of the device in the bloodstream, ensure a high siRNA loading and minimize their potential toxicity.[116-118,120,123-125] As reported by Choi *et al.*, the LbL nanoparticles containing siRNA between their layers led to the downregulation and silencing of BCL-2 expression, causing the apoptosis of blood cancer cells in culture and also in animal models (**Fig. 2.6**).[118] One issue to take into account in these capsules is their internalization by cells. The most important thing is not only the number of internalized capsules, but also the number of active molecules delivered, which depends on the loading capacity of the multilayer capsule.[126-128] Hence, several works are focused on the optimization and enhancement of the nucleic acid adsorption modifying the salt concentration of the incubating solution.[127,128]

The versatility of the LbL approach also allows the deposition of small molecules (e.g., drugs) into the polymeric membrane,[129] as well as the incorporation of growth factors (GFs).[130-132] Tissue regenerative medicine is a challenging field within biomedicine, which needs the intervention of several factors to help the tissue to regenerate. The use of GFs is a useful tool to enhance cell differentiation to the corresponding tissue. For this, some works developed LbL polymer capsules comprising within their membrane osteogenic factors such as recombinant human BMP-2 or osteogenic growth factors (OGF) to enhance bone tissue formation.[130,131]

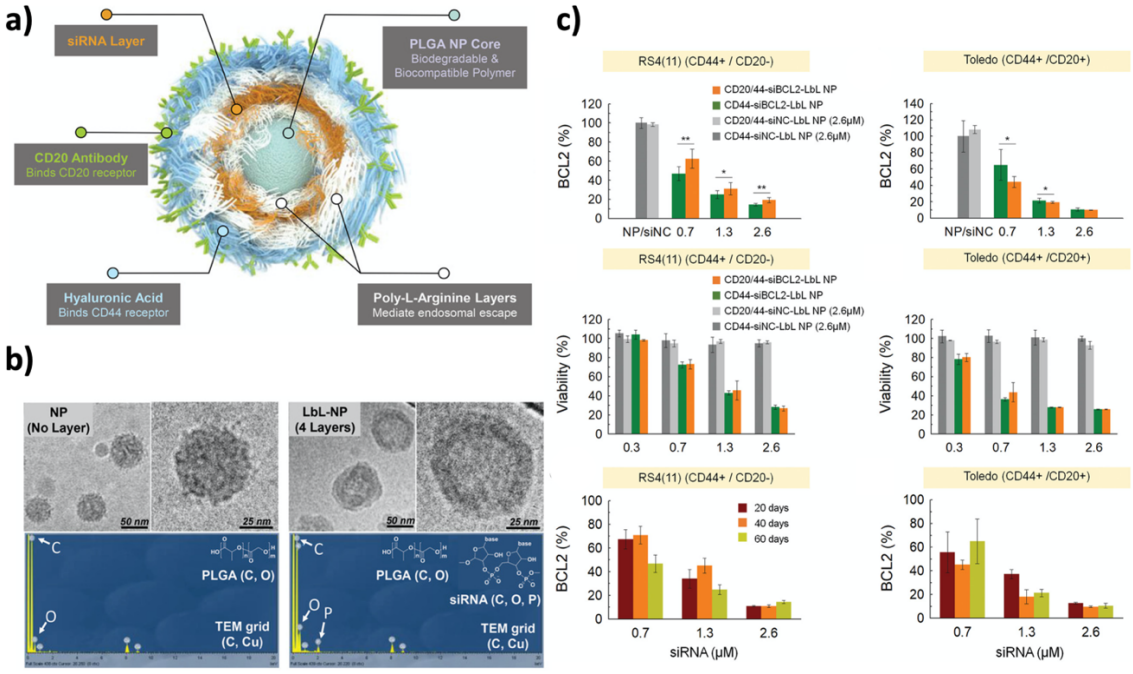

Fig. 2.6. *a) Schematic representation of dual-targeted (i.e., CD20 and CD44) nanoparticles for siRNA release for the treatment of haematological cancers presenting and up-regulation of antiapoptotic BCL-2 protein. b) Cryogenic TEM images and energy dispersive X-ray (EDX) spectra of PLGA core nanoparticles (left) and 4-layer LbL nanoparticles containing siRNA (right). The particles show a uniform nanolayer coating in TEM images and the incorporation of siRNA was analysed with EDX in which the presence of phosphate atoms confirms the presence of the nucleic acid. c) In vitro gene silencing effect of siRNA (i.e., siBCL2) containing nanoparticles. The presence of siBCL2 between the nanoparticle layers suppresses BCL2 gene expression (above) and, as a consequence, a decrease in the viability of the cells was observed (middle). The storage stability of the LbL nanoparticles was further analysed and the results show a gene silencing capacity after 60 days (below). Reprinted (adapted) with permission from Adv. Funct. Mater. 2019, 29, 20, 1900018. Copyright 2021 WILEY-VCH GmbH.*

The incorporation of the above-mentioned active agents usually relies on the electrostatic interaction between the building blocks. Consequently, the deposited active agent could be released before reaching the target site, thus losing its therapeutic potential and causing side effects associated with off-target accumulation. As an alternative to physical interactions, chemical conjugation techniques can be considered to improve the interaction between the constituents of the polymeric membrane.

2.3.2. Crosslinking and functionalization of the building blocks

Crosslinking of the building blocks constituting the multilayer membrane is regularly adopted to impart mechanical integrity and/or responsiveness to the polymeric capsules. Using thiol-modified polyelectrolytes for the LbL deposition and its subsequent crosslinking to form disulfide bonds results in redox responsive vehicles capable of releasing an encapsulated agent in response to the glutathione (GSH) levels encountered in the cellular microenvironment.[133-137] Thus, the fabricated capsules are stable at physiological pH but are deconstructed under reducing conditions allowing the targeted release of the cargo intracellularly.[134,135] This strategy is useful in vaccine formulations since traditional strategies have been unsuccessful in immunizing against many chronic diseases such as HIV.[135,137] The capsules are subjected to phagocytosis by antigen-presenting cells (APC) and to micropinocytosis by dendritic cells (DC), both being of utmost importance in the immune response coordination.[135] Within this field, Sexton and co-workers fabricated LbL capsules for vaccination, formed by a polymeric membrane of thiolated poly(methacrylic acid) (PMASH) and poly(vinylpyrrolidone) (PVPON) capable of encapsulating ovalbumin (OVA) peptide. They observed that these LbL capsules containing the peptide within their core were capable of efficiently stimulating T immune cells.[135] Furthermore, in comparison to the free protein, the encapsulated peptide antigen was able to induce an equivalent immune response using a lower dose.[135] Instead of using disulfide crosslinked polymeric membranes to protect and control the release of the encapsulated cargo, other authors employ polyelectrolytes that are sensitive to an external or internal trigger, such as UV light or pH change.[138,139] By covalently assembling poly(2-vinyl-4,4-dimethylazlactone) (PVDMA) with PEI, the degradation of the LbL occurred only at acidic pH values, allowing the release of the encapsulated cargo under these conditions.[139] Using poly(diallyldimethyl ammonium) chloride (PDADMAC) and poly[1-[4-(3-carboxy-4-hydroxyphenylazo)benzenesulfonamido]-1,2-ethanediyl, sodium salt] (PAZO) as the constituents of the polymeric membrane, the release of the cargo was controlled using UV light thanks to the formation of azobenzene (AZO) aggregates which induce a phase separation on the polymeric membrane.[139]

The conjugation of the active agent to a polyelectrolyte is a useful alternative to avoid the aforementioned limitations associated with the electrostatic adsorption of the building blocks onto the sacrificial template. The incorporation and encapsulation of small hydrophobic molecules is usually a challenge in the fabrication of LbL micro- and nanocapsules. Many works have described the conjugation of the drug or prodrug to one of the polyelectrolytes to improve its solubility, stability and transport of the therapeutic hydrophobic molecule.[140-146] Thanks to the conjugation, a better control over the release rate and an improvement in the targeting are achieved. This is very useful in pathologies like cancer, in which the control over the dosage and efficient targeting of the anticancer drug determines the success of the adopted approach.[145,146] Anticancer drugs like doxorubicin or paclitaxel have been successfully conjugated to a wide variety of polyelectrolytes.[141,144] Within this context, several strategies have been followed for the conjugation of the drug. Some of them use the amine bond formation for the conjugation of DOX to the polyelectrolyte used for the fabrication of the polymeric membrane (**Fig. 2.7a**).[141] Following this strategy, Ochs *et al.* observed a successful decrease in the viability of LIM 1899 human colon cancer cells after the treatment with the fabricated capsules, which were capable of releasing DOX in a controlled manner thanks to enzymatic degradation.[141] Another strategy to incorporate these hydrophobic drugs is the use of cyclodextrins, which are water-soluble oligosaccharides capable of hosting various guest molecules into their hydrophobic cavity (**Fig. 2.7a**).[144] For example, Jing and collaborators fabricated LbL capsules using a hyaluronic acid-cyclodextrin conjugate as a building block, which was subsequently loaded with paclitaxel. This system exhibited a controlled release and high effectiveness in reducing the viability of breast cancer cells (**Fig. 2.7b**). In cancer treatment, another strategy is the use of prodrugs conjugated to the polymer membrane layers. The use of Pt(II)-based drugs have been extensively reported since they are capable of inhibiting the growth of cancer cells interfering in transcription and other DNA-mediated cellular functions.[145] However, these drugs have limited solubility and lack of functional groups capable of facilitating their encapsulation, thus limiting their use in the clinic.[145] Moreover, they have a wide variety of side effects ranging from nephrotoxicity and cumulative neurotoxicity to ototoxicity.[145] The use of its prodrug (i.e., Pt(IV)) represents a promising alternative because it shows better pharmacokinetics and reduced side

effects.[145,146] Several works have conjugated the Pt(IV) prodrug to a polypeptide or a polysaccharide to exploit them as part of the polymeric membrane.[145,146] In this way, higher toxicity than free Pt(II) was observed thanks to a higher intracellular accumulation of Pt.[145] As reported by Zhang and co-workers, capsules fabricated *via* the LbL approach combining in their membrane Pt(IV)-chitosan conjugates and complementary anticancer drugs (e.g., gemcitabine (GEM)-conjugated to HA) were capable of releasing the active agents in a sustained manner, obtaining a synergistic effect that reduced lung cancer tumour while avoiding toxic effects in off-target organs and tissues.[146]

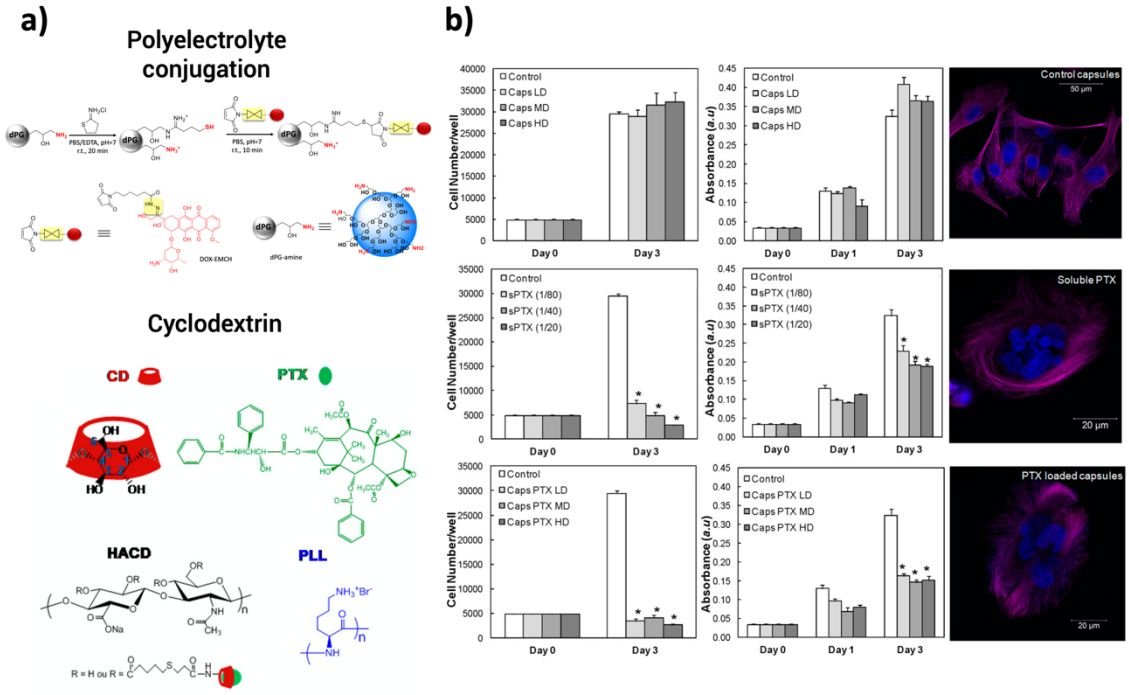

Fig. 2.7. *a) Chemical conjugation (above) vs. cyclodextrin complex formation (below) for the incorporation of poorly soluble molecules. The image below has been reprinted (adapted) with permission from Chem. Mater. 2013, 25, 19, 3867-3873. Copyright 2021 American Chemical Society b) Viability results and fluorescence micrographs of MDA-MB-231 cells in response to unloaded capsules (upper row), paclitaxel (PTX) in solution (middle row) and PTX-loaded capsules using cyclodextrin complex formation (row below). Capsules with the cyclodextrin-PTX complex induce a higher cell toxicity obtaining thus an efficient anticancer treatment. Reprinted (adapted) with permission from Chem. Mater. 2013, 25, 19, 3867-3873. Copyright 2021 American Chemical Society.*

Table 2. *Strategies to incorporate functionalities in the multilayer membrane of LbL capsules intended to be used in biomedical applications.*

Strategy	Active agent in the membrane	Encapsulated entity	Layer functionalization approach	Biomedical application	Outcomes	Ref.
Layer as the active agent	Iron oxide	N/A	Electrostatic interaction	Imaging, fate and biodistribution (*in vivo* and *in vitro* studies in MSC cells)	• Two-fold higher Fe uptake when encapsulated. • After intravenous administration, distribution of capsules was determined by MRI *in vivo*.	49
		N/A	Electrostatic interaction	Imaging, fate and biodistribution	• Capsules were accumulated in liver, as determined by MRI.	80
		N/A	Electrostatic interaction	Imaging, fate and biodistribution (degradation analysis)	• The signal intensity change did not exceed 25% with high Fe_3O_4 concentration. • The signal intensity change was 100% with low Fe_3O_4 concentration. • MRI contrast increase upon degradation.	81

Table 2. *Continued*

Strategy	Active agent in the membrane	Encapsulated entity	Layer functionalization approach	Biomedical application	Outcomes	Ref.
Layer as the active agent	Iron oxide	Doxycycline	Electrostatic interaction	Drug release	• The release of the drug is promoted by AMF. • Increasing the cell to capsule ratio increased the expression of endothelial growth factor receptor.	84
		RITC-BSA	Electrostatic interaction	Remote navigation (Localization in blood flow)	• Thanks to AMF guiding endothelium penetration is achieved in 30-40 minutes. • Accumulation of capsule accumulation did not block blood flow.	85
		N/A	Electrostatic interaction	Cancer	• AMF induced morphological change and disruption of the capsules.	86
		Doxorubicin	Electrostatic interaction	Imaging, guiding and drug release (studies in cancer cells)	• AMF guidance to the target site. • HIFU promoted the release of the drug.	88

Table 2. *Continued*

Strategy	Active agent in the membrane	Encapsulated entity	Layer functionalization approach	Biomedical application	Outcomes	Ref.
Layer as the active agent	Iron oxide and graphene oxide	Doxorubicin	Electrostatic interaction	Cancer (*in vitro* studies in HeLa cells and *in vivo* in HeLa bearing BALC/nude mice)	• HA and low magnet irradiation enhanced cell targeting. • On demand therapy. • Efficient tumour reduction.	87
	Gold	Doxorubicin	Electrostatic interaction	Cancer (*in vivo* and *in vitro* studies in MCF-7 cells)	• NIR promoted the release of the drug. • Reduced tumour volume *in vivo.*	90
		Dextran	Electrostatic interaction	Drug release in cancer (*in vitro* studies in MDA-MB-435 cells)	• Laser activated release into the cytosol.	93
	Cerium oxide	Luciferase	Electrostatic interaction	Oxidative stress (reactive oxygen species) attenuation	• Cell protection against 1.5 mM H_2O_2. • Enzyme activity retention.	103
		N/A	Electrostatic interaction	Oxidative stress (reactive oxygen species) attenuation	• B50 rat neuronal cell protection from high H_2O_2 doses. • Preservation of cell viability.	104

Table 2. *Continued*

Strategy	Active agent in the membrane	Encapsulated entity	Layer functionalization approach	Biomedical application	Outcomes	Ref.
Layer as the active agent	Graphene oxide	DOX	Hydrophobic interaction	Drug release	• After NIR irradiation nearly 80% of drug release.	107
	Glucose oxidase and catalase	Insulin	Electrostatic interaction	Diabetes	• In presence of glucose, capsules were capable of releasing nearly 55% of insulin.	111
		Insulin	Electrostatic interaction	Diabetes	• Release activity activated when glucose level increase. • 70% of insulin release in hyperglycaemia.	112
	siRNA	Doxorubicin and Indocyanine green dye	Electrostatic interactions	Cancer (*in vivo* and *in vitro* studies in A549 cells)	• Synergistic effect of thermal/gene/chemotherapies. • High tumour volume reduction. • High gene transfection.	116

Table 2. *Continued*

Strategy	Active agent in the membrane	Encapsulated entity	Layer functionalization approach	Biomedical application	Outcomes	Ref.
Layer as the active agent	siRNA	Doxorubicin and MRP1	Electrostatic interaction	Cancer (*in vivo* and *in vitro* studies in MDA-MB-468 cells)	• 4-8-fold tumour volume reduction.	117
		N/A	Electrostatic interaction	Cancer (Haematological BCL-2 protein silencing)	• BCL-2 protein reduction induced blood cancer cell apoptosis.	118
		N/A	Electrostatic interaction	Cancer (*in vivo* and *in vitro* studies in OVACAR8 cells)	• 54% knockdown of the target gene.	123
		Cisplatin	Electrostatic interaction	Cancer (Lung tumour targeting)	• Increased cytotoxicity *in vitro*. • RNAs and cisplatin combination enhanced tumour volume reduction.	124
		N/A	Electrostatic interaction	Gene transfection	• Enhanced transfection efficiency than commercial liposome-based transfection kits.	125

Table 2. *Continued*

Strategy	Active agent in the membrane	Encapsulated entity	Layer functionalization approach	Biomedical application	Outcomes	Ref.
Layer as the active agent	Growth factor	N/A	Electrostatic interaction	Bone regeneration	• Using BMP-2 and TGFβ1 bone regeneration was favoured in the absence of a cartilage template.	130
		Osteogenic peptide	Electrostatic interactions	Osteogenic differentiation	• Increased cell elongation/stretching. • Upregulation of bone related proteins.	131
Crosslinking and functionalization of the building blocks	Disulfide link	Ovalbumin	PMA functionalized with thiol groups and subsequent crosslinking	Vaccine (Chronic infections)	• Preferential degradation of the disulfide link intracellularly. • Ovalbumin stimulate T cell immunity.	135
	Doxorubicin	N/A	Click-chemistry	Cancer (*in vitro* studies in LIM1899 cells)	• Decreased cell viability (32%) and proliferation.	141
	KP9 peptide	N/A	Conjugation *via* disulfide link to PMA	Vaccine (Chronic infections)	• Stimulate lymphocyte immune response.	143
	Paclitaxel	N/A	Host-guest interaction with cyclodextrin	Cancer (*in vitro* studies in MDA-MB-231)	• Limited cell proliferation and metabolic activity.	144

Table 2. *Continued*

Strategy	Active agent in the membrane	Encapsulated entity	Layer functionalization approach	Biomedical application	Outcomes	Ref.
Crosslinking and functionalization of the building blocks	Pt (IV) pro	N/A	Covalent conjugation *via* amination to PLL	Cancer (*in vitro* studies in CT-26 cells)	• Higher intracellular accumulation of Pt. • Enhanced cytotoxicity.	145
		Gemcitabine	Covalent conjugation *via* amination to chitosan	Cancer (*in vitro* studies in NCl-H460 cells)	• Sustained release of the drugs. • Synergistic effect capable of reducing lung cancer and avoid toxicity in off-target organs and tissues.	146

2.4. Outer layer

It is evident from the previous sections that the LbL methodology offers numerous advantages including the colloidal stability, degradability, drug release and biocompatibility, among others.[147] These advantages derive through the careful design of the LbL micro/nanocapsules, that includes the selection of the appropriate components that act as the core, as well as the building blocks that are used as the coating layers and their functionalization. Although both the core and the multilayer membrane affect the *in vitro* and *in vivo* behaviour of the capsules, the most important component is the outer layer. The outer layer is the one that comes first into contact with the biological microenvironment defining the *in vitro/in vivo* fate of the capsules. Thus, a suitable functionalization can improve characteristics like circulation time in the blood and cell uptake or provide responsiveness to a physical, chemical or biological stimulus.

2.4.1. Colloidal stability and circulation time

Colloidal stability inside a biological environment is of crucial importance since it strongly affects the fate of the administered capsules. One of the most common techniques for improving the colloidal stability and circulation times (through opsonization inhibition) of nano- and microcapsules, is their surface-functionalization with poly (ethylene glycol) (PEG).[86,148-154] The ability of PEG to create brushes that inhibit the attachment of proteins present in the blood, and the steric hindrances that promote the individual stability (through aggregation inhibition) of each capsule, make PEG one of the best stability enhancement approaches. As an example, PEG was used as the final layer in a poly(L-lysine)/poly(glutamic acid) (PLL/PGA) capsule-based system aiming at improving its colloidal stability.[86] In this work, where the main objective was to prepare nanocapsules for hyperthermia applications, nanoemulsion droplets were used as the core around which the polyelectrolyte nanocapsule was formed. The Fe_3O_4 nanoparticles that were incorporated between the layers provided the responsiveness to alternating magnetic fields, whereas the PEG coating allowed for a long-term colloidal stability of 90 days, as demonstrated by dynamic light scattering studies. This long-term

colloidal stability, demonstrated the capability of the fabricated capsules to avoid the above-mentioned opsonins' adsorption onto the colloidal multilayer capsules and thus avoiding the unspecific clearance, *via* phagocytosis, of immune cells like macrophages.[149,151,152] In their work, Wattendorf and collaborators functionalized the outer layer of the fabricated microcapsules adding to the surface PEG-grafted PLL (PLL-g-PEG) and PGA (PGA-g-PEG) to analyse their stealth effect in human monocyte derived dendritic cells (DC) and macrophages (MΦ).[152] As they observed, PLL-g-PEG coated capsules were capable of resisting the internalization by DC and MΦ in comparison to the non-PEGylated counterparts. The capsules remained freely in the cellular microenvironment, thus reducing the uptake rate by about two-thirds and a half obtaining a drop in the phagocytosis mechanism by up to 85-90%.

However, this conventionally used PEG coatings present several limitations including, its degradation by oxidation, hypersensitivity, poor bioavailability, immunogenicity and non-biodegradability.[155] As an alternative, other brush-like structures have been studied and among them, poly(2-oxazoline)s (POxs) have emerged as interesting candidates. These POxs present excellent biocompatibility, a great stealth behaviour and protein repellence, and an ease of fabrication, thus increasing the circulation time and avoiding the clearance *via* phagocytic pathways.[155-158] In their work, Kempe *et al.* observed that capsules fabricated with these brush-like structures and incubated in model protein serums like BSA and lysozyme, were capable of reducing in 40% the association of proteins in comparison to its linear counterparts.[155] The better hydration and subsequent increased resistance to protein adhesion was the main reason behind the observed behaviour. In a similar work, it was observed that capsules fabricated with poly(2-ethyl-2-oxazoline) (PEtOx) and incubated in human serum presented a three-fold reduction in protein fouling with respect to the control systems in which poly(methacrylic acid) (PMA) and poly(2-diisopropylaminoethyl methacrylate) (PDPA) were used as the outer layer of the polymeric capsule.[157]

2.4.2. Targetability and selective internalization

Besides stability, surface functionalization using proteins or sugars on the surface of the capsules can improve cell internalization while enhancing the selective uptake by a

specific cell type. Additionally, a surface protein or sugar can be used as a recognition molecule rendering the capsules able to act as biosensors or biomolecule separators. In an interesting work,[159] fibrinogen was used to functionalize the surface of dextran/PLL/PGA multilayer capsules aiming at attracting the circulating platelets. Due to fibrinogen, the platelets adhered to the microcapsules *via* the αIIbβ3 integrin, forming a hybrid platelet-microcapsule system. The system was able to travel to the clot area and release the encapsulated anti-clotting factor VIII in an *in vitro* model of Haemophilia A. Notably, the release of the pro-clotting factor was achieved through the rupture of the capsules upon activated platelet contraction.

The use of lectin as a target is another approach that has been reported in the literature.[160] The authors of the study fabricated a sodium alginate/chitosan microcapsule coated with a lipid bilayer. This bilayer not only sealed the encapsulated drug daunorubicin, but also allowed the functionalization with a laboratory-synthesized glycolipid that shows high affinity to lectins. To further improve the targetability and selective uptake of the system, the authors used an additional lipid-based folate group (DSPE-PEG_{2000}-folate) that has the ability to target the MCF-7 cancer cells. A different system that also made use of lectin as a targeting group was reported by Zhang and co-workers.[161] In their work, the authors made a polyelectrolyte microcapsule constituted of poly(vinyl galactose esterco-methacryloxyethyl trimethylammonium chloride)s (PGEDMC) and PSS. PGEDMC contained galactose branches able to recognize membrane-bound galactose receptors (ASGPR). The *in vitro* studies revealed a peanut agglutinin (PNA) lectin recognition that allows adhesion to the HepG2 receptor, suggesting the potential of the system for hepatic targeting.

In another study,[162] surface functionalization of magnetic polyelectrolyte capsules using an antibody against horseradish peroxidase (HRP) led to the magnetic separation of HRP, proving the biomolecular recognition ability of these capsules through selective antibody functionalization. In a similar study, PEGylated microcapsules were functionalized with an antibody against collagen type IV, allowing their use for exclusive binding to collagen type IV substrates.[163] Following the same rationale,[164] PAH/polyacrylic acid (PAA) microcapsules were functionalized with antibodies (Y3, 5D3 and W6/32) against the major histocompatibility complex I (MHC I) (**Fig. 2.8a**). The

results of this study showed that the targeting towards this complex is selective and allotype specific (**Fig. 2.8b and 2.8c**). Additionally, when the microcapsules were coated with the staphylococcus aureus protein A before the antibody functionalization, then the targeting efficiency increased by 40-50% compared to the direct antibody functionalization (**Fig. 2.8c**). This was attributed to the specific orientation of the antibodies deriving from the optimized immobilization on the microcapsules' surface due to the protein A coating.

Enhanced targeting can be also achieved using antibodies specific to receptors that are overexpressed in various cells, like the endothelial growth factor receptor (EGFR) that is overexpressed, among others, in breast cancer. In a particular study, the authors fabricated quantum dots that were subsequently coated with PAA/PAH and functionalized with cetuximab, a monoclonal antibody against the EGFR.[165] The *in vitro* studies that were carried out in the MDA-MB-468 and MCF-7 human breast adenocarcinoma cell lines showed that the antibody-conjugated capsules interacted only with the MDA-MB-46 (EGFR positive), and not the MCF-7 (EGFR negative) cells. Other commonly overexpressed marker is A33, which is present in 95% of human colorectal tumour cells.[166] Functionalization of polymer capsules with the humanized A33 (HuA33) antibody, allowed their binding to corresponding receptors overexpressed in the LIM1215 colorectal cancer cell line. This binding was the first step towards an efficient internalization, and thanks to this, nearly all cells were capable of containing one particle, demonstrating an efficient targeting to the tumour site.[166]

Aside from proteins and antibodies, oligonucleotides like aptamers have also been used for surface functionalization.[167,168] In one of the works presented by Liao *et al.*, aptamer-functionalized microcapsules offered selective targeting and responsiveness to overexpressed cancer cell biomarkers like the vascular endothelial growth factor (VEGF) and adenosine triphosphate (ATP).[167] When the microcapsules were incubated with the cancer cells (MDA-MB-231), the VEGF on the surface of the cells or the intracellular ATP were bound to the anti-VEGF/anti-ATP on the surface of the capsules, leading to their unlocking (higher effectiveness with ATP functionalization) and releasing of the encapsulated drug doxorubicin. When the capsules were incubated with non-cancerous

MCF-10A cells, a lower toxicity was observed, suggesting that no doxorubicin was released.

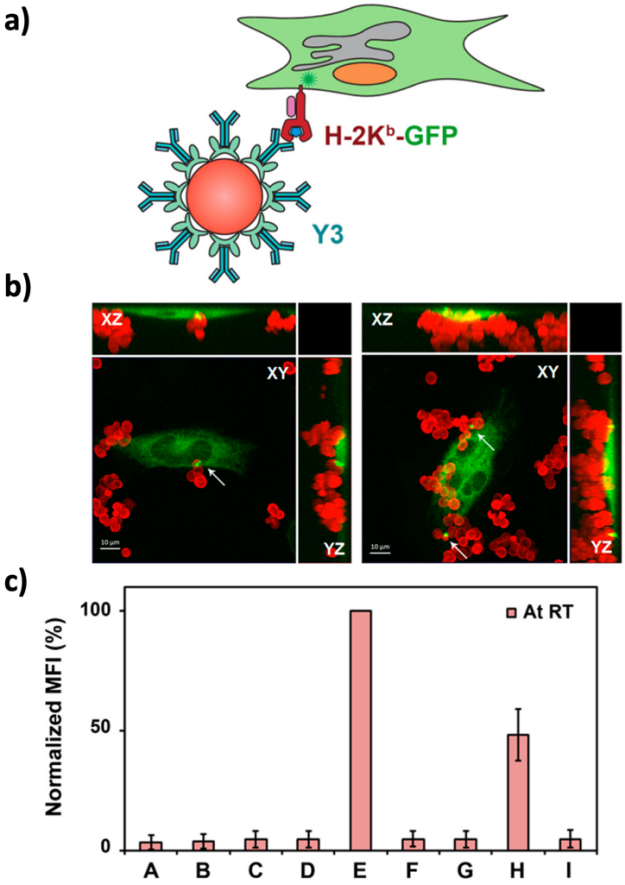

Fig. 2.8. *a) Schematic representation of (PAH/PAA)$_2$ microcapsules coated with protein A and post-functionalized with the murine Y3 antibody capable of specifically recognizing specific class I molecules at plasma membrane of STF1 cells. b) Confocal microscopy images showing the cell, antibody and allotype specific targeting of the capsules. In the particular case of these images, capsules post-functionalized with Y3 were attached after 3 h to STF1 cells. White arrows highlight the specific contact point between the cells and the capsules. c) Flow cytometry results summarizing the interaction study between the capsules functionalized with different antibodies and T1 cells. The used capsules were: (A) non functionalized, (B) coated with protein A, (C) functionalized with the Y3 antibody in optimized orientation, (D) functionalized with the 5D3 antibody in optimized orientation, (E) functionalized with the W6/32 antibody in optimized orientation. (F) Y3 antibody, (G) 5D3 antibody and (H) W6/32 antibodies were randomly orientated (I) BSA coated capsules. The results showed the allotype and cell specific tendency in this specific case using T1 cells. Optimizing the orientation of the antibodies, the targeting efficiency increased by 40-50%. Reprinted (adapted) with permission from ACS Appl. Mater. Interfaces 2017, 9, 13, 11506-11517. Copyright 2021 American Chemical Society.*

Other alternatives for the functionalization of the outer layer and the subsequent improvement of their targetability is the use of polysaccharides like hyaluronic acid (HA). HA presents great affinity to CD44, a cell surface receptor present in many cancer types, that plays a pivotal role in cancer progression and metastasis (**Fig. 2.9a**).[169,170] Within this context, many works have focused on the fabrication of capsules with a HA outer layer to enhance the targetability and also the internalization of the capsules (**Fig. 2.9b**).[87,118,169-171] Choi and collaborators fabricated capsules encapsulating siRNA to disable the B-cell lymphoma 2 (BCL-2) present in haematological cancers.[118] These capsules were functionalized with an outer HA layer conjugated to a specific antibody (CD20). As a result, the capsules were capable of binding to two different surface receptors obtaining a higher efficiency in the treatment. Furthermore, thanks to the presence of HA, capsules were internalized in an efficient way after their binding to the upregulated CD44 marker.

2.4.3. Providing stability and stimulus-responsive release

In the aforementioned sections we have already described how nanostructures like nanoparticles, in the intermediate layers of the LbL microcapsules, can provide advanced functionalities. However, nanoparticles and nanorods have also been used in the outer layer of various microcapsules aiming at improving the release properties by rendering the capsule responsive to a stimulus. As an example, silica[172-175] and titania[176] nanoparticles have been formed through *in situ* nucleation on the surface of PSS/PAH microcapsules resulting respectively in an ultrasound and UV/ultrasound-dependent release of Rhodamine-B and Dextran. Although the systems were not tested either *in vitro* or *in vivo*, the presented data suggested their potential use in the biomedical field. In another example, gold nanorods were used to decorate hydroxyapatite (HAP) /chitosan (CHI)/hyaluronic acid (HA) microcapsules aiming at the creation of a pH-responsive (chitosan) and NIR-responsive (gold) system.[177] The microcapsules showed a significant increase in the release of doxorubicin (~72%) when low pH (4.5) and NIR irradiation were combined. In the specific case of silica, apart from making the capsules capable of releasing a specific therapeutic agent in response to an external stimuli, this outer layer endowed the capsules with a greater robustness and reduced permeability

of the membrane, avoiding unspecific release, thanks to the blocking of the capsule pores.[174,175,178] Timin and collaborators observed that the capsules encapsulating doxorubicin and functionalized with an outer silica layer were capable of hindering the release of the encapsulated compound in the absence of an externa stimuli (i.e., ultrasound excitation or the presence of a reducing environment).[174] On the contrary, the drug was rapidly released under ultrasound treatment obtaining 87% of drug release after 120 s of stimulation and the same capsules in the presence of GSH were capable of releasing 71% at 48 h. Consequently, they obtained a selective drug delivery while maintaining the integrity of the encapsulated drug until the targeted site was reached.

Another way to obtain stimuli responsive capsules by functionalizing the outer layer of the polymeric membrane relies on the use of polysaccharides such as CHI and HA. One LbL system that made use of the pH-sensitivity of chitosan was presented by Verma *et al*.[179] In their chitosan/sodium alginate system, the surface was functionalized with Vitamin 12 aiming at its uptake in the intestine and through the intrinsic factor receptor-mediated endocytosis. The system was able to safely deliver the encapsulated insulin both *in vitro* and *in vivo* presenting a 4.3-fold increase in its absorption when loaded in the nano-capsules (< 250 nm), compared to the free insulin. HA, apart from its ability to target the overexpressed tumour marker CD44 mentioned in the previous section, is also capable of being hydrolysed by hyaluronidase which is usually overexpressed under bacterial infections and cancer environments (**Fig. 2.9a**).[180,181] Using this strategy, Zheng and co-workers developed a capsule with an outer layer of HA which was degraded in the presence of hyaluronidase, thus promoting the release of the encapsulated protein cytochrome C (Cyt).[180] In this way, capsules in the presence of hyaluronidase were capable of releasing 98% of the encapsulated protein after 96 h (**Fig. 2.9c**).

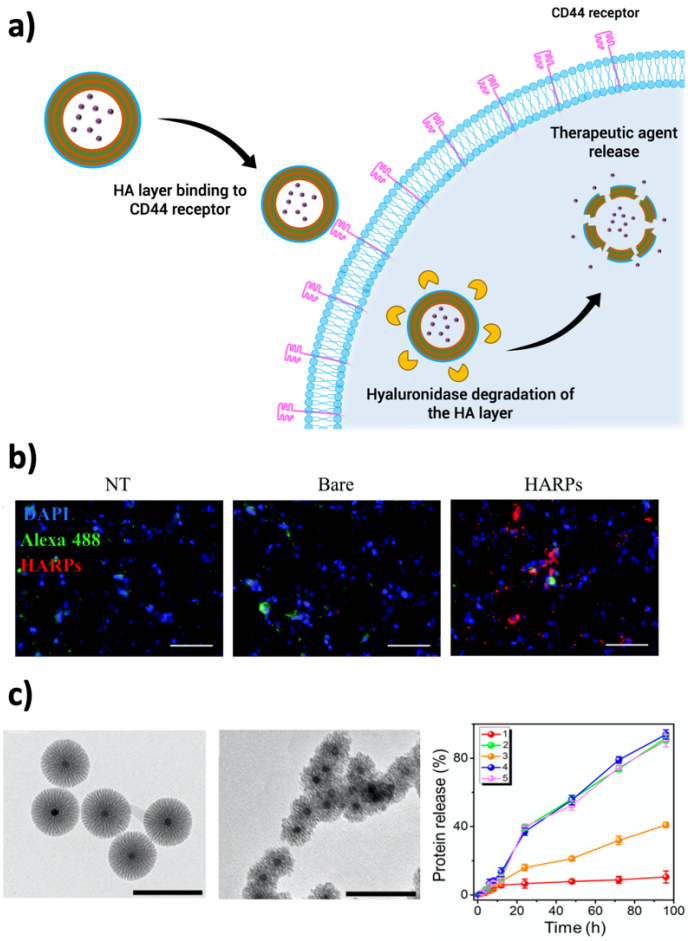

Fig. 2.9. *a) Schematic representation of the capability of HA to specifically bind to the CD44 receptor and subsequent hyaluronidase degradation allowing the release of the encapsulated therapeutic agent. b) Fluorescence micrographs showing the interaction between non treated capsules (NT), bare carboxylate-modified (CML) polystyrene latex beads (Bare) and HA functionalized capsules (HARPs). Nuclei of the cells were stained with DAPI, cell body structure with AlexaFluor 488 and capsules are shown in red. Republished with permission of Royal Society of Chemistry, from Enhancing chemoradiation of colorectal cancer through targeted delivery of raltitrexed by hyaluronic acid coated nanoparticles, Rosh J. et al., 11, 29, 2019; permission conveyed through Copyright Clearance Centre, Inc. c) TEM images of HA coated nanocapsules degradation by hyaluronidase after 0 h (left) and 96 h (middle). Encapsulated Cyt protein release percentage of the nanocapsules (right). The analysed capsule conformations were: (1) capsules coated with 163 mg/g HA, (2) capsules without HA coating, (3) capsules coated with 80 mg/g HA and (4) and (5) capsules coated with the considered amounts of HA in the presence of hyaluronidase. Reprinted (adapted) with permission from ACS Nano 2019, 13, 11, 12577-12590. Copyright 2021 American Chemical Society.*

2.4.4. Miscellaneous

Apart from the above-described properties that the LbL coatings offer, there are still a few attributes that are worth mentioning. As an example, improved stability, but this time in terms of degradation time of the polyelectrolyte layer was also studied after the coating of PAH/PSS capsules with bacterial self-assembled proteins isolated from *Bacillus thuringiensis*.[182] These proteins, called S-layers,[183] are composed of glycoprotein subunits that cover the outer layer of gram (+), gram (-) bacteria and archaea and have great potential to be used as biomimetic coatings.

Polydopamine has also been reported as an additional functionalization of the outer layer to improve the mechanical stability.[184] This stability could be attributed to the creation of covalent bonds between the repeated monomeric units that interconnect through the polyelectrolyte layers enhancing the mechanical strength of the polyelectrolyte system.

On a different approach, Dex/Parg LbL capsules were coated with a variety of liposomal formulations aiming at the activation of dendritic cells (DC) and a specific immune response.[185] The data of this study showed that the lipids acted as immunopotentiators enhancing DC activation with the combination of a lipid A derivative with 1,2-Dioleolyl-3-trimethylammonium-propane chloride salt (DOTAP)/1,2-dioleoyl-sn-glycero-3-phospho-ethanol-mine (DOPE), giving the strongest activation.

Finally, in a recent work by Cambell and co-workers, 16 different types of capsules were studied in terms of stability, by correlating the stability of the fabricated polyelectrolyte complexes (PECs) in the absence of the calcium carbonate template.[186] This study, that made use of various polyelectrolytes like heparin sulfate, dextran sulfate, chondroitin sulfate and hyaluronic acid, helped to identify polyelectrolyte pairs with the highest potential for drug delivery. Notably, it was shown that not all the pairs are suitable for LbL coating with several of these pairs not being able to form capsules after the removal of the core.

Table 3. *Strategies to incorporate functionalities on the outer layer of LbL capsules intended to be used in biomedical applications.*

Strategy	Encapsulated entity	Surface functionalization	Surface functionalization approach	Biomedical application	Outcomes	Ref.
Colloidal stability and circulation time	Iron oxide	PEG	PEG grafted on the PGA electrolyte	Cancer (Neither *in vitro*, nor *in vivo*)	• AMF-induced hyperthermia resulting to morphological alterations.	86
	$LaVO_4:Tb^{3+}$		PEGylation	Bioimaging (*in vitro*/*in vivo* toxicity)	• Fluorescence signal of capsules within cells and tissues.	148
	N/A		PEG grafted to PSS polyelectrolyte	Cancer (*in vitro* with LIM1215 and LIM2405 A33+ cells)	• Decreased non-specific binding. • HuA33 functionalization increase cell binding.	151
	N/A		PEG grafted to PLL and PGA polyelectrolytes	Shielding	• Capsules freely distributed and not adsorbed by macrophages and dendritic cells.	152
	N/A		PEG grafted to PLL polyelectrolyte	Shielding	• Reduced protein adsorption.	153
	N/A		Electrostatic interaction	Shielding	• Reduced adhesion to biological cells. • Reduced human serum albumin adsorption.	154

Table 3. *Continued*

Strategy	Encapsulated entity	Surface functionalization	Surface functionalization approach	Biomedical application	Outcomes	Ref.
Colloidal stability and circulation time	Urokinase plasminogen activator	Poly(2-ethyl-2-oxazoline)	Electrostatic interactions	Thrombolysis	• High platelet affinity. • Thrombin responsiveness and thrombus dissolution.	158
	N/A	Poly(2-oxazoline)	Electrostatic interactions	Antifouling	• 40% lower protein association in brush like POx than in linear.	155
	N/A	Poly(2-ethyl-2-oxazoline) copolymerized with methacrylic acid	Electrostatic interactions	Antifouling	• Preferential uptake of dendritic cells instead of macrophages.	156
	N/A	Poly(2-ethyl-2-oxazoline) copolymerized with methacrylic acid	Electrostatic interactions	Antifouling	• Three-fold reduction in human serum protein adsorption with poly(2-ethyl-2-oxazoline) copolymerized with methacrylic acid systems.	157

Table 3. *Continued*

Strategy	Encapsulated entity	Surface functionalization	Surface functionalization approach	Biomedical application	Outcomes	Ref.
Targetability and selective internalization	Factor VIII	Fibrinogen	Electrostatic interactions	Haemophilia A (*in vitro* with activated platelets)	• Delivery system exploiting platelets' contractile forces. • Faster haemostasis.	159
	Daunorubicin	• Lab-synthesized glycolipid • Commercial DSPE-PEG_{2000}-folate	Hydrophobic interactions	Breast cancer (*in vitro* with MCF-7 cells)	• High affinity towards lectin concavalin A and MCF-7 cells through the overexpressed folate receptor.	160
	Acyclovir	Galactose branches	Electrostatic interactions	Herpes & Hepatitis B	• Number of layers affects the release.	161
	Iron oxide nanoparticles	Anti-Horseradish peroxidase antibody	Covalent bonding	Biomolecular recognition (Neither *in vitro*, nor *in vivo*)	• Recognition, extraction and detection of HRP.	162
	N/A	PEG + Collagen type IV antibody	Biotin-streptavidin reaction	(Neither *in vitro*, nor *in vivo*)	• Enhanced binding affinity to collagen type IV.	163

Table 3. *Continued.*

Strategy	Encapsulated entity	Surface functionalization	Surface functionalization approach	Biomedical application	Outcomes	Ref.
Targetability and selective internalization	N/A	Y3, 5D3 and W6/32 antibodies	Covalent bonding	MHC I class receptors (*in vitro* with RMA, STF1 & T1 cells)	• Optimized antibody orientation through protein A coating resulting in enhanced targeting.	164
	QDs	Anti- endothelial growth factor receptor	Covalent bonding	Breast cancer (*in vitro* with MDA-MB-468 and MCF-7)	• Enhanced uptake by the MDA-MB-468 (EGFR expression) compared to the MCF-7 (no EGFR expression) cells.	165
	Doxorubicin	DNA crosslinked with anti-vascular endothelial growth factor or anti-adenosine triphosphate	Electrostatic interactions	Cancer (*in vitro* with MDA-MB-231 and MCF-10A)	• Selective uptake by cancer cells. • ATP-crosslinked capsules show higher toxicity on cancer cells compared to normal cells. No toxicity in all the cell lines when VEGF is used. • ATP overexpression results to DOX-D release.	167

Table 3. *Continued.*

Strategy	Encapsulated entity	Surface functionalization	Surface functionalization approach	Biomedical application	Outcomes	Ref.
Targetability and selective internalization	• TMR-D • CdSe/ZnS QDs • MP-11	DNA crosslinked with anti-ATP	Electrostatic interactions	Cancer (*in vitro* with MDA-MB-231) – not extensive study	• Multiple cargo loaded. • ATP-responsive release.	168
	N/A	HuA33	Physical adsorption	Cancer (*in vitro* in LIM1215 cells)	• Cell binding and rapid internalization. • Nearly all cells contain one particle within their cytosol.	166
	Raltitrexed	Hyaluronic acid with raltitrexed	Electrostatic interactions	Cancer (*in vitro* in CT26 and *in vivo*)	• Higher directed uptake of HA containing capsules. • Radiation and capsules combination increase tumour inhibition.	169
	siRNA	Hyaluronic acid and CD20 marker	• HA: Electrostatic interactions • CD20: click chemistry	Cancer (*in vitro* and *in vivo* haematological BCL-2 protein silencing)	• Successful directed internalization. • BCL-2 downregulation and cell apoptosis induction.	118

Table 3. *Continued.*

Strategy	Encapsulated entity	Surface functionalization	Surface functionalization approach	Biomedical application	Outcomes	Ref.
Targetability and selective internalization	Docetaxel and an anionic porphyrin ($TPPS_4$)	Hyaluronic acid	Electrostatic interactions	Cancer (*in vitro* in MD4-MB-231 and MCF-7 cells lines)	• Higher capsule adsorption in MDA-MB-231 cells (higher CD44 marker expression). • Both drug combination enables improvement in cell killing.	171
	Upconversion nanoparticles sensitive to UV and TiO_2	Hyaluronic acid	Electrostatic interactions	Cancer (*in vivo* and *in vitro* studies in HeLa cell line)	• Cancer cell apoptosis triggered by 808 nm light irradiation.	170
Loading stability and stimulus-responsive release	Rhodamine-B	Silica	*In situ* nucleation based on the hydrolysis of TEOS	Controlled drug delivery (Neither *in vitro*, nor *in vivo*)	• Ultrasound-dependent Rhodamine-B release.	172
	Dextran	Titania	*In situ* nucleation based on the hydrolysis of TIBO	Controlled drug delivery (Neither *in vitro*, nor *in vivo*)	• UV and Ultrasound-dependent release of TRITC-Dextran.	176

Table 3. *Continued.*

Strategy	Encapsulated entity	Surface functionalization	Surface functionalization approach	Biomedical application	Outcomes	Ref.
Loading stability and stimulus-responsive release	Doxorubicin	Au nanorods	Electrostatic interactions	Cancer (*in vitro* with MCF-7 cells)	• Controlled release. • Dual responsiveness.	177
	Insulin	Vitamin B12	Vitamin B12 grafted on the chitosan electrolyte	Diabetes, oral delivery (*in vitro* with Caco-2 cells and *ex vivo*/*in vivo* in male Wistar rats)	• The VitB12 capsules enhance 4.3 folds the absorption of insulin. • Sustained hypoglycaemic effect for 12 h.	179
	Upconversion nanoparticles sensitive to NIR and therapeutic protein cytochrome c	Hyaluronic acid	Electrostatic interactions	Cancer (*in vitro* studies in HeLa and NIH3T3 cell lines)	• Tracking and delivery of capsules *via* NIR. • In presence of hyaluronidase, capsules release 96% of the cargo in 96 h.	180

Table 3. *Continued.*

Strategy	Encapsulated entity	Surface functionalization	Surface functionalization approach	Biomedical application	Outcomes	Ref.
Loading stability and stimulus-responsive release	Tirapazamine and $TPPS_4$	Hyaluronic acid	Electrostatic interactions	Cancer (*in vitro* studies in SCC-7, MCF-7 AND COS 7 cell lines)	• NIR/MR imaging and guiding capability. • In presence of hyaluronidase 50-60% cargo release in 12 h. • Specific uptake obtained thanks to CD44 overexpression.	181
	Doxorubicin	Silica	*In situ* nucleation based on the hydrolysis of TEOS and TESPT	Cancer (*in vitro* studies in HeLa cells)	• Negligible drug release without any stimuli (silica shell protection). • Ultrasound stimuli: 87% release in 120 s. • GSH presence: 71% release in 48 h.	174
Miscellaneous	N/A	Bacterial self-assembled proteins	Recrystallization on the outer surface	Biocompatibility (*in vitro* with MG-63 cells)	• Improved stability towards degradation.	182
	Glucosidase	Polydopamine	Surface polymerization of dopamine	(Neither *in vitro*, nor *in vivo*)	• Improved mechanical stability.	184

Table 3. *Continued.*

Strategy	Encapsulated entity	Surface functionalization	Surface functionalization approach	Biomedical application	Outcomes	Ref.
Miscellaneous	N/A	Liposomal formulation	Electrostatic interactions	Immunomodulation (*in vitro* with DCs)	• Enhanced DC activation.	185
	N/A	N/A	N/A	N/A	• Stability studies among several polyelectrolyte layers showed specific pairs being more suitable for the formation of LbL capsules.	186

2.5. Towards multifunctional capsules

As described along this introduction, the LbL fabrication method allows the functionalization of almost all the components that form the polymeric capsule, from the inner cavity/core to the outermost layer through the polymeric membrane. However, the single functionalization of only one of these parts may limit their capability to overcome the challenges involved in complex pathologies. Consequently, the functionalization of various parts of the polymer capsules needs to be considered when adjusting to the individual particularities of a patient. Thus, taking advantage of the versatility of LbL approach, many works have developed capsules combining multiple functionalities within their structure, obtaining multifunctional micro- and nanoplatforms for a synergistic treatment adapted to the particular characteristics of the pathology.[39,58,116,123,159,165,171,187-193]

Theranostic nano- and microcapsules are excellent examples of these multifunctional systems. They are capable of interweaving diagnosis and therapeutic functionalities in the same single system, combining in their architecture imaging probes with therapeutic agents to simultaneously track and treat the target site.[123] The use of these theranostic nano- and microplatforms is a useful tool in cancer therapy to gain information about the tumour progression and promote its shrinking while avoiding the so common off-target side effects.[39,88,116,123,189,191] Traditionally, to impart imaging and diagnosis functionalities to the capsules, a combination of nanoparticles, such as iron oxide or quantum dots with encapsulated chemotherapeutic drugs has been adopted.[88,188,191] However, other employed alternatives rely on the use of ultrasound detectable polyelectrolyte pairs or chelating agents bind to an isotope detectable *via* positron emission tomography (PET).[39,189] Using the latest approach, Kozlovskaya and collaborators fabricated PVPON/TA layered capsules containing in their shell deferoxamine (DFO) chelating agent capable of binding to ^{89}Zr isotope.[189] This isotope provided a good balance between longer-term imaging and spatial resolution, maintained for 7 days. Furthermore, thanks to the rational selection of the polyelectrolyte pair, they were capable of releasing the encapsulated DOX using ultrasounds, sufficient to deliver the drug, but not being detrimental for the patient.

Additionally, they demonstrated that they were able to track the accumulation of the capsules in the course of time and while the therapeutic agent was released. However, these systems that make use the above-mentioned imaging probes are only capable of giving useful visual information of the target site and monitoring the release of the chemotherapeutic agent. Hence, the group of P. Hammond went a step further and fabricated nanoparticles capable of obtaining information about precise pathological changes, thus obtaining more dynamic systems not only focused in the local image information provided by the aforementioned counterparts.[123] The developed nanoparticles which included on their outer layer a urinary biosensing peptide, were activated by matrix metalloproteinase-9 (MMP-9) that is overexpressed in tumours. Simultaneously, the nanoparticles were capable of releasing encapsulated siRNA obtaining a prolonged gene silencing.

An additional way to efficiently treat tumours relies on the combination of targeting ligands in the outer layer and encapsulated chemotherapeutics in the core, in the same multifunctional nano- or microcarrier.[165,171,187,193] Using targeting ligands such as antibodies, the fabricated capsules are capable of binding to biomarkers present in the tumour to obtain an active accumulation.[165,193] Moreover, apart from using only traditional chemotherapeutic agents, different photosensitizing agents can be included in the polymeric shell to obtain a synergistic treatment, which combines commonly used chemotherapy with photodynamic therapy (PDT) capable of inducing a higher cell apoptosis and necrosis.[171,187] As an example, Gaio *et al.* fabricated capsules with a core containing chemotherapeutic docetaxel (DTX), a photosensitizer retained between the layers and an outer HA layer capable of binding to specific receptors like the CD44 or RHAMM present in various tumours.[187] Thanks to the co-delivery of both therapeutic agents, a strong synergism between them that resulted in a significant reduction in cell viability, was observed.

Other pathologies in which the multifunctional systems could be useful are cardiovascular and haemolytic pathologies.[159,192] Here, different strategies can be used to build the architecture of the capsules, guide them to the target and simultaneously treat it, by releasing therapeutic agents such as the recombinant tissue plasminogen activator (rtPA) or pro-clotting agents.[159,192] One of these examples relies on the use of

the platelet system as the sensor and actuator for the treatment. Thus, using fibrinogen as an outer layer, Hansen and co-workers were capable of attaching to the surface of their capsules platelets which actuated as capsule disrupters in the presence of thrombin, a clotting activator.[159] Capsules were capable of releasing VIII factor to increase fibrin formation and decrease clotting time to treat pro-clotting factor deficiency in Haemophilia A pathologies.

Based on the vast bibliography discussed along this introduction, the present thesis pretends to explore alternative polymer capsule configurations to yield multifunctional microreactors capable of alleviating the oxidative stress found in the cellular microenvironment.

References

(1) Williams, D. F. *The Williams Dictionary of Biomaterials*; Liverpool University Press, 1999. https://doi.org/10.5949/upo9781846314438.

(2) Williams, D. F. On the Nature of Biomaterials. *Biomaterials* **2009**, *30* (30), 5897–5909. https://doi.org/10.1016/j.biomaterials.2009.07.027.

(3) Oliva, N.; Unterman, S.; Zhang, Y.; Conde, J.; Song, H. S.; Artzi, N. Personalizing Biomaterials for Precision Nanomedicine Considering the Local Tissue Microenvironment. *Adv. Healthc. Mater.* **2015**, *4* (11), 1584–1599. https://doi.org/10.1002/adhm.201400778.

(4) Zhang, X.; Zhou, J.; Gu, Z.; Zhang, H.; Gong, Q.; Luo, K. Advances in Nanomedicines for Diagnosis of Central Nervous System Disorders. *Biomaterials* **2021**, *269* (May 2020), 120492. https://doi.org/10.1016/j.biomaterials.2020.120492.

(5) Luo, C.; Sun, B.; Wang, C.; Zhang, X.; Chen, Y.; Chen, Q.; Yu, H.; Zhao, H.; Sun, M.; Li, Z.; Zhang, H.; Kan, Q.; Wang, Y.; He, Z.; Sun, J. Self-Facilitated ROS-Responsive Nanoassembly of Heterotypic Dimer for Synergistic Chemo-Photodynamic Therapy. *J. Control. Release* **2019**, *302* (April), 79–89. https://doi.org/10.1016/j.jconrel.2019.04.001.

(6) Wang, H.; Zhao, Y.; Wu, Y.; Hu, Y. lin; Nan, K.; Nie, G.; Chen, H. Enhanced Anti-Tumor Efficacy by Co-Delivery of Doxorubicin and Paclitaxel with Amphiphilic Methoxy PEG-PLGA Copolymer Nanoparticles. *Biomaterials* **2011**, *32* (32), 8281–8290. https://doi.org/10.1016/j.biomaterials.2011.07.032.

(7) Decher, G. Fuzzy Nanoassemblies: Toward Layered Polymeric Multicomposites. *Science (80-.).* **1997**, *277* (5330), 1232–1237. https://doi.org/10.1126/science.277.5330.1232.

(8) Donath, E.; Sukhorukov, G. B.; Caruso, F.; Davis, S. A.; Möhwald, H. Novel Hollow Polymer Shells by Colloid-Templated Assembly of Polyelectrolytes. *Angew. Chem. Int. Ed. Engl.* **1998**, *37* (16), 2201–2205.

(9) Larrañaga, A.; Lomora, M.; Sarasua, J. R.; Palivan, C. G.; Pandit, A. Polymer Capsules as Micro-/Nanoreactors for Therapeutic Applications: Current Strategies

to Control Membrane Permeability. *Prog. Mater. Sci.* **2017**, *90*, 325–357. https://doi.org/10.1016/j.pmatsci.2017.08.002.

(10) Chen, Y.; Lin, X. Studies on the Drug Release Properties of Nano-Encapsulated Indomethacin Microparticles. *J. Microencapsul.* **2005**, *22* (1), 47–55. https://doi.org/10.1080/02652040500044972.

(11) Ai, H.; Jones, S. A.; De Villiers, M. M.; Lvov, Y. M. Nano-Encapsulation of Furosemide Microcrystals for Controlled Drug Release. *J. Control. Release* **2003**, *86* (1), 59–68. https://doi.org/10.1016/S0168-3659(02)00322-X.

(12) Ye, S.; Wang, C.; Liu, X.; Tong, Z. Deposition Temperature Effect on Release Rate of Indomethacin Microcrystals from Microcapsules of Layer-by-Layer Assembled Chitosan and Alginate Multilayer Films. *J. Control. Release* **2005**, *106* (3), 319–328. https://doi.org/10.1016/j.jconrel.2005.05.006.

(13) Pargaonkar, N.; Lvov, Y. M.; Li, N.; Steenekamp, J. H.; De Villiers, M. M. Controlled Release of Dexamethasone from Microcapsules Produced by Polyelectrolyte Layer-by-Layer Nanoassembly. *Pharm. Res.* **2005**, *22* (5), 826–835. https://doi.org/10.1007/s11095-005-2600-0.

(14) Agarwal, A.; Lvov, Y.; Sawant, R.; Torchilin, V. Stable Nanocolloids of Poorly Soluble Drugs with High Drug Content Prepared Using the Combination of Sonication and Layer-by-Layer Technology. *J. Control. Release* **2008**, *128* (3), 255–260. https://doi.org/10.1016/j.jconrel.2008.03.017.

(15) Yu, X.; Pishko, M. V. Nanoparticle-Based Biocompatible and Targeted Drug Delivery: Characterization and in Vitro Studies. *Biomacromolecules* **2011**, *12* (9), 3205–3212. https://doi.org/10.1021/bm200681m.

(16) Santos, A. C.; Pattekari, P.; Jesus, S.; Veiga, F.; Lvov, Y.; Ribeiro, A. J. Sonication-Assisted Layer-by-Layer Assembly for Low Solubility Drug Nanoformulation. *ACS Appl. Mater. Interfaces* **2015**, *7* (22), 11972–11983. https://doi.org/10.1021/acsami.5b02002.

(17) Zheng, Z.; Zhang, X.; Carbo, D.; Clark, C.; Nathan, C. A.; Lvov, Y. Sonication-Assisted Synthesis of Polyelectrolyte-Coated Curcumin Nanoparticles. *Langmuir* **2010**, *26* (11), 7679–7681. https://doi.org/10.1021/la101246a.

(18) Pattekari, P.; Zheng, Z.; Zhang, X.; Levchenko, T.; Torchilin, V.; Lvov, Y. Top-down and Bottom-up Approaches in Production of Aqueous Nanocolloids of Low Solubility Drug Paclitaxel. *Phys. Chem. Chem. Phys.* **2011**, *13* (19), 9014–9019. https://doi.org/10.1039/c0cp02549f.

(19) Zahr, A. S.; De Villiers, M.; Pishko, M. V. Encapsulation of Drug Nanoparticles in Self-Assembled Macromolecular Nanoshells. *Langmuir* **2005**, *21* (1), 403–410. https://doi.org/10.1021/la0478595.

(20) Zahr, A. S.; Pishko, M. V. Encapsulation of Paclitaxel in Macromolecular Nanoshells. *Biomacromolecules* **2007**, *8* (6), 2004–2010. https://doi.org/10.1021/bm070177m.

(21) Chen, Y.; Lin, X.; Park, H.; Greever, R. Study of Artemisinin Nanocapsules as Anticancer Drug Delivery Systems. *Nanomedicine Nanotechnology, Biol. Med.* **2009**, *5* (3), 316–322. https://doi.org/10.1016/j.nano.2008.12.005.

(22) Shutava, T. G.; Pattekari, P. P.; Arapov, K. A.; Torchilin, V. P.; Lvov, Y. M. Architectural Layer-by-Layer Assembly of Drug Nanocapsules with PEGylated Polyelectrolytes. *Soft Matter* **2012**, *8* (36), 9418–9427. https://doi.org/10.1039/c2sm25683e.

(23) Parekh, G.; Pattekari, P.; Joshi, C.; Shutava, T.; DeCoster, M.; Levchenko, T.; Torchilin, V.; Lvov, Y. Layer-by-Layer Nanoencapsulation of Camptothecin with Improved Activity. *Int. J. Pharm.* **2014**, *465* (1–2), 218–227. https://doi.org/10.1016/j.ijpharm.2014.01.041.

(24) Polomska, A.; Gauthier, M. A.; Leroux, J. C. In Vitro and In Vivo Evaluation of PEGylated Layer-by-Layer Polyelectrolyte-Coated Paclitaxel Nanocrystals. *Small* **2017**, *13* (2), 1–12. https://doi.org/10.1002/smll.201602066.

(25) Oshi, M. A.; Lee, J.; Naeem, M.; Hasan, N.; Kim, J.; Kim, H. J.; Lee, E. H.; Jung, Y.; Yoo, J. W. Curcumin Nanocrystal/PH-Responsive Polyelectrolyte Multilayer Core-Shell Nanoparticles for Inflammation-Targeted Alleviation of Ulcerative Colitis. *Biomacromolecules* **2020**, *21* (9), 3571–3581. https://doi.org/10.1021/acs.biomac.0c00589.

(26) Dai, Z.; Heilig, A.; Zastrow, H.; Donath, E.; Möhwald, H. Novel Formulations of

Vitamins and Insulin by Nanoengineering of Polyelectrolyte Multilayers around Microcrystals. *Chem. - A Eur. J.* **2004**, *10* (24), 6369–6374. https://doi.org/10.1002/chem.200400579.

(27) Song, L.; Zhi, Z. L.; Pickup, J. C. Nanolayer Encapsulation of Insulin- Chitosan Complexes Improves Efficiency of Oral Insulin Delivery. *Int. J. Nanomedicine* **2014**, *9* (1), 2127–2136. https://doi.org/10.2147/IJN.S59075.

(28) Fan, Y. F.; Wang, Y. N.; Fan, Y. G.; Ma, J. B. Preparation of Insulin Nanoparticles and Their Encapsulation with Biodegradable Polyelectrolytes *via* the Layer-by-Layer Adsorption. *Int. J. Pharm.* **2006**, *324* (2), 158–167. https://doi.org/10.1016/j.ijpharm.2006.05.062.

(29) Pechenkin, M. A.; Balabushevich, N. G.; Zorov, I. N.; Izumrudov, V. A.; Klyachko, N. L.; Kabanov, A. V.; Larionova, N. I. Use of Protease Inhibitors in Composite Polyelectrolyte Microparticles in Order to Increase the Bioavailability of Perorally Administered Encapsulated Proteins. *Pharm. Chem. J.* **2013**, *47* (1), 62–69. https://doi.org/10.1007/s11094-013-0898-1.

(30) Amancha, K. P.; Balkundi, S.; Lvov, Y.; Hussain, A. Pulmonary Sustained Release of Insulin from Microparticles Composed of Polyelectrolyte Layer-by-Layer Assembly. *Int. J. Pharm.* **2014**, *466* (1–2), 96–108. https://doi.org/10.1016/j.ijpharm.2014.02.006.

(31) Balabushevitch, N. G.; Sukhorukov, G. B.; Moroz, N. A.; Volodkin, D. V.; Larionova, N. I.; Donath, E.; Mohwald, H. Encapsulation of Proteins by Layer-by-Layer Adsorption of Polyelectrolytes onto Protein Aggregates: Factors Regulating the Protein Release. *Biotechnol. Bioeng.* **2001**, *76* (3), 207–213. https://doi.org/10.1002/bit.1184.

(32) Caruso, F.; Trau, D.; Möhwald, H.; Renneberg, R. Enzyme Encapsulation in Layer-by-Layer Engineered Polymer Multilayer Capsules. *Langmuir* **2000**, *16* (4), 1485–1488. https://doi.org/10.1021/la991161n.

(33) Jin, W.; Shi, X.; Caruso, F. High Activity Enzyme Microcrystal Multilayer Films [3]. *J. Am. Chem. Soc.* **2001**, *123* (33), 8121–8122. https://doi.org/10.1021/ja015807l.

(34) Yut, A.; Caruso, F. Thin Films of Polyelectrolyte-Encapsulated Catalase

Microcrystals for Biosensing. *Anal. Chem.* **2003**, *75* (13), 3031–3037. https://doi.org/10.1021/ac0340049.

(35) Trau, D.; Renneberg, R. Encapsulation of Glucose Oxidase Microparticles within a Nanoscale Layer-by-Layer Film: Immobilization and Biosensor Applications. *Biosens. Bioelectron.* **2003**, *18* (12), 1491–1499. https://doi.org/10.1016/S0956-5663(03)00119-2.

(36) Kudryavtseva, V.; Boi, S.; Read, J.; Gould, D.; Szewczyk, P. K.; Stachewicz, U.; Kiryukhin, M. V.; Pastorino, L.; Sukhorukov, G. B. Micro-Sized "Pelmeni" - A Universal Microencapsulation Approach Overview. *Mater. Des.* **2021**, *202*, 109527. https://doi.org/10.1016/j.matdes.2021.109527.

(37) Kudryavtseva, V.; Boi, S.; Read, J.; Guillemet, R.; Zhang, J.; Udalov, A.; Shesterikov, E.; Tverdokhlebov, S.; Pastorino, L.; Gould, D. J.; Sukhorukov, G. B. Biodegradable Defined Shaped Printed Polymer Microcapsules for Drug Delivery. *ACS Appl. Mater. Interfaces* **2021**, *13* (2), 2371–2381. https://doi.org/10.1021/acsami.0c21607.

(38) Wang, Y.; Yan, Y.; Cui, J.; Hosta-Rigau, L.; Heath, J. K.; Nice, E. C.; Caruso, F. Encapsulation of Water-Insoluble Drugs in Polymer Capsules Prepared Using Mesoporous Silica Templates for Intracellular Drug Delivery. *Adv. Mater.* **2010**, *22* (38), 4293–4297. https://doi.org/10.1002/adma.201001497.

(39) Chen, J.; Ratnayaka, S.; Alford, A.; Kozlovskaya, V.; Liu, F.; Xue, B.; Hoyt, K.; Kharlampieva, E. Theranostic Multilayer Capsules for Ultrasound Imaging and Guided Drug Delivery. *ACS Nano* **2017**, *11* (3), 3135–3146. https://doi.org/10.1021/acsnano.7b00151.

(40) Chaudhary, Z.; Khan, G. M.; Abeer, M. M.; Pujara, N.; Wan-Chi Tse, B.; McGuckin, M. A.; Popat, A.; Kumeria, T. Efficient Photoacoustic Imaging Using Indocyanine Green (ICG) Loaded Functionalized Mesoporous Silica Nanoparticles. *Biomater. Sci.* **2019**, *7* (12), 5002–5015. https://doi.org/10.1039/c9bm00822e.

(41) Chen, S.; McClements, D. J.; Jian, L.; Han, Y.; Dai, L.; Mao, L.; Gao, Y. Core-Shell Biopolymer Nanoparticles for Co-Delivery of Curcumin and Piperine: Sequential Electrostatic Deposition of Hyaluronic Acid and Chitosan Shells on the Zein Core.

ACS Appl. Mater. Interfaces **2019**, *11* (41), 38103–38115. https://doi.org/10.1021/acsami.9b11782.

(42) Chen, S.; McClements, D. J.; Jian, L.; Han, Y.; Dai, L.; Mao, L.; Gao, Y.; Huang, J.; Dai, L.; Du, J.; McClements, D. J.; Mao, L.; Liu, J.; Gao, Y. Fabrication and Characterization of Layer-by-Layer Composite Nanoparticles Based on Zein and Hyaluronic Acid for Codelivery of Curcumin and Quercetagetin. *ACS Appl. Mater. Interfaces* **2019**, *11* (18), 38103–38115. https://doi.org/10.1021/acsami.9b02529.

(43) Zelikin, A. N.; Becker, A. L.; Johnston, A. P. R.; Wark, K. L.; Turatti, F.; Caruso, F. A General Approach for DNA Encapsulation in Degradable Polymer Microcapsules. *ACS Nano* **2007**, *1* (1), 63–69. https://doi.org/10.1021/nn700063w.

(44) Price, A. D.; Zelikin, A. N.; Wang, Y.; Caruso, F. Triggered Enzymatic Degradation of DNA within Selectively Permeable Polymer Capsule Microreactors. *Angew. Chemie - Int. Ed.* **2009**, *48* (2), 329–332. https://doi.org/10.1002/anie.200804763.

(45) Li, L.; Puhl, S.; Meinel, L.; Germershaus, O. Silk Fibroin Layer-by-Layer Microcapsules for Localized Gene Delivery. *Biomaterials* **2014**, *35* (27), 7929–7939. https://doi.org/10.1016/j.biomaterials.2014.05.062.

(46) Donatan, S.; Yashchenok, A.; Khan, N.; Parakhonskiy, B.; Cocquyt, M.; Pinchasik, B. El; Khalenkow, D.; Möhwald, H.; Konrad, M.; Skirtach, A. Loading Capacity versus Enzyme Activity in Anisotropic and Spherical Calcium Carbonate Microparticles. *ACS Appl. Mater. Interfaces* **2016**, *8* (22), 14284–14292. https://doi.org/10.1021/acsami.6b03492.

(47) Zyuzin, M. V.; Cassani, M.; Barthel, M. J.; Gavilan, H.; Silvestri, N.; Escudero, A.; Scarpellini, A.; Lucchesi, F.; Teran, F. J.; Parak, W. J.; Pellegrino, T. Confining Iron Oxide Nanocubes inside Submicrometric Cavities as a Key Strategy to Preserve Magnetic Heat Losses in an Intracellular Environment. *ACS Appl. Mater. Interfaces* **2019**, *11* (45), 41957–41971. https://doi.org/10.1021/acsami.9b15501.

(48) Sharma, V.; Vijay, J.; Ganesh, M. R.; Sundaramurthy, A. Multilayer Capsules Encapsulating Nimbin and Doxorubicin for Cancer Chemo-Photothermal Therapy. *Int. J. Pharm.* **2020**, *582* (April), 119350.

https://doi.org/10.1016/j.ijpharm.2020.119350.

(49) Ashraf, S.; Taylor, A.; Sharkey, J.; Barrow, M.; Murray, P.; Wilm, B.; Poptani, H.; Rosseinsky, M. J.; Adams, D. J.; Lévy, R. *In Vivo* Fate of Free and Encapsulated Iron Oxide Nanoparticles after Injection of Labelled Stem Cells. *Nanoscale Adv.* **2019**, *1* (1), 367–377. https://doi.org/10.1039/c8na00098k.

(50) She, Z.; Wang, C.; Li, J.; Sukhorukov, G. B.; Antipina, M. N. Encapsulation of Basic Fibroblast Growth Factor by Polyelectrolyte Multilayer Microcapsules and Its Controlled Release for Enhancing Cell Proliferation. *Biomacromolecules* **2012**, *13* (7), 2174–2180. https://doi.org/10.1021/bm3005879.

(51) Kopach, O.; Pavlov, A. M.; Sindeeva, O. A.; Sukhorukov, G. B.; Rusakov, D. A. Biodegradable Microcapsules Loaded with Nerve Growth Factor Enable Neurite Guidance and Synapse Formation. *Pharmaceutics* **2021**, *13* (1), 1–15. https://doi.org/10.3390/pharmaceutics13010025.

(52) Larrañaga, A.; Isa, I. L. M.; Patil, V.; Thamboo, S.; Lomora, M.; Fernández-Yague, M. A.; Sarasua, J. R.; Palivan, C. G.; Pandit, A. Antioxidant Functionalized Polymer Capsules to Prevent Oxidative Stress. *Acta Biomater.* **2018**, *67*, 21–31. https://doi.org/10.1016/j.actbio.2017.12.014.

(53) Karamitros, C. S.; Yashchenok, A. M.; Möhwald, H.; Skirtach, A. G.; Konrad, M. Preserving Catalytic Activity and Enhancing Biochemical Stability of the Therapeutic Enzyme Asparaginase by Biocompatible Multilayered Polyelectrolyte Microcapsules. *Biomacromolecules* **2013**, *14* (12), 4398–4406. https://doi.org/10.1021/bm401341k.

(54) Tarakanchikova, Y. V.; Linnik, D. S.; Mashel, T.; Muslimov, A. R.; Pavlov, S.; Lepik, K. V.; Zyuzin, M. V.; Sukhorukov, G. B.; Timin, A. S. Boosting Transfection Efficiency: A Systematic Study Using Layer-by-Layer Based Gene Delivery Platform. *Mater. Sci. Eng. C* **2021**, *126* (April), 112161. https://doi.org/10.1016/j.msec.2021.112161.

(55) Kakran, M.; Muratani, M.; Tng, W. J.; Liang, H.; Trushina, D. B.; Sukhorukov, G. B.; Ng, H. H.; Antipina, M. N. Layered Polymeric Capsules Inhibiting the Activity of RNases for Intracellular Delivery of Messenger RNA. *J. Mater. Chem. B* **2015**, *3*

(28), 5842–5848. https://doi.org/10.1039/c5tb00615e.

(56) Zyuzin, M. V.; Antuganov, D.; Tarakanchikova, Y. V.; Karpov, T. E.; Mashel, T. V.; Gerasimova, E. N.; Peltek, O. O.; Alexandre, N.; Bruyere, S.; Kondratenko, Y. A.; Muslimov, A. R.; Timin, A. S. Radiolabeling Strategies of Micron- And Submicron-Sized Core-Shell Carriers for *in vivo* Studies. *ACS Appl. Mater. Interfaces* **2020**, *12* (28), 31137–31147. https://doi.org/10.1021/acsami.0c06996.

(57) German, S. V.; Novoselova, M. V.; Bratashov, D. N.; Demina, P. A.; Atkin, V. S.; Voronin, D. V.; Khlebtsov, B. N.; Parakhonskiy, B. V.; Sukhorukov, G. B.; Gorin, D. A. High-Efficiency Freezing-Induced Loading of Inorganic Nanoparticles and Proteins into Micron- and Submicron-Sized Porous Particles. *Sci. Rep.* **2018**, *8* (1), 1–10. https://doi.org/10.1038/s41598-018-35846-x.

(58) Novoselova, M. V.; Voronin, D. V.; Abakumova, T. O.; Demina, P. A.; Petrov, A. V.; Petrov, V. V.; Zatsepin, T. S.; Sukhorukov, G. B.; Gorin, D. A. Focused Ultrasound-Mediated Fluorescence of Composite Microcapsules Loaded with Magnetite Nanoparticles: In Vitro and in Vivo Study. *Colloids Surfaces B Biointerfaces* **2019**, *181* (June), 680–687. https://doi.org/10.1016/j.colsurfb.2019.06.025.

(59) Brkovic, N.; Zhang, L.; Peters, J. N.; Kleine-Doepke, S.; Parak, W. J.; Zhu, D. Quantitative Assessment of Endosomal Escape of Various Endocytosed Polymer-Encapsulated Molecular Cargos upon Photothermal Heating. *Small* **2020**, *16* (46), 1–18. https://doi.org/10.1002/smll.202003639.

(60) Son, K. J.; Yoon, H. J.; Kim, J. H.; Jang, W. D.; Lee, Y.; Koh, W. G. Photosensitizing Hollow Nanocapsules for Combination Cancer Therapy. *Angew. Chemie - Int. Ed.* **2011**, *50* (50), 11968–11971. https://doi.org/10.1002/anie.201102658.

(61) Trushina, D. B.; Akasov, R. A.; Khovankina, A. V.; Borodina, T. N.; Bukreeva, T. V.; Markvicheva, E. A. Doxorubicin-Loaded Biodegradable Capsules: Temperature Induced Shrinking and Study of Cytotoxicity in Vitro. *J. Mol. Liq.* **2019**, *284*, 215–224. https://doi.org/10.1016/j.molliq.2019.03.152.

(62) Novoselova, M. V.; Loh, H. M.; Trushina, D. B.; Ketkar, A.; Abakumova, T. O.; Zatsepin, T. S.; Kakran, M.; Brzozowska, A. M.; Lau, H. H.; Gorin, D. A.; Antipina, M. N.; Brichkina, A. I. Biodegradable Polymeric Multilayer Capsules for Therapy of

Lung Cancer. *ACS Appl. Mater. Interfaces* **2020**, *12* (5), 5610–5623. https://doi.org/10.1021/acsami.9b21381.

(63) Mandapalli, P. K.; Labala, S.; Vanamala, D.; Koranglekar, M. P.; Sakimalla, L. A.; Venuganti, V. V. K. Influence of Charge on Encapsulation and Release Behavior of Small Molecules in Self-Assembled Layer-by-Layer Microcapsules. *Drug Deliv.* **2014**, *21* (8), 605–614. https://doi.org/10.3109/10717544.2013.867381.

(64) Sivakumar, S.; Bansal, V.; Cortez, C.; Chong, S. F.; Zelikin, A. N.; Caruso, F. Degradable, Surfactant-Free, Monodisperse Polymer-Encapsulated Emulsions as Anticancer Drug Carriers. *Adv. Mater.* **2009**, *21* (18), 1820–1824. https://doi.org/10.1002/adma.200802475.

(65) Liu, X.; Gao, C.; Shen, J.; Möhwald, H. Multilayer Microcapsules as Anti-Cancer Drug Delivery Vehicle: Deposition, Sustained Release, and in Vitro Bioactivity. *Macromol. Biosci.* **2005**, *5* (12), 1209–1219. https://doi.org/10.1002/mabi.200500176.

(66) Gao, C.; Donath, E.; Möhwald, H.; Shen, J. Spontaneous Deposition of Water-Soluble Substances into Microcapsules: Phenomenon, Mechanism, and Application. *Angew. Chemie* **2002**, *114* (20), 3943–3947. https://doi.org/10.1002/1521-3757(20021018)114:20<3943::aid-ange3943>3.0.co;2-k.

(67) Gao, C.; Liu, X.; Shen, J.; Möhwald, H. Spontaneous Deposition of Horseradish Peroxidase into Polyelectrolyte Multilayer Capsules to Improve Its Activity and Stability. *Chem. Commun.* **2002**, *1* (17), 1928–1929. https://doi.org/10.1039/b204583d.

(68) Zhao, Q.; Zhang, S.; Tong, W.; Gao, C.; Shen, J. Polyelectrolyte Microcapsules Templated on Poly(Styrene Sulfonate)-Doped $CaCO_3$ Particles for Loading and Sustained Release of Daunorubicin and Doxorubicin. *Eur. Polym. J.* **2006**, *42* (12), 3341–3351. https://doi.org/10.1016/j.eurpolymj.2006.09.005.

(69) De Cock, L. J.; De Wever, O.; Van Vlierberghe, S.; Vanderleyden, E.; Dubruel, P.; De Vos, F.; Vervaet, C.; Remon, J. P.; De Geest, B. G. Engineered (Hep/PARG) 2 Polyelectrolyte Capsules for Sustained Release of Bioactive TGF-B1. *Soft Matter*

2012, *8* (4), 1146–1154. https://doi.org/10.1039/c1sm06618h.

(70) Kurapati, R.; Raichur, A. M. Composite Cyclodextrin-Calcium Carbonate Porous Microparticles and Modified Multilayer Capsules: Novel Carriers for Encapsulation of Hydrophobic Drugs. *J. Mater. Chem. B* **2013**, *1* (25), 3175–3184. https://doi.org/10.1039/c3tb20192a.

(71) Becker, A. L.; Orlotti, N. I.; Folini, M.; Cavalieri, F.; Zelikin, A. N.; Johnston, A. P. R.; Zaffaroni, N.; Caruso, F. Redox-Active Polymer Microcapsules for the Delivery of a Survivin-Specific siRNA in Prostate Cancer Cells. *ACS Nano* **2011**, *5* (2), 1335–1344. https://doi.org/10.1021/nn103044z.

(72) Ibarz, G.; Dähne, L.; Donath, E.; Möhwald, H. Smart Micro- and Nanocontainers for Storage, Transport, and Release. *Adv. Mater.* **2001**, *13* (17), 1324–1327. https://doi.org/10.1002/1521-4095(200109)13:17<1324::AID-ADMA1324>3.0.CO;2-L.

73) Itoh, Y.; Matsusaki, M.; Kida, T.; Akashi, M. Locally Controlled Release of Basic Fibroblast Growth Factor from Multilayered Capsules. *Biomacromolecules* **2008**, *9* (8), 2202–2206. https://doi.org/10.1021/bm800321w.

(74) Balabushevich, N. G.; Tiourina, O. P.; Volodkin, D. V.; Larionova, N. I.; Sukhorukov, G. B. Loading the Multilayer Dextran Sulfate/Protamine Microsized Capsules with Peroxidase. *Biomacromolecules* **2003**, *4* (5), 1191–1197. https://doi.org/10.1021/bm0340321.

(75) Lvov, Y.; Antipov, A. A.; Mamedov, A.; Möhwald, H.; Sukhorukov, G. B. Urease Encapsulation in Nanoorganized Microshells. *Nano Lett.* **2001**, *1* (3), 125–128. https://doi.org/10.1021/nl0100015.

(76) She, Z.; Antipina, M. N.; Li, J.; Sukhorukov, G. B. Mechanism of Protein Release from Polyelectrolyte Multilayer Microcapsules. *Biomacromolecules* **2010**, *11* (5), 1241–1247. https://doi.org/10.1021/bm901450r.

(77) Timin, A. S.; Muslimov, A. R.; Petrova, A. V.; Lepik, K. V.; Okilova, M. V.; Vasin, A. V.; Afanasyev, B. V.; Sukhorukov, G. B. Hybrid Inorganic-Organic Capsules for Eficient Intracellular Delivery of Novel siRNAs against Influenza A (H1N1) Virus Infection. *Sci. Rep.* **2017**, *7* (1), 1–12. https://doi.org/10.1038/s41598-017-00200-

0.

(78) von Montfort, C.; Alili, L.; Teuber-Hanselmann, S.; Brenneisen, P. Redox-Active Cerium Oxide Nanoparticles Protect Human Dermal Fibroblasts from PQ-Induced Damage. *Redox Biol.* **2015**, *4*, 1–5. https://doi.org/10.1016/j.redox.2014.11.007.

(79) Navolokin, N. A.; German, S. V.; Bucharskaya, A. B.; Godage, O. S.; Zuev, V. V.; Maslyakova, G. N.; Pyataev, N. A.; Zamyshliaev, P. S.; Zharkov, M. N.; Terentyuk, G. S.; Gorin, D. A.; Sukhorukov, G. B. Systemic Administration of Polyelectrolyte Microcapsules: Where Do They Accumulate and When? *In vivo* and *ex vivo* Study. *Nanomaterials* **2018**, *8* (10), 1–14. https://doi.org/10.3390/nano8100812.

(80) Yi, Q.; Li, D.; Lin, B.; Pavlov, A. M.; Luo, D.; Gong, Q.; Song, B.; Ai, H.; Sukhorukov, G. B. Magnetic Resonance Imaging for Monitoring of Magnetic Polyelectrolyte Capsule *in vivo* Delivery. *Bionanoscience* **2014**, *4* (1), 59–70. https://doi.org/10.1007/s12668-013-0117-2.

(81) German, S. V.; Bratashov, D. N.; Navolokin, N. A.; Kozlova, A. A.; Lomova, M. V.; Novoselova, M. V.; Burilova, E. A.; Zyev, V. V.; Khlebtsov, B. N.; Bucharskaya, A. B.; Terentyuk, G. S.; Amirov, R. R.; Maslyakova, G. N.; Sukhorukov, G. B.; Gorin, D. A. *In vitro* and *in vivo* MRI Visualization of Nanocomposite Biodegradable Microcapsules with Tunable Contrast. *Phys. Chem. Chem. Phys.* **2016**, *18* (47), 32238–32246. https://doi.org/10.1039/C6CP03895F.

(82) Carregal-Romero, S.; Guardia, P.; Yu, X.; Hartmann, R.; Pellegrino, T.; Parak, W. J. Magnetically Triggered Release of Molecular Cargo from Iron Oxide Nanoparticle Loaded Microcapsules. *Nanoscale* **2015**, *7* (2), 570–576. https://doi.org/10.1039/c4nr04055d.

(83) Stavarache, C. E.; Paniwnyk, L. Controlled Rupture of Magnetic LbL Polyelectrolyte Capsules and Subsequent Release of Contents Employing High Intensity Focused Ultrasound. *J. Drug Deliv. Sci. Technol.* **2018**, *45* (November 2017), 60–69. https://doi.org/10.1016/j.jddst.2018.02.011.

(84) Luo, D.; Poston, R. N.; Gould, D. J.; Sukhorukov, G. B. Magnetically Targetable Microcapsules Display Subtle Changes in Permeability and Drug Release in Response to a Biologically Compatible Low Frequency Alternating Magnetic Field.

Mater. Sci. Eng. C **2019**, *94*, 647–655. https://doi.org/10.1016/j.msec.2018.10.031.

(85) Voronin, D. V.; Sindeeva, O. A.; Kurochkin, M. A.; Mayorova, O.; Fedosov, I. V.; Semyachkina-Glushkovskaya, O.; Gorin, D. A.; Tuchin, V. V.; Sukhorukov, G. B. *In vitro* and *in vivo* Visualization and Trapping of Fluorescent Magnetic Microcapsules in a Bloodstream. *ACS Appl. Mater. Interfaces* **2017**, *9* (8), 6885–6893. https://doi.org/10.1021/acsami.6b15811.

(86) Cristofolini, L.; Szczepanowicz, K.; Orsi, D.; Rimoldi, T.; Albertini, F.; Warszynski, P. Hybrid Polyelectrolyte/Fe_3O_4 Nanocapsules for Hyperthermia Applications. *ACS Appl. Mater. Interfaces* **2016**, *8* (38), 25043–25050. https://doi.org/10.1021/acsami.6b05917.

(87) Deng, L.; Li, Q.; Al-Rehili, S.; Omar, H.; Almalik, A.; Alshamsan, A.; Zhang, J.; Khashab, N. M. Hybrid Iron Oxide-Graphene Oxide-Polysaccharides Microcapsule: A Micro-Matryoshka for On-Demand Drug Release and Antitumor Therapy in Vivo. *ACS Appl. Mater. Interfaces* **2016**, *8* (11), 6859–6868. https://doi.org/10.1021/acsami.6b00322.

(88) Novoselova, M. V.; German, S. V.; Abakumova, T. O.; Perevoschikov, S. V.; Sergeeva, O. V.; Nesterchuk, M. V.; Efimova, O. I.; Petrov, K. S.; Chernyshev, V. S.; Zatsepin, T. S.; Gorin, D. A. Multifunctional Nanostructured Drug Delivery Carriers for Cancer Therapy: Multimodal Imaging and Ultrasound-Induced Drug Release. *Colloids Surfaces B Biointerfaces* **2021**, *200* (September 2020), 111576. https://doi.org/10.1016/j.colsurfb.2021.111576.

(89) Guo, C.; Wang, J.; Dai, Z. Selective Content Release from Light-Responsive Microcapsules by Tuning the Surface Plasmon Resonance of Gold Nanorods. *Microchim. Acta* **2011**, *173* (3–4), 375–382. https://doi.org/10.1007/s00604-011-0570-y.

(90) Shao, J.; Xuan, M.; Si, T.; Dai, L.; He, Q. Biointerfacing Polymeric Microcapsules for in Vivo Near-Infrared Light-Triggered Drug Release. *Nanoscale* **2015**, *7* (45), 19092–19098. https://doi.org/10.1039/c5nr06350g.

(91) Xu, S.; Shi, J.; Feng, D.; Yang, L.; Cao, S. Hollow Hierarchical

Hydroxyapatite/Au/Polyelectrolyte Hybrid Microparticles for Multi-Responsive Drug Delivery. *J. Mater. Chem. B* **2014**, *20* (38), 6500–6507. https://doi.org/10.1039/c4tb01066c.

(92) Guo, C.; Wang, J.; Dai, Z.; Javiern, A. M.; Del Pino, P.; Bedard, M. F.; Ho, D.; Skirtach, A. G.; Sukhorukov, G. B.; Plank, C.; Parak, W. J.; Shao, J.; Xuan, M.; Si, T.; Dai, L.; He, Q.; Pavlov, A. M.; Saez, V.; Cobley, A.; Graves, J.; Sukhorukov, G. B.; Mason, T. J. Controlled Protein Release from Microcapsules with Composite Shells Using High Frequency Ultrasound - Potential for *in vivo* Medical Use. *Soft Matter* **2011**, *7* (3–4), 4341–4347. https://doi.org/10.1021/la802448z.

(93) Javier, A. M.; Del Pino, P.; Bedard, M. F.; Ho, D.; Skirtach, A. G.; Sukhorukov, G. B.; Plank, C.; Parak, W. J. Photoactivated Release of Cargo from the Cavity of Polyelectrolyte Capsules to the Cytosol of Cells. *Langmuir* **2008**, *24* (21), 12517–12520. https://doi.org/10.1021/la802448z.

(94) Del Mercato, L. L.; Ferraro, M. M.; Baldassarre, F.; Mancarella, S.; Greco, V.; Rinaldi, R.; Leporatti, S. Biological Applications of LbL Multilayer Capsules: From Drug Delivery to Sensing. *Adv. Colloid Interface Sci.* **2014**, *207* (1), 139–154. https://doi.org/10.1016/j.cis.2014.02.014.

(95) Luo, G. F.; Xu, X. D.; Zhang, J.; Yang, J.; Gong, Y. H.; Lei, Q.; Jia, H. Z.; Li, C.; Zhuo, R. X.; Zhang, X. Z. Encapsulation of an Adamantane-Doxorubicin Prodrug in pH-Responsive Polysaccharide Capsules for Controlled Release. *ACS Appl. Mater. Interfaces* **2012**, *4* (10), 5317–5324. https://doi.org/10.1021/am301258a.

(96) Chen, J.; Wang, D.; Xi, J.; Au, L.; Siekkinen, A.; Warsen, A.; Li, Z. Y.; Zhang, H.; Xia, Y.; Li, X. Immuno Gold Nanocages with Tailored Optical Properties for Targeted Photothermal Destruction of Cancer Cells. *Nano Lett.* **2007**, *7* (5), 1318–1322. https://doi.org/10.1021/nl070345g.

(97) Von Maltzahn, G.; Park, J. H.; Agrawal, A.; Bandaru, N. K.; Das, S. K.; Sailor, M. J.; Bhatia, S. N. Computationally Guided Photothermal Tumor Therapy Using Long-Circulating Gold Nanorod Antennas. *Cancer Res.* **2009**, *69* (9), 3892–3900. https://doi.org/10.1158/0008-5472.CAN-08-4242.

(98) Hainfeld, J. F.; Lin, L.; Slatkin, D. N.; Avraham Dilmanian, F.; Vadas, T. M.;

Smilowitz, H. M. Gold Nanoparticle Hyperthermia Reduces Radiotherapy Dose. *Nanomedicine Nanotechnology, Biol. Med.* **2014**, *10* (8), 1609–1617. https://doi.org/10.1016/j.nano.2014.05.006.

(99) Neshastehriz, A.; Tabei, M.; Maleki, S.; Eynali, S.; Shakeri-Zadeh, A. Photothermal Therapy Using Folate Conjugated Gold Nanoparticles Enhances the Effects of 6 MV X-Ray on Mouth Epidermal Carcinoma Cells. *J. Photochem. Photobiol. B Biol.* **2017**, *172* (January), 52–60. https://doi.org/10.1016/j.jphotobiol.2017.05.012.

(100) Jiang, Y.; Yang, D.; Zhang, L.; Sun, Q.; Sun, X.; Li, J.; Jiang, Z. Preparation of Protamine-Titania Microcapsules through Synergy between Layer-by-Layer Assembly and Biomimetic Mineralization. *Adv. Funct. Mater.* **2009**, *19* (1), 150–156. https://doi.org/10.1002/adfm.200800974.

(101) Caruso, F.; Caruso, R. A.; Möhwald, H. Nanoengineering of Inorganic and Hybrid Hollow Spheres by Colloidal Templating. *Science (80-.).* **1998**, *282* (5391), 1111–1114. https://doi.org/10.1126/science.282.5391.1111.

(102) Wang, D.; Rogach, A. L.; Caruso, F. Semiconductor Quantum Dot-Labeled Microsphere Bioconjugates Prepared by Stepwise Self-Assembly. *Nano Lett.* **2002**, *2* (8), 857–861. https://doi.org/10.1021/nl025624c.

(103) Popov, A. L.; Popova, N.; Gould, D. J.; Shcherbakov, A. B.; Sukhorukov, G. B.; Ivanov, V. K. Ceria Nanoparticles-Decorated Microcapsules as a Smart Drug Delivery/Protective System: Protection of Encapsulated P. Pyralis Luciferase. *ACS Appl. Mater. Interfaces* **2018**, *10* (17), 14367–14377. https://doi.org/10.1021/acsami.7b19658.

(104) Popov, A. L.; Popova, N. R.; Tarakina, N. V.; Ivanova, O. S.; Ermakov, A. M.; Ivanov, V. K.; Sukhorukov, G. B. Intracellular Delivery of Antioxidant CeO_2 Nanoparticles *via* Polyelectrolyte Microcapsules. *ACS Biomater. Sci. Eng.* **2018**, *4* (7), 2453–2462. https://doi.org/10.1021/acsbiomaterials.8b00489.

(105) Del Mercato, L. L.; Guerra, F.; Lazzari, G.; Nobile, C.; Bucci, C.; Rinaldi, R. Biocompatible Multilayer Capsules Engineered with a Graphene Oxide Derivative: Synthesis, Characterization and Cellular Uptake. *Nanoscale* **2016**, *8* (14), 7501–7512. https://doi.org/10.1039/c5nr07665j.

(106) Kurapati, R.; Raichur, A. M. Graphene Oxide Based Multilayer Capsules with Unique Permeability Properties: Facile Encapsulation of Multiple Drugs. *Chem. Commun.* **2012**, *48* (48), 6013–6015. https://doi.org/10.1039/c2cc32248j.

(107) Kurapati, R.; Raichur, A. M. Near-Infrared Light-Responsive Graphene Oxide Composite Multilayer Capsules: A Novel Route for Remote Controlled Drug Delivery. *Chem. Commun.* **2013**, *49* (7), 734–736. https://doi.org/10.1039/c2cc38417e.

(108) Fang, M.; Grant, P. S.; McShane, M. J.; Sukhorukov, G. B.; Golub, V. O.; Lvov, Y. M. Magnetic Bio/Nanoreactor with Multilayer Shells of Glucose Oxidase and Inorganic Nanoparticles. *Langmuir* **2002**, *18* (16), 6338–6344. https://doi.org/10.1021/la025731m.

(109) Caruso, F.; Schüler, C. Enzyme Multilayers on Colloid Particles: Assembly, Stability, and Enzymatic Activity. *Langmuir* **2000**, *16* (24), 9595–9603. https://doi.org/10.1021/la000942h.

(110) Qi, W.; Yan, X.; Duan, L.; Cui, Y.; Yang, Y.; Li, J. Glucose-Sensitive Microcapsules from Glutaraldehyde Cross-Linked Hemoglobin and Glucose Oxidase. *Biomacromolecules* **2009**, *10* (5), 1212–1216. https://doi.org/10.1021/bm801502r.

(111) Qi, W.; Yan, X.; Fei, J.; Wang, A.; Cui, Y.; Li, J. Triggered Release of Insulin from Glucose-Sensitive Enzyme Multilayer Shells. *Biomaterials* **2009**, *30* (14), 2799–2806. https://doi.org/10.1016/j.biomaterials.2009.01.027.

(112) Xu, C.; Lei, C.; Huang, L.; Zhang, J.; Zhang, H.; Song, H.; Yu, M.; Wu, Y.; Chen, C.; Yu, C. Glucose-Responsive Nanosystem Mimicking the Physiological Insulin Secretion *via* an Enzyme-Polymer Layer-by-Layer Coating Strategy. *Chem. Mater.* **2017**, *29* (18), 7725–7732. https://doi.org/10.1021/acs.chemmater.7b01804.

(113) Schüler, C.; Caruso, F. Preparation of Enzyme Multilayers on Colloids for Biocatalysis. *Macromol. Rapid Commun.* **2000**, *21* (11), 750–753. https://doi.org/10.1002/1521-3927(20000701)21:11<750::AID-MARC750>3.0.CO;2-3.

(114) Liang, Z.; Wang, C.; Tong, Z.; Ye, W.; Ye, S. Bio-Catalytic Nanoparticles with Urease

Immobilized in Multilayer Assembled through Layer-by-Layer Technique. *React. Funct. Polym.* **2005**, *63* (1), 85–94. https://doi.org/10.1016/j.reactfunctpolym.2005.02.009.

(115) Lvov, Y.; Caruso, F. Biocolloids with Ordered Urease Multilayer Shells as Enzymatic Reactors. *Anal. Chem.* **2001**, *73* (17), 4212–4217. https://doi.org/10.1021/ac010118d.

(116) Rui, Y.; Pang, B.; Zhang, J.; Liu, Y.; Hu, H.; Liu, Z.; Ama Baidoo, S.; Liu, C.; Zhao, Y.; Li, S. Near-Infrared Light-Activatable siRNA Delivery by Microcapsules for Combined Tumour Therapy. *Artif. Cells, Nanomedicine Biotechnol.* **2018**, *46* (sup2), 15–24. https://doi.org/10.1080/21691401.2018.1449752.

(117) Deng, Z. J.; Morton, S. W.; Ben-Akiva, E.; Dreaden, E. C.; Shopsowitz, K. E.; Hammond, P. T. Layer-by-Layer Nanoparticles for Systemic Codelivery of an Anticancer Drug and siRNA for Potential Triple-Negative Breast Cancer Treatment. *ACS Nano* **2013**, *7* (11), 9571–9584. https://doi.org/10.1021/nn4047925.

(118) Choi, K. Y.; Correa, S.; Min, J.; Li, J.; Roy, S.; Laccetti, K. H.; Dreaden, E.; Kong, S.; Heo, R.; Roh, Y. H.; Lawson, E. C.; Palmer, P. A.; Hammond, P. T. Binary Targeting of siRNA to Hematologic Cancer Cells *in vivo* Using Layer-by-Layer Nanoparticles. *Adv. Funct. Mater.* **2019**, *29* (20), 0–31. https://doi.org/10.1002/adfm.201900018.

(119) Gomes-Da-Silva, L. C.; Fonseca, N. A.; Moura, V.; Pedroso De Lima, M. C.; Simões, S.; Moreira, J. N. Lipid-Based Nanoparticles for siRNA Delivery in Cancer Therapy: Paradigms and Challenges. *Acc. Chem. Res.* **2012**, *45* (7), 1163–1171. https://doi.org/10.1021/ar300048p.

(120) Young Choi, K.; Silvestre, O. F.; Huang, X.; Hida, N.; Liu, G.; Ho, D. N.; Lee, S.; Wook Lee, S.; In Hong, J.; Chen, X. A Nanoparticle Formula for Delivering siRNA or miRNAs to Tumor Cells in Cell Culture and *in vivo*. *Nat. Protoc.* **2015**, *9* (8), 1900–1915. https://doi.org/10.1038/nprot.2014.128.A.

(121) Leng, O.; Woodle, M. C.; Lu, P. Y.; Mixson, A. J. Advances in Systemic siRNA Delivery. *Drugs Future* **2009**, *34* (9), 721–737.

https://doi.org/10.1358/dof.2009.034.09.1413267.

(122) Pan, X.; Thompson, R.; Meng, X.; Wu, D.; Xu, L. Tumor-Targeted RNA-Interference: Functional Non-Viral Nanovectors. *Am. J. Cancer Res.* **2011**, *1* (1), 25–42.

(123) Boehnke, N.; Correa, S.; Hao, L.; Wang, W.; Straehla, J. P.; Bhatia, S. N.; Hammond, P. T. Theranostic Layer-by-Layer Nanoparticles for Simultaneous Tumor Detection and Gene Silencing. *Angew. Chemie - Int. Ed.* **2020**, *02115*, 2–10. https://doi.org/10.1002/anie.201911762.

(124) Gu, L.; Deng, Z. J.; Roy, S.; Hammond, P. T. A Combination RNAi-Chemotherapy Layer-by-Layer Nanoparticle for Systemic Targeting of KRAS/P53 with Cisplatin to Treat Non–Small Cell Lung Cancer. *Clin. Cancer Res.* **2017**, *23* (23), 7312–7323. https://doi.org/10.1158/1078-0432.CCR-16-2186.

(125) Timin, A. S.; Muslimov, A. R.; Lepik, K. V.; Epifanovskaya, O. S.; Shakirova, A. I.; Mock, U.; Riecken, K.; Okilova, M. V.; Sergeev, V. S.; Afanasyev, B. V.; Fehse, B.; Sukhorukov, G. B. Efficient Gene Editing *via* Non-Viral Delivery of CRISPR–Cas9 System Using Polymeric and Hybrid Microcarriers. *Nanomedicine Nanotechnology, Biol. Med.* **2018**, *14* (1), 97–108. https://doi.org/10.1016/j.nano.2017.09.001.

(126) Elbakry, A.; Wurster, E. C.; Zaky, A.; Liebl, R.; Schindler, E.; Bauer-Kreisel, P.; Blunk, T.; Rachel, R.; Goepferich, A.; Breunig, M. Layer-by-Layer Coated Gold Nanoparticles: Size-Dependent Delivery of DNA into Cells. *Small* **2012**, *8* (24), 3847–3856. https://doi.org/10.1002/smll.201201112.

(127) Borden, M. A.; Caskey, C. F.; Little, E.; Gillies, R. J.; Ferrara, K. W. DNA and Polylysine Adsorption and Multilayer Construction onto Cationic Lipid-Coated Microbubbles. *Langmuir* **2007**, *23* (18), 9401–9408. https://doi.org/10.1021/la7009034.

(128) Correa, S.; Boehnke, N.; Deiss-Yehiely, E.; Hammond, P. T. Solution Conditions Tune and Optimize Loading of Therapeutic Polyelectrolytes into Layer-by-Layer Functionalized Liposomes. *ACS Nano* **2019**, *13* (5), 5623–5634. https://doi.org/10.1021/acsnano.9b00792.

(129) Khopade, A. J.; Arulsudar, N.; Khopade, S. A.; Hartmann, J. Ultrathin Antibiotic

Walled Microcapsules. *Biomacromolecules* **2005**, *6* (1), 229–234. https://doi.org/10.1021/bm049554a.

(130) Facca, S.; Cortez, C.; Mendoza-Palomares, C.; Messadeq, N.; Dierich, A.; Johnston, A. P. R.; Mainard, D.; Voegel, J. C.; Caruso, F.; Benkirane-Jessel, N. Active Multilayered Capsules for *in vivo* Bone Formation. *Proc. Natl. Acad. Sci. U. S. A.* **2010**, *107* (8), 3406–3411. https://doi.org/10.1073/pnas.0908531107.

(131) Zhang, B. J.; Han, Z. W.; Duan, K.; Mu, Y. D.; Weng, J. Multilayered Pore-Closed PLGA Microsphere Delivering OGP and BMP-2 in Sequential Release Patterns for the Facilitation of BMSCs Osteogenic Differentiation. *J. Biomed. Mater. Res. - Part A* **2018**, *106* (1), 95–105. https://doi.org/10.1002/jbm.a.36210.

(132) Go, D. P.; Gras, S. L.; Mitra, D.; Nguyen, T. H.; Stevens, G. W.; Cooper-White, J. J.; O'Connor, A. J. Multilayered Microspheres for the Controlled Release of Growth Factors in Tissue Engineering. *Biomacromolecules* **2011**, *12* (5), 1494–1503. https://doi.org/10.1021/bm1014574.

(133) Cheng, R.; Feng, F.; Meng, F.; Deng, C.; Feijen, J.; Zhong, Z. Glutathione-Responsive Nano-Vehicles as a Promising Platform for Targeted Intracellular Drug and Gene Delivery. *J. Control. Release* **2011**, *152* (1), 2–12. https://doi.org/10.1016/j.jconrel.2011.01.030.

(134) Zelikin, A. N.; Quinn, J. F.; Caruso, F. Disulfide Cross-Linked Polymer Capsules: En Route to Biodeconstructible Systems. *Biomacromolecules* **2006**, *7* (1), 27–30. https://doi.org/10.1021/bm050832v.

(135) Sexton, A.; Whitney, P. G.; Chong, S.; Zelikin, A. N.; Johnston, A. P. R.; De Rose, R.; Brooks, A. G.; Caruso, F.; Kent, S. J. A Protective Vaccine Delivery System for *in vivo* T Cell Stimulation Using Nanoengineered Polymer Hydrogel Capsules. *ACS Nano* **2009**, *3* (11), 3391–3400.

(136) Zelikin, A. N.; Li, Q.; Caruso, F. Disulfide-Stabilized Poly (Methacrylic Acid) Capsules: Formation, Cross-Linking, and Degradation Behavior. *Chem. Mater.* **2008**, *20* (12), 2655–2661.

(137) Chong, S. F.; Sexton, A.; De Rose, R.; Kent, S. J.; Zelikin, A. N.; Caruso, F. A Paradigm for Peptide Vaccine Delivery Using Viral Epitopes Encapsulated in Degradable

Polymer Hydrogel Capsules. *Biomaterials* **2009**, *30* (28), 5178–5186. https://doi.org/10.1016/j.biomaterials.2009.05.078.

(138) Guo, X.; Carter, M. C. D.; Appadoo, V.; Lynn, D. M. Tunable and Selective Degradation of Amine-Reactive Multilayers in Acidic Media. *Biomacromolecules* **2019**, *20* (9), 3464–3474. https://doi.org/10.1021/acs.biomac.9b00756.

(139) Yi, Q.; Sukhorukov, G. B. UV-Induced Disruption of Microcapsules with Azobenzene Groups. *Soft Matter* **2014**, *10* (9), 1384–1391. https://doi.org/10.1039/c3sm51648b.

(140) Reum, N.; Fink-Straube, C.; Klein, T.; Hartmann, R. W.; Lehr, C. M.; Schneider, M. Multilayer Coating of Gold Nanoparticles with Drug-Polymer Coadsorbates. *Langmuir* **2010**, *26* (22), 16901–16908. https://doi.org/10.1021/la103109b.

(141) Ochs, C. J.; Such, G. K.; Yan, Y.; Van Koeverden, M. P.; Caruso, F. Biodegradable Click Capsules with Engineered Drug-Loaded Multilayers. *ACS Nano* **2010**, *4* (3), 1653–1663. https://doi.org/10.1021/nn9014278.

(142) Mohanta, V.; Madras, G.; Patil, S. Albumin-Mediated Incorporation of Water-Insoluble Therapeutics in Layer-by-Layer Assembled Thin Films and Microcapsules. *J. Mater. Chem. B* **2013**, *1* (37), 4819–4827. https://doi.org/10.1039/c3tb20592d.

(143) De Rose, R.; Zelikin, A. N.; Johnston, A. P. R.; Sexton, A.; Chong, S. F.; Cortez, C.; Mulholland, W.; Caruso, F.; Kent, S. J. Binding, Internalization, and Antigen Presentation of Vaccine-Loaded Nanoengineered Capsules in Blood. *Adv. Mater.* **2008**, *20* (24), 4698–4703. https://doi.org/10.1002/adma.200801826.

(144) Jing, J.; Szarpak-Jankowska, A.; Guillot, R.; Pignot-Paintrand, I.; Picart, C.; Auzély-Velty, R. Cyclodextrin/Paclitaxel Complex in Biodegradable Capsules for Breast Cancer Treatment. *Chem. Mater.* **2013**, *25* (19), 3867–3873. https://doi.org/10.1021/cm4019925.

(145) Zhou, D.; Xiao, H.; Meng, F.; Zhou, S.; Guo, J.; Li, X.; Jing, X.; Huang, Y. Layer-by-Layer Assembled Polypeptide Capsules for Platinum-Based pro-Drug Delivery. *Bioconjug. Chem.* **2012**, *23* (12), 2335–2343. https://doi.org/10.1021/bc300144e.

(146) Zhang, R.; Ru, Y.; Gao, Y.; Li, J.; Mao, S. Layer-by-Layer Nanoparticles Co-Loading Gemcitabine and Platinum (IV) Prodrugs for Synergistic Combination Therapy of Lung Cancer. *Drug Des. Devel. Ther.* **2017**, *11*, 2631–2642. https://doi.org/10.2147/DDDT.S143047.

(147) Tong, W.; Song, X.; Gao, C. Layer-by-Layer Assembly of Microcapsules and Their Biomedical Applications. *Chem. Soc. Rev.* **2012**, *41* (18), 6103–6124. https://doi.org/10.1039/c2cs35088b.

(148) Dhanya, C. R.; Jeyaraman, J.; Janeesh, P. A.; Shukla, A.; Sivakumar, S.; Abraham, A. Bio-Distribution and: *in vivo* / *in vitro* Toxicity Profile of PEGylated Polymer Capsules Encapsulating $LaVO_4:Tb^{3+}$ Nanoparticles for Bioimaging Applications. *RSC Adv.* **2016**, *6* (60), 55125–55134. https://doi.org/10.1039/c6ra06719k.

(149) Ochs, C. J.; Such, G. K.; Städler, B.; Caruso, F. Low-Fouling, Biofunctionalized and Biodegradable Click Capsules. *Biomacromolecules* **2008**, *9* (12), 3389–3396. https://doi.org/10.1021/bm800794w.

(150) Johnston, A. P. R.; Such, G. K.; Ng, S. L.; Caruso, F. Challenges Facing Colloidal Delivery Systems: From Synthesis to the Clinic. *Curr. Opin. Colloid Interface Sci.* **2011**, *16* (3), 171–181. https://doi.org/10.1016/j.cocis.2010.11.003.

(151) Cortez, C.; Tomaskovic-crook, E.; Johnston, A. P. R.; Scott, A. M.; Nice, E. C.; Heath, J. K.; Caruso, F. Influence of Size , Surface , Cell Line , and Colorectal Cancer Cells. *ACS Nano* **2007**, *1* (2), 93–102.

(152) Wattendorf, U.; Kreft, O.; Textor, M.; Sukhorukov, G. B.; Merkle, H. P. Stable Stealth Function for Hollow Polyelectrolyte Microcapsules through a Poly(Ethylene Glycol) Grafted Polyelectrolyte Adlayer. *Biomacromolecules* **2008**, *9* (1), 100–108. https://doi.org/10.1021/bm700857s.

(153) Heuberger, R.; Sukhorukov, G.; Vörös, J.; Textor, M.; Möhwald, H. Biofunctional Polyelectrolyte Multilayers and Microcapsules: Control of Non-Specific and Bio-Specific Protein Adsorption. *Adv. Funct. Mater.* **2005**, *15* (3), 357–366. https://doi.org/10.1002/adfm.200400063.

(154) Khopade, A. J.; Caruso, F. Surface-Modification of Polyelectrolyte Multilayer-Coated Particles for Biological Applications. *Langmuir* **2003**, *19* (15), 6219–6225.

https://doi.org/10.1021/la030016d.

(155) Kempe, K.; Ng, S. L.; Noi, K. F.; Müllner, M.; Gunawan, S. T.; Caruso, F. Clickable Poly(2-Oxazoline) Architectures for the Fabrication of Low-Fouling Polymer Capsules. *ACS Macro Lett.* **2013**, *2* (12), 1069–1072. https://doi.org/10.1021/mz400522e.

(156) Kempe, K.; Xiang, S. D.; Wilson, P.; Rahim, M. A.; Ju, Y.; Whittaker, M. R.; Haddleton, D. M.; Plebanski, M.; Caruso, F.; Davis, T. P. Engineered Hydrogen-Bonded Glycopolymer Capsules and Their Interactions with Antigen Presenting Cells. *ACS Appl. Mater. Interfaces* **2017**, *9* (7), 6444–6452. https://doi.org/10.1021/acsami.6b15459.

(157) Kempe, K.; Ng, S. L.; Gunawan, S. T.; Noi, K. F.; Caruso, F. Intracellularly Degradable Hydrogen-Bonded Polymer Capsules. *Adv. Funct. Mater.* **2014**, *24* (39), 6187–6194. https://doi.org/10.1002/adfm.201401397.

(158) Gunawan, S. T.; Kempe, K.; Bonnard, T.; Cui, J.; Alt, K.; Law, L. S.; Wang, X.; Westein, E.; Such, G. K.; Peter, K.; Hagemeyer, C. E.; Caruso, F. Multifunctional Thrombin-Activatable Polymer Capsules for Specific Targeting to Activated Platelets. *Adv. Mater.* **2015**, *27* (35), 5153–5157. https://doi.org/10.1002/adma.201502243.

(159) Hansen, C. E.; Myers, D. R.; Baldwin, W. H.; Sakurai, Y.; Meeks, S. L.; Lyon, L. A.; Lam, W. A. Platelet-Microcapsule Hybrids Leverage Contractile Force for Targeted Delivery of Hemostatic Agents. *ACS Nano* **2017**, *11* (6), 5579–5589. https://doi.org/10.1021/acsnano.7b00929.

(160) Qi, W.; Wang, A.; Yang, Y.; Du, M.; Bouchu, M. N.; Boullanger, P.; Li, J. The Lectin Binding and Targetable Cellular Uptake of Lipid-Coated Polysaccharide Microcapsules. *J. Mater. Chem.* **2010**, *20* (11), 2121–2127. https://doi.org/10.1039/b920469p.

(161) Zhang, F.; Wu, Q.; Chen, Z. C.; Zhang, M.; Lin, X. F. Hepatic-Targeting Microcapsules Construction by Self-Assembly of Bioactive Galactose-Branched Polyelectrolyte for Controlled Drug Release System. *J. Colloid Interface Sci.* **2008**, *317* (2), 477–484. https://doi.org/10.1016/j.jcis.2007.09.065.

(162) Valdepérez, D.; del Pino, P.; Sánchez, L.; Parak, W. J.; Pelaz, B. Highly Active Antibody-Modified Magnetic Polyelectrolyte Capsules. *J. Colloid Interface Sci.* **2016**, *474*, 1–8. https://doi.org/10.1016/j.jcis.2016.04.003.

(163) Deo, D. I.; Gautrot, J. E.; Sukhorukov, G. B.; Wang, W. Biofunctionalization of PEGylated Microcapsules for Exclusive Binding to Protein Substrates. *Biomacromolecules* **2014**, *15* (7), 2555–2562. https://doi.org/10.1021/bm500412d.

(164) Kolesnikova, T. A.; Kiragosyan, G.; Le, T. H. N.; Springer, S.; Winterhalter, M. Protein A Functionalized Polyelectrolyte Microcapsules as a Universal Platform for Enhanced Targeting of Cell Surface Receptors. *ACS Appl. Mater. Interfaces* **2017**, *9* (13), 11506–11517. https://doi.org/10.1021/acsami.7b01313.

(165) Nifontova, G.; Kalenichenko, D.; Baryshnikova, M.; Gomes, F. R.; Alves, F.; Karaulov, A.; Nabiev, I.; Sukhanova, A. Biofunctionalized Polyelectrolyte Microcapsules Encoded with Fluorescent Semiconductor Nanocrystals for Highly Specific Targeting and Imaging of Cancer Cells. *Photonics* **2019**, *6* (4). https://doi.org/10.3390/photonics6040117.

(166) Cortez, C.; Tomaskovic-Crook, E.; Johnston, A. P. R.; Radt, B.; Cody, S. H.; Scott, A. M.; Nice, E. C.; Heath, J. K.; Caruso, F. Targeting and Uptake of Multilayered Particles to Colorectal Cancer Cells. *Adv. Mater.* **2006**, *18* (15), 1998–2003. https://doi.org/10.1002/adma.200600564.

(167) Chen, W. H.; Liao, W. C.; Sohn, Y. S.; Fadeev, M.; Cecconello, A.; Nechushtai, R.; Willner, I. Stimuli-Responsive Nucleic Acid-Based Polyacrylamide Hydrogel-Coated Metal–Organic Framework Nanoparticles for Controlled Drug Release. *Adv. Funct. Mater.* **2018**, *28* (8), 1–9. https://doi.org/10.1002/adfm.201705137.

(168) Liao, W. C.; Lu, C. H.; Hartmann, R.; Wang, F.; Sohn, Y. S.; Parak, W. J.; Willner, I. Adenosine Triphosphate-Triggered Release of Macromolecular and Nanoparticle Loads from Aptamer/DNA-Cross-Linked Microcapsules. *ACS Nano* **2015**, *9* (9), 9078–9086. https://doi.org/10.1021/acsnano.5b03223.

(169) Rosch, J. G.; Landry, M. R.; Thomas, C. R.; Sun, C. Enhancing Chemoradiation of Colorectal Cancer through Targeted Delivery of Raltitrexed by Hyaluronic Acid

Coated Nanoparticles. *Nanoscale* **2019**, *11* (29), 13947–13960. https://doi.org/10.1039/c9nr04320a.

(170) Hou, Z.; Deng, K.; Li, C.; Deng, X.; Lian, H.; Cheng, Z.; Jin, D.; Lin, J. 808 nm Light-Triggered and Hyaluronic Acid-Targeted Dual-Photosensitizers Nanoplatform by Fully Utilizing Nd^{3+}-Sensitized Upconversion Emission with Enhanced Anti-Tumor Efficacy. *Biomaterials* **2016**, *101*, 32–46. https://doi.org/10.1016/j.biomaterials.2016.05.024.

(171) Maiolino, S.; Moret, F.; Conte, C.; Fraix, A.; Tirino, P.; Ungaro, F.; Sortino, S.; Reddi, E.; Quaglia, F. Hyaluronan-Decorated Polymer Nanoparticles Targeting the CD44 Receptor for the Combined Photo/Chemo-Therapy of Cancer. *Nanoscale* **2015**, *7* (13), 5643–5653. https://doi.org/10.1039/c4nr06910b.

(172) Gao, H.; Wen, D.; Sukhorukov, G. B. Composite Silica Nanoparticle/Polyelectrolyte Microcapsules with Reduced Permeability and Enhanced Ultrasound Sensitivity. *J. Mater. Chem. B* **2015**, *3* (9), 1888–1897. https://doi.org/10.1039/c4tb01717j.

(173) Song, F.; Gao, H.; Li, D.; Petrov, A. V.; Petrov, V. V.; Wen, D.; Sukhorukov, G. B. Low Intensity Focused Ultrasound Responsive Microcapsules for Non-Ablative Ultrafast Intracellular Release of Small Molecules. *J. Mater. Chem. B* **2021**, *9* (10), 2384–2393. https://doi.org/10.1039/d0tb02788j.

(174) Timin, A. S.; Muslimov, A. R.; Lepik, K. V.; Okilova, M. V.; Tcvetkov, N. Y.; Shakirova, A. I.; Afanasyev, B. V.; Gorin, D. A.; Sukhorukov, G. B. Intracellular Breakable and Ultrasound-Responsive Hybrid Microsized Containers for Selective Drug Release into Cancerous Cells. *Part. Part. Syst. Charact.* **2017**, *34* (5), 1–10. https://doi.org/10.1002/ppsc.201600417.

(175) Zyuzin, M. V.; Timin, A. S.; Sukhorukov, G. B. Multilayer Capsules Inside Biological Systems: State-of-the-Art and Open Challenges. *Langmuir* **2019**, *35* (13), 4747–4762. https://doi.org/10.1021/acs.langmuir.8b04280.

(176) Gao, H.; Wen, D.; Tarakina, N. V.; Liang, J.; Bushby, A. J.; Sukhorukov, G. B. Bifunctional Ultraviolet/Ultrasound Responsive Composite TiO_2/Polyelectrolyte Microcapsules. *Nanoscale* **2016**, *8* (9), 5170–5180. https://doi.org/10.1039/c5nr06666b.

(177) Song, Z.; Liu, Y.; Shi, J.; Ma, T.; Zhang, Z.; Ma, H.; Cao, S. Hydroxyapatite/Mesoporous Silica Coated Gold Nanorods with Improved Degradability as a Multi-Responsive Drug Delivery Platform. *Mater. Sci. Eng. C* **2018**, *83* (June 2017), 90–98. https://doi.org/10.1016/j.msec.2017.11.012.

(178) Gao, H.; Goriacheva, O. A.; Tarakina, N. V.; Sukhorukov, G. B. Intracellularly Biodegradable Polyelectrolyte/Silica Composite Microcapsules as Carriers for Small Molecules. *ACS Appl. Mater. Interfaces* **2016**, *8* (15), 9651–9661. https://doi.org/10.1021/acsami.6b01921.

(179) Verma, A.; Sharma, S.; Gupta, P. K.; Singh, A.; Teja, B. V.; Dwivedi, P.; Gupta, G. K.; Trivedi, R.; Mishra, P. R. Vitamin B12 Functionalized Layer by Layer Calcium Phosphate Nanoparticles: A Mucoadhesive and PH Responsive Carrier for Improved Oral Delivery of Insulin. *Acta Biomater.* **2016**, *31*, 288–300. https://doi.org/10.1016/j.actbio.2015.12.017.

(180) Zheng, F.; Wang, C.; Meng, T.; Zhang, Y.; Zhang, P.; Shen, Q.; Zhang, Y.; Zhang, J.; Li, J.; Min, Q.; Chen, J.; Zhu, J. J. Outer-Frame-Degradable Nanovehicles Featuring Near-Infrared Dual Luminescence for *in vivo* Tracking of Protein Delivery in Cancer Therapy. *ACS Nano* **2019**, *13* (11), 12577–12590. https://doi.org/10.1021/acsnano.9b03424.

(181) Chen, W. H.; Luo, G. F.; Qiu, W. X.; Lei, Q.; Liu, L. H.; Wang, S. B.; Zhang, X. Z. Mesoporous Silica-Based Versatile Theranostic Nanoplatform Constructed by Layer-by-Layer Assembly for Excellent Photodynamic/Chemo Therapy. *Biomaterials* **2017**, *117*, 54–65. https://doi.org/10.1016/j.biomaterials.2016.11.057.

(182) Habibi, N.; Pastorino, L.; Babolmorad, G.; Ruggiero, C.; Guda, T.; Ong, J. L. Polyelectrolyte Multilayers and Capsules: S-Layer Functionalization for Improving Stability and Biocompatibility. *J. Drug Deliv. Sci. Technol.* **2017**, *38*, 1–8. https://doi.org/10.1016/j.jddst.2016.12.004.

(183) Fagan, R. P.; Fairweather, N. F. Biogenesis and Functions of Bacterial S-Layers. *Nat. Rev. Microbiol.* **2014**, *12* (3), 211–222. https://doi.org/10.1038/nrmicro3213.

(184) Zhang, C.; Jin, T.; Cheng, G.; Yuan, S.; Sun, Z.; Li, N. W.; Yu, L.; Ding, S. Functional Polymers in Electrolyte Optimization and Interphase Design for Lithium Metal Anodes. *J. Mater. Chem. A* **2021**, *9* (23), 13388–13401. https://doi.org/10.1039/d1ta02297k.

(185) De Temmerman, M. L.; Rejman, J.; Lucas, B.; Vandenbroucke, R. E.; Libert, C.; Demeester, J.; De Smedt, S. C. Modulation of Dendritic Cells by Lipid Grafted Polyelectrolyte Microcapsules. *Adv. Funct. Mater.* **2012**, *22* (20), 4236–4243. https://doi.org/10.1002/adfm.201103151.

(186) Campbell, J.; Abnett, J.; Kastania, G.; Volodkin, D.; Vikulina, A. S. Which Biopolymers Are Better for the Fabrication of Multilayer Capsules? A Comparative Study Using Vaterite $CaCO_3$ as Templates. *ACS Appl. Mater. Interfaces* **2021**, *13* (2), 3259–3269. https://doi.org/10.1021/acsami.0c21194.

(187) Gaio, E.; Conte, C.; Esposito, D.; Miotto, G.; Quaglia, F.; Moret, F.; Reddi, E. Co-Delivery of Docetaxel and Disulfonate Tetraphenyl Chlorin in One Nanoparticle Produces Strong Synergism between Chemo- and Photodynamic Therapy in Drug-Sensitive and -Resistant Cancer Cells. *Mol. Pharm.* **2018**, *15* (10), 4599–4611. https://doi.org/10.1021/acs.molpharmaceut.8b00597.

(188) Nifontova, G.; Krivenkov, V.; Zvaigzne, M.; Samokhvalov, P.; Efimov, A. E.; Agapova, O. I.; Agapov, I. I.; Korostylev, E.; Zarubin, S.; Karaulov, A.; Nabiev, I.; Sukhanova, A. Controlling Charge Transfer from Quantum Dots to Polyelectrolyte Layers Extends Prospective Applications of Magneto-Optical Microcapsules. *ACS Appl. Mater. Interfaces* **2020**, *12* (32), 35882–35894. https://doi.org/10.1021/acsami.0c08715.

(189) Kozlovskaya, V.; Alford, A.; Dolmat, M.; Ducharme, M.; Caviedes, R.; Radford, L.; Lapi, S. E.; Kharlampieva, E. Multilayer Microcapsules with Shell-Chelated ^{89}Zr for PET Imaging and Controlled Delivery. *ACS Appl. Mater. Interfaces* **2020**, *12* (51), 56792–56804. https://doi.org/10.1021/acsami.0c17456.

(190) Quarta, A.; Rodio, M.; Cassani, M.; Gigli, G.; Pellegrino, T.; Del Mercato, L. L. Multilayered Magnetic Nanobeads for the Delivery of Peptides Molecules Triggered by Intracellular Proteases. *ACS Appl. Mater. Interfaces* **2017**, *9* (40),

35095–35104. https://doi.org/10.1021/acsami.7b05709.

(191) Alford, A.; Rich, M.; Kozlovskaya, V.; Chen, J.; Sherwood, J.; Bolding, M.; Warram, J.; Bao, Y.; Kharlampieva, E. Ultrasound-Triggered Delivery of Anticancer Therapeutics from MRI-Visible Multilayer Microcapsules. *Adv. Ther.* **2018**, *1* (5), 1–16. https://doi.org/10.1002/adtp.201800051.

(192) Correa-Paz, C.; Navarro Poupard, M. F.; Polo, E.; Rodríguez-Pérez, M.; Taboada, P.; Iglesias-Rey, R.; Hervella, P.; Sobrino, T.; Vivien, D.; Castillo, J.; del Pino, P.; Campos, F.; Pelaz, B. *In vivo* Ultrasound-Activated Delivery of Recombinant Tissue Plasminogen Activator from the Cavity of Sub-Micrometric Capsules. *J. Control. Release* **2019**, *308* (February), 162–171. https://doi.org/10.1016/j.jconrel.2019.07.017.

(193) Drachuk, I.; Harbaugh, S.; Kelley-Loughnane, N. Improving the Activity of DNA-Encoded Sensing Elements through Confinement in Silk Microcapsules. *ACS Appl. Mater. Interfaces* **2020**, *12* (43), 48329–48339. https://doi.org/10.1021/acsami.0c13713.

CHAPTER 3.

Encapsulation of manganese dioxide nanoparticles into layer-by-layer polymer capsules for the fabrication of antioxidant microreactors

CHAPTER 3. Encapsulation of manganese dioxide nanoparticles into layer-by-layer polymer capsules for the fabrication of antioxidant microreactors

Abstract

Oxidative stress is caused by the accumulation of reactive oxygen and nitrogen species (ROS and RNS) in the cellular microenvironment. These ROS and RNS damage important cell structures leading to cell apoptosis and senescence, thus causing a detrimental effect on numerous disease pathologies such as osteoarthritis, neuro- degeneration and cardiovascular diseases. For this reason, there is a growing interest in the development of antioxidant biomaterials that can eventually regulate the levels of ROS/RNS and prevent oxidative stress. The encapsulation of antioxidant enzymes (e.g., catalase or superoxide dismutase) on polymer microcapsules fabricated *via* the layer-by-layer (LbL) approach represents a promising strategy within this context. The diffusion of reagents and by-products through the shell of these microcapsules is timely and spatially controlled, allowing the bio-chemical reaction between ROS/RNS and the encapsulated enzyme. However, natural enzymes usually present low stability, high cost and difficult storage, which could limit their potential application in the bio- medical field. Hence, nanomaterials with intrinsic enzyme-like characteristics (i.e., nanozymes) have been considered as inorganic alternatives. In the present chapter, manganese dioxide nanoparticles were encapsulated into LbL polymer microcapsules to yield synthetic antioxidant microreactors. These microreactors efficiently scavenged hydrogen peroxide (H_2O_2) from solution and protected cells from oxidative stress in an *in vitro* model. The versatility of the synthetic procedure presented herein allows the fabrication of capsules with either positive or negative surface charge, which has a direct impact on the cytotoxicity and cell interaction.

3.1. Introduction

Reactive oxygen species (ROS) such as hydrogen peroxide (H_2O_2), hydroxyl (·OH) and superoxide anion radicals (O_2^-) are reactive molecules which play an essential role in numerous cell signalling processes.[1] In normal cellular activity conditions, cells are capable of regulating efficiently the levels of ROS through several antioxidant enzymes

and molecules. However, an overproduction of these ROS can overwhelm the antioxidant capacity of the cells and induce oxidative stress, which is the cause of numerous pathologies like neurodegeneration, cancer, osteoarthritis and cardiovascular diseases.[1-4]

For the reduction of the overproduced ROS, different alternatives based on biomaterials have been widely studied, including polymer micro- and nanocapsules fabricated *via* the layer-by-layer (LbL) approach. These consist on the alternate deposition of oppositely charged polyelectrolytes on a colloidal template, which is subsequently removed.[5] This process allows the fabrication of tailor-made micro- and nanocapsules with the possibility to adapt their physical, chemical, morphological and mechanical properties to the required application.[6,7] More precisely, the thickness of the polymeric membrane and the amount of polyelectrolyte attached to the sacrificial template can be tuned changing the polymerization degree of the polyelectrolytes, adjusting the ionic strength of the polyelectrolyte solution or modulating the template-polyelectrolyte amount ratio to ensure an efficient layer adhesion.[8] To impart advanced functionalities to the fabricated polymer micro- and nanocapsules, the outer layer can be chemically functionalized with several biomolecules.[9] Alternatively, inorganic nanoparticles can be incorporated either within the capsule or between the layers to create stimulus-responsive micro- and nanocapsules.[10-13]

Thanks to the versatility of this process, the fabricated capsules have been used for different biomedical applications such as drug delivery vehicles,[14-16] imaging,[17,18] or, more recently, as micro- and nanoreactors.[19,20] In the latter case, the capsules accommodate within their core active biomolecules such as enzymes, which act *in situ* allowing the continuous transfer of reagents and products through the polymeric membrane. Enzymes like catalase [19] or superoxide dismutase (SOD) have been widely studied for the reduction of the overproduced ROS. However, the exposure of these enzymes to diverse environmental conditions (e.g., extreme pH, high temperature, organic solvent) has a detrimental effect on their catalytic activity, thus limiting their practical application.[21]

As an inorganic alternative to these antioxidant enzymes, nanozymes (e.g., CeO_2 [20,22] or MnO_2[1,23-25]) have gained interest in nanobiotechnology owing to their high catalytic

efficiency and robust stability.[21,23,25,27] Manganese dioxide nanoparticles are of particular interest as ROS scavengers because of their multienzyme nature that mimic simultaneously the activity of both catalase and SOD.[23] Furthermore, the decomposition of these nanoparticles in Mn^{2+} and H_2O, preventing their accumulation in the body, makes manganese dioxide a good inorganic alternative for the treatment of oxidative stress.[1]

In this chapter, it was hypothesized that MnO_2-loaded polymer microcapsules would protect cells from H_2O_2-induced oxidative stress. We fabricated polymer capsules loaded with MnO_2 nanoparticles *via* the LbL process, depositing alternately poly(sodium 4-styrenesulfonate) (PSS) and poly(allylamine hydrochloride) (PAH) on a MnO_2-decorated $CaCO_3$ sacrificial template. After the $CaCO_3$ template removal, antioxidant polymer capsules loaded with MnO_2 nanoparticles were obtained. The capsules were thoroughly characterized in terms of physico-chemical, morphological and functional properties and, as a proof of concept, their therapeutic potential was evaluated in a preliminary *in vitro* model of oxidative stress using HeLa cells.

3.2. Materials and methods

3.2.1. Materials

Calcium chloride ($CaCl_2$), sodium carbonate (Na_2CO_3), sodium chloride (NaCl), potassium permanganate ($KMnO_4$), hydrogen peroxide (H_2O_2) (30% wt. in H_2O), poly(allylamine hydrochloride) (PAH) (M_w ~17,500 g/mol), poly(sodium 4-styrenesulfonate) (PSS) (M_w ~70,000 g/mol), ethylenediaminetetraacetic acid disodium salt dihydrate (EDTA), fluorescein 5-isothiocyanate (FITC), Phosphate Buffer Saline (PBS), Hank's Balanced Salt Solution (HBSS), Triton X-100, Tween 20 and bovine serum albumin (BSA) were purchased from Sigma Aldrich. Dulbecco's modified Eagle's medium (DMEM), fetal bovine serum (FBS), penicillin-streptomycin solution (P/S), AlamarBlue® cell viability reagent, rhodamine-phalloidin, 4',6-diamidino-2-phenylindole dihydrochloride (DAPI) and 16% Formaldehyde Solution (w/v) were purchased from Thermo Fischer Scientific.

3.2.2. Synthesis and characterization of MnO_2 nanoparticles

3.2.2.1. Synthesis of MnO_2 nanoparticles

MnO_2 nanoparticles were synthesized using a modified procedure as previously reported.[1,3,28] Briefly, 4.125 mmol of $KMnO_4$ was dissolved in 150 mL of distilled water inside a conical flask, and left under stirring (300 rpm) for 15 min. In parallel and in a smaller conical flask, 1.072 mM of PAH was dissolved in 50 mL of distilled water and stirred (300 rpm) again for 15 min. After 15 min, the stirring speed of the $KMnO_4$ solution was increased at 600 rpm and the aqueous solution of PAH was added. The mixed solution was stirred for 24 h and then freeze dried for 48-96 h. The freeze-dried sample was resuspended in 10 mL of distilled water inside a 15 mL falcon tube with the help of an ultrasonic probe (90% amplification for 5 min), and then was washed 3 times by centrifugation at 7000 g. After each centrifugation, the precipitate was redispersed in distilled water either by shaking or vortexing. After the third spinning, the precipitate was dispersed in distilled water using an ultrasonic probe for 1 h (90% amplification) inside an ice bath. The dispersion was kept at 4 ^{o}C until further use.

3.2.2.2. Characterization of MnO_2 nanoparticles

The morphological analysis of the MnO_2 nanoparticles was carried out by means of Scanning Electron Microscopy (SEM: FEI 200) at a working voltage and working current of 10 kV and 43 pA, respectively and by Transmission Electron Microscopy (TEM: JEM 1011, Jeol, Tokyo, Japan) at an accelerating voltage of 100 keV. The samples for the TEM were prepared by drop-casting 6 µl of solution previously diluted onto ultrathin C-film 150 mesh Cu grids.

Fourier-transform infrared spectroscopy (FTIR) was performed using a Shimadzu Miracle 10. The number of scans was set to 45, the scanning range was set from 4000 to 400 cm^{-1} and the resolution step at 4 cm^{-1}.

The size distribution as well as the surface charge were measured using a Zetasizer NanoZS90, Malvern instruments LTD. The measurements were carried out at 25 ^{o}C in distilled water at a concentration of 200 µg/mL. The size and the surface charge measurements represent the mean ± SD of three different measurements, with ten runs of ten seconds for each measurement. Before each measurement, the samples were sonicated for ten seconds using a Bandelin ultrasonic probe at 8 W, to avoid the presence of aggregates during measurements.

3.2.3. Fabrication and characterization of polymer capsules

3.2.3.1. Fabrication of polymer capsules

Polymer capsules were fabricated *via* the LbL process using $CaCO_3$ microparticles as a sacrificial template and PSS and PAH as negative and positive polyelectrolytes, respectively. $CaCO_3$ particles stabilized with PSS were obtained by the fast precipitation reaction between $CaCl_2$ and Na_2CO_3, similar to previous reports.[29] Briefly, aqueous solutions of 0.2 M $CaCl_2$ and Na_2CO_3 were prepared separately. 0.2 M Na_2CO_3 solution was prepared in the presence of PSS (4 mg/mL). The $CaCl_2$ solution was quickly poured into the PSS-Na_2CO_3 solution in an equal volume. After 30 s of vigorous stirring, the solution was incubated for 15 min. The obtained dispersion was centrifuged at 2000 g (1 min) and the particles were washed 3 times with distilled water. Then the particles

were resuspended in a 4 mg/mL MnO_2 aqueous solution (4 mg MnO_2 nanoparticles:10 mg $CaCO_3$ microparticles) and incubated in an orbital shaker at 300 rpm (30 min). After the incubation, the dispersion of particles was washed three times with a 0.005 M NaCl solution to remove the excess of MnO_2 nanoparticles. The amount of adsorbed MnO_2 nanoparticles onto the $CaCO_3$ templates was assessed by dissolving the template within a 0.1 M EDTA solution. First, a calibration curve of MnO_2 in a 0.1 M EDTA solution was prepared. $CaCO_3$ templates were incubated with different concentrations of MnO_2 nanoparticles and after the washing steps described above, templates were immersed in the EDTA solution thrice. The supernatant of each incubation step was collected and the MnO_2 concentration was determined by UV-VIS (Perkin Elmer lambda 365) at λ = 385 nm. Thereafter, the particles were resuspended in a 2 mg/mL PSS solution in 0.5 M NaCl (pH 6.5) and after ten minutes of incubation, the particles were centrifuged and washed thrice with a 0.005 M NaCl solution. After that, the particles were resuspended in a 2 mg/mL PAH solution in 0.5 M NaCl (pH 6.5) and incubated for ten minutes. This process was repeated until the desired number of layers was deposited. Finally, the particles were immersed in a 0.1 M EDTA solution to remove the template. After 5 minutes of incubation with EDTA, the particles were centrifuged and recovered. This process was repeated three times to ensure the complete removal of the sacrificial template (**Fig. 3.1**). The resulting capsules were washed several times with PBS or distilled water for the following use and characterization.

In a particular case, FITC-labelled PAH was used for the fabrication of fluorescently-labelled capsules to analyse the internalization of the polymer capsules by the cells. To do so, PAH and FITC were mixed at a ratio of 100 mol amide group of PAH per 1 mol of FITC. Briefly, PAH was dissolved in a 500 mM carbonate buffer (pH = 9.5) and then FITC solution (1 mg/mL in DMSO) was added dropwise to this solution sheltered from light. After 30 min of incubation, the solution was dialyzed for 48 h against distilled water, using a dialysis tubing cellulose membrane (avg. flat with 10 mm) (Sigma Aldrich). Once the dialysis process finished, the solution was freeze-dried (Telstar LyoQuest).

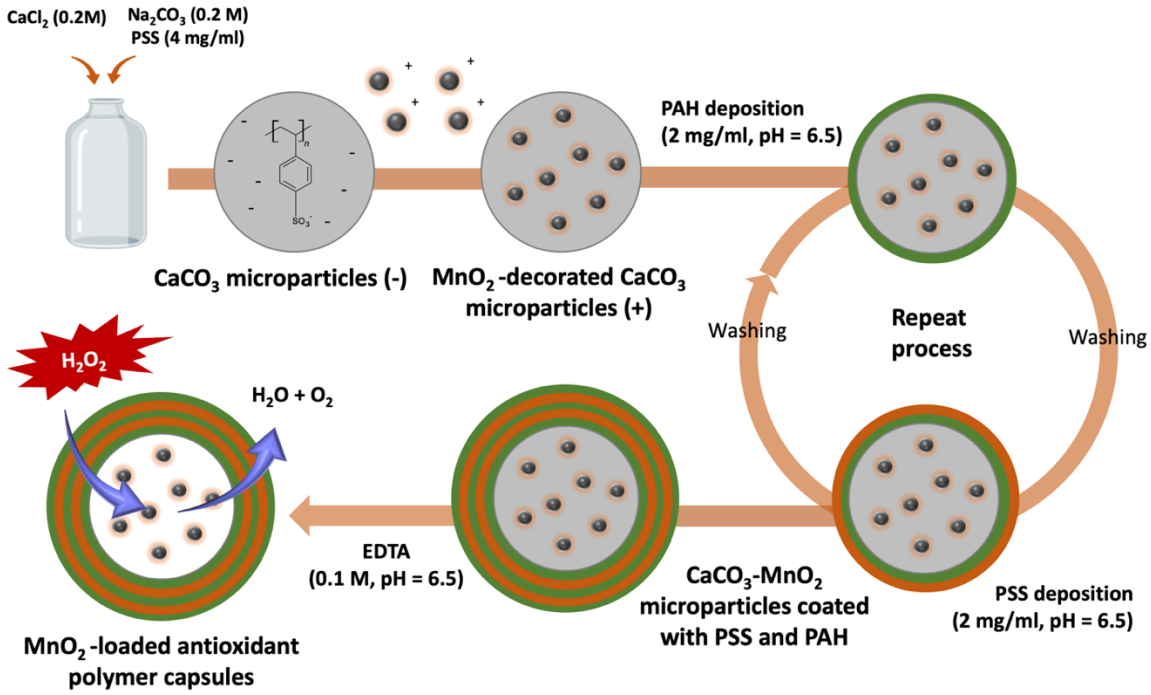

Fig. 3.1. *Schematic representation of the fabrication of MnO_2-loaded antioxidant polymer capsules.*

3.2.3.2. Physico-chemical and morphological characterization

The morphological analysis of the $CaCO_3$ microparticles and polymer capsules was carried out by means of Scanning Electron Microscopy (SEM: Hitachi S-4800) at a working voltage and working current of 5 kV and 2 nA, respectively.

To confirm the presence of MnO_2 nanoparticles in the $CaCO_3$ microparticles, X-ray Diffraction (XRD) analysis was performed using a PHILIPS X`PERT PRO automatic diffractometer operating at 40 kV and 40 mA, in theta-theta configuration, secondary monochromator with Cu-Kα radiation (λ = 1.5418 Å) and a PIXcel solid state detector.

The size distribution of the $CaCO_3$ microparticles was obtained in a Laser Scattering Particle Size Distribution Analyzer (HORIBA LA-350).

The ζ-potential of the particles after each polyelectrolyte deposition was measured from a minimum of ten runs using a Malvern Instrument Zetasizer (ZEN 3690).

Infrared spectra of the polyelectrolytes and capsules before and after the $CaCO_3$ sacrificial template removal was measured using a Nicolet AVATAR 370 operating in the

Attenuated Total Reflectance (ATR-FTIR). Spectra were taken with a resolution of 2 cm^{-1} and averaged over 64 scans.

The complete removal of the template was further confirmed *via* energy dispersive X-ray spectroscopy (EDS) using a FEI 200 SEM with a built-in Bruker Nano XFlash 5010 detector. The voltage was set at 20 kV and the scanning time at one minute. All the samples were coated with gold at 25 mA for 70 s before analysis.

The antioxidant capacity of the polymer capsules in the presence of biologically relevant H_2O_2 concentration (i.e., 10 µM and 50 µM) was evaluated using a Fluorimetric Hydrogen Peroxide Assay Kit (Sigma Aldrich). Briefly, polymer capsules at a final concentration of $1{\cdot}10^5$, $1{\cdot}10^6$, $1{\cdot}10^7$ or $1{\cdot}10^8$ polymer capsules/mL were incubated in a 10 or 50 µM H_2O_2 solution for 30 min. Afterwards, the dispersion of polymer capsules was centrifuged and 50 µL of the supernatant was transferred to a well in a 96-well plate together with another 50 µL of master mix containing horseradish peroxidase and red peroxidase substrate. After incubating for 20 min sheltered from light, the fluorescence intensity was measured (λ_{ex}=540 nm/λ_{em}=590 nm) on a microplate reader (BioTek Synergy H1M) to determine the H_2O_2 concentration.

The capacity of the capsules to scavenge H_2O_2 after being exposed to several cycles of H_2O_2 was also evaluated. For this purpose, polymer capsules at a final concentration of $1{\cdot}10^8$ capsules/mL were incubated in a 10 or 50 µM H_2O_2 solution for 30 min and subsequently centrifuged. The supernatant was collected to determine the H_2O_2 concentration following the procedure described above (Cycle 1). The polymer capsules were then resuspended in H_2O_2 solution (10 or 50 µM) and incubated for another 30 min. After being centrifuged, the supernatant was collected to determine the H_2O_2 concentration (Cycle 2). This process was repeated until cycle 4.

The H_2O_2 scavenging capacity of the polymer capsules after being sterilized with ethanol was also determined. Here, polymer capsules at a final concentration of $1{\cdot}10^7$ or $1{\cdot}10^8$ polymer capsules/mL were incubated in a 10 µM H_2O_2 solution for 30 min and subsequently centrifuged. The supernatant was collected to determine the H_2O_2 concentration following the procedure described above (non-sterilized sample). The polymer capsules were then resuspended in ethanol for 10 min. They were then collected by centrifugation and incubated in a 10 µM H_2O_2 solution for 30 min. The

supernatant was finally collected after centrifugation to determine the H_2O_2 concentration (sterilized sample).

3.2.4. *In vitro* studies

3.2.4.1. HeLa cell seeding

HeLa cells (ATCC) were grown in T-75 flasks with complete medium (DMEM + 10% FBS + 1% P/S) and incubated at 37 ^{o}C in a 5% CO_2 atmosphere. For the metabolic activity measurement and H_2O_2 scavenging analysis, the cells were seeded at a density of 50,000 or 5,000 cells/well on a 24 or 96-well plate, respectively.

3.2.4.2. Preliminary cytocompatibility test

To evaluate the cytotoxicity of the capsules, the metabolic activity of HeLa cells in the presence of polymer capsules was measured using the AlamarBlue® assay. Cells were seeded in 24-well plates and treated with MnO_2-loaded capsules with different surface charge (positive or negative) at three different capsules-to-cell ratios (10, 100 and 1000 polymer capsules/cell). Cells cultured in the absence of capsules were used as a control. At the selected time points (24 h or 72 h), the culture media was removed and replaced by fresh complete media containing AlamarBlue® (10% v/v). Cells were then incubated for 75 min at 37 ^{o}C in 5% CO_2 atmosphere sheltered from light. Finally, 200 µL of the assay media was transferred to a 96-well plate and the fluorescence intensity (λ_{ex}=545 nm/λ_{em}=590 nm) was read on a microplate reader (BioTek Synergy H1M).

The internalization of the FITC-labelled capsules by the cells was also analysed. After 24 h incubation of the cells in the presence of polymer capsules (10 capsules/cell), the culture media was removed and the cells were washed with HBSS and fixed with 4% paraformaldehyde. Cells were then washed with HBSS and permeabilized with 0.5% Triton X-100 in PBS for 10 minutes. After that, the cells were washed twice with PBS and incubated in a 1% BSA solution in PBS in the presence of rhodamine-phalloidin (0.066 µM) and DAPI (300 nM) for 15 minutes. Finally, cells were washed twice with PBS-T (0.1% Tween 20) and once with PBS before being observed in an inverted fluorescence microscope (Nikon Eclipse Ts2).

3.2.4.3. Therapeutic potential of the polymer capsules in H_2O_2-induced in vitro model

To evaluate the capacity of the capsules to protect cells in a H_2O_2-induced oxidative stress model, cells were first seeded at a concentration of 5,000 cells/well in a 96-well plate in complete medium. After cell adhesion (4 hours), polymer capsules with either positive or negative surface charge were added at a final ratio of 10, 100 and 1000 capsules/cell and incubated overnight. After this incubation, three stimuli of a biologically relevant H_2O_2 concentration (100 µM) were applied at different time points (0 h, 12 h, 24 h). The metabolic activity was measured using AlamarBlue® assay at the selected time points (8 h, 24 h, 32 h from the first stimulus addition) as described above.

3.2.5. Statistical analysis

All quantitative data related to the fabrication and characterization of polymer capsules are presented as the mean ± standard deviation (SD). For the *in vitro* studies six technical replicates (n=6) were employed and the results are presented as the mean ± standard deviation (SD). The statistical difference between groups was tested by one-way analysis of variance (ANOVA), using the Bonferroni post-hoc test and a confidence level of 95% ($p<0.05$).

3.3. Results and discussion

3.3.1. Synthesis of MnO_2 nanoparticles

Following the experimental procedure described above, we were able to acquire MnO_2 nanoparticles of spherical morphology and an average size of ~50 nm (**Fig. 3.2a, 3.2b**). The FTIR spectrum presented in **Fig. 3.2c** shows the characteristic peaks resulting from the PAH-stabilized MnO_2 nanoparticles. More specifically, the peaks in the range of 550-650 cm^{-1} can be attributed to the stretching vibration of Mn-O. Shifting to higher wavenumbers, the stretching vibration of C-H of the PAH coating can be seen in the range of 1435-1485 cm^{-1}, while the asymmetric vibration of N-H can be observed in the range of 1570-1650 cm^{-1}. Finally, the broad peaks in the range of 2800-3000 cm^{-1} and 3140-3400 cm^{-1} are respectively attributed to the symmetric stretching vibrations of O-H and N-H. Dynamic light scattering measurements were performed to assess the colloidal stability of the synthesized nanoparticles. The results presented in **Fig. 3.2d** and 3.**2e** show respectively the Gaussian distributions of the hydrodynamic diameter (average size: 129.7 ± 5.1 nm) and of the surface charge (average ζ-potential: +42.4 ± 0.05 mV). The higher hydrodynamic diameter deriving from the DLS measurements can be attributed to the PAH-coating. This coating is also responsible for the positive surface charge as well as the polydispersity (PDI) value of 0.35 ± 0.04. This PDI value suggests a moderate nanoparticle dispersion which can be attributed to the hydrogen bonds that are created between the PAH and the water molecules, affecting the hydrodynamic diameter. However, the strong positive surface charge that indicates strong repulsive electrostatic interactions, as well as the small size of nanoparticles suggest an increased colloidal stability.

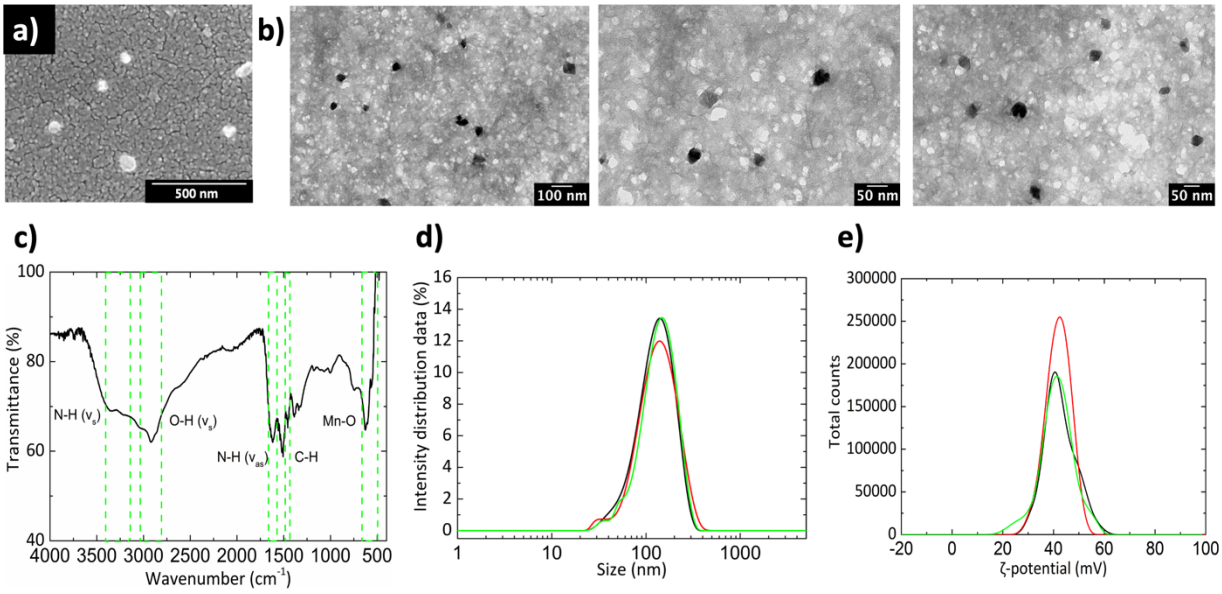

Fig. 3.2. *a) Scanning electron micrograph depicting the morphology and size of the synthesized MnO_2 nanoparticles, b) Transmission electron micrograph depicting the morphology and size of the synthesized MnO_2 nanoparticles, c) FTIR spectrum presenting the characteristic peaks of the synthesized nanoparticles, d) size and e) ζ-potential (surface charge) distributions of the synthesized nanoparticles, respectively.*

3.3.2. Fabrication of MnO_2-decorated $CaCO_3$ template

For the fabrication of $CaCO_3$ sacrificial template, $CaCl_2$ and Na_2CO_3 salts were mixed in the presence of PSS. The process resulted in vaterite-like spherical particles with a porous surface and a slightly uniform size distribution (**Fig. 3.3a**). The obtained microparticles had a mean diameter size of 2.73 ± 1.0 µm (**Fig. 3.3d, left**). The addition of PSS plays a pivotal role in the fabrication of the $CaCO_3$ sacrificial template, preventing the recrystallization of the microparticles to calcite-like structure[29] and endowing this $CaCO_3$ template with stability. Furthermore, PSS helps in the achievement of a narrower particle diameter distribution and a strong negative surface charge, which would improve the subsequent incorporation of positively charged MnO_2 nanoparticles through electrostatic interactions. Although alternative templates (e.g., polystyrene beads, silica nanoparticles) could yield smaller particles with a narrower distribution of sizes, the use of $CaCO_3$ microparticles brings the opportunity to fabricate capsules by

using mild conditions (i.e., avoiding the use of organic solvents and/or extremely acidic/basic conditions for core removal). This is vital to preserve the integrity of the assembled layers. Great efforts are being made to improve the polydispersity of $CaCO_3$-based templates by using, among others, PSS, ethylene glycol (EG) or glycerol as additional reagents in the precipitation reaction.[30-33]

After the incubation process of the $CaCO_3$ sacrificial templates with the MnO_2 nanoparticles, particles of 2.99 ± 1.1 µm (**Fig. 3.3d, right**) were obtained. No significant differences were observed in size distribution and morphology between the MnO_2-decorated $CaCO_3$ templates and non-decorated templates (**Fig. 3.3a and 3.3b**). The successful incorporation of MnO_2 in the sacrificial template was confirmed by XRD analysis, where diffraction peaks at 19° and 38° associated to MnO_2 appeared in the diffractogram (**Fig. 3.3c**).

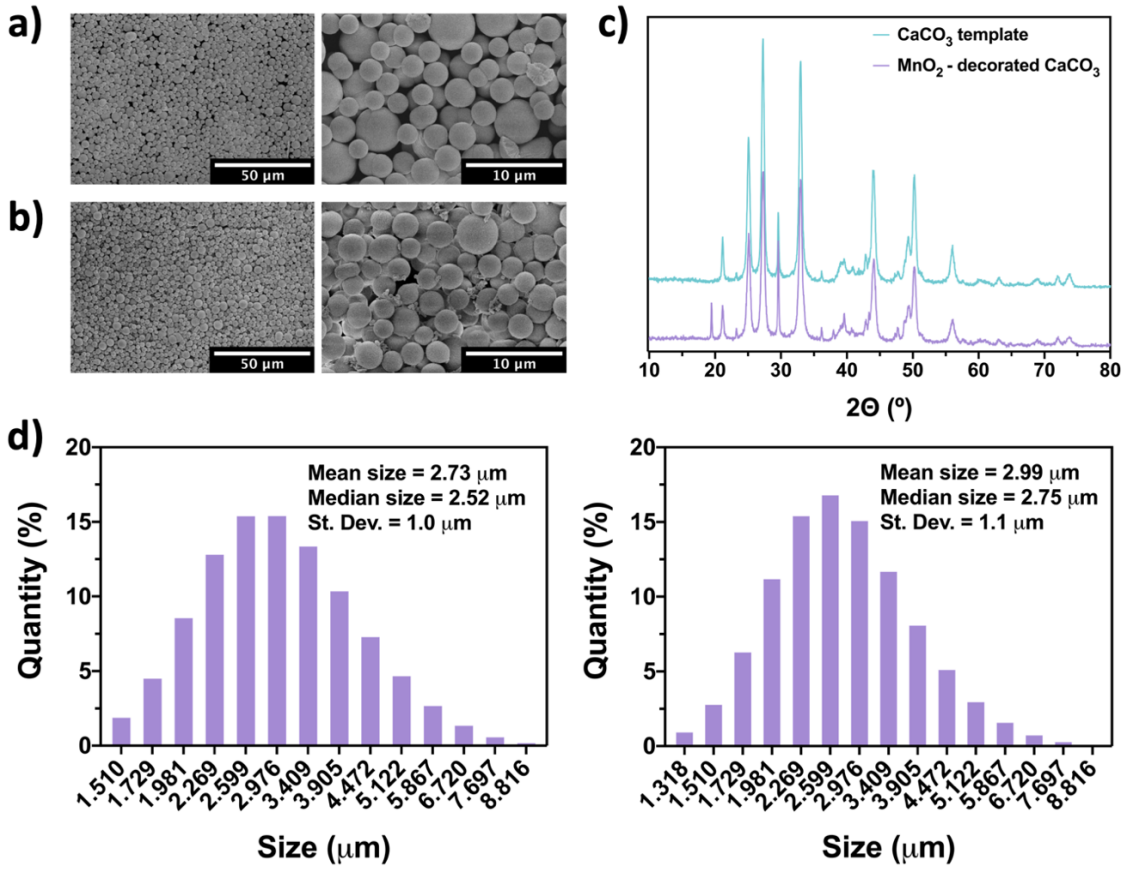

Fig. 3.3. *Morphological characterization via SEM (a,b) of $CaCO_3$ templates (a) and MnO_2-decorated $CaCO_3$ templates (b). c) XRD spectra of the sacrificial template. d) Size distribution of $CaCO_3$ microparticles (left) and MnO_2-decorated $CaCO_3$ microparticles (right).*

As the adsorbed MnO_2 quantity will affect the H_2O_2 scavenging capacity, the ratio 4 mg MnO_2: 10 mg $CaCO_3$ microparticles was chosen to maximize the adsorbed MnO_2 quantity. To optimize this ratio, $CaCO_3$ microparticles were incubated with different amounts of MnO_2 nanoparticles (e.g., 2, 4, 8 and 10 mg of MnO_2 with 10 mg of $CaCO_3$ microparticles) and after the dissolution of the template with EDTA a similar MnO_2 adsorption was observed at all the studied ratios (**Fig. 3.4**), suggesting that an excess of MnO_2 that ensures maximum MnO_2 adsorption was employed in all the cases.

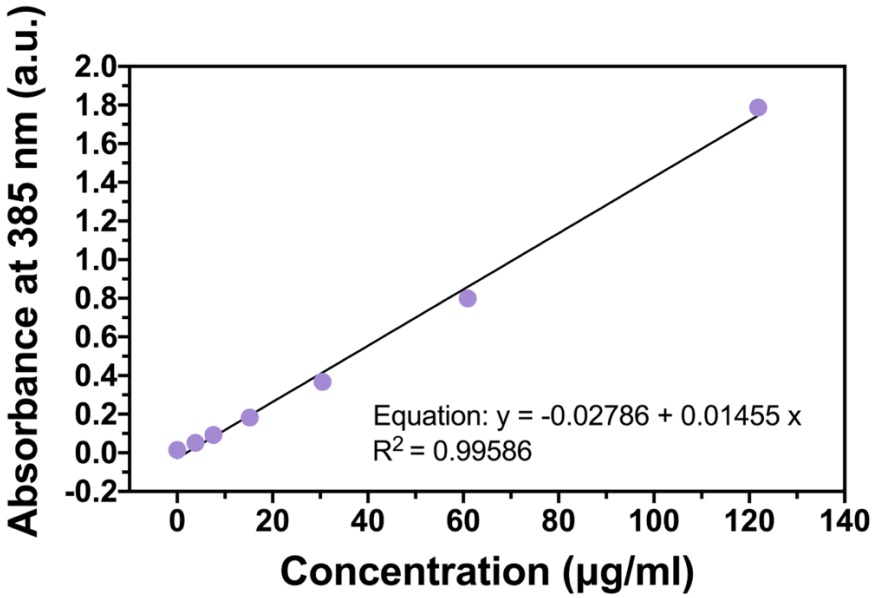

	Adsorbed MnO_2 (µg)				
Concentration	**M1**	**M2**	**M3**	**Mean (µg)**	**SD**
2:10	124.7	125.5	86.5	112.2	22.3
4:10	98.7	117.9	97.2	104.6	11.5
8:10	99.5	135.1	-	117.3	25.2
10:10	143.1	155.1	121.3	139.8	17.2

Fig. 3.4. *Calibration curve of different MnO_2 concentrations at 385 nm (above)Amount of adsorbed MnO_2 (µg) in 10 mg of $CaCO_3$ template at different MnO_2:$CaCO_3$ ratios (2:10, 4:10, 8:10, 10:10) (below).*

3.3.3. Fabrication of capsules *via* de layer-by-layer approach

For the fabrication of polymer capsules, positively charged PAH and negatively charged PSS were deposited alternately onto $CaCO_3$ cores. These polyelectrolytes were chosen

for the formation of the shell, due to their active use, as model polyelectrolytes, in the fabrication of different therapeutic systems.[34-37] In the development of advanced materials for biomedical applications, the use of biodegradable polymers such as chitosan and alginate are highly desirable. However, for the particular application of polymer capsules as nano- and microreactors, a fast degradation of the polymeric shell could be detrimental. Therefore, a timely degradation of the polymer capsule while ensuring the diffusion of reagents and by-products through the polymeric shell should be ensured, which can be achieved by the precise control of the crosslinking degree.

The initial surface charge of the $CaCO_3$ template was positive in the case of MnO_2-decorated sacrificial templates, whereas it was negative in the non-decorated templates. MnO_2-decorated $CaCO_3$ microparticles were first incubated with PSS and the surface charge shifted from +5.0 mV to -21.5 mV (**Fig. 3.5c**). In the case of $CaCO_3$ microparticles without MnO_2, the first layer was made of PAH and the ζ–potential value changed from -17.7 mV to -1.7 mV (**Fig. 3.5c**). Thereafter, polyelectrolyte layers were assembled alternately and a sequential charge reversal was observed in the ζ–potential, demonstrating the successful assembly of the layers (**Fig. 3.5c**).

After the LbL process, the $CaCO_3$ sacrificial template was removed by the immersion of the microparticles in 0.1 M EDTA. As observed by SEM (**Fig. 3.5a and 3.5b**), after the EDTA incubation, the capsules were hollow, owing to their collapsed shape. To confirm the complete removal of the sacrificial template, FTIR and EDS spectra were acquired. In the FTIR spectra (**Fig. 3.5f**), the two main bands of the $CaCO_3$ at 1384 cm^{-1} and 870 cm^{-1} were observed before the EDTA immersion. After the EDTA addition, these bands disappeared and only the characteristic bands of PAH and PSS were detected. In the EDS (**Fig. 3.5d and 3.5e**), no traces of calcium were observed in the spectrum after the EDTA addition, confirming the complete removal of the template.

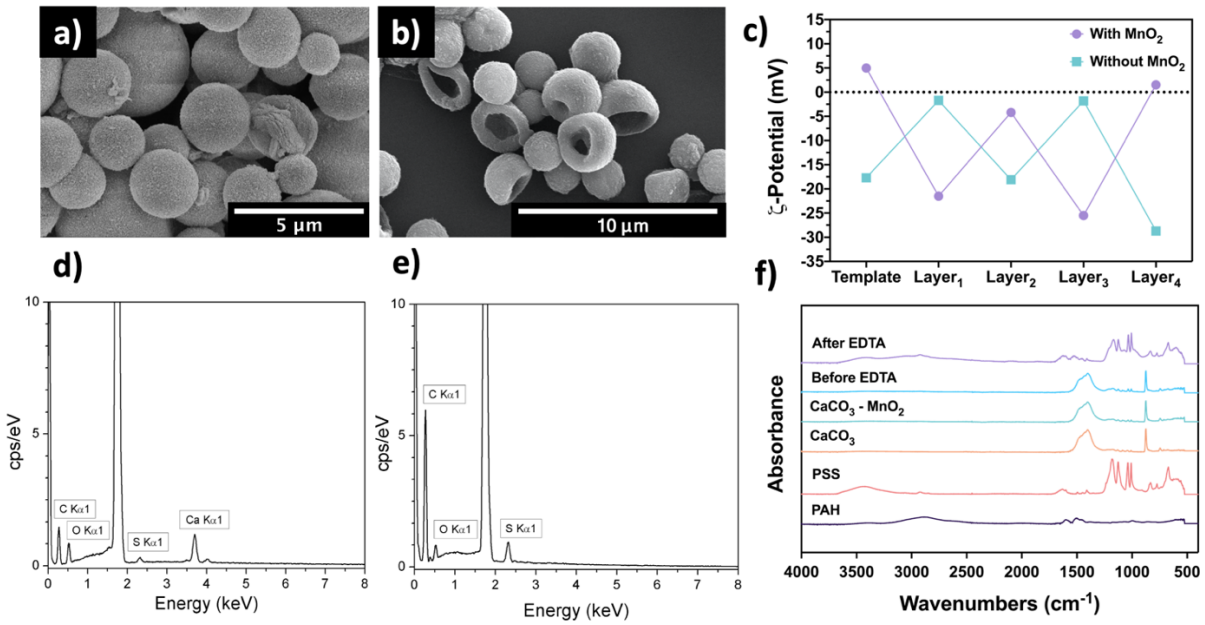

Fig. 3.5. *Morphological characterization via SEM (a and b) of polymer capsules a) before and b) after 0.1 M EDTA addition. c) ζ–potential of $CaCO_3$ microparticles and MnO_2-decorated microparticles after each polyelectrolyte deposition. EDS spectra of polymer capsules d) before and e) after 0.1 M EDTA addition. f) FTIR spectra of polymer capsules before and after 0.1 M EDTA addition.*

The resulting hollow polymer capsules were incubated with two biologically relevant H_2O_2 concentrations (10 µM and 50 µM) at a final concentration of $1{\cdot}10^5$, $1{\cdot}10^6$, $1{\cdot}10^7$, $1{\cdot}10^8$ polymer capsules/mL for 30 min to assess their antioxidant capacity. At the 50 µM H_2O_2 concentration, a significant ($p<0.05$) decrease in the H_2O_2 concentration was observed only in the case of $1{\cdot}10^8$ capsules/mL (from 100 ± 6% to 45 ± 3%) (**Fig. 6a**). At the 10 µM H_2O_2 concentration, significant decreases ($p<0.05$) in the H_2O_2 concentration were observed with the concentrations of $1{\cdot}10^6$, $1{\cdot}10^7$ and $1{\cdot}10^8$ polymer capsules/mL, from the initial value of 100 ± 6% to 84 ± 4%, 64 ± 2% and 6 ± 1%, respectively (**Fig. 3.6a**). Taken together, these results confirm the H_2O_2 scavenging capacity of the developed capsules. The reaction between the MnO_2 nanoparticles embedded in the polymer capsules and H_2O_2 results in the generation of O_2 as previously reported.[1,3,38-40]

To test the regeneration capacity of the capsules to scavenge H_2O_2, capsules were subjected to several H_2O_2 scavenging cycles. Capsules were incubated with two different H_2O_2 concentrations (10 and 50 µM) in four subsequent cycles at a concentration of $1{\cdot}10^8$ capsules/mL. The supernatant of each incubation was collected to analyse the

H_2O_2 reduction capacity (**Fig. 3.6b**), considering 100% reduction capacity the reduction observed in the first cycle. In both cases, a significant decrease ($p<0.05$) of the H_2O_2 scavenging capacity was observed after the second cycle. However, the capsules were able to maintain a 34 ± 6% and 58 ± 1% of their activity after the fourth cycle for the H_2O_2 concentrations of 50 and 10 μM, respectively.

To analyse the effect of sterilization on the scavenging capacity, the capsules were sterilized with ethanol and subsequently incubated with 10 μM H_2O_2 at different concentrations ($1{\cdot}10^7$ and $1{\cdot}10^8$ polymer capsules/mL). In the case of $1{\cdot}10^7$ capsules/mL, there was a significant decrease ($p<0.05$) in the H_2O_2 scavenging capacity of the sterilized capsules with respect to the non-sterilized ones (**Fig. 3.6c**). This can be associated to the reversible reorganization of the polyelectrolytes in the water/ethanol mixture that causes an increased permeability of the shell and subsequent loss of MnO_2 nanoparticles from the interior of the capsule.[41] Nevertheless, capsules were able to maintain a 69 ± 6% H_2O_2 scavenging capacity after their sterilization with ethanol. At $1{\cdot}10^8$ capsules/mL, no significant change ($p<0.05$) in the scavenging capacity was observed after the sterilization process. Therefore, the stability of the capsules facing different processes is significant and ensures the utility of these capsules in the disease treatment.

The leakage of MnO_2 nanoparticles was confirmed by incubating polymer capsules in PBS and measuring the concentration of MnO_2 nanoparticles in the supernatant by means of UV-VIS at different time points (i.e., day 1, 2 and 3). It was observed that almost all the loaded MnO_2 (104.6 ± 11.5 μg) was released after three days in PBS (**Fig. 3.7**), suggesting an increased permeability of the polymer shell that contributes to the leakage of the embedded nanoparticles.

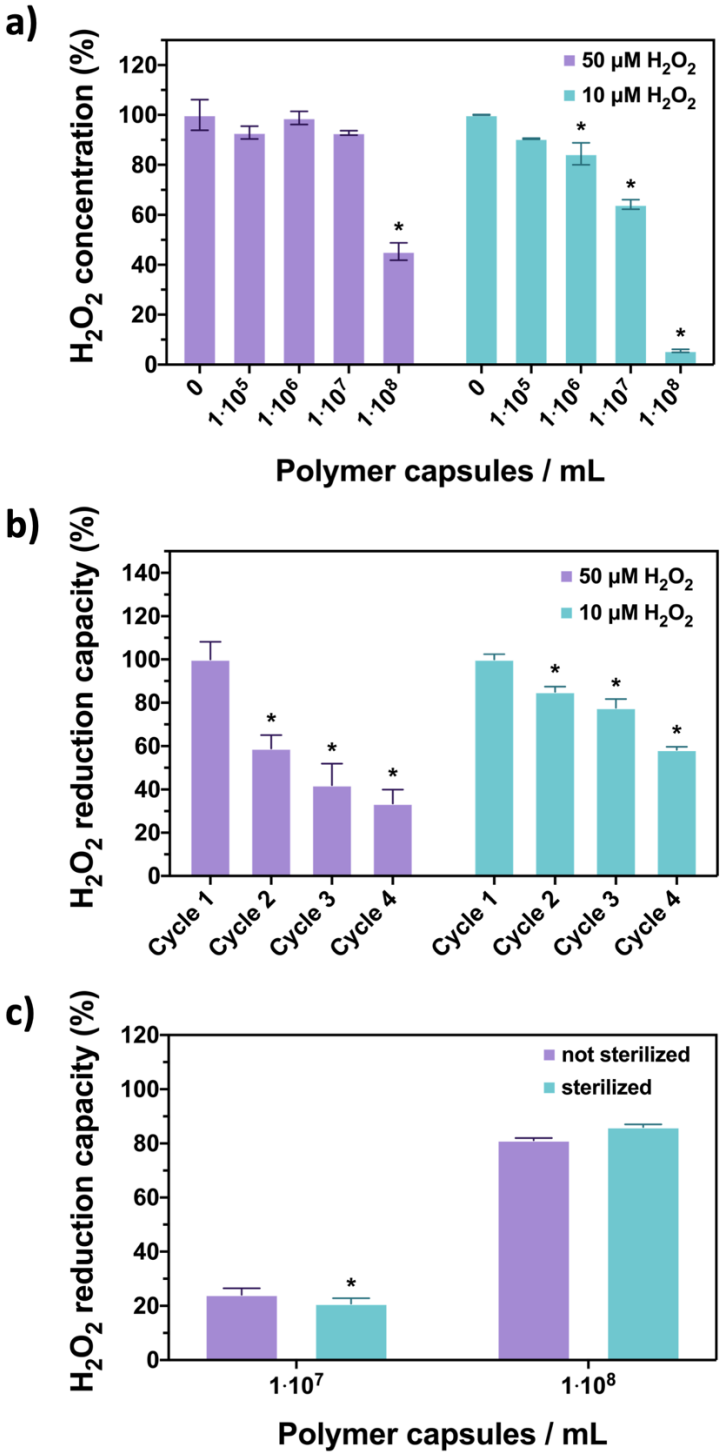

Fig. 3.6. *a) H_2O_2 scavenging capacity of the polymer capsules at biologically relevant H_2O_2 concentrations (10 µM and 50 µM). b) H_2O_2 scavenging capacity of the polymer capsules after four H_2O_2 (10 µM and 50 µM) cycles. Capsules were incubated at a concentration of $1{\cdot}10^8$ capsules/mL and it was considered 100% reduction capacity the reduction obtained in the first cycle. c) H_2O_2 scavenging capacity of the polymer capsules at 10 µM H_2O_2 after the sterilization process. Asterisks (*) indicate significant differences ($p<0.05$) with respect to each control (0 capsules/mL in (a), cycle 1 in (b), non-sterilized capsules in (c)).*

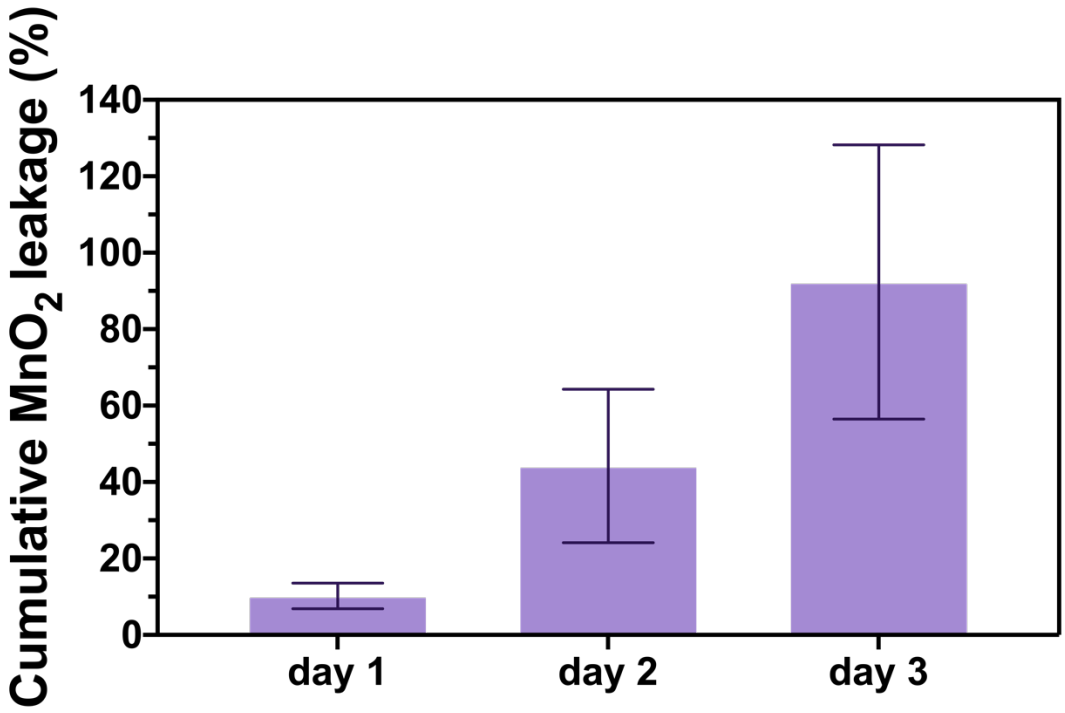

Fig. 3.7. *MnO_2 nanoparticle leakage in PBS.*

3.3.4. Metabolic activity of HeLa cells in the presence of capsules and capsule internalization

To evaluate the *in vitro* cytocompatibility of the developed capsules, either positively (i.e., PSS-PAH-PSS-PAH) or negatively charged (PSS-PAH-PSS-PAH-PSS) capsules were incubated with HeLa cells at different capsule per cell ratios (10, 100, 1000 capsules/cell) and the metabolic activity of cells was measured after one and three days by means of AlamarBlue® assay. In the case of positively charged capsules, a significant decrease ($p<0.05$) in the metabolic activity of cells was observed after one day of incubation at all the studied ratios (**Fig. 3.8a**). Note that the metabolic activity was below the threshold value (i.e., 70%) in the cases of 100 and 1000 capsules/cell. In contrast, cells were able to maintain higher metabolic activities in the presence of negatively charged capsules and, in this case, the metabolic activity of the cells was above 79 ± 7% in all the cases (**Fig. 3.8a**).

At day three, no significant differences ($p<0.05$) were observed in the metabolic activity of cells in the presence of 10 capsules/cell with respect to the control (i.e., in the absence

of capsules). The metabolic activity of cells was below the threshold value (i.e., 70%) at 100 and 1000 capsules/cell in the case of positively charged capsules. In contrast, cells were able to maintain a metabolic activity >81 ± 5% at 100 capsules/cell in the case of negatively charged capsules and only in the case of 1000 capsules/cell the metabolic activity was below the threshold value (i.e., 70%). Taken together, the results indicate a lower cytotoxicity of the negatively charged capsules with respect to the positively charged ones. Regarding the Mn^{2+} production after the reaction with H_2O_2, it has been reported that an excessive and chronic exposure to high concentrations and the accumulation of manganese can lead to neurotoxicity and irreversible brain disease.[40,42-44] Despite this controversial effects, other studies suggest that Mn^{2+} ions can be physically metabolized without a long retention in the body and any toxic effect.[28,45,46] Furthermore, as demonstrated by the cytotoxic evaluation, the amount of manganese used in this work (5.2 μg/well) is not enough to induce any cytotoxic effect.

To determine the uptake and distribution of the capsules in the cellular microenvironment, polymer capsules were observed under optical and fluorescence microscope. As observed in **Fig. 3.8b**, negatively charged capsules were uniformly distributed and few capsules were attached to the cells. In contrast, positively charged capsules were accumulated generally around the cells (**Fig. 3.8b, right**). For the fluorescence microscope analysis, capsules were fabricated using FITC-labelled PAH. **Fig. 3.8c** shows the internalization of the negatively and positively charged capsules, respectively. In both cases, few capsules were localized in the cytoplasm and showed a collapsed shape, whereas some other capsules were observed around the cell membrane retaining their spherical shape. Based on the micrographs obtained with the fluorescent microscope, the differences between positively and negatively charged polymer capsules were not relevant. We believe that the polymer capsules developed in this work primarily reduce the ROS from the extracellular microenvironment. The uptake of the capsules for an efficient reduction of intracellular ROS could be promoted by using either smaller capsules or surface functionalization strategies.[47-49]

The obtained results in the metabolic activity analysis and the internalization and distribution demonstrate that, as reported in bibliography, positively charged capsules are preferably taken up or attached to the cells but they induce a higher cytotoxic

response.[50] The cytoplasmic membrane of cells is typically negatively charged. Consequently, positively charged capsules display a higher cellular binding as it is observed in the obtained results.[51,52] As observed in the fluorescent micrographs, most of the capsules were accumulated preferably around the cellular membrane and low internalization was observed.

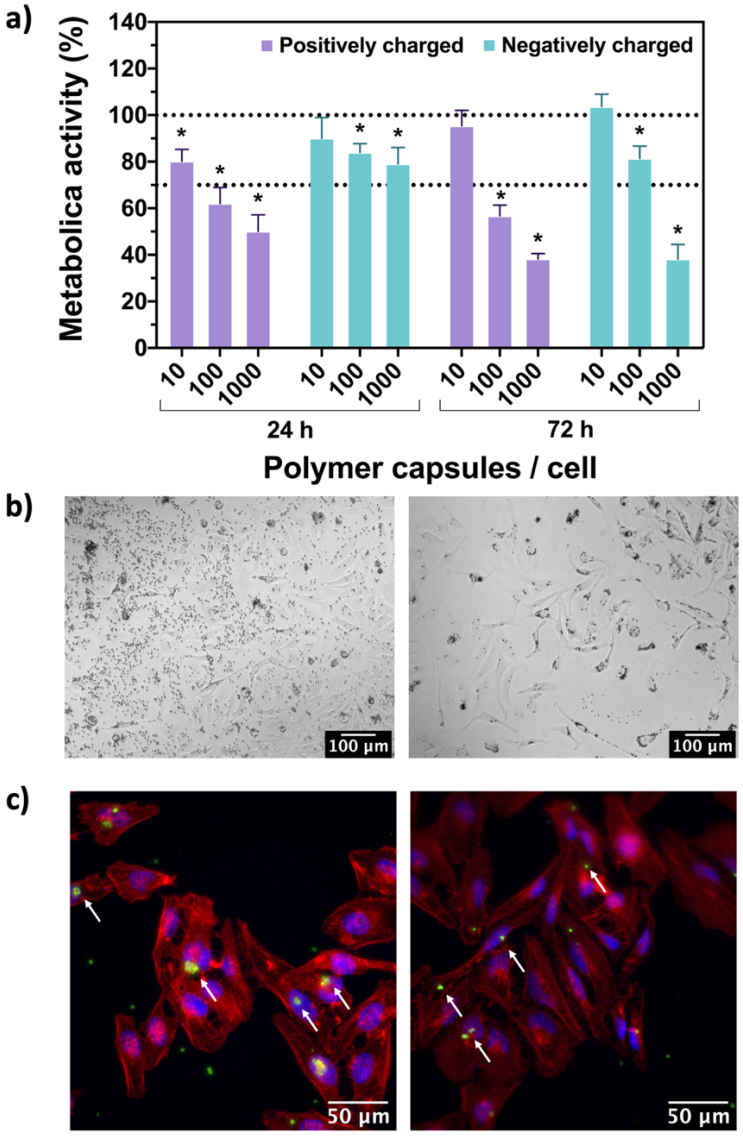

Fig. 3.8. *a) Metabolic activity of HeLa cells in the presence of polymer capsules. Asterisks (*) indicate significant differences (p<0.05) with respect to the control (0 capsules/mL). b) Distribution of negatively (left) and positively (right) charged polymer capsules in the cellular microenvironment. c) Fluorescent micrographs of HeLa cells in the presence of negatively (left) and positively (right) charged polymer capsules (Nuclei-DAPI: Blue / Actin filaments-Rhodamine Phalloidin: Red / Polymer capsules-FITC: Green). White arrows highlight the presence of FITC-labelled polymer capsules.*

3.3.5. Therapeutic potential of the polymer capsules in a H_2O_2-induced oxidative stress *in vitro* model

The therapeutic potential of the polymer capsules was evaluated in a H_2O_2-induced *in vitro* model with positively and negatively charged capsules. In this model, 100 µM H_2O_2 stimuli were added every 12 hours to the cells to induce oxidative stress. Metabolic activity of the cells was measured by the AlamarBlue® assay at the selected time points (8, 24 and 32 h after the first stimulus). The concentration of the H_2O_2 stimuli (100 µM) was chosen after an analysis of different H_2O_2 concentrations to ensure an extreme situation which can cause cell death and/or significant reduction in the observed metabolic activity. As a negative control, HeLa cells were cultured in the absence of capsules and H_2O_2 stimuli. As a positive control, HeLa cells in the absence of capsules but with 100 µM H_2O_2 stimuli were used.

As expected from the previously performed *in vitro* cytocompatibility test (**Fig. 3.8a**), the positively charged capsules had a detrimental effect on the metabolic activity of cells at the higher ratios (i.e., 100 and 1000 capsules/cell), thus limiting their therapeutic potential (**Fig. 3.9**). The metabolic activity of the cells at 8 h and 24 h in the presence of capsules was not significantly different ($p<0.05$) with respect to the controls, with the exception of the positively charged capsules at the concentrations of 100 and 1000 capsules/cell and negatively charged capsules at the concentration of 1000 capsules/cell. In these cases, a significant decrease ($p<0.05$) in the metabolic activity was observed with respect to the negative control (**Fig. 3.9**).

At 24 h, a significant difference ($p<0.05$) was observed between the positive and negative control, which became larger at 32 h due to the induced oxidative stress (**Fig. 3.9**). Interestingly, the addition of positively charged capsules at a concentration of 10 capsules/cell and negatively charged capsules at a concentration of 10 or 100 capsules/cell resulted in a significant increase ($p<0.05$) in the metabolic activity with respect to the positive control, thus suggesting a protective effect towards oxidative stress. In view of these results, to obtain an efficient therapeutic effect against the overproduction of H_2O_2, both the concentration and surface charge of the capsules should be carefully considered.

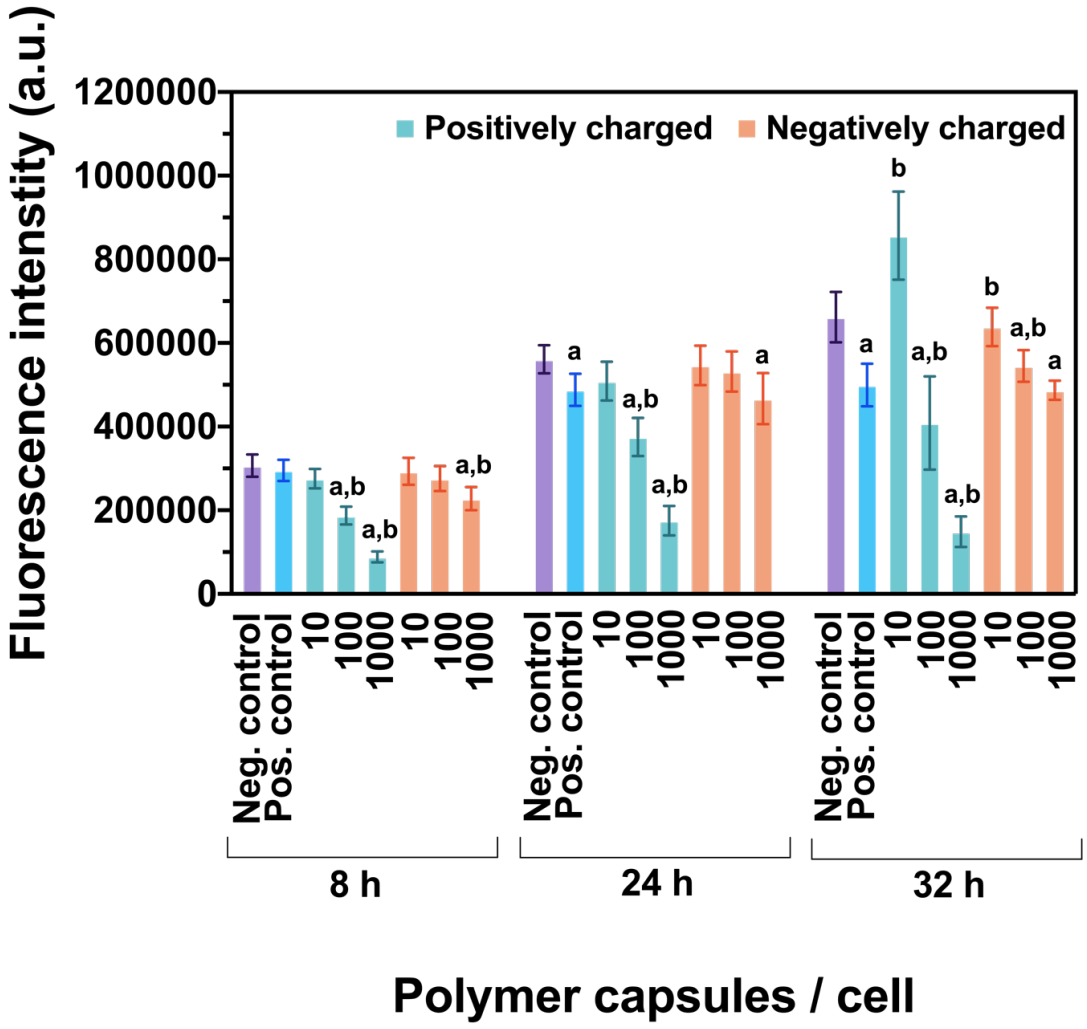

Fig. 3.9. *Metabolic activity of HeLa cells in the presence of H_2O_2 stimuli (100 µM) and polymer capsules. The "a" and "b" indicate significant differences ($p<0.05$) with respect to the negative (cells in the absence of capsules and H_2O_2) and the positive control (cells in the absence of capsules but with the addition of H_2O_2), respectively (n=6).*

3.4. Conclusions

In the present chapter, we fabricated MnO_2-loaded polymer capsules *via* the LbL approach. The developed capsules acted as antioxidant microreactors and were able to reduce H_2O_2 from solution at biologically relevant concentrations. The capsules were robust, as demonstrated by their capacity to scavenge H_2O_2 from solution after several cycles and after being sterilized with ethanol. The stability towards ethanol sterilization is of particular interest for the potential use of these capsules in biomedical applications. The cytocompatibility of the developed capsules was assessed *in vitro*, where significant differences between the positively and negatively charged capsules were observed. Positively charged capsules were accumulated around the cells and caused a detrimental effect on their metabolic activity at the higher concentrations (100 and 1000 capsules/cell), thus limiting their therapeutic potential. In contrast, negatively charged capsules were uniformly distributed in the cellular microenvironment and preserved the metabolic activity of cells better. In the developed H_2O_2-induced oxidative stress model, some beneficial response was observed for the concentration of 10 capsules/cell in positively charged capsules and for 10 and 100 capsules/cell in negatively charged capsules. This study represents a novel strategy for the fabrication of antioxidant polymer microreactors, where the traditional encapsulation of antioxidant enzymes has been replaced by manganese dioxide nanoparticles, thus providing a more robust and stable inorganic alternative.

References

(1) Tapeinos, C.; Larrañaga, A.; Sarasua, J. R.; Pandit, A. Functionalised Collagen Spheres Reduce H_2O_2 Mediated Apoptosis by Scavenging Overexpressed ROS. *Nanomedicine Nanotechnology, Biol. Med.* **2018**, *14* (7), 2397–2405. https://doi.org/10.1016/j.nano.2017.03.022.

(2) De Gracia Lux, C.; Joshi-Barr, S.; Nguyen, T.; Mahmoud, E.; Schopf, E.; Fomina, N.; Almutairi, A. Biocompatible Polymeric Nanoparticles Degrade and Release Cargo in Response to Biologically Relevant Levels of Hydrogen Peroxide. *J. Am. Chem. Soc.* **2012**, *134* (38), 15758–15764. https://doi.org/10.1021/ja303372u.

(3) Pereira, D. R.; Tapeinos, C.; Rebelo, A. L.; Oliveira, J. M.; Reis, R. L.; Pandit, A. Scavenging Nanoreactors That Modulate Inflammation. *Adv. Biosyst.* **2018**, *2* (6), 1–13. https://doi.org/10.1002/adbi.201800086.

(4) Van De Bittner, G. C.; Dubikovskaya, E. A.; Bertozzi, C. R.; Chang, C. J. *In Vivo* Imaging of Hydrogen Peroxide Production in a Murine Tumor Model with a Chemoselective Bioluminescent Reporter. *Proc. Natl. Acad. Sci. U. S. A.* **2010**, *107* (50), 21316–21321. https://doi.org/10.1073/pnas.1012864107.

(5) Larrañaga, A.; Lomora, M.; Sarasua, J. R.; Palivan, C. G.; Pandit, A. Polymer Capsules as Micro-/Nanoreactors for Therapeutic Applications: Current Strategies to Control Membrane Permeability. *Prog. Mater. Sci.* **2017**, *90*, 325–357. https://doi.org/10.1016/j.pmatsci.2017.08.002.

(6) Donatan, S.; Yashchenok, A.; Khan, N.; Parakhonskiy, B.; Cocquyt, M.; Pinchasik, B. El; Khalenkow, D.; Möhwald, H.; Konrad, M.; Skirtach, A. Loading Capacity versus Enzyme Activity in Anisotropic and Spherical Calcium Carbonate Microparticles. *ACS Appl. Mater. Interfaces* **2016**, *8* (22), 14284–14292. https://doi.org/10.1021/acsami.6b03492.

(7) Ping, Y.; Guo, J.; Ejima, H.; Chen, X.; Richardson, J. J.; Sun, H.; Caruso, F. PH-Responsive Capsules Engineered from Metal-Phenolic Networks for Anticancer Drug Delivery. *Small* **2015**, *11* (17), 2032–2036. https://doi.org/10.1002/smll.201403343.

(8) Schneider, G.; Decher, G. Functional Core/Shell Nanoparticles *via* Layer-by-Layer Assembly. Investigation of the Experimental Parameters for Controlling Particle Aggregation and for Enhancing Dispersion Stability. *Langmuir* **2008**, *24* (5), 1778–1789. https://doi.org/10.1021/la7021837.

(9) Boehnke, N.; Correa, S.; Hao, L.; Wang, W.; Straehla, J. P.; Bhatia, S. N.; Hammond, P. T. Theranostic Layer-by-Layer Nanoparticles for Simultaneous Tumor Detection and Gene Silencing. *Angew. Chemie - Int. Ed.* **2020**, *02115*, 2–10. https://doi.org/10.1002/anie.201911762.

(10) Timin, A. S.; Muslimov, A. R.; Zyuzin, M. V.; Peltek, O. O.; Karpov, T. E.; Sergeev, I. S.; Dotsenko, A. I.; Goncharenko, A. A.; Yolshin, N. D.; Sinelnik, A.; Krause, B.; Baumbach, T.; Surmeneva, M. A.; Chernozem, R. V.; Sukhorukov, G. B.; Surmenev, R. A. Multifunctional Scaffolds with Improved Antimicrobial Properties and Osteogenicity Based on Piezoelectric Electrospun Fibers Decorated with Bioactive Composite Microcapsules. *ACS Appl. Mater. Interfaces* **2018**, *10* (41), 34849–34868. https://doi.org/10.1021/acsami.8b09810.

(11) Valdepérez, D.; del Pino, P.; Sánchez, L.; Parak, W. J.; Pelaz, B. Highly Active Antibody-Modified Magnetic Polyelectrolyte Capsules. *J. Colloid Interface Sci.* **2016**, *474*, 1–8. https://doi.org/10.1016/j.jcis.2016.04.003.

(12) Gao, H.; Wen, D.; Tarakina, N. V.; Liang, J.; Bushby, A. J.; Sukhorukov, G. B. Bifunctional Ultraviolet/Ultrasound Responsive Composite TiO_2/Polyelectrolyte Microcapsules. *Nanoscale* **2016**, *8* (9), 5170–5180. https://doi.org/10.1039/c5nr06666b.

(13) Gorin, D. A.; Portnov, S. A.; Inozemtseva, O. A.; Luklinska, Z.; Yashchenok, A. M.; Pavlov, A. M.; Skirtach, A. G.; Möhwald, H.; Sukhorukov, G. B. Magnetic/Gold Nanoparticle Functionalized Biocompatible Microcapsules with Sensitivity to Laser Irradiation. *Phys. Chem. Chem. Phys.* **2008**, *10* (45), 6899–6905. https://doi.org/10.1039/b809696a.

(14) Pavlov, A. M.; Saez, V.; Cobley, A.; Graves, J.; Sukhorukov, G. B.; Mason, T. J. Controlled Protein Release from Microcapsules with Composite Shells Using High Frequency Ultrasound - Potential for in Vivo Medical Use. *Soft Matter* **2011**, *7* (9),

4341–4347. https://doi.org/10.1039/c0sm01536a.

(15) Timin, A. S.; Muslimov, A. R.; Lepik, K. V.; Epifanovskaya, O. S.; Shakirova, A. I.; Mock, U.; Riecken, K.; Okilova, M. V.; Sergeev, V. S.; Afanasyev, B. V.; Fehse, B.; Sukhorukov, G. B. Efficient Gene Editing *via* Non-Viral Delivery of CRISPR–Cas9 System Using Polymeric and Hybrid Microcarriers. *Nanomedicine Nanotechnology, Biol. Med.* **2018**, *14* (1), 97–108. https://doi.org/10.1016/j.nano.2017.09.001.

(16) Timin, A. S.; Muslimov, A. R.; Lepik, K. V.; Okilova, M. V.; Tcvetkov, N. Y.; Shakirova, A. I.; Afanasyev, B. V.; Gorin, D. A.; Sukhorukov, G. B. Intracellular Breakable and Ultrasound-Responsive Hybrid Microsized Containers for Selective Drug Release into Cancerous Cells. *Part. Part. Syst. Charact.* **2017**, *34* (5), 1–10. https://doi.org/10.1002/ppsc.201600417.

(17) Voronin, D. V.; Sindeeva, O. A.; Kurochkin, M. A.; Mayorova, O.; Fedosov, I. V.; Semyachkina-Glushkovskaya, O.; Gorin, D. A.; Tuchin, V. V.; Sukhorukov, G. B. *In vitro* and *in vivo* Visualization and Trapping of Fluorescent Magnetic Microcapsules in a Bloodstream. *ACS Appl. Mater. Interfaces* **2017**, *9* (8), 6885–6893. https://doi.org/10.1021/acsami.6b15811.

(18) German, S. V.; Bratashov, D. N.; Navolokin, N. A.; Kozlova, A. A.; Lomova, M. V.; Novoselova, M. V.; Burilova, E. A.; Zyev, V. V.; Khlebtsov, B. N.; Bucharskaya, A. B.; Terentyuk, G. S.; Amirov, R. R.; Maslyakova, G. N.; Sukhorukov, G. B.; Gorin, D. A. *In vitro* and *in vivo* MRI Visualization of Nanocomposite Biodegradable Microcapsules with Tunable Contrast. *Phys. Chem. Chem. Phys.* **2016**, *18* (47), 32238–32246. https://doi.org/10.1039/C6CP03895F.

(19) Larrañaga, A.; Isa, I. L. M.; Patil, V.; Thamboo, S.; Lomora, M.; Fernández-Yague, M. A.; Sarasua, J. R.; Palivan, C. G.; Pandit, A. Antioxidant Functionalized Polymer Capsules to Prevent Oxidative Stress. *Acta Biomater.* **2018**, *67*, 21–31. https://doi.org/10.1016/j.actbio.2017.12.014.

(20) Popov, A. L.; Popova, N.; Gould, D. J.; Shcherbakov, A. B.; Sukhorukov, G. B.; Ivanov, V. K. Ceria Nanoparticles-Decorated Microcapsules as a Smart Drug Delivery/Protective System: Protection of Encapsulated P. Pyralis Luciferase. *ACS*

Appl. Mater. Interfaces **2018**, *10* (17), 14367–14377. https://doi.org/10.1021/acsami.7b19658.

(21) Wang, Q.; Wei, H.; Zhang, Z.; Wang, E.; Dong, S. Nanozyme: An Emerging Alternative to Natural Enzyme for Biosensing and Immunoassay. *TrAC - Trends Anal. Chem.* **2018**, *105*, 218–224. https://doi.org/10.1016/j.trac.2018.05.012.

(22) Popov, A. L.; Popova, N. R.; Tarakina, N. V.; Ivanova, O. S.; Ermakov, A. M.; Ivanov, V. K.; Sukhorukov, G. B. Intracellular Delivery of Antioxidant CeO_2 Nanoparticles *via* Polyelectrolyte Microcapsules. *ACS Biomater. Sci. Eng.* **2018**, *4* (7), 2453–2462. https://doi.org/10.1021/acsbiomaterials.8b00489.

(23) Li, W.; Liu, Z.; Liu, C.; Guan, Y.; Ren, J.; Qu, X. Manganese Dioxide Nanozymes as Responsive Cytoprotective Shells for Individual Living Cell Encapsulation. *Angew. Chemie - Int. Ed.* **2017**, *56* (44), 13661–13665. https://doi.org/10.1002/anie.201706910.

(24) Bao, Y.-W.; Hua, X.-W.; Zeng, J.; Wu, F.-G. Bacterial Template Synthesis of Multifunctional Nanospindles for Glutathione Detection and Enhanced Cancer-Specific Chemo-Chemodynamic Therapy. *Research* **2020**, *2020*, 9301215. https://doi.org/10.34133/2020/9301215.

(25) Xu, K. F.; Jia, H. R.; Zhu, Y. X.; Liu, X.; Gao, G.; Li, Y. H.; Wu, F. G. Cholesterol-Modified Dendrimers for Constructing a Tumor Microenvironment-Responsive Drug Delivery System. *ACS Biomater. Sci. Eng.* **2019**, *5* (11), 6072–6081. https://doi.org/10.1021/acsbiomaterials.9b01386.

(26) Lin, Y.; Ren, J.; Qu, X. Catalytically Active Nanomaterials: A Promising Candidate for Artificial Enzymes. *Acc. Chem. Res.* **2014**, *47* (4), 1097–1105. https://doi.org/10.1021/ar400250z.

(27) Chen, Q.; Feng, L.; Liu, J.; Zhu, W.; Dong, Z.; Wu, Y.; Liu, Z. Intelligent Albumin–MnO_2 Nanoparticles as pH-/H_2O_2-Responsive Dissociable Nanocarriers to Modulate Tumor Hypoxia for Effective Combination Therapy. *Adv. Mater.* **2016**, *28* (33), 7129–7136. https://doi.org/10.1002/adma.201601902.

(28) Prasad, P.; Gordijo, C. R.; Abbasi, A. Z.; Maeda, A.; Ip, A.; Rauth, M.; Dacosta, R. S.; Wu, X. Y. Multifunctional Albumin - MnO_2 Nanoparticles Modulate Solid Tumor

Microenvironment by Attenuating Enhance Radiation Response. **2014**, No. 4, 3202–3212. https://doi.org/10.1021/nn405773r.

(29) Wang, C.; He, C.; Tong, Z.; Liu, X.; Ren, B.; Zeng, F. Combination of Adsorption by Porous $CaCO_3$ Microparticles and Encapsulation by Polyelectrolyte Multilayer Films for Sustained Drug Delivery. *Int. J. Pharm.* **2006**, *308* (1–2), 160–167. https://doi.org/10.1016/j.ijpharm.2005.11.004.

(30) Cai, A.; Xu, X.; Pan, H.; Tao, J.; Liu, R.; Tang, R.; Cho, K. Direct Synthesis of Hollow Vaterite Nanospheres from Amorphous Calcium Carbonate Nanoparticles *via* Phase Transformation. *J. Phys. Chem. C* **2008**, *112* (30), 11324–11330. https://doi.org/10.1021/jp801408k.

(31) Facchinetto, S. E.; Bortolotto, T.; Neumann, G. E.; Vieira, J. C. B.; De Menezes, B. B.; Giacomelli, C.; Schmidt, V. Synthesis of Submicrometer Calcium Carbonate Particles from Inorganic Salts Using Linear Polymers as Crystallization Modifiers. *J. Braz. Chem. Soc.* **2017**, *28* (4), 547–556. https://doi.org/10.5935/0103-5053.20160196.

(32) Tarakanchikova, Y.; Alzubi, J.; Pennucci, V.; Follo, M.; Kochergin, B.; Muslimov, A.; Skovorodkin, I.; Vainio, S.; Antipina, M. N.; Atkin, V.; Popov, A.; Meglinski, I.; Cathomen, T.; Cornu, T. I.; Gorin, D. A.; Sukhorukov, G. B.; Nazarenko, I. Biodegradable Nanocarriers Resembling Extracellular Vesicles Deliver Genetic Material with the Highest Efficiency to Various Cell Types. *Small* **2019**. https://doi.org/10.1002/smll.201904880.

(33) Trushina, D. B.; Bukreeva, T. V.; Antipina, M. N. Size-Controlled Synthesis of Vaterite Calcium Carbonate by the Mixing Method: Aiming for Nanosized Particles. *Cryst. Growth Des.* **2016**, *16* (3), 1311–1319. https://doi.org/10.1021/acs.cgd.5b01422.

(34) Ashraf, S.; Taylor, A.; Sharkey, J.; Barrow, M.; Murray, P.; Wilm, B.; Poptani, H.; Rosseinsky, M. J.; Adams, D. J.; Lévy, R. *In Vivo* Fate of Free and Encapsulated Iron Oxide Nanoparticles after Injection of Labelled Stem Cells . *Nanoscale Adv.* **2019**, *1* (1), 367–377. https://doi.org/10.1039/c8na00098k.

(35) Luo, D.; Poston, R. N.; Gould, D. J.; Sukhorukov, G. B. Magnetically Targetable

Microcapsules Display Subtle Changes in Permeability and Drug Release in Response to a Biologically Compatible Low Frequency Alternating Magnetic Field. *Mater. Sci. Eng. C* **2019**, *94*, 647–655. https://doi.org/10.1016/j.msec.2018.10.031.

(36) Guo, C.; Wang, J.; Dai, Z. Selective Content Release from Light-Responsive Microcapsules by Tuning the Surface Plasmon Resonance of Gold Nanorods. *Microchim. Acta* **2011**, *173* (3–4), 375–382. https://doi.org/10.1007/s00604-011-0570-y.

(37) Yashchenok, A. M.; Bratashov, D. N.; Gorin, D. A.; Lomova, M. V.; Pavlov, A. M.; Sapelkin, A. V.; Shim, B. S.; Khomutov, G. B.; Kotov, N. A.; Sukhorukov, G. B.; Möhwald, H.; Skirtach, A. G. Carbon Nanotubes on Polymeric Microcapsules: Freestanding Structures and Point-Wise Laser Openings. *Adv. Funct. Mater.* **2010**, *20* (18), 3136–3142. https://doi.org/10.1002/adfm.201000846.

(38) Bizeau, J.; Tapeinos, C.; Marella, C.; Larrañaga, A.; Pandit, A. Synthesis and Characterization of Hyaluronic Acid Coated Manganese Dioxide Microparticles That Act as ROS Scavengers. *Colloids Surfaces B Biointerfaces* **2017**, *159*, 30–38. https://doi.org/10.1016/j.colsurfb.2017.07.081.

(39) Tapeinos, C.; Tomatis, F.; Battaglini, M.; Larrañaga, A.; Marino, A.; Telleria, I. A.; Angelakeris, M.; Debellis, D.; Drago, F.; Brero, F.; Arosio, P.; Lascialfari, A.; Petretto, A.; Sinibaldi, E.; Ciofani, G. Cell Membrane-Coated Magnetic Nanocubes with a Homotypic Targeting Ability Increase Intracellular Temperature Due to ROS Scavenging and Act as a Versatile Theranostic System for Glioblastoma Multiforme. *Adv. Healthc. Mater.* **2019**, *8* (18). https://doi.org/10.1002/adhm.201900612.

(40) Smith, M. R.; Fernandes, J.; Go, Y.; Jones, D. P. Redox Dynamics of Manganese as a Mitochondrial Life-Death Switch Matthew. *Biochem. Biophys. Res. Commun.* **2017**, *482* (3), 388–398. https://doi.org/10.1016/j.bbrc.2016.10.126.Redox.

(41) Lvov, Y.; Antipov, A. A.; Mamedov, A.; Möhwald, H.; Sukhorukov, G. B. Urease Encapsulation in Nanoorganized Microshells. *Nano Lett.* **2001**, *1* (3), 125–128. https://doi.org/10.1021/nl0100015.

(42) Reaney, S. H.; Bench, G.; Smith, D. R. Brain Accumulation and Toxicity of Mn(II) and Mn(III) Exposures. *Toxicol. Sci.* **2006**, *93* (1), 114–124. https://doi.org/10.1093/toxsci/kfl028.

(43) Zhang Danhui, Kanthasamy Arthi, Anantharama Vellareddy, K. A. Effects of Manganese on Tyrosine Hydroxylase (TH) Activity and TH-Phosphorylation in a Dopaminergic Neural Cell Line. *Toxicol. Appl. Pharmacol.* **2008**, *254* (2), 65–71. https://doi.org/10.1038/jid.2014.371.

(44) Afeseh Ngwa, H.; Kanthasamy, A.; Gu, Y.; Fang, N.; Anantharam, V.; Kanthasamy, A. G. Manganese Nanoparticle Activates Mitochondrial Dependent Apoptotic Signaling and Autophagy in Dopaminergic Neuronal Cells. *Toxicol. Appl. Pharmacol.* **2011**, *256* (3), 227–240. https://doi.org/10.1016/j.taap.2011.07.018.

(45) Hu, D. R.; Chen, L. J.; Qu, Y.; Peng, J. R.; Chu, B. Y.; Shi, K.; Hao, Y.; Zhong, L.; Wang, M. Y.; Qian, Z. Y. Oxygen-Generating Hybrid Polymeric Nanoparticles with Encapsulated Doxorubicin and Chlorin E6 for Trimodal Imaging-Guided Combined Chemo-Photodynamic Therapy. *Theranostics* **2018**, *8* (6), 1558–1574. https://doi.org/10.7150/thno.22989.

(46) Xu, K.; Zhang, J.; Xue, W.; Tong, H.; Zhang, W.; Xu, K.; Zhang, J.; Xue, W.; Tong, H.; Zhang, W.; Zhao, Z.; Liu, H. Albumin-Stabilized Manganese-Based Nanocomposites with Sensitive Tumor Microenvironment Responsivity and Their Application for Efficient SiRNA Delivery in Brain Tumors. *J. Mater. Chem. B* **2020**, *8* (7), 1507–1515. https://doi.org/10.1039/c9tb02341k.

(47) Cortez, C.; Tomaskovic-Crook, E.; Johnston, A. P. R.; Radt, B.; Cody, S. H.; Scott, A. M.; Nice, E. C.; Heath, J. K.; Caruso, F. Targeting and Uptake of Multilayered Particles to Colorectal Cancer Cells. *Adv. Mater.* **2006**, *18* (15), 1998–2003. https://doi.org/10.1002/adma.200600564.

(48) El-Sayed, A.; Khalil, I. A.; Kogure, K.; Futaki, S.; Harashima, H. Octaarginine- and Octalysine-Modified Nanoparticles Have Different Modes of Endosomal Escape. *J. Biol. Chem.* **2008**, *283* (34), 23450–23461. https://doi.org/10.1074/jbc.M709387200.

(49) Cui, J.; Ju, Y.; Houston, Z. H.; Glass, J. J.; Fletcher, N. L.; Alcantara, S.; Dai, Q.;

Howard, C. B.; Mahler, S. M.; Wheatley, A. K.; De Rose, R.; Brannon, P. T.; Paterson, B. M.; Donnelly, P. S.; Thurecht, K. J.; Caruso, F.; Kent, S. J. Modulating Targeting of Poly(Ethylene Glycol) Particles to Tumor Cells Using Bispecific Antibodies. *Adv. Healthc. Mater.* **2019**, *8* (9), 1–10. https://doi.org/10.1002/adhm.201801607.

(50) Fröhlich, E. The Role of Surface Charge in Cellular Uptake and Cytotoxicity of Medical Nanoparticles. *Int. J. Nanomedicine* **2012**, *7*, 5577–5591. https://doi.org/10.2147/IJN.S36111.

(51) Johnston, A. P. R.; Such, G. K.; Ng, S. L.; Caruso, F. Challenges Facing Colloidal Delivery Systems: From Synthesis to the Clinic. *Curr. Opin. Colloid Interface Sci.* **2011**, *16* (3), 171–181. https://doi.org/10.1016/j.cocis.2010.11.003.

(52) Zyuzin, M. V.; Timin, A. S.; Sukhorukov, G. B. Multilayer Capsules Inside Biological Systems: State-of-the-Art and Open Challenges. *Langmuir* **2019**, *35* (13), 4747–4762. https://doi.org/10.1021/acs.langmuir.8b04280.

CHAPTER 4.

Smart layer-by-layer polymeric microreactors: pH-triggered drug release and attenuation of cellular oxidative stress as prospective combination therapy

CHAPTER 4. Smart layer-by-layer polymeric microreactors: pH-triggered drug release and attenuation of cellular oxidative stress as prospective combination therapy

Abstract

Polymer capsules fabricated *via* the layer-by-layer (LbL) approach have emerged as promising biomedical systems for the release of a wide variety of therapeutic agents, owing to their tunable and controllable structure and the possibility to include several functionalities in the polymeric membrane during the fabrication process. However, the limitation of the capsules with a single functionality to overcome the challenges involved in the treatment of complex pathologies denotes the need to develop multifunctional capsules capable of targeting several mediators and/or mechanisms. Oxidative stress is caused by the accumulation of reactive oxygen species [e.g., hydrogen peroxide (H_2O_2), hydroxyl radicals (·OH), and superoxide anion radicals $\cdot O_2^-$)] in the cellular microenvironment and is a key modulator in the pathology of a broad range of inflammatory diseases. The disease microenvironment is also characterized by the presence of proinflammatory cytokines, increased levels of matrix metalloproteinases, and acidic pH, all of which could be exploited to trigger the release of therapeutic agents. In the present chapter, multifunctional capsules were fabricated *via* the LbL approach. Capsules were loaded with an antioxidant enzyme (catalase) and functionalized with a model drug (doxorubicin), which was conjugated to an amine-containing dendritic polyglycerol through a pH-responsive linker. These capsules efficiently scavenge H_2O_2 from solution, protecting cells from oxidative stress, and release the model drug in acidic microenvironments.

4.1. Introduction

The Layer-by-Layer (LbL) technique is a simple and versatile method that allows the modification of a wide variety of substrates (e.g., planar structures, fibers, colloidal particles) through the alternate deposition of oppositely charged polyelectrolytes.[1-4] This technique has evolved from the application on planar substrates to colloidal micro- and nanoparticles in the late 1990s thanks to the intensive investigations by Möhwald and collaborators.[5-8] In these pioneering studies, highly charged polyelectrolytes were

deposited onto colloidal particles by taking advantage of their stability, selectivity and permeability.[7,9] The colloidal core was subsequently removed giving rise to hollow polymer capsules.

Recent progresses in the field of bioscience and polymer synthesis allows the fabrication of polymer capsules using alternative biodegradable synthetic and natural polymers, proteins or inorganic nanoparticles, among others, being their properties tunable for the specific biomedical requirements.[2,8,10-12] Thus, taking advantage of this versatility and capability to fabricate polymer capsules with tailor-made properties, capsules have been fabricated for a wide variety of applications, including drug/protein/gene delivery vehicles,[13-16] polymer capsules for imaging applications,[17-19] or micro- and nanoreactors.[19,20-22] The latest contain active entities in their core and allow the diffusion of reagents and by-products through the polymer shell. The active compounds [e.g., enzymes or nanozymes[23] (i.e., synthetic nanomaterials with enzyme-like characteristics)] are protected from the outer microenvironment and act *in situ*.[1,20]

However, in most of these applications, capsules are endowed with a single functionality, which may limit their potential to overcome the challenges involved in the treatment of complex pathologies, and to adapt to patient specific characteristics.[24] This denotes the need to develop multifunctional capsules, which respond to different physiological stimuli and adjust to the individual particularities of the patient.[11,24,25] Excellent examples of such multifunctional capsules are theranostic micro- and nanocapsules, which are capable of simultaneously diagnosing and treating the damaged site, while acting also as imaging agents.[26-30] To impart these advanced functionalities, the polyelectrolytes employed for the fabrication of the polymeric membrane can be modified incorporating several functionalities and (bio)molecules (e.g., drugs, antibodies or proteins) which will respond to specific external or local stimuli.[1,29]

The deconstruction of the capsule is usually required for the efficient triggered delivery of the encapsulated therapeutic agent. Either internal (i.e., local) or external stimuli can facilitate the disruption of the capsule by different mechanisms. For example, a decrease in the pH (e.g., mimicking endosomal pH conditions) cause charge repulsion between the polyelectrolytes, leading to rapid release of the encapsulated cargo.[31] Decorating

the polymeric membrane with magnetic- (e.g., iron oxide nanoparticles[32]), ultrasound- (e.g., gold nanoparticles[14]) and near-infrared-responsive (e.g., graphene oxide[33]) nanoparticles allows the disassembly of the polymeric shell and subsequent release of the encapsulated therapeutic. All these strategies are clearly inappropriate when microcapsules are intended to be used as microreactors. Ideally for the application we intend to pursue, the polymeric capsule should maintain its structural integrity when the complementary drug is released to ensure the protection of the encapsulated enzyme.

In this approach, the use of dendritic polyglycerols (dPG) is envisioned as an unexplored strategy to impart additional functionalities to the capsules while preserving their structural integrity. Dendritic polymers present a high solubility, biocompatibility and a high functionality.[34,35] Hence, a wide variety of active compounds, such as bioactive molecules or targeting moieties can be conjugated to the dPG branches using cleavable bonds which will respond to the stimuli and specific conditions of the damaged area (e.g., acidic pH, overexpressed enzymes or reducing media).[34-37]

When the native cellular regulation of reactive oxygen species (ROS) production (e.g., hydrogen peroxide (H_2O_2), hydroxyl radicals (·OH), superoxide anion radicals ($\cdot O_2^-$)) is overwhelmed, oxidative stress, which is implicated in numerous pathologies such as neurodegeneration, cancer, osteoarthritis or cardiovascular diseases, occurs.[38-40] Furthermore, oxidative stress is usually accompanied by dysregulated inflammatory responses and a reduction in the environmental pH.[40-42] Thus, to overcome the complexity of an oxidative stress microenvironment, multifunctional biomedical systems mentioned above will be of great interest.

In this chapter, it was hypothesized that the LbL approach, in combination with dendritic polyglycerol-drug conjugates, could be exploited to create multifunctional polymer capsules capable of simultaneously reducing the levels of ROS while releasing a model drug in response to a biologically relevant stimulus (i.e., pH). We fabricated multifunctional polymer capsules by depositing alternate layers of poly(sodium 4-styrenesulfonate) (PSS), poly(allylamine hydrochloride) (PAH) and an amine containing dPG conjugated to doxorubicin (dPG-DOX), which was employed as a model drug to test the potential of the system, on a CAT-loaded $CaCO_3$ sacrificial template. DOX was

conjugated to dPG through a pH responsive linker. After the removal of the $CaCO_3$ template, multifunctional capsules were obtained. The physicochemical, morphological, and functional properties of the capsules were thoroughly determined. A preliminary *in vitro* model of oxidative stress with HeLa cells was used to assess the therapeutic potential of the capsules.

4.2. Materials and Methods

4.2.1. Materials

The following reagents were purchased from Thermo Fisher Scientific: Dulbecco's modified Eagle's medium, fetal bovine serum, penicillin−streptomycin, AlamarBlue cell viability reagent, 4',6-diamidino-2-phenylindole dihydrochloride (DAPI), and 16% formaldehyde solution (w/v). Anhydrous dimethyl formamide (DMF) and anhydrous tetrahydrofuran (THF) were obtained from Scharlab. dPG (M_W = 9 KDa, PDI = 1.6 and approximately 121 −OH groups) was prepared according to the published procedure.[43] The hydrazone derivative of doxorubicin (DOX−EMCH, i.e., DOX bound to 3,3'-N-[ε-maleimidocaproic acid]) was prepared as described previously.[44] The other reagents were purchased from Sigma-Aldrich and used as received. PAH and PSS had molecular weights of Mw = 17,500 and 70,000 g/mol, respectively.

4.2.2. Synthesis of dPG-Amine

The synthesis of dPG-amine was carried out in the following steps.[45]

4.2.2.1. Mesylation of dPG

dPG mesylate was synthesized by reacting dendritic polyglycerol with mesyl chloride (MsCl). To a solution of dPG in anhydrous dimethylformamide (DMF) MsCl was added dropwise in ice bath over a period of 30 min under stirring. The resulting mixture was stirred overnight at room temperature. DMF was removed after 12 h and the product was dialyzed against methanol:acetone (70:30) solution for two days changing the solvent twice. The final product, dPG mesylate (dPG-Ms) was obtained as a yellowish oil after complete evaporation of the solvent with 18 mol% degree of functionalization of mesyl groups.

^{1}H NMR (300 MHz, D_2O): δ 4.2-3.4 ppm (m, 5 H, dPG backbone), δ 3.2 (s, 1 H, CH_3, OMs).

4.2.2.2. Azidation of dPG

For the synthesis of dPG azide, dPG-Ms was dissolved in anhydrous DMF with addition of 3 equiv of sodium azide per mesyl group. The mixture was then stirred at 60 ^{o}C for 72 h. The resultant solution was cooled down to room temperature and filtered using celite to remove the unreacted sodium azide. Finally, the product was dialyzed against methanol:chloroform (70:30) solution for 48 h changing the solvent twice. The final product was obtained after evaporation of the solvent. The functionalization of the dPG with azide groups was confirmed with the complete disappearance of the mesyl (CH_3) peaks at 3.2 ppm indicating 15 mol% azide functionalization.

^{1}H NMR (300 MHz, D_2O): δ 4.2-3.5 ppm (m, 5 H, dPG backbone).

4.2.2.3. Amination of dPG

The amination of dPG was carried out by the reduction of azide moieties using triphenyl phosphine (PPh_3) as the reducing agent. The azide functionalized dPG was dissolved in water and 4 equiv of PPh_3 (in THF) per azide group was added twice in a period of 24 h and the reaction was carried out at 40 ^{o}C for 48 h. The resultant solution was filtered to remove PPh_3 salt and dialyzed against methanol for 48 h changing the solvent twice. The functionalization of dPG with 15 mol% amine groups was confirmed with NMR.

^{1}H NMR (300 MHz, D_2O): δ 4.2-3.2 ppm (m, 5 H, dPG backbone), δ 2.8-3.2 ppm (m, 1 H, -CH), δ 2.4-2.8 ppm (m, 2H, -CH_2).

4.2.3. Synthesis of dPG-DOX conjugate

The conjugation of DOX and dPG-amine takes place in two steps in one-pot synthesis. The first step comprises the thiolation of dPG-amine followed by the conjugation of thiolated dPG with DOX-EMCH using hydrazone bond formation. For the thiolation step, dPG-amine (10 mg/mL) was dissolved in 50 mM sodium phosphate (pH 7.0) containing 5 mM EDTA solution followed by the addition of a solution of 2-iminothiolane (1.5 eq per dPG molecule). The mixture was stirred at room temperature for 20 min. After 20 min, a solution of DOX-EMCH (1.2 eq per dPG molecule) in 10 mM sodium phosphate buffer (pH 5.8) was added to the reaction mixture and the solution was stirred at room

temperature for 2 h. The resultant reaction mixture was concentrated using amicon filter (molecular weight cut-off 3 kDa) followed by purification using Sephadex G-25 column chromatography using 10 mM sodium phosphate buffer (pH = 7). Conjugate formation was confirmed by appearance of a faster band on the Sephadex G-25 superfine column. After purification, the conjugate was lyophilized to obtain the product in dry state.

4.2.4. Physicochemical characterization of polymer-drug conjugates

Nuclear magnetic resonance spectroscopy (NMR) was carried out at a frequency of 300 MHz using deuterated water as solvent for all the samples. The ζ-potential measurements and hydrodynamic sizes were performed on a Zetasizer Nano ZS analyzer using Malvern Instrument. Fresh polymer solutions were prepared at 1 mg/mL in 10 mM sodium phosphate buffer. All measurements were done at 25 ^{o}C and pH = 7.4 using a standard rectangular quartz cuvette and for a minimum of 10 runs. Fourier-transform infrared spectroscopy (FTIR) was performed using a Nicolet Avatar 370 operating in the Attenuated Total Reflectance (ATR-FTIR). The spectra of the samples before and after the amination of dPG were taken with a resolution of 2 cm^{-1} and averaged over 64 scans. The amount of conjugated DOX to the dPG backbone was determined by measuring the conjugated drug release at pH = 4.0 using UV-Vis Spectroscopy. All samples were prepared in water of Millipore quality (resistivity 18 MΩ cm^{-1}, pH 5.6 ± 0.2).

4.2.5. Fabrication and characterization of polymer capsules

4.2.5.1. Fabrication of polymer capsules

Polymer capsules were fabricated *via* the LbL approach, as previously described.[20] Na_2CO_3 (1 M in distilled water) and catalase (2 mg/mL in Tris-HCl 0.05, pH = 7.0) solutions were poured into $CaCl_2$ (1 M in distilled water) solution. After 30 s of stirring at 1100 rpm, the particles were allowed to settle down for 15 min. After this, the particles were collected by centrifugation at 2000g and washed (×3) with a 0.005 M NaCl solution. As the $CaCO_3$−catalase microparticles have a negative surface charge, PAH [2 mg/mL in 0.5 M NaCl (pH = 6.5)] was used as the first polyelectrolyte. After an incubation time of 12

min, the particles were collected by centrifugation and washed (×3) with 0.005 M NaCl solution. Following the same procedure, the second layer (i.e., PSS) was deposited. After the assembly of the first two polyelectrolyte layers, dPG−DOX conjugate or dPG-amine was used as the positive layer in the following layer depositions, following the same procedure. The particles were resuspended in 2 mg/mL dPG-DOX/dPG-amine solution in 0.5 M NaCl and subsequently washed with 0.005 NaCl. Particles containing six layers were fabricated with a final shell architecture of (PAH/PSS) $(dPG\text{-}DOX/PSS)_2$ or (PAH/PSS) $(dPG\text{-}amine/PSS)_2$. To remove the template, the particles were immersed in 0.1 M EDTA solution (three times, 5 min for each incubation) (**Fig. 4.1**).

The successful encapsulation of the enzyme was assessed by using FITC-labelled CAT (CAT-FITC) in the fabrication process. To do so, CAT and FITC at a ratio of 50−100 µg of FITC per milligram of protein were mixed, as previously described.[20]

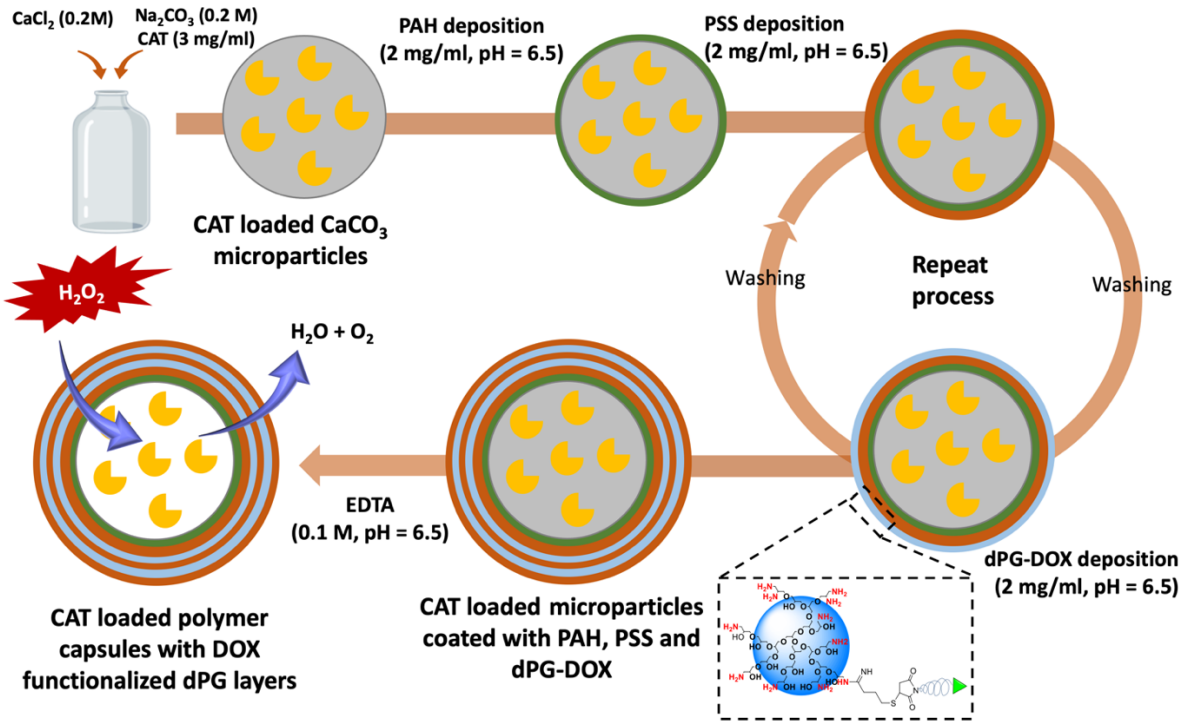

Fig. 4.1. *Schematic representation of the fabrication of multifunctional polymer capsules.*

4.2.5.2. Physico-chemical and morphological characterization of microcapsules

A scanning electron microscope (Hitachi S-4800) was used to analyse the morphological aspects of the polymer capsules. The microscope was operated at a working voltage of 5 kV and a working current of 10 nA.

The ζ-potential was monitored after each polyelectrolyte deposition step by means of a Malvern Instrument Zetasizer (ZEN 3690).

A laser scattering particle size distribution analyser (HORIBA LA-350) provided information about the size distribution of the template.

The successful template removal was assessed *via* FTIR spectroscopy (Nicolet Avatar 370), operating in the attenuated total reflectance (ATR−FTIR), as previously described.[23]

To confirm the DOX adsorption, polymer capsules were observed in an inverted fluorescence microscope (Nikon Eclipse Ts2). After the template removal, the capsules were washed thrice with distilled water, and a drop of the solution was taken out and observed under the fluorescence microscope. As a control, polymer capsules fabricated with dPG without the model drug (dPG-amine) were used. The amount of adsorbed DOX was determined by measuring the dPG-DOX concentration in the polyelectrolyte solution before and after each layer deposition. 100 µL samples were taken out from the initial polyelectrolyte solution and from the supernatant of the particle dispersion after the layer incubation. The samples were diluted to 1:5, and the fluorescence intensity (λ_{ex} = 480 nm/λ_{em} = 595 nm) was measured on a microplate reader (BioTek Synergy H1M) to determine the dPG-DOX concentration.

The stability of the fabricated capsules was analysed by means of SEM. After the template removal, capsules were incubated in PBS at 37 ^{o}C, and samples were taken out at different time points (e.g., 4, 24, and 72 h). The images were acquired using SEM, with the same instrument and conditions mentioned above.

The antioxidant capacity of polymer capsules was evaluated using a fluorimetric hydrogen peroxide assay kit (Sigma-Aldrich), as described in the previous chapter.

The H_2O_2 scavenging capacity of the polymer capsules after ethanol sterilization was also determined. Here, sterilized and non-sterilized polymer capsules at $1 \cdot 10^6$ or $1 \cdot 10^7$ polymer capsules/mL were incubated in 10 and 50 µM H_2O_2 solutions for 30 min. After the subsequent centrifugation, the H_2O_2 concentration in the supernatant was determined, following the aforementioned procedure.

4.2.6. pH-dependent drug release

The release of DOX was performed in the presence of four different buffers. Phosphate buffers (100 mM, pH 6.0 and 7.4) and sodium acetate buffers (100 mM, pH 4.0 and 5.0) were used, and the release study was performed at 37 ^{o}C. After their fabrication, the capsules were centrifuged and the supernatant was removed. Then, they were resuspended in 0.5 mL of each buffer and placed in an orbital shaker at 37 ^{o}C. At specific time points (30 min, 4 h, and 24 h), the capsule dispersion was centrifuged and the supernatant was collected. After the supernatant removal, the same volume of fresh buffer was added. The fluorescence intensity (λ_{ex} = 480 nm/λ_{em} = 595 nm) of the supernatant was measured on a microplate reader (BioTek Synergy H1M) to determine the released DOX concentration.

DOX release was also assessed qualitatively by the analysis of the decrease of DOX fluorescence intensity. To do so, polymer capsules were fabricated containing CAT-FITC, following the procedure detailed above. The capsule dispersion was split and centrifuged. After this, the two buffer solutions (pH = 5.0 and pH = 7.4) were added and the polymer capsules were incubated at 37 ^{o}C. At specific time points (4 and 24 h), the polymer capsules were collected and washed with distilled water to observe them under an inverted fluorescence microscope (Nikon Eclipse Ts2).

4.2.7. *In vitro* studies

4.2.7.1. HeLa cell seeding

HeLa cells (ATCC) were seeded, following the same protocol described in the previous chapter. A density of 5,000 cells/well on a 96-well plate was used for metabolic activity

measurements. A density of 10,000 cells/well on a 24-well plate was used for internalization studies.

4.2.7.2. Preliminary cytocompatibility test

The cytotoxicity of the capsules was evaluated as described in chapter 3. Three capsule-to-cell ratios (10, 100, and 1000 polymer capsules/cell) and two time points (24 and 72 h) were analysed, and AlamarBlue was used to measure the metabolic activity of cells. The uptake of the capsules by HeLa cells was also analysed.

Polymer capsules at 10 capsules/cell were incubated with cells during 2, 4, and 24 h. Afterward, the cells were fixed and stained, following the same procedure described before.[23] The cells were observed under an inverted fluorescence microscope (Nikon Eclipse Ts2).

4.2.7.3. Therapeutic potential of the multifunctional capsules in a H_2O_2-induced in vitro model

To assess the capacity of the fabricated capsules to protect cells from a H_2O_2-induced oxidative stress, we used our previously reported model (chapter 3). Three capsule-to-cell ratios (10, 100, and 1000 polymer capsules/cell) were analysed. Two stimuli of 50 and 100 µM H_2O_2 were added at different time points (0 and 24 h). AlamarBlue assay was used to check the metabolic activity of the cells at the selected time points (8, 24, 32, and 48 h).

4.2.8. Statistical analysis

Data related to the fabrication and characterization of polymer capsules are presented as mean ± standard deviation (SD). In the *in vitro* studies, the results are presented as mean ± SD, with n = 4. One-way analysis of variance (ANOVA) was used to test the statistical differences between groups, with the Bonferroni post-hoc test and a confidence level of 95% ($p < 0.05$).

4.3. Results and discussion

4.3.1. Synthesis of dPG-DOX conjugate

Polyglycerol amine (dPG-amine) was synthesized following a three-step protocol. The -OH of dPG were first converted to mesyl (Ms) groups followed by the conversion of Ms groups to azide functionalities. The azide groups were subsequently transformed into amine groups using triphenylphosphine as the reducing agent. **Fig. 4.2** shows the schematics and the reaction conditions for the synthesis of dPG-amine from dPG as starting material. All samples were well characterized using nuclear magnetic resonance (NMR) spectroscopy (**Fig. 4.3-4.5**) and a total of 15 mol% amine grafting was obtained (i.e., 18 NH_2 and 103 OH groups, in average). The conversion of azide groups to amine moieties was further confirmed by the disappearance of the characteristic peak of azide groups at 2100 cm^{-1} after reduction reaction (**Fig. 4.6**). The zeta potential of the dPG-amine was 12 ± 2 mV, confirming the presence of amine functionalities on dPG moieties. The hydrodynamic sizes of dPG-amine were found to be around 20-25 nm with a high polydispersity index (PDI = 0.7) owing to the aggregation of the particles in solution.

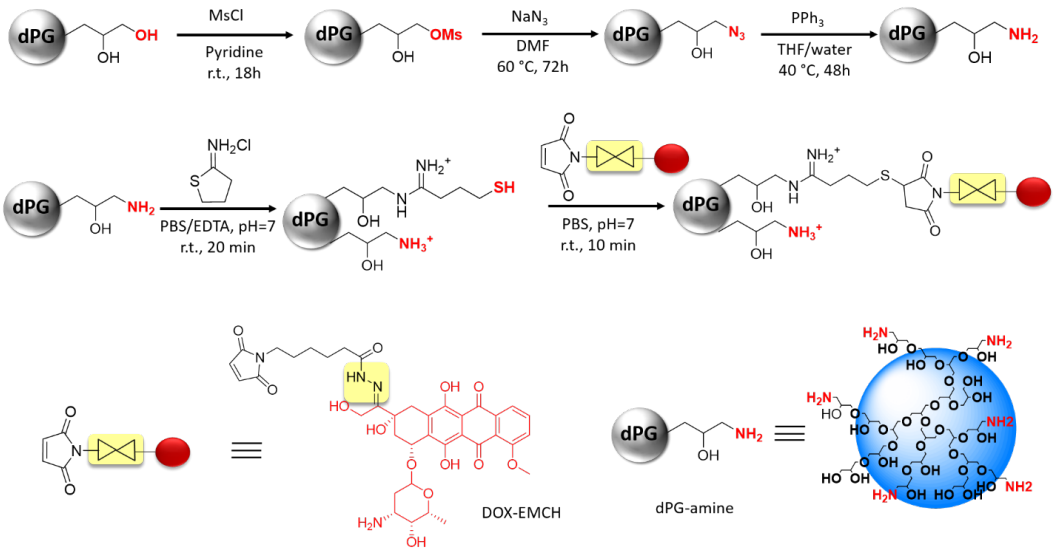

Fig 4.2. *Reaction pathways for the synthesis of dPG-amine and dPG-DOX conjugate. The depicted structure of dPG-amine represents only a fraction of the total polymer.*

The conjugate of dPG-DOX was synthesized through a one-pot synthesis as stated in earlier publications.[36,46] A schematic representation of the conjugation reaction

between DOX-EMCH (i.e., DOX bearing a pH-cleavable hydrazone bond, with a maleimide group for conjugation) and dPG-amine containing 15 mol% amino groups is shown in **Fig. 4.2**. First, dPG-amine was thiolated to yield, on average, one thiol per dPG molecule. After thiolation, DOX-EMCH was added to the dPG-thiol solution to allow the reaction between the thiols and the maleimide groups through a selective Michael-type addition. After the reconstitution of the lyophilized samples in PBS buffer, the concentration of DOX was determined photometrically using the molar absorption coefficient of DOX at 495 nm. The first assessment of the pH-triggered cleavage and DOX release was performed by dispersing the dPG-DOX conjugate in sodium acetate buffer at pH 4.0 and applied on a G-25 Sephadex column. The amount of DOX conjugated to the dPG backbone was calculated to be ∼2 wt% or one DOX per three molecules of dPG using UV/vis spectroscopy at 495 nm (ε 495 = 10645 M^{-1} cm^{-1}). It should be noted that such rather low drug loading was aimed in order to enable the predominance of $–NH_3^+$ at the surface of the conjugates for their further incorporation into the microcapsules during the LbL deposition process. The hydrodynamic sizes of the conjugates remained in the same size range as dPG-amine. The zeta potential of the dPG-DOX was 9 ± 0.5 mV, confirming the presence of amine functionalities on dPG moieties incorporating an overall positive charge on dPG even after DOX conjugation.

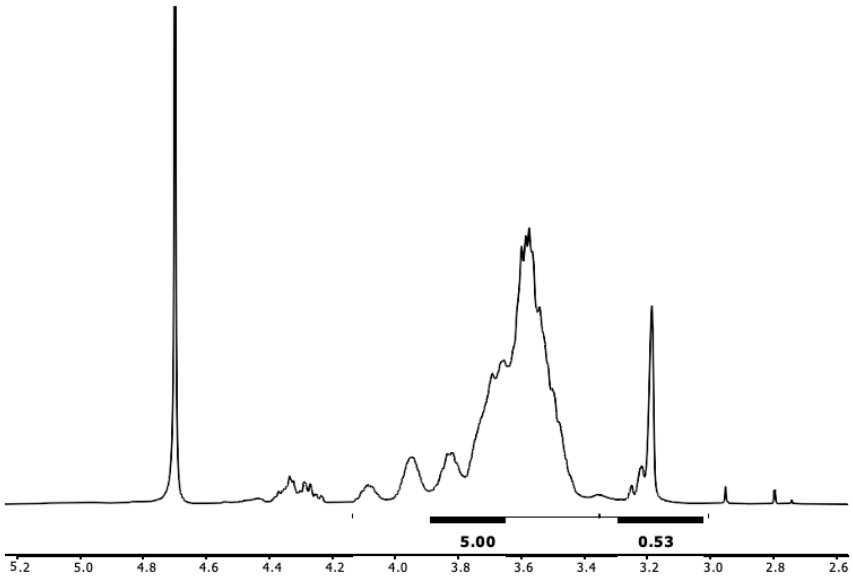

Fig. 4.3. *^{1}H NMR (300 MHz, D_2O) spectra of dPG mesyl: δ 4.2-3.4 ppm (m, 5H, dPG backbone), δ 3.2 (s, 1 H, CH_3, OMs).*

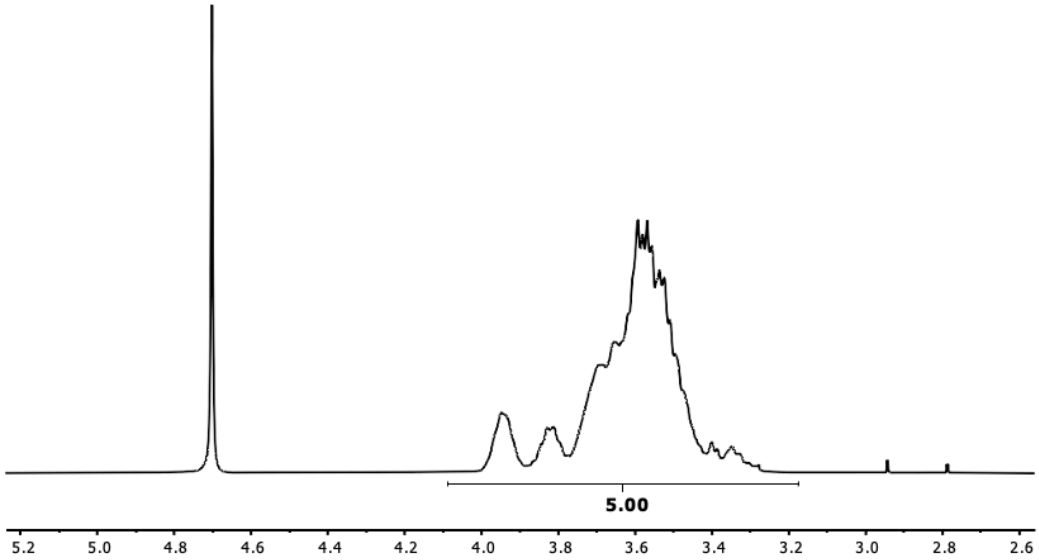

Fig. 4.4. *^{1}H NMR (300 MHz, D_2O) spectra of dPG mesyl: δ 4.2-3.5 ppm (m, 5H, dPG backbone).*

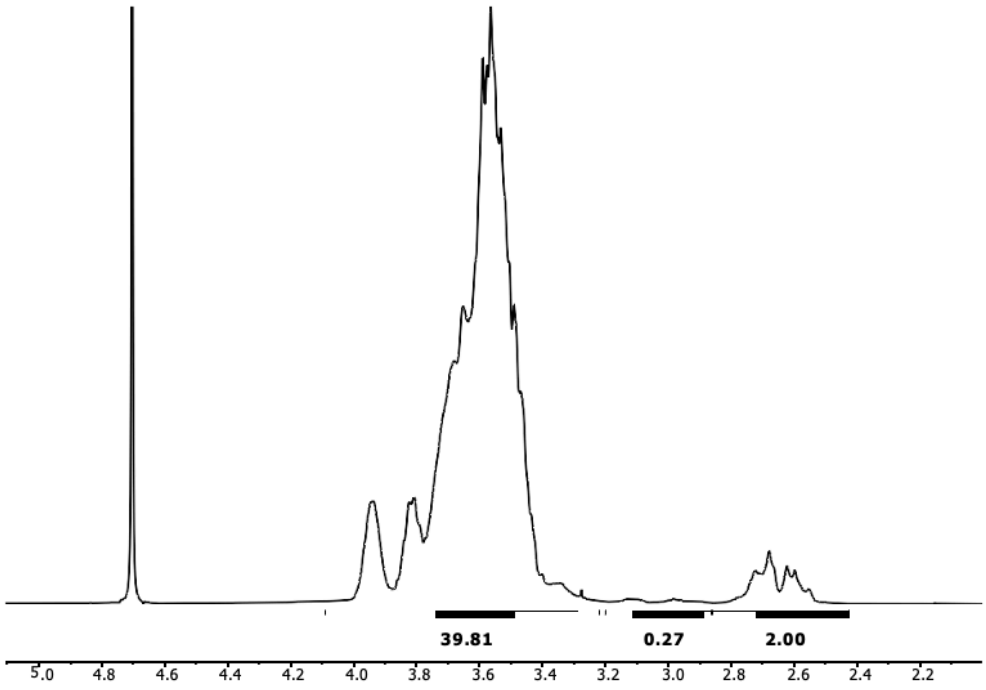

Fig. 4.5. *^{1}H NMR (300 MHz, D_2O) spectra of dPG-amine: δ 4.2-3.2 ppm (m, 5H, dPG backbone), δ 2.8-3.2 ppm (s, 1 H, -CH), δ 2.4-2.8 ppm (m, 2 H, -CH_2).*

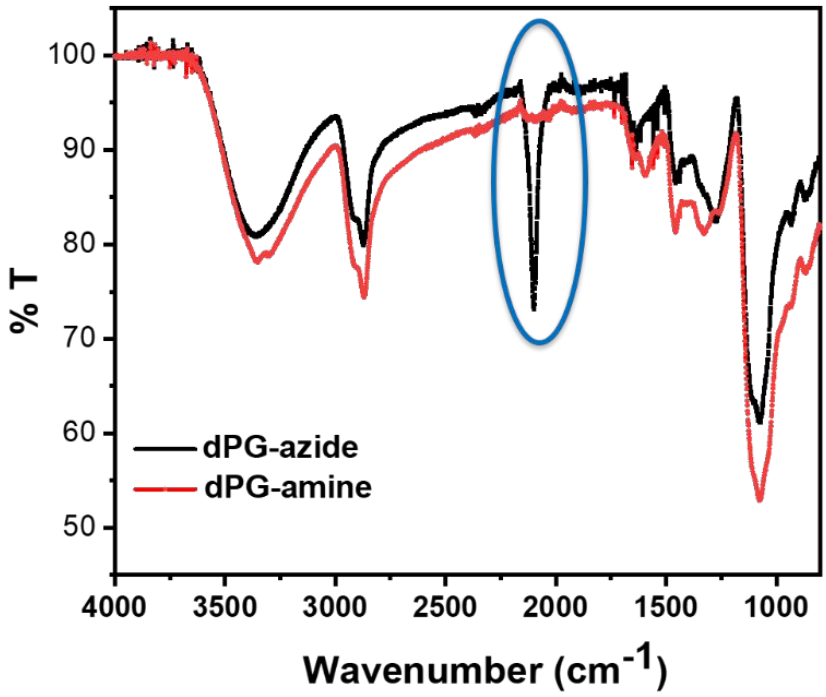

Fig. 4.6. *FTIR spectra of dPG-azide (black) and dPG-amine (red). The disappearance of the characteristic peak of azide at 2100 cm^{-1} after reduction to amine is highlighted in the figure.*

4.3.2. Fabrication of polymer capsules *via* de LbL approach

For the fabrication of polymer capsules, $CaCO_3$ sacrificial template was first synthesized through the co-precipitation of CAT, $CaCl_2$ and Na_2CO_3 (**Fig. 4.1**) because of the reported higher encapsulation efficiency in comparison to alternative methods.[47,48] The process resulted in CAT loaded $CaCO_3$ spherical microparticles with a mean diameter of 3.9 ± 1.6 µm, which slightly differed from the $CaCO_3$ sacrificial template without the enzyme (3.1 ± 1.2 µm) (**Fig. 4.7**). $CaCO_3$ microparticles were selected as sacrificial template as they are easily dissolved using a calcium chelating agent (i.e., ethylenediaminetetraacetic acid disodium salt dehydrate (EDTA)) and enable to avoid harsh conditions (i.e., organic solvents and/or extremely high/low pH) in the subsequent template removal step, thus protecting the integrity of polyelectrolytes, the encapsulated enzyme, and the chemically conjugated drug.[49] Contrary to other templates such as polystyrene beads[50] and melamine formaldehyde cores,[51] the protocol used herein allows the pre-encapsulation of the enzyme. Post-encapsulation of (bio)macromolecules in templated LbL capsules usually rely on an increased permeability of the polymeric membrane

promoted by a change in solvent composition,[52] pH[53] or temperature.[54] These conditions could have a detrimental effect on the conformational integrity of the encapsulated enzyme, thus jeopardizing its catalytic activity.

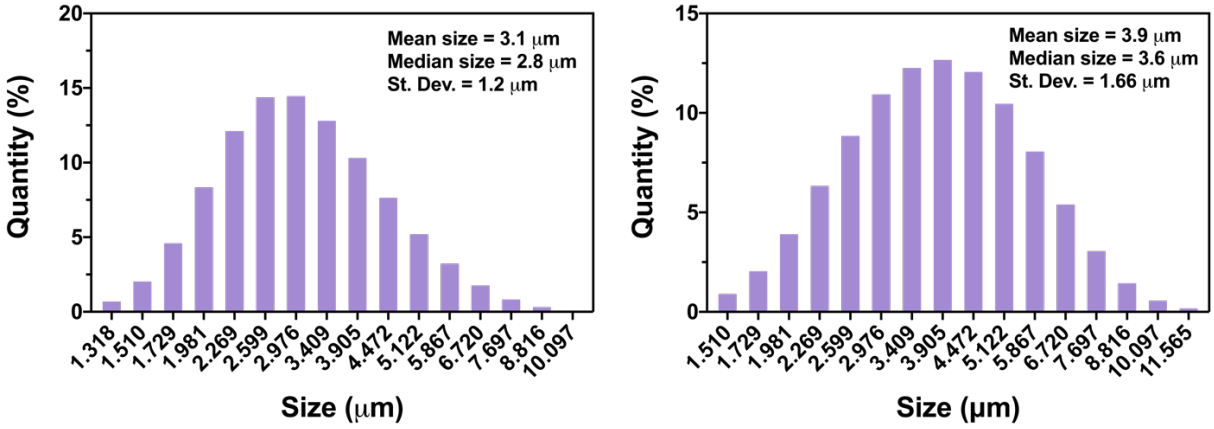

Fig. 4.7. *Size distribution of $CaCO_3$ microparticles without (left) and with (right) co-precipitated CAT.*

Capsules containing six layers were fabricated using PAH as the first positive layer and dPG-DOX or dPG without the conjugated drug (dPG-amine) for the subsequent positive layers (**Fig. 4.1**), resulting in (PAH/PSS)(dPG-DOX/PSS)$_2$ and (PAH/PSS)(dPG-amine/PSS)$_2$ architectures, respectively. PAH and PSS polyelectrolytes were chosen due to their extensive use as model polyelectrolytes in the fabrication of many therapeutic systems and their robust structure enabling the transfer of substrates across the polymeric membrane, while protecting the active compound from the external environment.[49,55-57] Although LbL capsules based on biodegradable polyelectrolytes are of high interest in several biomedical applications (e.g., nanovehicles for the transfer of genetic material[58] or drugs[59]), biodegradability may be an undesirable property when capsules are intended to be used as microreactors. If the degradation process is not carefully controlled, the encapsulated enzyme would be exposed to the external physiological conditions and suffer protease degradation and denaturation.

The sacrificial template was initially negatively charged (pI_{CAT} = 5.4). Therefore, CAT loaded $CaCO_3$ microparticles were first incubated with PAH, resulting in a shift in their surface charge from -9.4 ± 0.6 mV to -5.0 ± 0.3 mV in the case of capsules fabricated using dPG-DOX (**Fig. 4.8a**) and from -10.5 ± 0.3 mV to -8.9 ± 1.2 mV in the case of

capsules fabricated using dPG-amine (**Fig. 4.8a**). Afterwards, polyelectrolyte layers were assembled alternately and a change in the ζ-potential value was observed after each deposition step, confirming the successful layer assembly (**Fig. 8a**).

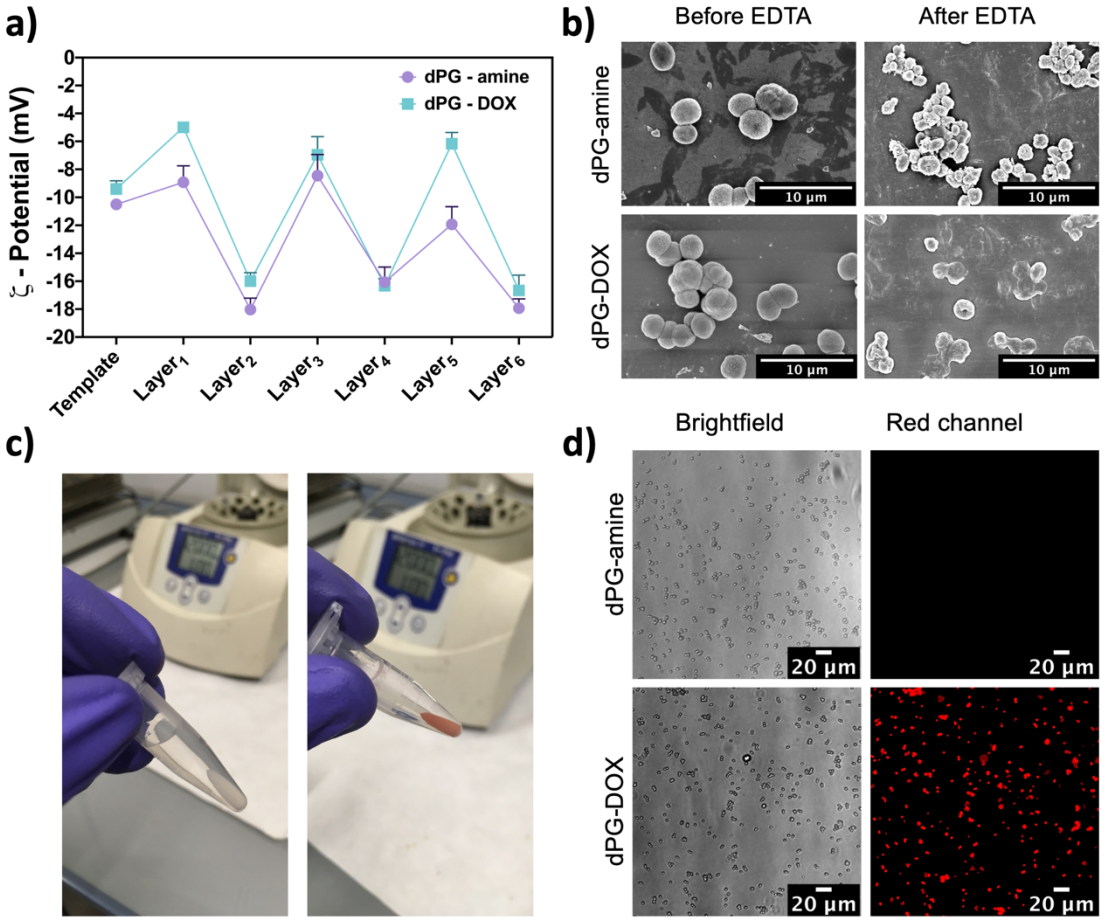

Fig. 4.8. *a) ζ-potential of (PAH/PSS)(dPG-DOX/PSS)$_2$ and (PAH/PSS)(dPG-amine/PSS)$_2$ polymer capsules, b) Morphological characterization via SEM of polymer capsules, c) Polymer capsules before (left) and after (right) incubation with dPG-DOX, d) Fluorescence micrographs of capsules fabricated with dPG-amine or dPG-DOX.*

After the LbL process, the microparticles were immersed in 0.1 M EDTA solution to allow the removal of the $CaCO_3$ sacrificial template (**Fig. 4.1**). As observed in SEM micrographs, the fabricated capsules before EDTA addition had a spherical shape with a mean diameter size ~ 3-4 µm (**Fig. 4.8b**). After EDTA incubation, capsules fabricated with dPG-DOX and with dPG-amine were hollow, as suggested by their collapsed shape (**Fig. 4.8b**). Fourier transform infrared spectra (FTIR) (**Fig. 4.9**), where the two main bands

associated to $CaCO_3$ at 1384 cm^{-1} and 870 cm^{-1} disappeared after the incubation with EDTA, confirmed the successful elimination of the sacrificial template.

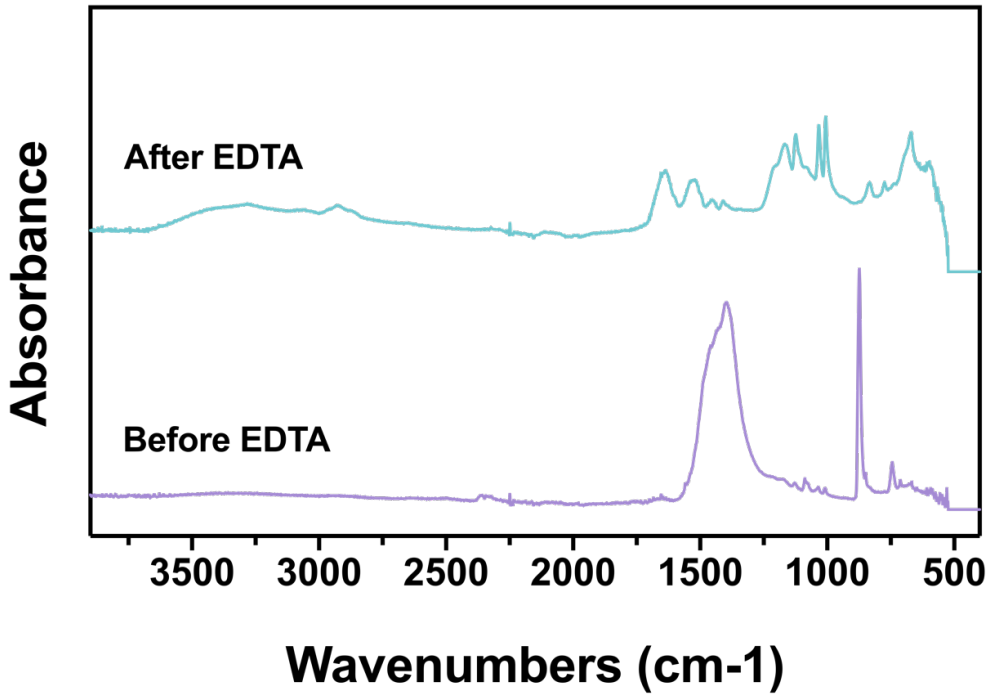

Fig 4.9. *FTIR spectra of polymer capsules before (purple) and after (green) template removal.*

To test their stability, microcapsules were immersed in PBS at 37 ^{o}C and micrographs were acquired at different time points (4, 24 and 72 h). As observed in SEM, capsules maintained their spherical and collapsed shape at the selected time points, confirming their stability over time (**Fig. 4.10**).

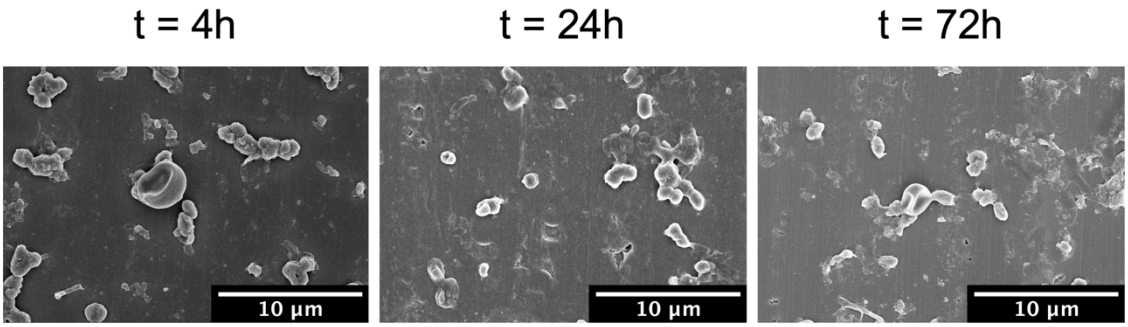

Fig. 4.10. *Morphological characterization via SEM of the stability of the polymercapsules over time.*

The successful adsorption of DOX was quantitatively and qualitatively assessed. After the incubation of the capsules with the dPG-DOX, a change in the color of the microcapsule pellet was observed (**Fig. 4.8c**). The successful incorporation of dPG-DOX was quantitatively confirmed by measuring the concentration of dPG-DOX in the supernatant before and after each layer deposition. The obtained results showed a decrease in the dPG-DOX concentration in the solution after each incubation, confirming the adsorption of the drug conjugate onto the capsules (**Fig. 4.11**). The adsorbed quantity of DOX was 1.9 µg per 10 mg of $CaCO_3$ sacrificial template. Finally, the presence of DOX was qualitatively confirmed by means of fluorescence microscopy after the template removal. Red fluorescence was observed in the case of the capsules fabricated with dPG-DOX, whereas capsules fabricated with dPG-amine were not visible (**Fig. 4.8d**).

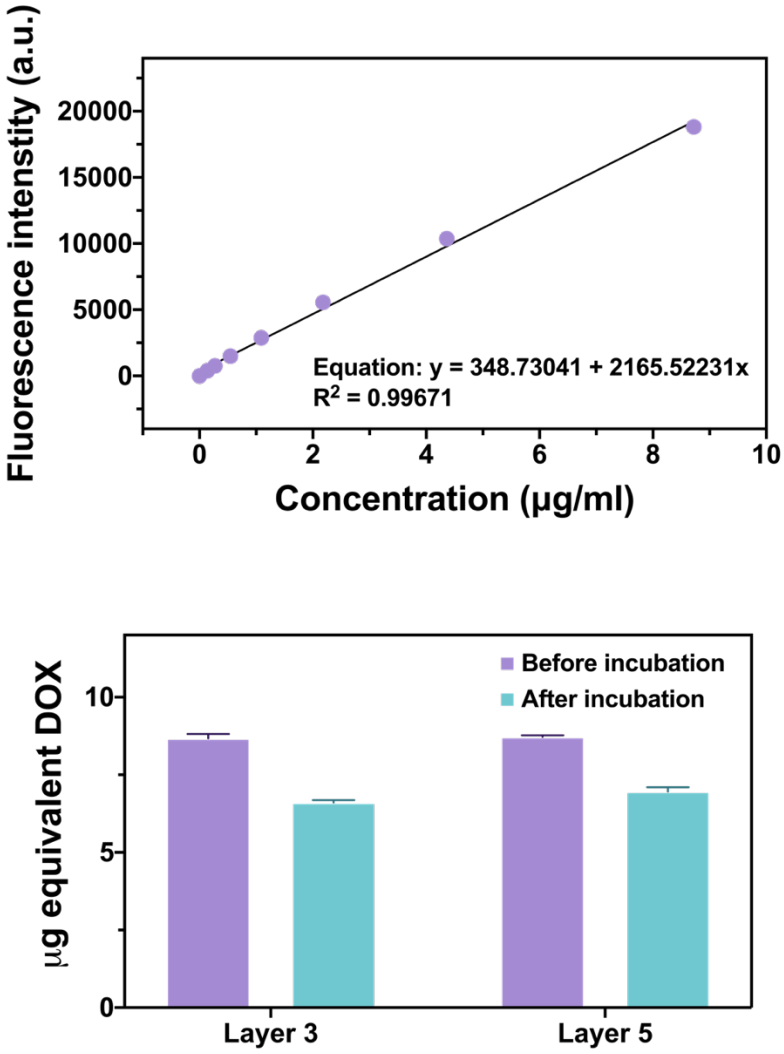

Fig. 4.11. *a) Calibration curve of dPG-DOX dissolved in 0.5 M NaCl, b) Adsorbed dPG-DOX in polymer capsules after de 3rd and 5th layer incubation.*

4.3.3. Antioxidant capacity and pH-dependent drug release of the polymer capsules

To assess the antioxidant capacity, two biologically relevant H_2O_2 concentrations (10 µM and 50 µM) were used. Capsules were incubated at a final polymer capsule concentration of $1{\cdot}10^4$, $1{\cdot}10^5$, $1{\cdot}10^6$ and $1{\cdot}10^7$ polymer capsules/mL for 30 minutes. The concentration of H_2O_2 in the solution decreased in a polymer capsule concentration-dependent manner (**Fig. 4.12a**). At the concentration of 10 µM H_2O_2, a significant decrease ($p<0.05$) in the H_2O_2 concentration was observed at the polymer capsule concentrations of $1{\cdot}10^5$, $1{\cdot}10^6$ and $1{\cdot}10^7$ polymer capsules/mL, from the initial value of 100 ± 2.3% to 91.2 ± 3.2%, 53.8 ± 2.4% and 2 ± 0.1%, respectively (**Fig. 4.12a**). In the case of 50 µM, the concentration of H_2O_2 decreased significantly ($p<0.05$) from an initial value of 100 ± 0.6% to 94.8 ± 1.8%, 60.6 ± 2% and -12.4 ± 0.2% using the polymer capsule concentrations of $1{\cdot}10^5$, $1{\cdot}10^6$ and $1{\cdot}10^7$ polymer capsules/mL respectively (**Fig. 4.12a**). Taken together, the obtained results confirmed the H_2O_2 scavenging capacity of the developed polymer capsules, indicating that the activity of the encapsulated enzyme is preserved and the reagents are able to diffuse through the polymeric membrane. The use of antioxidant enzymes is gaining increasing attention for biomedical applications over alternative nonenzymatic antioxidants (e.g., vitamins, flavonoids) thanks to their specificity and efficacy. Furthermore, contrarily to nonenzymatic antioxidants, they are not consumed in reaction with ROS.[60,61] However, due to their susceptibility to undergo protease degradation and denaturation, several encapsulation strategies (e.g., liposomes,[62] polymersomes,[63] poly(lactide-co-glycolide) particles[64]) are being considered. The LbL approach does not require complex chemistries, avoids the use of organic/harmful solvents and conditions and important aspects of the resulting capsules (e.g., size, shape, stiffness) can be easily controlled, thus representing a robust strategy over other alternatives.

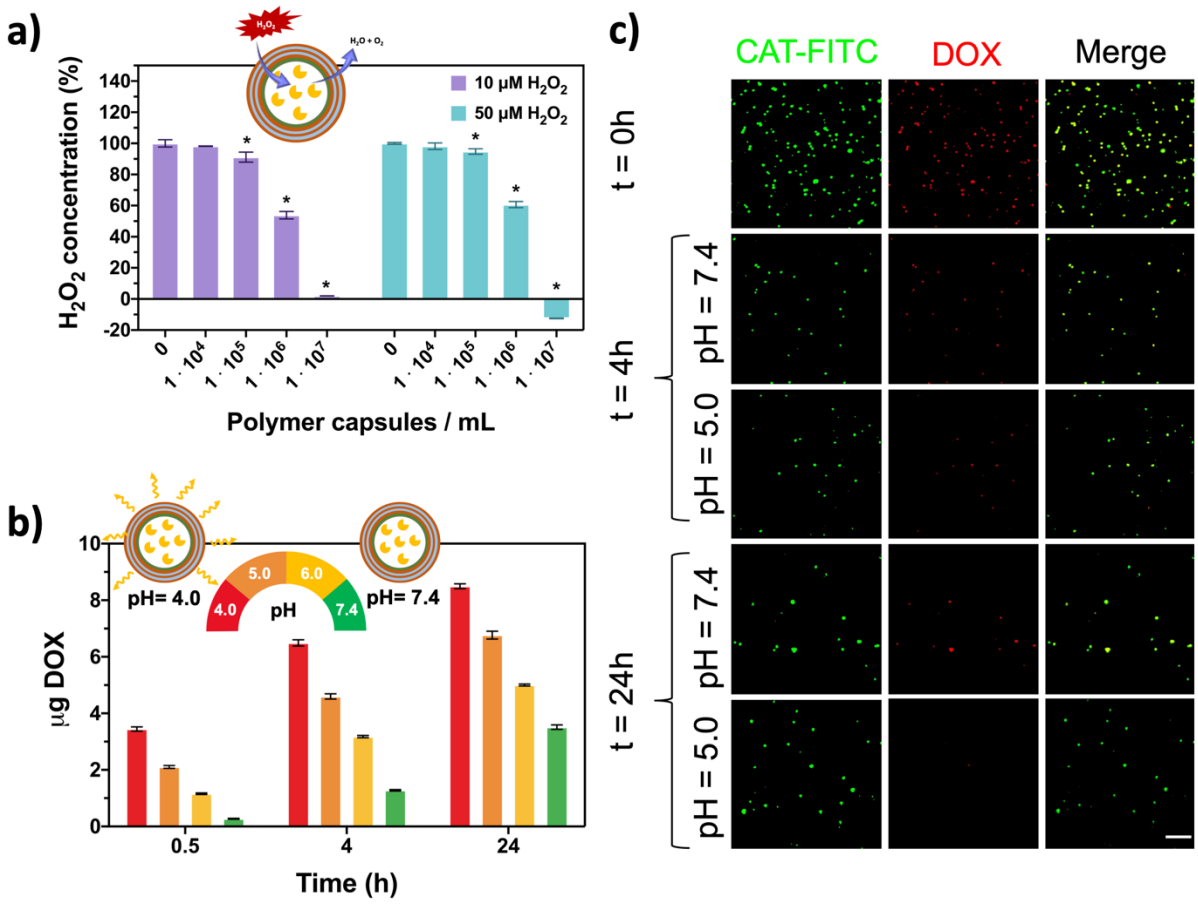

Fig. 4.12. *a) H_2O_2 scavenging capacity of polymer capsules at biologically relevant H_2O_2 concentrations (10 μM and 50 μM). Asterisks (*) indicate significant differences ($p < 0.05$) with respect to each control (0 capsules/mL in (a)), b) DOX release at different pH values, c) Fluorescence micrographs of DOX release at different pH values (FITC-CAT: green/ DOX: red). Scale bar: 50 μm.*

The scavenging capacity of the encapsulated enzyme after a sterilization process was also evaluated. After submerging the capsules in ethanol (70%), they were incubated with 10 μM and 50 μM H_2O_2 at a final concentration of $1{\cdot}10^6$ and $1{\cdot}10^7$ polymer capsules/mL. Regardless of the H_2O_2 concentration, a significant decrease ($p<0.05$) in the scavenging capacity of the capsules was observed due to the sterilization with ethanol (**Fig. 4.13**). In the case of 10 μM H_2O_2 concentration, polymer capsules reduced 94.1 ± 0.6% and 37.9 ± 0.9% of the initial H_2O_2 from the solution, using concentrations of $1{\cdot}10^7$ and $1{\cdot}10^6$ polymer capsules/mL respectively, whereas the sterilized counterparts reduced 47.9 ± 2.1% and 0.7 ± 1.2% of H_2O_2 (**Fig. 4.13**). At the concentration of 50 μM H_2O_2, significant differences were also observed in both polymer

capsule concentrations. Using $1{\cdot}10^7$ and $1{\cdot}10^6$ polymer capsules/mL, H_2O_2 reduction values were determined to be 97.3 ± 2.8% and 35.2 ± 1.8% respectively, whereas in the case of sterilized capsules the values were 40.2 ± 4.1% and 18.4 ± 2.4% (**Fig. 4.13**). The encapsulation of enzymes into LbL capsules and alternative polymeric systems (e.g., single-enzyme nanogels,[65,66] polymersomes,[67] and so on) commonly results in an improved stability of the encapsulated enzyme towards proteolytic degradation, organic solvents, changes in pH and temperature, and so forth.[68,69] However, in the particular case of LbL capsules exposed to water/ethanol mixtures, an increased permeability has been reported, which is associated to the rearrangement of the polyelectrolytes forming the shell.[70] This can have a deleterious effect on the catalytic activity of the enzyme and, at the same time, result in its leakage from the polymeric capsule. Therefore, sterilization with ethanol was not considered for the subsequent *in vitro* studies and alternative approaches to prevent contamination where acquired.

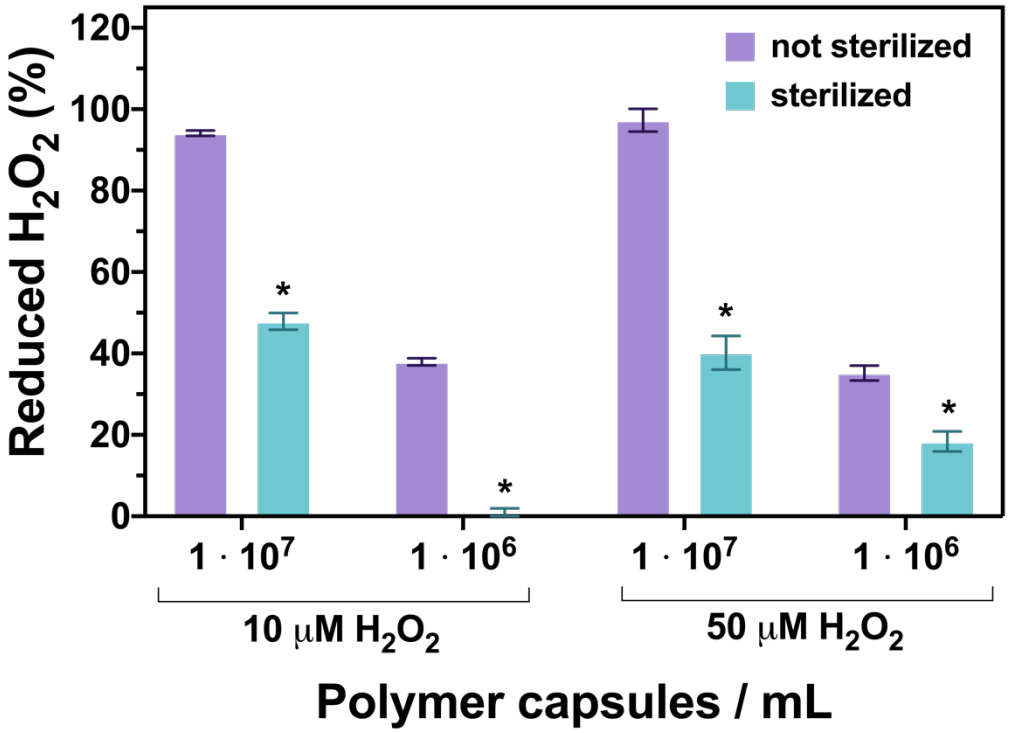

Fig. 4.13. *Reduced H_2O_2 by the polymer capsules at 10 μM and 50 μM H_2O_2 after the sterilization process. 100% reduction refers to the complete removal of H_2O_2 from the solution. Asterisks (*) indicate significant differences ($p<0.05$) with respect to the control (non-sterilized capsules).*

To assess the capacity of the capsules to release a model drug in response to the microenvironment pH, the fabricated polymer capsules were incubated in four different pH buffers (pH = 4.0, 5.0, 6.0 and 7.4). We chose to work with DOX-EMCH as it is a well-established prodrug currently in clinical trials that is stable at neutral pH but undergoes hydrazone cleavage at pH values lower than 6 to release the antiproliferative drug doxorubicin. Supernatants were collected after 30 min, 4 h and 24 h and their fluorescence intensities were measured using a microplate reader. After 30 min, the capsules showed an initial release of the model drug of 0.3, 1.2, 2.1, and 3.5 μg at pH = 7.4, 6.0, 5.0, and 4.0, respectively (**Fig. 4.12b**). As expected, a higher initial release was observed in the more acidic environment. After 24 h, polymer capsules released a total DOX amount of 3.5, 5.0, 6.8, and 8.5 μg at pH = 7.4, 6.0, 5.0, and 4.0, respectively, thus confirming the pH-dependent release of the fabricated polymer capsules (**Fig. 4.12b**). In comparison to other LbL capsules that rely on a diffusion process to release the encapsulated cargo, our approach allows the delivery of the model drug (i.e., DOX) only in acidic conditions. This is of high relevance for the potential translation of this system to biomedical applications, as the off-target effects of the administered drug would be minimized. Diffusion mediated drug release, apart from being nonspecific to any biologically relevant stimulus, is usually accompanied by an initial burst release. For example, around 80% of the encapsulated DOX was released from capsules made out of PAH/PSS multilayers in less than 300 minutes.[71] In another example using PSS and poly(amidoamine) dendrimer to fabricate hollow polymer capsules, capsule degradation and/or high ionic strengths were needed to ensure the complete release of the encapsulated DOX.[72]

The pH dependent release of the fabricated polymer capsules was further confirmed by means of fluorescence microscopy. For this purpose, CAT was stained with FITC (CAT-FITC) prior to the co-precipitation process. After the LbL process and template removal, the capsules were immersed in two of the buffers mentioned above (pH = 5.0 *vs.* pH = 7.4) and fluorescent micrographs were acquired after 4 and 24 h. Most of the polymer capsules immersed in pH 7.4 buffer maintained their fluorescence intensity at the assessed time points (4 and 24 h) in both channels (red and green), compared to the capsules before their immersion (0 h) (**Fig. 4.12c**). In contrast, polymer capsules

immersed in the acidic pH buffer were able to emit fluorescence signal only in the green channel (CAT-FITC) but the fluorescence signal in the red channel (DOX) was not visible after 24 h, suggesting a substantial release of the drug (**Fig. 4.12c**). Although the drug seems to be completely released, the stability of the polymer capsules immersed in pH = 5.0 buffer was preserved, keeping their spherical shape and integrity. Several studies have employed LbL capsules as delivery vehicles for the release of DOX and other therapeutic agents. Most of them rely on the Fickian diffusion release mechanism, where the diffusion is governed by the concentration gradient between the two sides of the polymeric shell, which acts as a barrier. Accordingly, tuning the thickness of the polymeric shell (e.g., by changing the number of deposited layers[71]) or its density (e.g., by promoting shrinkage of the capsules through a thermal treatment[59] or crosslinking reactions[73]) have been reported as a valid strategy to control the release kinetics of the encapsulated DOX. In this sense, the release of DOX from polymer capsules made out of PAH and dendritic porphyrin was delayed when the polymer layers were crosslinked *via* the carbodiimide chemistry.[73] To achieve a more specific release at the site of interest, biologically relevant stimuli have been employed as triggers for the disassembly of the capsules and the subsequent delivery of the cargo. Yan *et al.*[74] fabricated LbL polymer capsules stabilized with disulfide bonds that underwent deconstruction during intracellular trafficking due to the reducing environment, thereby leading to DOX release. The acidic microenvironment has been similarly employed to promote the disassembly of hydrazone-bonded polymer capsules, which resulted in a much faster release of the entrapped DOX in comparison to the one observed at neutral pH.[75] Contrary to these two last examples, our approach allows the release of DOX in response to a biologically relevant stimulus (i.e., acidic pH) while preventing the disassembly of the capsule, which is a must to preserve the protection of catalase and act as a long lasting microreactor.

Based on these results, we confirm the multifunctional identity of the fabricated capsules, which are able to simultaneously scavenge H_2O_2 from the microenvironment in a dose-dependent manner and release DOX in acidic microenvironments.

4.3.4. Metabolic activity of HeLa cells in the presence of multifunctional capsules and internalization

The *in vitro* cytocompatibility of polymer capsules (i.e., (PAH/PSS)(dPG-amine/PSS)$_2$) was tested in HeLa cells. The metabolic activity of cells in the presence of various capsule per cell ratios (10, 100, 1000 capsules/cell) was measured after 24 and 72 h by means of AlamarBlue® assay. Cells without capsules were used as a negative control. Cells were able to maintain a normal metabolic activity above the threshold value (i.e., 70%) in the presence of capsules. In fact, after 72 h, no decrease in their metabolic activity ($p<0.05$) was observed with respect to the negative control (**Fig. 4.14a**). Although LbL capsules composed of polyelectrolytes are believed to be nontoxic for cells, some studies have reported detrimental effects on cell proliferation and viability at concentrations above 50 capsules per cell.[76] Besides, the incorporation of inorganic nanoparticles (e.g., magnetic nanoparticles,[77] manganese dioxide nanoparticles[23]) to provide advanced functionalities also resulted in an increased cytotoxicity of the fabricated capsules in comparison to the non-functionalized counterparts, thus reducing the threshold at which these capsules can be employed in the subsequent biological studies. The LbL approach is a highly versatile method that allows to easily tune the surface charge of the resulting capsules. In principle, positively charged capsules improve cell uptake (presumably because of the electrostatic interaction between the surface of the particle and the cell membrane) and can be a valid strategy for some particular applications where internalization is a must (e.g., gene therapy[78]). At the same time, it is generally accepted that positively charged micro- and nanocapsules induce a higher cytotoxicicity.[79] Based on this "rule of thumb" and on our previous experience,[23] we engineered the capsules to display an external negative charge. To further confirm the effect of the polymer capsules, cells were observed under the optical microscope. Compared to the negative control (i.e., cells in absence of polymer capsules), no changes were observed in the morphology of the cells and cell density in the presence of polymer capsules (**Fig. 4.14b**). Taken together, the results indicate no cytotoxic effect of the fabricated capsules in any of the capsule to cell ratios.

The internalization of polymer capsules by both innate immune cells (e.g., macrophages, monocytes, dendritic cells) and potential target cells must be carefully considered.

Phagocytosis by immune cells may be desirable for specific applications, including vaccine carriers. In many other cases (e.g., drug delivery), polymer capsules should escape from the uptake by immune cells to reach the target cells. In any case, the LbL approach offers huge versatility in controlling those key parameters that will determine cell uptake, including size,[80] shape,[81,82] surface charge,[83] stiffness[84] and surface chemistry,[56,85,86] among others. There is a vast literature aimed at unravelling the interplay between these parameters and various internalization mechanisms, sometimes drawing contradictory conclusions. As reported by Novoselova *et al.,*[80] increasing the size of the LbL capsules from 500 nm to 2 μm reduced the uptake by both macrophages and lung cancer cells from 80% to 20% (approximate values), suggesting that an increased size could be employed as a strategy to avoid macrophage internalization. In another example,[82] bowl-like microcapsules where preferentially internalized by both smooth muscle cells and macrophages in comparison to spherical counterparts, indicating that isotropic-shaped capsules (i.e., spheres) could be used over anisotropic ones to evade macrophages. However, Shimoni *et al.*[81] reported that capsules with high aspect ratios (i.e., rod-shaped capsules) were poorly internalized by HeLa cells in comparison to spherical ones. This highlights the complexity of endocytosis/phagocytosis processes and their dependence on cell type. Stiffness of the capsules, which can be modulated by the number of layers,[84] crosslinking reactions or incorporation of nanoparticles[87] also seems to determine the uptake efficiency, the softer capsules with lower stiffness being preferentially internalized by cells with respect to stiffer ones. Tuning the surface chemistry of the capsules can be used to either facilitate or avoid cellular uptake. Engineering the surface of the capsules by attaching bioactive molecules (e.g., peptides, antibodies, etc.) on the outermost layer allows the recognition of receptors and target the intended cells *via* the antibody-antigen interaction.[85] Surface PEGylation and similar approaches, in contrast, evade immune clearance and has also been applied to LbL capsules.[86]

Performing a systematic study to analyse the internalization mechanisms of our capsules is beyond the scope of this chapter. Polymer capsules are transported into cells by endocytosis but, determining the exact mechanism (e.g., caveolae-mediated endocytosis, clathrin-mediated endocytosis, etc.[88]) requires deeper analyses by

blocking/inhibiting various cellular endocytic pathways.[82] Herein, a preliminary study was designed to assess the internalization of the capsules by HeLa cells. Polymer capsules (i.e., (PAH/PSS)(dPG-DOX/PSS)$_2$) were incubated at a concentration of 10 polymer capsules/cell and fixed at different time points (2, 4 and 24 h) prior to their observation under the fluorescence microscope. As discussed above, at the selected time points, negligible release of DOX from the capsules is expected. This was further confirmed in the image merged with the brightfield, where DOX was clearly associated to the round-shaped capsules (**Fig. 4.14c, right**). As observed in **Fig. 4.14c**, polymer capsules showed a tendency to localize near the nucleus. A progressive accumulation of polymer capsules within the cells was observed along incubation time and, as a result, most of the capsules were accumulated around the perinuclear region at 24 h. A similar tendency was also reported in bibliography, in which a perinuclear accumulation of carriers was observed.[35,36]

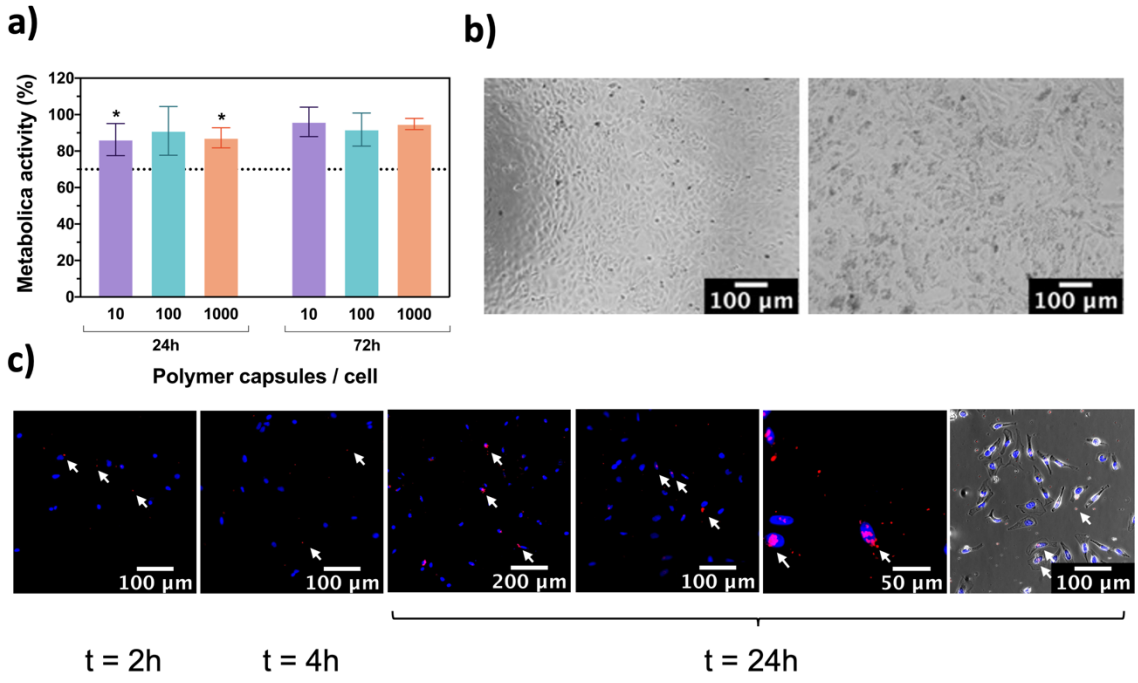

Fig. 4.14. *a) Metabolic activity of HeLa cells in the presence of polymer capsules. Asterisks (*) indicate significant differences ($p<0.05$) with respect to the control (cells in absence of capsules), b) Cell in absence of polymer capsules (left) and in the presence of polymer capsules (1000 polymer capsules / cell) (right), c) Fluorescence micrographs of HeLa cell in presence of polymer capsules at different time points (Nuclei-DAPI: blue / Polymer capsules functionalized with DOX: red). White arrows highlight the presence of DOX containing polymer capsules.*

4.3.5. Therapeutic potential of the polymer capsules in a H_2O_2-induced oxidative stress *in vitro* model

Oxidative stress leads to cellular apoptosis and senescence by damaging important cell structures, thus aggravating numerous disease pathologies such as cancer, neurodegeneration or osteoarthritis. Accordingly, a plethora of biomaterials to control oxidative stress has been developed in the last years including, among others, natural antioxidant-based micro- and nanoparticles (e.g., vitamin-E,[89] flavonoids,[90] etc.), synthetic polymeric nanoparticles with intrinsic antioxidant capacity[91] and nanozymes based on cerium oxide,[21] manganese dioxide[92] or carbon derivatives.[93] Although nanozymes represent a promising inorganic alternative to natural enzymes, showing a unique multienzyme mimetic activity, important challenges need to be addressed in terms of long-term cytotoxicity, biodistribution, *in vivo* uptake, etc. prior to their translation into biomedical applications.[94] In our present approach, inspired by compartmentalization strategies found at the cellular and subcellular levels, we encapsulated an antioxidant enzyme (i.e., catalase) into synthetic polymer capsules, resembling artificial organelles. This strategy provides increased robustness to the system by protecting the fragile enzymes from environmental harsh conditions, extending accordingly the storage time and its resistance to temperature, changes in pH, and so forth[95], while maintaining its recycling stability (i.e., capacity to efficiently perform successive batch reactions).[69] All these benefits, together with their cytocompatibility and the possibility to incorporate complementary entities as described above, make LbL capsules an excellent therapeutic platform to protect cells from oxidative stress.

An *in vitro* model with HeLa cells was used to evaluate the therapeutic potential of the fabricated polymer capsules. Cells were stimulated every 24 h with two biologically relevant H_2O_2 concentrations (i.e., 50 µM and 100 µM) to induce oxidative stress (**Fig. 4.15a**). This H_2O_2 extracellular concentrations are assumed to induce deleterious responses on cells, ultimately leading to oxidative distress.[96] Metabolic activity of the cells was assessed by the AlamarBlue® assay at different time points (8, 24, 32 and 48 h after the initial stimulus) (**Fig. 4.15a**). The H_2O_2 concentrations were chosen after a preliminary analysis to evaluate the effect of different concentrations on metabolic

activity. HeLa cells cultured in the absence of polymer capsules and H_2O_2 stimuli were used as negative control. Cells in absence of capsules but with H_2O_2 stimuli were considered as positive control. The concentrations of polymer capsules employed were 10, 100 and 1000 polymer capsules/cell, and they were not sterilized due to the aforementioned detrimental effect of the ethanol in the CAT scavenging capacity (**Fig. 4.13**). Alternatively, capsules were fabricated in clean conditions and all the employed solutions were sterile-filtered. No bacterial or other type of contamination was observed during the course of the experiment. In this particular experiment, capsules without DOX (i.e., (PAH/PSS) (dPG-amine/PSS)$_2$) were employed to avoid any possible toxic effect that could mask the protection of capsules against H_2O_2-induced oxidative stress.

At a H_2O_2 concentration of 50 μM, the metabolic activity of the cells decreased significantly ($p<0.05$) over time at both the positive control and with 10 polymer capsules/cell, with no significant differences between these two conditions (**Fig. 4.15b**). This suggested no therapeutic effect of the capsules at this concentration. However, with the addition of higher capsule-to-cell ratios (i.e., 100 and 1000 polymer capsules/cell) a beneficial effect was observed specially with the concentration of 1000 polymer capsules/cell (**Fig. 4.15b**). At the concentration of 100 polymer capsules/cell, the mean metabolic activity of the cells was always above the positive control, obtaining a significant difference ($p<0.05$) at 32 h (**Fig. 4.15b**). At 1000 polymer capsules/cell, significant differences ($p<0.05$) were observed at all the time-points with respect to the positive control, with the exception of the first time point (i.e., 8 h).

Using 100 μM H_2O_2 stimuli, a similar trend was observed. In the case of the positive control and 10 polymer capsules/cell concentration, the metabolic activity values were respectively 17.1 ± 4.6% and 23.4 ± 0.6% after 48 h. At 100 and 1000 polymer capsules/cell, the therapeutic effect of the capsules was again validated. With both polymer capsule-to-cell concentrations, the metabolic activity was significantly higher ($p<0.05$) than in the positive control at all the studied time points. Furthermore, at 1000 polymer capsules/cell, no differences in the metabolic activity were observed in comparison to the negative control (i.e., cells in absence of polymer capsules and H_2O_2) at the first two time points (i.e., 8 and 24 h), and the metabolic activity value was above 80%. These results suggest a therapeutic potential of these capsules to scavenge H_2O_2.

Although HeLa cells are not representative of any particular disease associated to oxidative stress, their response to H_2O_2 is similar to the one observed in other relevant cells. To study the effect of oxidative stress in various diseases (e.g., myocardial infarction, neurodegenerative processes, age-related macular degeneration, and so on), a wide variety of cells (e.g., cardiomyocytes, astrocytes, neural stem cells, human retinal pigment epithelial cells) have been exposed to H_2O_2.[97-100] In the reported studies, a H_2O_2 concentration of 100 µM induced a significant decrease in cell viability. Thus, we believe that the effect of the capsules observed herein with a well-established cell line could be translated to other validated disease models.

To further confirm the obtained results with the AlamarBlue® assay, cells were observed under the optical microscope. In the case of 50 µM of H_2O_2, some of the cells in the positive control were dead, while in the presence of capsules at a concentration of 1000 polymer capsules/cell, cells were able to maintain their density with less cell death (**Fig. 4.15c**), confirming the results obtained with the AlamarBlue® assay. In the case of 100 µM of H_2O_2, a higher quantity of dead cells was appreciable in the positive control (**Fig. 4.15c).** Contrarily, cells incubated in the presence of 1000 polymer capsules/cell were alive, and maintained their shape and density (**Fig. 4.15c**).

Taken together, these results confirm a therapeutic effect of the fabricated polymer capsules at the higher capsule-to-cell ratios (i.e., 100 and 1000 polymer capsules/cell) especially with 1000 polymer capsules/cell. At 10 polymer capsules/cell, no therapeutic effect was appreciated, suggesting that the concentration was not enough to protect cell from the H_2O_2-induced cell death.

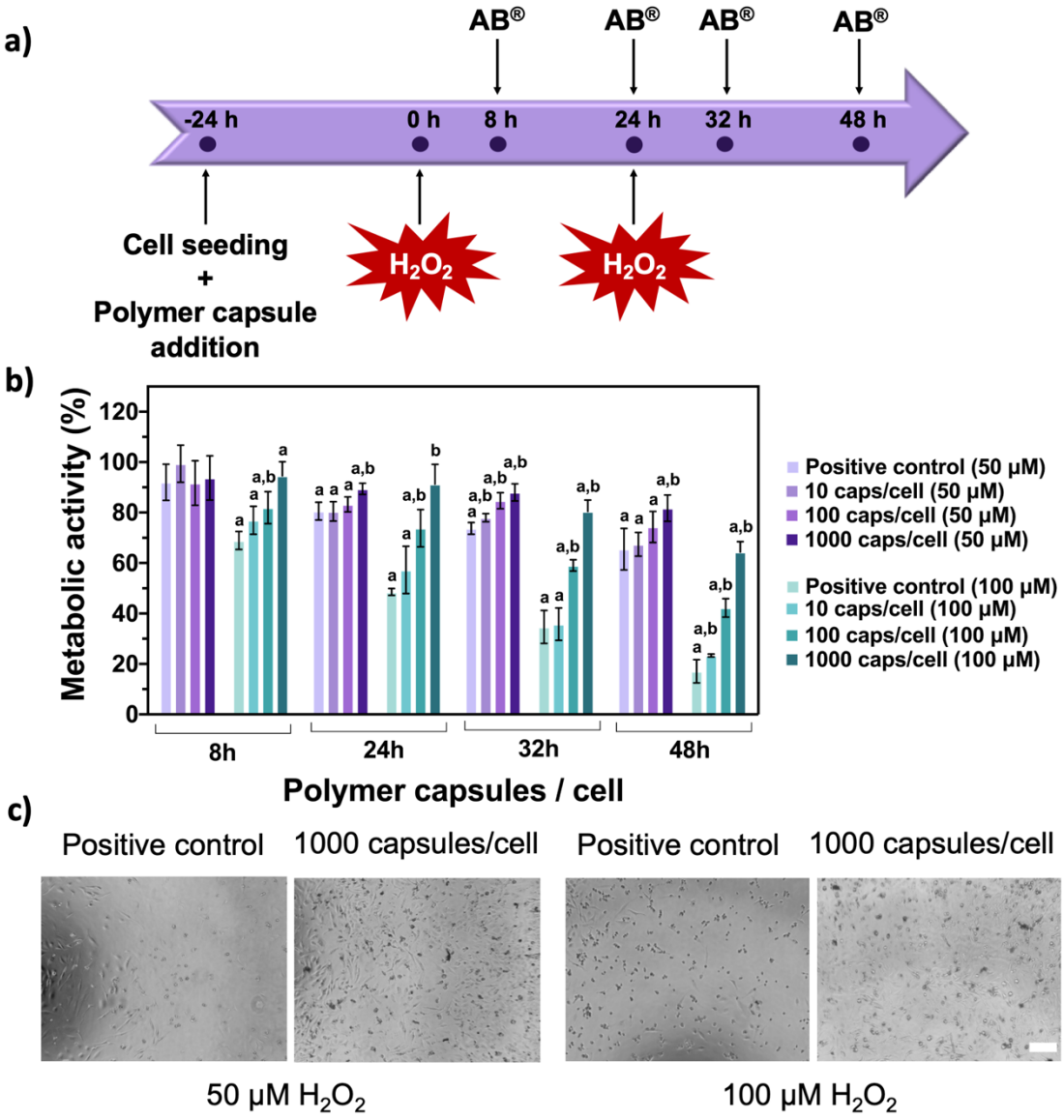

Fig. 4.15. *a) Schematic temporal distribution of stimuli addition and metabolic activity measurements, b) Metabolic activity of HeLa cells in the presence of H_2O_2 stimuli (50 µM and 100 µM) and polymer capsules. The "a" and "b" indicate significant differences with respect to the negative control (cells in the absence of capsules and H_2O_2) and the positive control (cells in the absence of capsules but with the addition of 50 µM or 100 µM of H_2O_2) respectively (n=4). 100% of metabolic activity was ascribed to the negative control, c) Optical micrographs of cells in absence of capsules and with the addition of H_2O_2 stimuli (left column), and cells with 1000 polymer capsules/cell and H_2O_2 stimuli (right column). Scale bar: 200 µm.*

4.4. Conclusions

In this chapter, we fabricated polymeric capsules *via* the LbL approach and exploited the versatility of this method to incorporate several functionalities into a single polymeric microplatform. The fabricated polymer capsules acted as antioxidant microreactors thanks to the encapsulation of catalase in their core and were able to release a model drug (i.e., DOX) in response to a biologically relevant stimulus (i.e., acidic pH) due to the incorporation of functionalized dPGs in their shell. Contrarily to previously reported delivery systems, our capsules preserve their structural integrity after the drug release process, thus avoiding the leakage of the encapsulated entity and functioning as robust microreactors that perform therapeutic biocatalytic reactions. The cytocompatibility of the developed capsules, which were internalized by cells and preferentially accumulated in the perinuclear region, was confirmed *in vitro*. In our validated oxidative stress model, the use of the higher polymer capsule concentrations resulted in a positive response, showing significant differences in the metabolic activity of the cells in comparison to the positive control (cell without capsules but stimulated with H_2O_2). Accordingly, the strategy proposed herein could be used in the development of multifunctional microreactors for the treatment of complex pathologies requiring complementary therapies.

References

(1) Zyuzin, M. V.; Timin, A. S.; Sukhorukov, G. B. Multilayer Capsules Inside Biological Systems: State-of-the-Art and Open Challenges. *Langmuir* **2019**, *35* (13), 4747–4762. https://doi.org/10.1021/acs.langmuir.8b04280.

(2) Costa, R. R.; Castro, E.; Arias, F. J.; Rodríguez-Cabello, J. C.; Mano, J. F. Multifunctional Compartmentalized Capsules with a Hierarchical Organization from the Nano to the Macro Scales. *Biomacromolecules* **2013**, *14* (7), 2403–2410. https://doi.org/10.1021/bm400527y.

(3) Aslan, S.; Deneufchatel, M.; Hashmi, S.; Li, N.; Pfefferle, L. D.; Elimelech, M.; Pauthe, E.; Van Tassel, P. R. Carbon Nanotube-Based Antimicrobial Biomaterials Formed *via* Layer-by-Layer Assembly with Polypeptides. J. Colloid Interface Sci. 2012, 388 (1), 268–273. https://doi.org/10.1016/j.jcis.2012.08.025

(4) Burke, S. E.; Barrett, C. J. PH-Responsive Properties of Multilayered Poly(L-Lysine)/ Hyaluronic Acid Surfaces. *Biomacromolecules* **2003**, *4* (6), 1773–1783. https://doi.org/10.1021/bm034184w.

(5) Keller, S. W.; Johnson, S. A.; Brigham, E. S.; Yonemoto, E. H.; Mallouk, T. E.; Johnson, S. A. Photoinduced Charge Separation in Multilayer Thin Films Grown by Sequential Adsorption of Polyelectrolytes. *J. Am. Chem. Soc.* **1995**, *117* (51), 12879–12880. https://doi.org/10.1021/ja00156a034.

(6) Caruso, F.; Caruso, R. A.; Möhwald, H. Nanoengineering of Inorganic and Hybrid Hollow Spheres by Colloidal Templating. *Science (80-.).* **1998**, *282* (5391), 1111–1114. https://doi.org/10.1126/science.282.5391.1111.

(7) Donath, E.; Sukhorukov, G. B.; Caruso, F.; Davis, S. A.; Möhwald, H. Novel Hollow Polymer Shells by Colloid-Templated Assembly of Polyelectrolytes. *Angew. Chem. Int. Ed. Engl.* **1998**, *37* (16), 2201–2205.

(8) Sukhorukov, G. B.; Donath, E.; Davis, S.; Lichtenfeld, H.; Caruso, F.; Popov, V. I.; Möhwald, H. Stepwise Polyelectrolyte Assembly on Particle Surfaces: A Novel Approach to Colloid Design. *Polym. Adv. Technol.* **1998**, *9* (10–11), 759–767. https://doi.org/10.1002/(SICI)1099-1581(1998100)9:10/11<759::AID-

PAT846>3.0.CO;2-Q.

(9) Lavalle, P.; Gergely, C.; Cuisinier, F. J. G.; Decher, G.; Schaaf, P.; Voegel, J. C.; Picart, C. Comparison of the Structure of Polyelectrolyte Multilayer Films Exhibiting a Linear and an Exponential Growth Regime: An *in situ* Atomic Force Microscopy Study. *Macromolecules* **2002**, *35* (11), 4458–4465. https://doi.org/10.1021/ma0119833.

(10) Rui, Y.; Pang, B.; Zhang, J.; Liu, Y.; Hu, H.; Liu, Z.; Ama Baidoo, S.; Liu, C.; Zhao, Y.; Li, S. Near-Infrared Light-Activatable siRNA Delivery by Microcapsules for Combined Tumour Therapy. *Artif. Cells, Nanomedicine Biotechnol.* **2018**, *46* (sup2), 15–24. https://doi.org/10.1080/21691401.2018.1449752.

(11) Cristofolini, L.; Szczepanowicz, K.; Orsi, D.; Rimoldi, T.; Albertini, F.; Warszynski, P. Hybrid Polyelectrolyte/Fe_3O_4 Nanocapsules for Hyperthermia Applications. *ACS Appl. Mater. Interfaces* **2016**, *8* (38), 25043–25050. https://doi.org/10.1021/acsami.6b05917.

(12) Popov, A. L.; Popova, N.; Gould, D. J.; Shcherbakov, A. B.; Sukhorukov, G. B.; Ivanov, V. K. Ceria Nanoparticles-Decorated Microcapsules as a Smart Drug Delivery/Protective System: Protection of Encapsulated P. Pyralis Luciferase. *ACS Appl. Mater. Interfaces* **2018**, *10* (17), 14367–14377. https://doi.org/10.1021/acsami.7b19658.

(13) Timin, A. S.; Muslimov, A. R.; Petrova, A. V.; Lepik, K. V.; Okilova, M. V.; Vasin, A. V.; Afanasyev, B. V.; Sukhorukov, G. B. Hybrid Inorganic-Organic Capsules for Eficient Intracellular Delivery of Novel siRNAs against Influenza A (H1N1) Virus Infection. *Sci. Rep.* **2017**, *7* (1), 1–12. https://doi.org/10.1038/s41598-017-00200-0.

(14) Pavlov, A. M.; Saez, V.; Cobley, A.; Graves, J.; Sukhorukov, G. B.; Mason, T. J. Controlled Protein Release from Microcapsules with Composite Shells Using High Frequency Ultrasound - Potential for in Vivo Medical Use. *Soft Matter* **2011**, *7* (9), 4341–4347. https://doi.org/10.1039/c0sm01536a.

(15) Timin, A. S.; Muslimov, A. R.; Lepik, K. V.; Epifanovskaya, O. S.; Shakirova, A. I.; Mock, U.; Riecken, K.; Okilova, M. V.; Sergeev, V. S.; Afanasyev, B. V.; Fehse, B.;

Sukhorukov, G. B. Efficient Gene Editing *via* Non-Viral Delivery of CRISPR–Cas9 System Using Polymeric and Hybrid Microcarriers. *Nanomedicine Nanotechnology, Biol. Med.* **2018**, *14* (1), 97–108. https://doi.org/10.1016/j.nano.2017.09.001.

(16) Ping, Y.; Guo, J.; Ejima, H.; Chen, X.; Richardson, J. J.; Sun, H.; Caruso, F. PH-Responsive Capsules Engineered from Metal-Phenolic Networks for Anticancer Drug Delivery. *Small* **2015**, *11* (17), 2032–2036. https://doi.org/10.1002/smll.201403343.

(17) Voronin, D. V.; Sindeeva, O. A.; Kurochkin, M. A.; Mayorova, O.; Fedosov, I. V.; Semyachkina-Glushkovskaya, O.; Gorin, D. A.; Tuchin, V. V.; Sukhorukov, G. B. *In Vitro* and *in Vivo* Visualization and Trapping of Fluorescent Magnetic Microcapsules in a Bloodstream. *ACS Appl. Mater. Interfaces* **2017**, *9* (8), 6885–6893. https://doi.org/10.1021/acsami.6b15811.

(18) German, S. V.; Bratashov, D. N.; Navolokin, N. A.; Kozlova, A. A.; Lomova, M. V.; Novoselova, M. V.; Burilova, E. A.; Zyev, V. V.; Khlebtsov, B. N.; Bucharskaya, A. B.; Terentyuk, G. S.; Amirov, R. R.; Maslyakova, G. N.; Sukhorukov, G. B.; Gorin, D. A. *In Vitro* and *in Vivo* MRI Visualization of Nanocomposite Biodegradable Microcapsules with Tunable Contrast. *Phys. Chem. Chem. Phys.* **2016**, *18* (47), 32238–32246. https://doi.org/10.1039/C6CP03895F.

(19) Adamczak, M.; Hoel, H. J.; Gaudernack, G.; Barbasz, J.; Szczepanowicz, K.; Warszyński, P. Polyelectrolyte Multilayer Capsules with Quantum Dots for Biomedical Applications. *Colloids Surfaces B Biointerfaces* **2012**, *90* (1), 211–216. https://doi.org/10.1016/j.colsurfb.2011.10.028.

(20) Larrañaga, A.; Isa, I. L. M.; Patil, V.; Thamboo, S.; Lomora, M.; Fernández-Yague, M. A.; Sarasua, J. R.; Palivan, C. G.; Pandit, A. Antioxidant Functionalized Polymer Capsules to Prevent Oxidative Stress. *Acta Biomater.* **2018**, *67*, 21–31. https://doi.org/10.1016/j.actbio.2017.12.014.

(21) Popov, A. L.; Popova, N. R.; Tarakina, N. V.; Ivanova, O. S.; Ermakov, A. M.; Ivanov, V. K.; Sukhorukov, G. B. Intracellular Delivery of Antioxidant CeO_2 Nanoparticles *via* Polyelectrolyte Microcapsules. *ACS Biomater. Sci. Eng.* **2018**, *4* (7), 2453–2462.

https://doi.org/10.1021/acsbiomaterials.8b00489.

(22) Larrañaga, A.; Lomora, M.; Sarasua, J. R.; Palivan, C. G.; Pandit, A. Polymer Capsules as Micro-/Nanoreactors for Therapeutic Applications: Current Strategies to Control Membrane Permeability. *Prog. Mater. Sci.* **2017**, *90*, 325–357. https://doi.org/10.1016/j.pmatsci.2017.08.002.

(23) Marin, E.; Tapeinos, C.; Lauciello, S.; Ciofani, G.; Sarasua, J. R.; Larrañaga, A. Encapsulation of Manganese Dioxide Nanoparticles into Layer-by-Layer Polymer Capsules for the Fabrication of Antioxidant Microreactors. *Mater. Sci. Eng. C* **2020**, *117* (April), 111349. https://doi.org/10.1016/j.msec.2020.111349.

(24) Gao, H.; Wen, D.; Tarakina, N. V.; Liang, J.; Bushby, A. J.; Sukhorukov, G. B. Bifunctional Ultraviolet/Ultrasound Responsive Composite TiO2/Polyelectrolyte Microcapsules. *Nanoscale* **2016**, *8* (9), 5170–5180. https://doi.org/10.1039/c5nr06666b.

(25) Xu, S.; Shi, J.; Feng, D.; Yang, L.; Cao, S. Hollow Hierarchical Hydroxyapatite/Au/Polyelectrolyte Hybrid Microparticles for Multi-Responsive Drug Delivery. *J. Mater. Chem. B* **2014**, *20* (38), 6500–6507. https://doi.org/10.1039/c4tb01066c.

(26) Passi, M.; Kumar, V.; Packirisamy, G. Theranostic Nanozyme: Silk Fibroin Based Multifunctional Nanocomposites to Combat Oxidative Stress. *Mater. Sci. Eng. C* **2020**, *107* (September 2019). https://doi.org/10.1016/j.msec.2019.110255.

(27) Jing, Y.; Zhu, Y.; Yang, X.; Shen, J.; Li, C. Ultrasound-Triggered Smart Drug Release from Multifunctional Core-Shell Capsules One-Step Fabricated by Coaxial Electrospray Method. *Langmuir* **2011**, *27* (3), 1175–1180. https://doi.org/10.1021/la1042734.

(28) Chen, Y.; Chen, H.; Zeng, D.; Tian, Y.; Chen, F.; Feng, J.; Shi, J. Core/Shell Structured Hollow Mesoporous Nanocapsules: A Potential Platform for Simultaneous Cell Imaging and Anticancer Drug Delivery. *ACS Nano* **2010**, *4* (10), 6001–6013. https://doi.org/10.1021/nn1015117.

(29) Chen, H.; Di, Y.; Chen, D.; Madrid, K.; Zhang, M.; Tian, C.; Tang, L.; Gu, Y. Combined Chemo- and Photo-Thermal Therapy Delivered by Multifunctional Theranostic

Gold Nanorod-Loaded Microcapsules. *Nanoscale* **2015**, *7* (19), 8884–8897. https://doi.org/10.1039/c5nr00473j.

(30) Boehnke, N.; Correa, S.; Hao, L.; Wang, W.; Straehla, J. P.; Bhatia, S. N.; Hammond, P. T. Theranostic Layer-by-Layer Nanoparticles for Simultaneous Tumor Detection and Gene Silencing. *Angew. Chemie - Int. Ed.* **2020**, *02115*, 2–10. https://doi.org/10.1002/anie.201911762.

(31) Liang, K.; Such, G. K.; Johnston, A. P. R.; Zhu, Z.; Ejima, H.; Richardson, J. J.; Cui, J.; Caruso, F. Endocytic PH-Triggered Degradation of Nanoengineered Multilayer Capsules. *Adv. Mater.* **2014**, *26* (12), 1901–1905. https://doi.org/10.1002/adma.201305144.

(32) Carregal-Romero, S.; Guardia, P.; Yu, X.; Hartmann, R.; Pellegrino, T.; Parak, W. J. Magnetically Triggered Release of Molecular Cargo from Iron Oxide Nanoparticle Loaded Microcapsules. *Nanoscale* **2015**, *7* (2), 570–576. https://doi.org/10.1039/c4nr04055d.

(33) Deng, L.; Li, Q.; Al-Rehili, S.; Omar, H.; Almalik, A.; Alshamsan, A.; Zhang, J.; Khashab, N. M. Hybrid Iron Oxide-Graphene Oxide-Polysaccharides Microcapsule: A Micro-Matryoshka for On-Demand Drug Release and Antitumor Therapy in Vivo. *ACS Appl. Mater. Interfaces* **2016**, *8* (11), 6859–6868. https://doi.org/10.1021/acsami.6b00322.

(34) Calderón, M.; Graeser, R.; Kratz, F.; Haag, R. Development of Enzymatically Cleavable Prodrugs Derived from Dendritic Polyglycerol. *Bioorganic Med. Chem. Lett.* **2009**, *19* (14), 3725–3728. https://doi.org/10.1016/j.bmcl.2009.05.058.

(35) Calderón, M.; Welker, P.; Licha, K.; Fichtner, I.; Graeser, R.; Haag, R.; Kratz, F. Development of Efficient Acid Cleavable Multifunctional Prodrugs Derived from Dendritic Polyglycerol with a Poly(Ethylene Glycol) Shell. *J. Control. Release* **2011**, *151* (3), 295–301. https://doi.org/10.1016/j.jconrel.2011.01.017.

(36) Baabur-Cohen, H.; Vossen, L. I.; Krüger, H. R.; Eldar-boock, A.; Yeini, E.; Landa-Rouben, N.; Tiram, G.; Wedepohl, S.; Markovsky, E.; Leor, J.; Calderón, M.; Satchi-Fainaro, R. In Vivo Comparative Study of Distinct Polymeric Architectures Bearing a Combination of Paclitaxel and Doxorubicin at a Synergistic Ratio. *J. Control.*

Release **2017**, *257*, 118–131. https://doi.org/10.1016/j.jconrel.2016.06.037.

(37) Sousa-Herves, A.; Würfel, P.; Wegner, N.; Khandare, J.; Licha, K.; Haag, R.; Welker, P.; Calderón, M. Dendritic Polyglycerol Sulfate as a Novel Platform for Paclitaxel Delivery: Pitfalls of Ester Linkage. *Nanoscale* **2015**, *7* (9), 3923–3932. https://doi.org/10.1039/c4nr04428b.

(38) Finkel, T. Oxidant Signals and Oxidative Stress. *Curr. Opin. Cell Biol.* **2003**, *15* (2), 247–254. https://doi.org/10.1016/S0955-0674(03)00002-4.

(39) Van Oppen, L. M. P. E.; Abdelmohsen, L. K. E. A.; Van Emst-De Vries, S. E.; Welzen, P. L. W.; Wilson, D. A.; Smeitink, J. A. M.; Koopman, W. J. H.; Brock, R.; Willems, P. H. G. M.; Williams, D. S.; Van Hest, J. C. M. Biodegradable Synthetic Organelles Demonstrate ROS Shielding in Human-Complex-I-Deficient Fibroblasts. *ACS Cent. Sci.* **2018**, *4* (7), 917–928. https://doi.org/10.1021/acscentsci.8b00336.

(40) Pereira, D. R.; Tapeinos, C.; Rebelo, A. L.; Oliveira, J. M.; Reis, R. L.; Pandit, A. Scavenging Nanoreactors That Modulate Inflammation. *Adv. Biosyst.* **2018**, *2* (6), 1–13. https://doi.org/10.1002/adbi.201800086.

(41) Pu, H. L.; Chiang, W. L.; Maiti, B.; Liao, Z. X.; Ho, Y. C.; Shim, M. S.; Chuang, E. Y.; Xia, Y.; Sung, H. W. Nanoparticles with Dual Responses to Oxidative Stress and Reduced PH for Drug Release and Anti-Inflammatory Applications. *ACS Nano* **2014**, *8* (2), 1213–1221. https://doi.org/10.1021/nn4058787.

(42) Yu, Z.; Ma, L.; Ye, S.; Li, G.; Zhang, M. Construction of an Environmentally Friendly Octenylsuccinic Anhydride Modified PH-Sensitive Chitosan Nanoparticle Drug Delivery System to Alleviate Inflammation and Oxidative Stress. *Carbohydr. Polym.* **2020**, *236* (January). https://doi.org/10.1016/j.carbpol.2020.115972.

(43) Haag, R.; Tuerk, H.; Mecking, S. Preparation of Highly Branched Polyols Based on Glycosides Useful as an Additive in Paints and Adhesives, Additive and Crosslinker in Polymers, in Cosmetics, Preparation of Nano Particles and Active Substance Carrier. DE10211664 A1, 2003.

(44) Willner, D.; Trail, P. A.; Hofstead, S. J.; King, H. D.; Lasch, S. J.; Braslawsky, G. R.; Greenfield, R. S.; Kaneko, T.; Firestone, R. A. (6-maleimidocaproyl)hydrazone of Doxorubicin. A New Derivative for the Preparation of Immunoconjugates of

Doxorubicin. *Bioconjug. Chem.* **1993**, *4* (6), 521–527. https://doi.org/10.1021/bc00024a015.

(45) Roller, S.; Zhou, H.; Haag, R. High-Loading Polyglycerol Supported Reagents for Mitsunobu- and Acylation-Reactions and Other Useful Polyglycerol Derivatives. *Mol. Divers.* **2005**, *9* (4), 305–316. https://doi.org/10.1007/s11030-005-8117-y.

(46) Hussain, A. F.; Krüger, H. R.; Kampmeier, F.; Weissbach, T.; Licha, K.; Kratz, F.; Haag, R.; Calderón, M.; Barth, S. Targeted Delivery of Dendritic Polyglycerol-Doxorubicin Conjugates by ScFv-SNAP Fusion Protein Suppresses EGFR+ Cancer Cell Growth. *Biomacromolecules* **2013**, *14* (8), 2510–2520. https://doi.org/10.1021/bm400410e.

(47) Feoktistova, N. A.; Vikulina, A. S.; Balabushevich, N. G.; Skirtach, A. G.; Volodkin, D. Bioactivity of Catalase Loaded into Vaterite $CaCO_3$ Crystals *via* Adsorption and Co-Synthesis. *Mater. Des.* **2019**, *185*, 108223. https://doi.org/10.1016/j.matdes.2019.108223.

(48) Petrov, A. I.; Volodkin, D. V.; Sukhorukov, G. B. Protein-Calcium Carbonate Coprecipitation: A Tool for Protein Encapsulation. *Biotechnol. Prog.* **2005**, *21* (3), 918–925. https://doi.org/10.1021/bp0495825.

(49) Donatan, S.; Yashchenok, A.; Khan, N.; Parakhonskiy, B.; Cocquyt, M.; Pinchasik, B. El; Khalenkow, D.; Möhwald, H.; Konrad, M.; Skirtach, A. Loading Capacity versus Enzyme Activity in Anisotropic and Spherical Calcium Carbonate Microparticles. *ACS Appl. Mater. Interfaces* **2016**, *8* (22), 14284–14292. https://doi.org/10.1021/acsami.6b03492.

(50) Sadasivan, S.; Sukhorukov, G. B. Fabrication of Hollow Multifunctional Spheres Containing MCM-41 Nanoparticles and Magnetite Nanoparticles Using Layer-by-Layer Method. *J. Colloid Interface Sci.* **2006**, *304* (2), 437–441. https://doi.org/10.1016/j.jcis.2006.09.010.

(51) Gao, C.; Moya, S.; Lichtenfeld, H.; Casoli, A.; Fiedler, H.; Donath, E.; Möhwald, H. The Decomposition Process of Melamine Formaldehyde Cores: The Key Step in the Fabrication of Ultrathin Polyelectrolyte Multilayer Capsules. *Macromol. Mater. Eng.* **2001**, *286* (6), 355–361. https://doi.org/10.1002/1439-

2054(20010601)286:6<355::AID-MAME355>3.0.CO;2-9.

(52) Antipov, A.; Shchukin, D.; Fedutik, Y.; Zanaveskina, I.; Klechkovskaya, V.; Sukhorukov, G.; Möhwald, H. Urease-Catalyzed Carbonate Precipitation inside the Restricted Volume of Polyelectrolyte Capsules. *Macromol. Rapid Commun.* **2003**, *24* (3), 274–277. https://doi.org/10.1002/marc.200390041.

(53) Sukhorukov, G. B.; Antipov, A. A.; Voigt, A.; Donath, E.; Ḿhwald, H. PH-Controlled Macromolecule Encapsulation in and Release from Polyelectrolyte Multilayer Nanocapsules. *Macromol. Rapid Commun.* **2001**, *22* (1), 44–46. https://doi.org/10.1002/1521-3927(20010101)22:1<44::AID-MARC44>3.0.CO;2-U.

(54) Shi, J.; Wang, X.; Xu, S.; Wu, Q.; Cao, S. Reversible Thermal-Tunable Drug Delivery across Nano-Membranes of Hollow PUA/PSS Multilayer Microcapsules. *J. Memb. Sci.* **2016**, *499*, 307–316. https://doi.org/10.1016/j.memsci.2015.10.065.

(55) Tiourina, O. P.; Antipov, A. A.; Sukhorukov, G. B.; Larionova, N. I.; Lvov, Y.; Möhwald, H. Entrapment of -Chymotrypsin into Hollow Polyelectrolyte Microcapsules. *Macromol. Biosci.* **2001**, *1* (5), 209–214. https://doi.org/10.1002/1616-5195(20010701)1:5<209::aid-mabi209>3.3.co;2-p.

(56) Valdepérez, D.; del Pino, P.; Sánchez, L.; Parak, W. J.; Pelaz, B. Highly Active Antibody-Modified Magnetic Polyelectrolyte Capsules. *J. Colloid Interface Sci.* **2016**, *474*, 1–8. https://doi.org/10.1016/j.jcis.2016.04.003.

(57) Fakhrullin, R. F.; Bikmullin, A. G.; Nurgaliev, D. K. Magnetically Responsive Calcium Carbonate Microcrystals. *ACS Appl. Mater. Interfaces* **2009**, *1* (9), 1847–1851. https://doi.org/10.1021/am9003864.

(58) Tarakanchikova, Y.; Alzubi, J.; Pennucci, V.; Follo, M.; Kochergin, B.; Muslimov, A.; Skovorodkin, I.; Vainio, S.; Antipina, M. N.; Atkin, V.; Popov, A.; Meglinski, I.; Cathomen, T.; Cornu, T. I.; Gorin, D. A.; Sukhorukov, G. B.; Nazarenko, I. Biodegradable Nanocarriers Resembling Extracellular Vesicles Deliver Genetic Material with the Highest Efficiency to Various Cell Types. *Small* **2019**. https://doi.org/10.1002/smll.201904880.

(59) Trushina, D. B.; Akasov, R. A.; Khovankina, A. V.; Borodina, T. N.; Bukreeva, T. V.; Markvicheva, E. A. Doxorubicin-Loaded Biodegradable Capsules: Temperature Induced Shrinking and Study of Cytotoxicity *in vitro*. *J. Mol. Liq.* **2019**, *284*, 215–224. https://doi.org/10.1016/j.molliq.2019.03.152.

(60) Christofidou-Solomidou, M.; Muzykantov, V. R. Antioxidant Strategies in Respiratory Medicine. *Treat. Respir. Med.* **2006**, *5* (1), 47–78. https://doi.org/10.2165/00151829-200605010-00004.

(61) Hood, E.; Simone, E.; Wattamwar, P.; Dziubla, T.; Muzykantov, V. Nanocarriers for Vascular Delivery of Antioxidants. *Nanomedicine* **2011**, *6* (7), 1257–1272. https://doi.org/10.2217/nnm.11.92.

(62) Yoshimoto, M. Stabilization of Enzymes through Encapsulation in Liposomes. *Methods Mol. Biol.* **2011**, *679*, 9–18. https://doi.org/10.1007/978-1-60761-895-9_2.

(63) Tanner, P.; Balasubramanian, V.; Palivan, C. G. Aiding Nature's Organelles: Artificial Peroxisomes Play Their Role. *Nano Lett.* **2013**, *13* (6), 2875–2883. https://doi.org/10.1021/nl401215n.

(64) Petro, M.; Jaffer, H.; Yang, J.; Kabu, S.; Morris, V. B.; Labhasetwar, V. Tissue Plasminogen Activator Followed by Antioxidant-Loaded Nanoparticle Delivery Promotes Activation/Mobilization of Progenitor Cells in Infarcted Rat Brain. *Biomaterials* **2016**, *81*, 169–180. https://doi.org/10.1016/j.biomaterials.2015.12.009.

(65) Beloqui, A.; Baur, S.; Trouillet, V.; Welle, A.; Madsen, J.; Bastmeyer, M.; Delaittre, G. Single-Molecule Encapsulation: A Straightforward Route to Highly Stable and Printable Enzymes. *Small* **2016**, *12* (13), 1716–1722.

(66) Beloqui, A.; Kobitski, A. Y.; Nienhaus, G. U.; Delaittre, G. A Simple Route to Highly Active Single-Enzyme Nanogels. *Chem. Sci.* **2018**, *9* (4), 1006–1013. https://doi.org/10.1039/c7sc04438k.

(67) Blackman, L. D.; Varlas, S.; Arno, M. C.; Houston, Z. H.; Fletcher, N. L.; Thurecht, K. J.; Hasan, M.; Gibson, M. I.; O'Reilly, R. K. Confinement of Therapeutic Enzymes in Selectively Permeable Polymer Vesicles by Polymerization-Induced Self-

Assembly (PISA) Reduces Antibody Binding and Proteolytic Susceptibility. *ACS Cent. Sci.* **2018**, *4* (6), 718–723. https://doi.org/10.1021/acscentsci.8b00168.

(68) Caruso, F.; Trau, D.; Möhwald, H.; Renneberg, R. Enzyme Encapsulation in Layer-by-Layer Engineered Polymer Multilayer Capsules. *Langmuir* **2000**, *16* (4), 1485–1488. https://doi.org/10.1021/la991161n.

(69) Shi, J.; Zhang, W.; Zhang, S.; Wang, X.; Jiang, Z. Synthesis of Organic-Inorganic Hybrid Microcapsules through *in situ* Generation of an Inorganic Layer on an Adhesive Layer with Mineralization-Inducing Capability. *J. Mater. Chem. B* **2015**, *3* (3), 465–474. https://doi.org/10.1039/c4tb01802h.

(70) Lvov, Y.; Antipov, A. A.; Mamedov, A.; Möhwald, H.; Sukhorukov, G. B. Urease Encapsulation in Nanoorganized Microshells. *Nano Lett.* **2001**, *1* (3), 125–128. https://doi.org/10.1021/nl0100015.

(71) Zhao, Q.; Zhang, S.; Tong, W.; Gao, C.; Shen, J. Polyelectrolyte Microcapsules Templated on Poly(Styrene Sulfonate)-Doped $CaCO_3$ Particles for Loading and Sustained Release of Daunorubicin and Doxorubicin. *Eur. Polym. J.* **2006**, *42* (12), 3341–3351. https://doi.org/10.1016/j.eurpolymj.2006.09.005.

(72) Khopade, A. J.; Caruso, F. Stepwise Self-Assembled Poly(amidoamine) Dendrimer and Poly(styrenesulfonate) Microcapsules as Sustained Delivery Vehicles. *Biomacromolecules* **2002**, *3* (6), 1154–1162. https://doi.org/10.1021/bm025562k.

(73) Son, K. J.; Yoon, H. J.; Kim, J. H.; Jang, W. D.; Lee, Y.; Koh, W. G. Photosensitizing Hollow Nanocapsules for Combination Cancer Therapy. *Angew. Chemie - Int. Ed.* **2011**, *50* (50), 11968–11971. https://doi.org/10.1002/anie.201102658.

(74) Yan, Y.; Johnston, A. P. R.; Dodds, S. J.; Kamphuis, M. M. J.; Ferguson, C.; Parton, R. G.; Nice, E. C.; Heath, J. K.; Caruso, F. Uptake and Intracellular Fate of Disulfide-Bonded Polymer Hydrogel Capsules for Doxorubicin Delivery to Colorectal Cancer Cells. *ACS Nano* **2010**, *4* (5), 2928–2936. https://doi.org/10.1021/nn100173h.

(75) Luo, G. F.; Xu, X. D.; Zhang, J.; Yang, J.; Gong, Y. H.; Lei, Q.; Jia, H. Z.; Li, C.; Zhuo, R. X.; Zhang, X. Z. Encapsulation of an Adamantane-Doxorubicin Prodrug in pH-Responsive Polysaccharide Capsules for Controlled Release. *ACS Appl. Mater.*

Interfaces **2012**, *4* (10), 5317–5324. https://doi.org/10.1021/am301258a.

(76) She, Z.; Wang, C.; Li, J.; Sukhorukov, G. B.; Antipina, M. N. Encapsulation of Basic Fibroblast Growth Factor by Polyelectrolyte Multilayer Microcapsules and Its Controlled Release for Enhancing Cell Proliferation. *Biomacromolecules* **2012**, *13* (7), 2174–2180. https://doi.org/10.1021/bm3005879.

(77) Pavlov, A. M.; Gabriel, S. A.; Sukhorukov, G. B.; Gould, D. J. Improved and Targeted Delivery of Bioactive Molecules to Cells with Magnetic Layer-by-Layer Assembled Microcapsules. *Nanoscale* **2015**, *7* (21), 9686–9693. https://doi.org/10.1039/c5nr01261a.

(78) Tarakanchikova, Y.; Muslimov, A.; Sergeev, I.; Lepik, K.; Yolshin, N.; Goncharenko, A.; Vasilyev, K.; Eliseev, I.; Bukatin, A.; Sergeev, V.; Pavlov, S.; Popov, A.; Meglinski, I.; Afanasiev, B.; Parakhonskiy, B.; Sukhorukov, G.; Gorin, D. A Highly Efficient and Safe Gene Delivery Platform Based on Polyelectrolyte Core-Shell Nanoparticles for Hard-to-Transfect Clinically Relevant Cell Types. *J. Mater. Chem. B* **2020**, *8* (41), 9576–9588. https://doi.org/10.1039/d0tb01359e.

(79) Fröhlich, E. The Role of Surface Charge in Cellular Uptake and Cytotoxicity of Medical Nanoparticles. *Int. J. Nanomedicine* **2012**, *7*, 5577–5591. https://doi.org/10.2147/IJN.S36111.

(80) Novoselova, M. V.; Loh, H. M.; Trushina, D. B.; Ketkar, A.; Abakumova, T. O.; Zatsepin, T. S.; Kakran, M.; Brzozowska, A. M.; Lau, H. H.; Gorin, D. A.; Antipina, M. N.; Brichkina, A. I. Biodegradable Polymeric Multilayer Capsules for Therapy of Lung Cancer. *ACS Appl. Mater. Interfaces* **2020**, *12* (5), 5610–5623. https://doi.org/10.1021/acsami.9b21381.

(81) Shimoni, O.; Yan, Y.; Wang, Y.; Caruso, F. Shape-Dependent Cellular Processing of Polyelectrolyte Capsules. *ACS Nano* **2013**, *7* (1), 522–530. https://doi.org/10.1021/nn3046117.

(82) Li, H.; Zhang, W.; Tong, W.; Gao, C. Enhanced Cellular Uptake of Bowl-like Microcapsules. *ACS Appl. Mater. Interfaces* **2016**, *8* (18), 11210–11214. https://doi.org/10.1021/acsami.6b02965.

(83) Brueckner, M.; Jankuhn, S.; Jülke, E. M.; Reibetanz, U. Cellular Interaction of a

Layer-by-Layer Based Drug Delivery System Depending on Material Properties and Cell Types. *Int. J. Nanomedicine* **2018**, *13*, 2079–2091. https://doi.org/10.2147/IJN.S153701.

(84) Hartmann, R.; Weidenbach, M.; Neubauer, M.; Fery, A.; Parak, W. J. Stiffness-Dependent *in vitro* Uptake and Lysosomal Acidification of Colloidal Particles. *Angew. Chemie - Int. Ed.* **2015**, *54* (4), 1365–1368. https://doi.org/10.1002/anie.201409693.

(85) Kolesnikova, T. A.; Kiragosyan, G.; Le, T. H. N.; Springer, S.; Winterhalter, M. Protein A Functionalized Polyelectrolyte Microcapsules as a Universal Platform for Enhanced Targeting of Cell Surface Receptors. *ACS Appl. Mater. Interfaces* **2017**, *9* (13), 11506–11517. https://doi.org/10.1021/acsami.7b01313.

(86) Dhanya, C. R.; Jeyaraman, J.; Janeesh, P. A.; Shukla, A.; Sivakumar, S.; Abraham, A. Bio-Distribution and: *in vivo* / *in vitro* Toxicity Profile of PEGylated Polymer Capsules Encapsulating $LaVO_4$:Tb^{3+} Nanoparticles for Bioimaging Applications. *RSC Adv.* **2016**, *6* (60), 55125–55134. https://doi.org/10.1039/c6ra06719k.

(87) Del Mercato, L. L.; Guerra, F.; Lazzari, G.; Nobile, C.; Bucci, C.; Rinaldi, R. Biocompatible Multilayer Capsules Engineered with a Graphene Oxide Derivative: Synthesis, Characterization and Cellular Uptake. *Nanoscale* **2016**, *8* (14), 7501–7512. https://doi.org/10.1039/c5nr07665j.

(88) Almeida, M. S. De; Susnik, E.; Drasler, B.; Rothen-rutishauser, B. Understanding Nanoparticle Endocytosis to Improve Targeting Strategies in Nanomedicine. **2021**. https://doi.org/10.1039/d0cs01127d.

(89) Bizeau, J.; Tapeinos, C.; Marella, C.; Larrañaga, A.; Pandit, A. Synthesis and Characterization of Hyaluronic Acid Coated Manganese Dioxide Microparticles That Act as ROS Scavengers. *Colloids Surfaces B Biointerfaces* **2017**, *159*, 30–38. https://doi.org/10.1016/j.colsurfb.2017.07.081.

(90) Roy, P.; Parveen, S.; Ghosh, P.; Ghatak, K.; Dasgupta, S. Flavonoid Loaded Nanoparticles as an Effective Measure to Combat Oxidative Stress in Ribonuclease A. *Biochimie* **2019**, *162*, 185–197. https://doi.org/10.1016/j.biochi.2019.04.023.

(91) Wattamwar, P. P.; Mo, Y.; Wan, R.; Palli, R.; Zhang, Q.; Dziubla, T. D. Antioxidant Activity of Degradable Polymer Poly(trolox ester) to Suppress Oxidative Stress Injury in the Cells. *Adv. Funct. Mater.* **2010**, *20* (1), 147–154. https://doi.org/10.1002/adfm.200900839.

(92) Tapeinos, C.; Tomatis, F.; Battaglini, M.; Larrañaga, A.; Marino, A.; Telleria, I. A.; Angelakeris, M.; Debellis, D.; Drago, F.; Brero, F.; Arosio, P.; Lascialfari, A.; Petretto, A.; Sinibaldi, E.; Ciofani, G. Cell Membrane-Coated Magnetic Nanocubes with a Homotypic Targeting Ability Increase Intracellular Temperature Due to ROS Scavenging and Act as a Versatile Theranostic System for Glioblastoma Multiforme. *Adv. Healthc. Mater.* **2019**, *8* (18). https://doi.org/10.1002/adhm.201900612.

(93) Mu, X.; He, H.; Wang, J.; Long, W.; Li, Q.; Liu, H.; Gao, Y.; Ouyang, L.; Ren, Q.; Sun, S.; Wang, J.; Yang, J.; Liu, Q.; Sun, Y.; Liu, C.; Zhang, X. D.; Hu, W. Carbogenic Nanozyme with Ultrahigh Reactive Nitrogen Species Selectivity for Traumatic Brain Injury. *Nano Lett.* **2019**, *19* (7), 4527–4534. https://doi.org/10.1021/acs.nanolett.9b01333.

(94) Liang, M.; Yan, X. Nanozymes: From New Concepts, Mechanisms, and Standards to Applications. *Acc. Chem. Res.* **2019**, *52* (8), 2190–2200. https://doi.org/10.1021/acs.accounts.9b00140.

(95) Shi, J.; Yang, C.; Zhang, S.; Wang, X.; Jiang, Z.; Zhang, W.; Song, X.; Ai, Q.; Tian, C. Polydopamine Microcapsules with Different Wall Structures Prepared by a Template-Mediated Method for Enzyme Immobilization. *ACS Appl. Mater. Interfaces* **2013**, *5* (20), 9991–9997. https://doi.org/10.1021/am403523d.

(96) Sies, H. Hydrogen Peroxide as a Central Redox Signaling Molecule in Physiological Oxidative Stress: Oxidative Eustress. *Redox Biol.* **2017**, *11* (December 2016), 613–619. https://doi.org/10.1016/j.redox.2016.12.035.

(97) Konyalioglu, S.; Armagan, G.; Yalcin, A.; Atalayin, C.; Dagci, T. Effects of Resveratrol on Hydrogen Peroxide-Induced Oxidative Stress in Embryonic Neural Stem Cells. *Neural Regen. Res.* **2013**, *8* (6), 485–495. https://doi.org/10.3969/j.issn.1673-5374.2013.06.001.

(98) Zhang, Y.; Liu, X.; Zhang, L.; Li, X.; Zhou, Z.; Jiao, L.; Shao, Y.; Li, M.; Leng, B.; Zhou, Y.; Liu, T.; Liu, Q.; Shan, H.; Du, Z. Metformin Protects against H_2O_2-Induced Cardiomyocyte Injury by Inhibiting the MiR-1a-3p/GRP94 Pathway. *Mol. Ther. - Nucleic Acids* **2018**, *13* (December), 189–197. https://doi.org/10.1016/j.omtn.2018.09.001.

(99) Zhao, H.; Wang, R.; Ye, M.; Zhang, L. Genipin Protects against H_2O_2 -Induced Oxidative Damage in Retinal Pigment Epithelial Cells by Promoting Nrf2 Signaling. *Int. J. Mol. Med.* **2019**, *43* (2), 936–944. https://doi.org/10.3892/ijmm.2018.4027.

(100) Amri, F.; Ghouili, I.; Amri, M.; Carrier, A.; Masmoudi-Kouki, O. Neuroglobin Protects Astroglial Cells from Hydrogen Peroxide-Induced Oxidative Stress and Apoptotic Cell Death. *J. Neurochem.* **2017**, *140* (1), 151–169. https://doi.org/10.1111/jnc.13876.

CHAPTER 5.

Layer-by-layer polymer capsules with antioxidant outer inorganic and organic layer as microplatforms to perform cascade reactions

CHAPTER 5. Layer-by-layer polymer capsules with antioxidant outer inorganic and organic layer as microplatforms to perform cascade reactions

Abstract

Enzymatic (bio)chemical cascade reactions play a pivotal role in the regular cell functioning. The alteration of these cascades may have a detrimental effect on cell homeostasis, growth and differentiation. Hence, the recovery of those aberrant cellular pathways becomes a fundamental factor in the restoration of the (bio)chemical stability. Within this context, the use of polymer capsules fabricated *via* the layer-by-layer (LbL) approach has emerged as a promising tool. The tuneable architecture of these capsules may allow the positioning of active entities on any of the constituent parts of the capsules by different functionalization and encapsulation techniques. In the present chapter, the formation of an inorganic (i.e., in situ formation of a MnO_2 layer) or organic (i.e., catalase loaded single enzyme nanogels (SENs)) antioxidant outer layer has been exploited to perform cascade reactions. These capsules efficiently scavenge H_2O_2 from the solution in both of the analysed systems. Furthermore, those capsules with an outer organic layer were capable of efficiently performing cascade reactions.

5.1. Introduction

The alteration in the metabolism of an enzyme interferes on regular (bio)chemical cascade reactions, these having drastic effects in homeostasis, growth and differentiation of cells.[1] In those cases, the fine-tunning of these cascade reactions and the whole replacement of the damaged cellular pathways, are fundamental to recover the proper functioning of cell metabolism.[1] Thus, inspired by the compartmentalization strategies found at the cellular and subcellular level, several replacing strategies based on biomaterials, such as liposomes or polymersomes, have been proposed.[1-3]

As an alternative to these methods, the use of polymer capsules fabricated *via* the layer-by-layer (LbL) approach is considered within the framework of the present chapter. As described along this PhD thesis, this technique allows the fabrication of micro- and

nanocapsules with *ad hoc* physical, chemical, morphological and mechanical properties.[4,5] Taking advantage of this versatility, this approach has been extensively used in the fabrication of drug/gene/protein delivery vehicles,[6-9] capsules for imaging applications[10-13] and in the fabrication of micro- and nanoreactors.[14-17] The latest are capable of encapsulating active entities like enzymes, and allow the continuous diffusion of reagents and by-products through the polymeric membrane while protecting them from proteases degradation and denaturation.[14,18,19] Furthermore, this fabrication technique enables the positioning of the active entities not only within the inner cavity but also in the polymeric shell by a simple electrostatic adsorption or by using different functionalization and encapsulation/entrapment techniques.[20-23]

In this chapter, we hypothesized that the LbL approach could be exploited to create polymer capsules with an outer antioxidant organic or inorganic layer, capable of performing cascade reactions. For the organic outer layer the single encapsulation of an individual protein molecule, denoted as Single Enzyme Nanogels (SENs), is considered.[24,25] In this SENs, the enzyme is wrapped within a thin polymeric mantle, increasing accordingly the stability of the active core under the physiological denaturing and degrading environments.[24,25] Thanks to the controlled thickness of the membrane, the encapsulated active entity is capable of maintaining similar properties to the free enzyme in terms of size[25] and, more importantly, in terms of reactivity and catalysis,[24] making them prone to be used in a wide variety of applications.[26-30]

However, despite the advances in the encapsulation and protection of the enzymes, their fabrication still remains expensive and laborious.[31,32] Within this context, inorganic alternatives like nanozymes (e.g., CeO_2[15,16] or MnO_2[33-36]) have emerged as promising tools to mimic the activity of organic enzymes while offering a higher robustness, ease of fabrication and lower cost.[32,37] Herein, MnO_2 particles are of particular interest in the scavenging of reactive oxygen species (ROS), due to their multienzyme activity which consist on mimicking the activity of superoxide dismutase (SOD) and catalase (CAT).[38-40] One promising way to incorporate this antioxidant scavenger into polymer nano- and microcapsules is *via* a mineralization process, in which a MnO_2 layer is created *in situ* through a simple reaction onto the polymer capsules or even onto individual living cells.[40]

In this chapter, we fabricated polymer capsules by depositing alternately layers of poly(sodium 4-styrenesulfonate) (PSS) and poly(allylamine hydrochloride) (PAH), on a glucose oxidase (GOx)-loaded $CaCO_3$ sacrificial template. GOx was employed as a proof of concept to test the capability of the proposed system to accomplish cascade reactions. For the outer inorganic antioxidant layer, an *in situ* mineralization process using $KMnO_4$ was followed, whereas the organic outer layer was obtained after the incubation of the fabricated polymer particles with CAT-loaded SENs. The physicochemical, morphological and functional properties of the capsules were thoroughly determined. This last experimental chapter represents accordingly a significant advance in the development of LbL polymer microreactors as platforms to perform cascade reactions and thus replace in the future damaged cellular pathways.

5.2. Materials and methods

5.2.1. Materials

Calcium chloride ($CaCl_2$), sodium carbonate (Na_2CO_3), sodium chloride (NaCl), potassium permanganate ($KMnO_4$), hydrogen peroxide (H_2O_2) (30% wt. in H_2O), poly (allylamine hydrochloride) (PAH) ($M_w \sim 17{,}500$ g/mol), poly (sodium 4-styrenesulfonate) (PSS) ($M_w \sim 70{,}000$ g/mol), o-toluidine, glacial acetic acid, ethylenediaminetetraacetic acid disodium salt dihydrate (EDTA), glucose oxidase (GOx) from *Aspergillus niger*, glucose, tetramethylrhodamine isothiocyanate (TRITC), Phosphate Buffer Saline (PBS) and Hank's Balanced Salt Solution were purchased from Sigma Aldrich. Dulbecco's modified Eagle's medium (DMEM), fetal bovine serum (FBS), penicillin-streptomycin solution (P/S) and AlamarBlue® cell viability reagents were purchased from Thermo Fisher Scientific.

5.2.2. Fabrication of single enzyme nanogels (SENs)

SENs were kindly provided by our collaborators and were synthesized following their well-established protocols.[25] Briefly, catalase (CAT) (8.9 g/L, 2 mL in sodium phosphate 50 mM buffer, pH 6.1) was deoxygenated by bubbling N_2 for 45 min. After that, sucrose (5%, w/v), together with acrylamide (AA) and bisacrylamide (BIS) in deoxygenated sodium phosphate buffer (50 mM, pH = 6.1), and carboxyethyl acrylate (CEA) in deoxygenated DMSO (10% v/v, 33 mM) were added to the enzyme solution. Monomer ratios were kept constant (AA/protein 600:1 mol/mol; BIS/protein 600:1 mol/mol; CEA/protein 1000:1 mol/mol). In continuous nitrogen bubbling, ammonium persulfate (APS/protein 500:1 mol/mol) and tetramethylethylenediamine (TEMED/APS 2:1 w/w) were added to the enzyme/AA/BIS/CEA mixture. The reaction was kept under N_2 and shaken at room temperature for 2 h. The obtained SENs were dialyzed against PBS buffer to remove low-molar mass reagents and passed through a Sephadex G-75 column to remove non-encapsulated enzymes and protein-free polymer hydrogels. Negatively charged SENs were obtained with a ζ-potential value of -17.2 ± 2.2 mV.

5.2.3. Fabrication and characterization of polymer capsules with an antioxidant outer layer

5.2.3.1. Fabrication of polymer capsules

Polymer capsules were fabricated *via* the LbL approach using $CaCO_3$ microparticles as sacrificial template and PSS and PAH as negative and positive polyelectrolytes respectively. GOx loaded $CaCO_3$ templates were obtained by the co-precipitation of $CaCl_2$, Na_2CO_3 and GOx, similar to previous reports.[14] Separately prepared Na_2CO_3 1M aqueous solution and 3 mg/mL GOx solution dissolved in Tris-HCl 0.05 M (pH = 7.0) were poured into the $CaCl_2$ 1M aqueous solution and after 30 s of vigorous stirring (1100 rpm) the solution was incubated for 15 min. The obtained dispersion was centrifuged at 2000 g (1 min) and the particles were washed thrice with a 0.005 M NaCl solution. As the GOx containing $CaCO_3$ microparticles have a negative surface charge, the collected microparticles were then resuspended in a 2 mg/mL PAH solution in 0.5 M NaCl (pH = 6.5). After 12 min of incubation, the dispersion was centrifuged and washed three times with 0.005 M NaCl solution. Subsequently, the particles were resuspended in a 2 mg/mL PSS solution in 0.5 M NaCl (pH = 6.5) and after 12 min of incubation the particles were collected and washed thrice with 0.005 M NaCl solution. Particles containing five layers were fabricated with a final PAH layer to allow the following mineralization process and deposition of negatively charged SEN by electrostatic interactions. The mineralization process was carried out following the direct redox reaction between PAH and $KMnO_4$ reported in previous works.[39,41] For this, after the deposition of the last PAH layer, microparticles were incubated with an aqueous $KMnO_4$ solution at different concentrations (i.e.., 2.5, 5, 10, 20, 50 and 100 mM) for 15 min. Thereafter, particles were thoroughly washed thrice with a 0.005 M NaCl solution. In the case of SENs, 10 µg/mL and 25 µg/mL solutions in 0.5 M NaCl were incubated with the positively charged microparticle suspension for 12 min and after that, the microparticles were washed three times with 0.005 M NaCl solution. Finally, both systems were immersed in 0.1 M EDTA solution to remove the template following the same protocol described in previous chapters **(Fig. 5.1).** After that, the particles were washed several times with PBS or distilled water for the following analysis.

In a particular case, TRITC-labelled GOx (GOx-TRITC) was used for the fabrication of capsules to check the successful encapsulation of the enzyme. For this a protocol provided by Thermo Scientific was followed with slight modifications.[42] Briefly, GOx was dissolved in a 100 mM carbonate buffer (pH = 9.5) at a concentration of 6.5 mg/mL, and 35 µL of a TRITC solution (1 mg/mL in DMSO) were added dropwise. The mixture was mixed thoroughly and incubated overnight at room temperature sheltered from light. After that, the solution was filtered using a PD 10 desalting column to remove the excess of TRITC using as filtering buffer Tris-HCl 0.05 M (pH = 7.0). The obtained solution was stored at 4 ^{o}C until use.

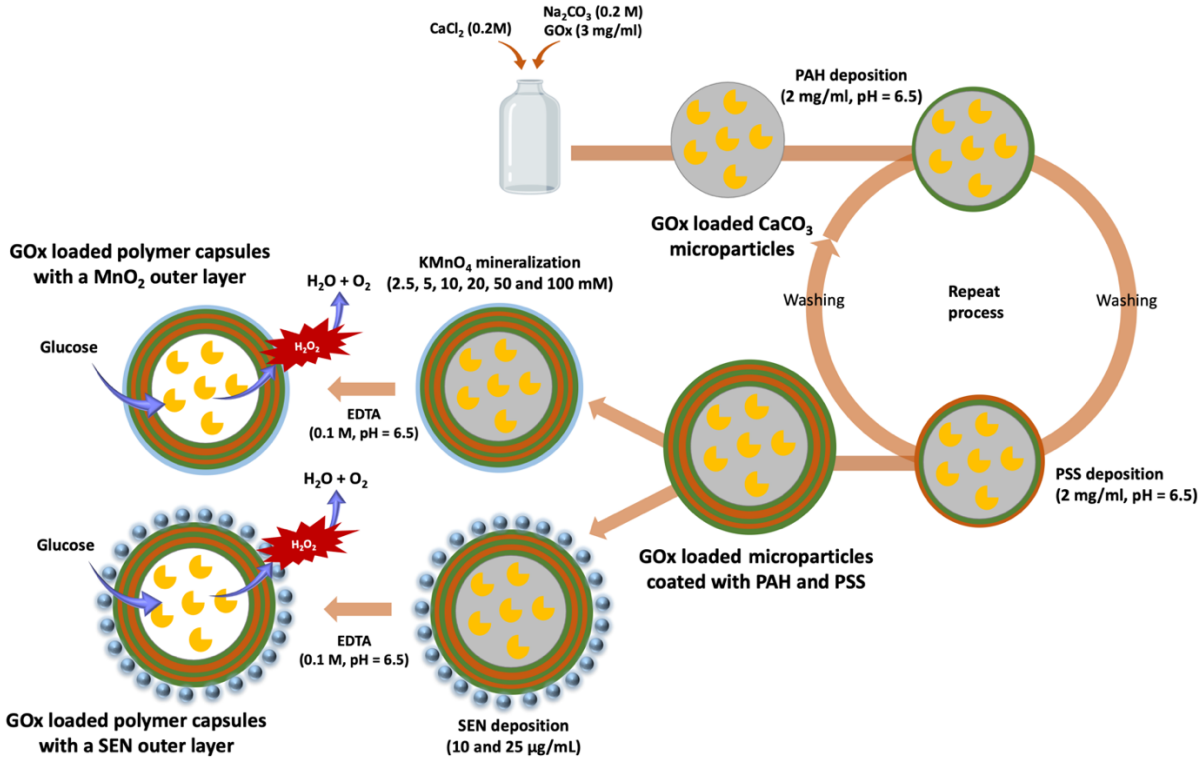

Fig. 5.1. *Schematic representation of the fabrication of antioxidant polymer capsules.*

5.2.3.2. Physico-chemical and morphological characterization

The morphological analysis of the polymer capsules was carried out by means of Scanning Electron Microscopy (SEM: HITACHI S-4800) at a working voltage and working current of 5 kV and 10 nA respectively.

The ζ-potential after each polyelectrolyte deposition was measured from a minimum of ten runs using a Malvern Instrument Zetasizer (ZEN 3690).

To confirm the presence of the MnO_2 in the outer layer capsules were analysed under X-ray photoelectron spectroscopy (XPS: SPECS (Berlin, Germany)) equipped with Phoibos 150 1D-DLD analyser and an Al Kα monochromatic radiation source (1486.7 eV). An initial analysis was made to determine the main elements present (wide scan: step energy 1 eV, dwell time 0.1 s, pass energy 80 eV) and after that a detailed analysis was carried out to the detected main elements (detail scan: step energy 0.08 eV, dwell time 0.1 s, pass energy 30 eV) using an electron output angle of 90º. The spectrometer was previously calibrated with Ag (Ag 3d5/2, 368.26 eV).

The presence of MnO_2 was further confirmed by UV-VIS (Perkin Elmer lambda 365) measuring the wavelength spectra of $KMnO_4$ solution and capsules after $KMnO_4$ incubation.

The encapsulation of GOx and the incorporation of SENs was confirmed by mean of confocal laser scanning microscopy (CLSM). Images were captured using a Leica TCS SP STED confocal microscope (Germany) equipped with a 63x oil immersion objective.

To further confirm the distribution of the fluorescently labelled GOx (GOx-TRITC) and SENs (CAT-FITC), the fabricated polymer capsules were analysed by means of Fluorescent Activated Cell Sorter (FACS: MoFlo Astrios EQs Sorter, Beckman Coulter, US). For the analysis, 100,000 events were made per sample (λ_{ex} = 488 nm/λ_{em} = 519-526 nm for green fluorescence and λ_{ex} = 561 nm/λ_{em} = 579-616 nm for red fluorescence). The obtained results were analysed with the FlowJo software (Tree Star, Inc., USA).

5.2.4. Glucose reduction and antioxidant capacity of the capsules

The antioxidant capacity of the polymer capsules with the outer inorganic and organic layer was measured using a Fluorimetric Hydrogen Peroxide Assay Kit (Sigma Aldrich). To do so, capsules at a final concentration of $1 \cdot 10^7$ and $1 \cdot 10^8$ polymer capsules/mL were incubated for 30 min in the presence of biologically relevant H_2O_2 concentrations (i.e., 10 µM and 50 µM). After that, the dispersion of capsules was centrifuged and 50 µL of the supernatant were incubated in a 96-well plate with 50 µL of master mix containing horseradish peroxidase and red peroxidase substrate. The mixture was incubated protected from light for 20 min protected from light and after that, the fluorescence

intensity was measured (λ_{ex} = 540 nm/λ_{em} = 590 nm) on a microplate reader (BioTek Synergy H1M) to determine the H_2O_2 concentration.

Glucose reduction was measured using a o-toluidine and a glacial acetic acid incubation solution similar to previous reports.[43] O-toluidine (6.0% v/v) was dissolved in glacial acetic acid and the mixture was allowed to age for a week at room temperature protected from light. Once the incubating solution was prepared, this was mixed with the corresponding samples in a relation of 1 mL of sample per 3 mL of incubation solution and the mixture was immersed in a 100 ^{o}C water bath for 8 min. After that, the absorbance signal at 360 nm was measured using a microplate reader (BioTek Synergy H1M) to determine the glucose concentration of the solution.

5.2.5. Glucose oxidase and SEN cascade reaction

The cascade reaction between the encapsulated GOx and the catalase from the SENs was assessed using a Fluorimetric Hydrogen Peroxide Assay Kit (Sigma Aldrich). Briefly, capsules with and without the external SEN layer and at a final concentration of $1{\cdot}10^7$ and $1{\cdot}10^8$ polymer capsules/mL were incubated with three glucose concentration (i.e., 100 µM, 250 µM and 500 µM) for 30 min. After incubating for 20 min protected from light, fluorescence intensity was measured (λ_{ex} = 540 nm/λ_{em} = 590 nm) on a microplate reader (BioTek Synergy H1M) to determine the H_2O_2 concentration.

5.2.6. *In vitro* studies

5.2.6.1. MRC-5 cell seeding

MRC-5 fibroblast cells were seeded following the same protocol described in the previous chapters for HeLa cells. A density of 5,000 cells/well on a 96-well plate was used for metabolic activity measurements.

5.2.6.2. Preliminary cytocompatibility test

The cytotoxicity of the capsules was evaluated as described in Chapters 3 and 4. Three capsule concentrations ($1{\cdot}10^6$, $1{\cdot}10^7$ and $1{\cdot}10^8$ polymer capsules/mL) and two time

points (24 and 72 h) were analysed, and AlamarBlue was used to measure the metabolic activity of cells.

5.2.7. Statistical analysis

All quantitative data related to the fabrication and characterization of polymer capsules are presented as the mean ± standard deviation (SD). In the *in vitro* studies the results are presented as mean ± SD, with n = 4. The statistical difference between groups was tested by one-way analysis of variance (ANOVA), using the Bonferroni post-hoc test and a confidence level of 95% ($p<0.05$).

5.3. Results and discussion

5.3.1. Fabrication of polymer capsules *via* the layer-by-layer approach and formation of the antioxidant layer

For the fabrication of polymer capsules, $CaCO_3$ template was first synthesized through the co-precipitation of GOx together with $CaCl_2$ and Na_2CO_3 salts (**Fig. 5.1**), due to the reported high encapsulation efficiency of this method comparing to other alternatives.[44,45] As observed in SEM images, the obtained microparticles presented a porous spherical shape with a mean diameter size of ∼3−4 μm (**Fig. 5.2c**). $CaCO_3$ was selected as the sacrificial template not only for its capability to efficiently encapsulate large molecules but also due to its ease of preparation and subsequent dissolution using calcium chelating agents (i. e., ethylenediaminetetraacetic acid disodium salt dehydrate (EDTA)) thus avoiding the use of harsh conditions (i.e., organic solvents and/or extremely high/low pH) in template removal.[4] The protocol used for the encapsulation of GOx allows the pre-encapsulation of the enzyme avoiding this way post-encapsulation methods used in other type of templates, which usually rely on the change in the permeability of the polymeric membrane.[46,47] For this, changes in solvent composition,[48] pH[49] or temperature[50] are employed leading usually to a loss in the integrity and catalytic activity of the enzyme.

Once the sacrificial template was obtained, positively charged PAH and negatively charged PSS were deposited alternately onto GOx loaded $CaCO_3$ ($CaCO_3$-GOx) cores. These polyelectrolytes were chosen due to their extensive use as model polyelectrolytes in the fabrication of LbL capsules for different therapeutic systems and because of their robustness.[51-54] Thanks to this, capsules are capable of enabling the transfer of reagents and by-products across the polymeric membrane while protecting the encapsulated entity from external microenvironment. This attribute is a key factor in the fabrication of LbL nano- and microreactors since the uncontrolled degradation of the polymeric membrane could have a detrimental effect in the encapsulated enzyme, exposing it to external physiological conditions which can lead to protease degradation and denaturation.

As the initial surface charge of the sacrificial template was negative (pI_{GOx} = 4.2), $CaCO_3$-GOx microparticles were first incubated with PAH. In the case of capsules mineralized *in situ* to create the antioxidant MnO_2 layer this resulted in a surface charge shift from -13.0 ± 0.5 mV to -2.4 ± 0.4 mV for $KMnO_4$ values of 2.5 mM, 5 mM and 10 mM and from -13.2 ± 0.4 mV to 0.2 ± 0.1 mV for $KMnO_4$ values of 20 mM, 50 mM and 100 mM (**Fig. 5.2b**). After that, polyelectrolyte layers were assembled alternately and a reversal ζ-potential value change was observed after each deposition step, confirming the successful layer assembly (**Fig. 5.2b**). Capsules with 5 layers were fabricated with a final PAH layer, which will allow the subsequent mineralization process.

In nature, the creation of mineral shells can play a pivotal role in the protection of different organism acting as a shield for hostile stressors and external environments.[40,55] Mimicking this biomineralization process, different works proposed this method for the protection of bacteria and cells.[40,55] In our work, a simple mineralization process was proposed for the *in situ* fabrication of an antioxidant outer layer capable of reducing ROS present in the microenvironment. Taking advantage of the affinity of amine groups from PAH to metal ions, a direct redox reaction between the last PAH layer and $KMnO_4$ at different concentrations was carried out (**Fig. 5.2a**). After the incubation, the colour of the particle pellet changed from white to dark brown, as reported in other works,[56] suggesting the formation of the MnO_2 layer onto the capsules (**Fig. 5.3a**). After this process, the sacrificial template was removed by immersing in a 0.1 M EDTA solution (**Fig. 5.1**). As observed in SEM micrographs after the EDTA incubation, polymer capsules presented a collapsed shape suggesting the complete removal of the sacrificial core (**Fig. 5.2d**)

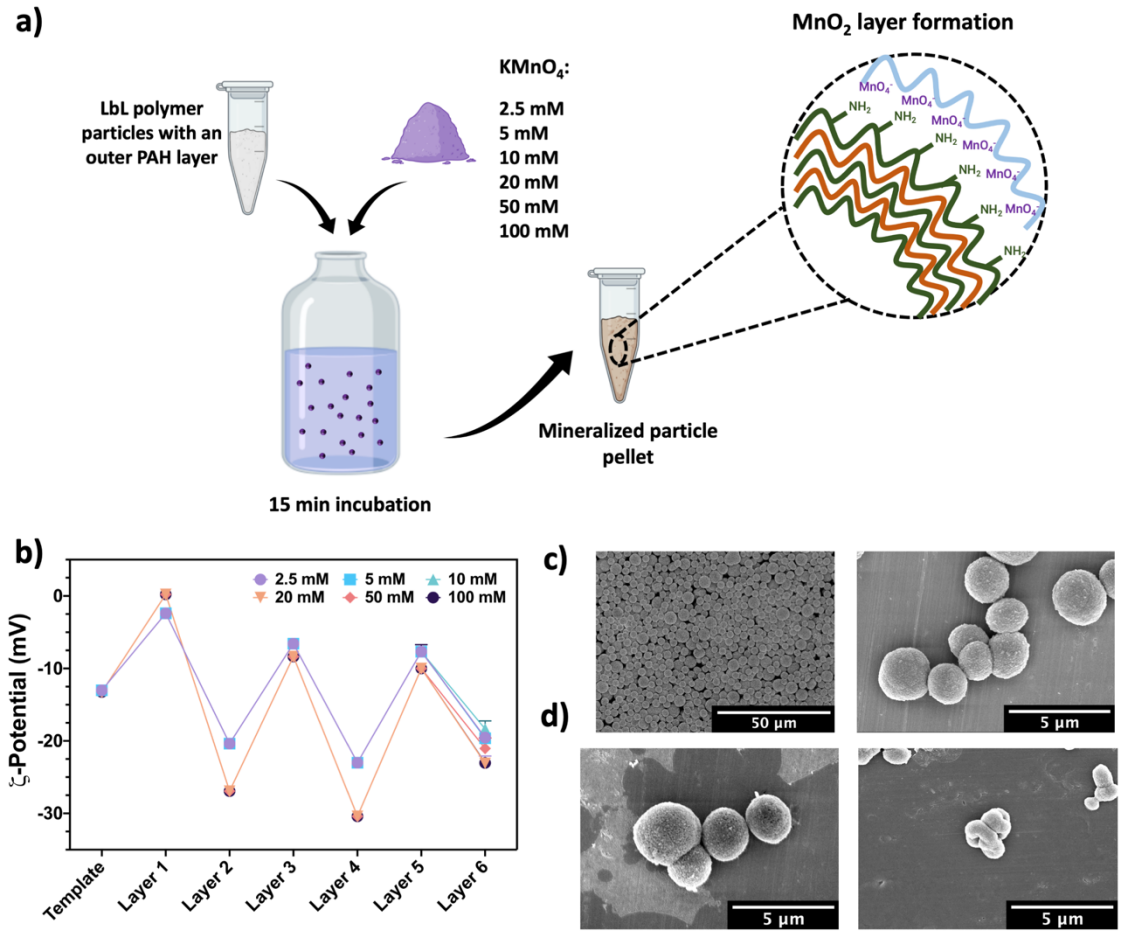

Fig. 5.2. *a) Schematic representation of the mineralization process of the fabricated polymer capsules. b) ζ-potential of $CaCO_3$-GOx microparticles after each layer deposition using for the fabrication of the final antioxidant layer different $KMnO_4$ concentrations (e. g., 2.5, 5, 10, 20, 50 and 100 mM). c) Morphological characterization via SEM of $CaCO_3$-GOx templates. d) Morphological characterization of $KMnO_4$ mineralized polymer capsules before (left) and after (right) 0.1 M EDTA incubation*.

The successful fabrication of MnO_2 layer onto the fabricated capsules was firstly assessed by means of UV-vis. After the incubation of the particles with $KMnO_4$ and the subsequent template removal, the UV-vis spectra of them was measured and compared with the raw $KMnO_4$ solution spectra. The obtained results showed that the characteristic peaks of $KMnO_4$ (i.e., 315, 525 and 545 nm) disappeared after its incubation with polymer particles bearing an external PAH layer (**Fig. 5.3b**). The particles showed one single wide band around 300 nm regardless the $KMnO_4$ concentration used, suggesting the formation of MnO_2 onto the polymer particles (**Fig. 5.3b**). This tendency

was observed in other works, in which the presence of this peak around 300 nm was attributed to the plasmon band of colloidal manganese dioxide.[39]

To further confirm the presence of MnO_2 in the capsules, they were analysed by means of XPS using capsules without the last mineralization step as a control. In the obtained results it was observed that the binding energy related to the Mn 2p 3/2 peak was 642.1 eV which corresponds to the binding energy of MnO_2 as reported in XPS handbook (**Fig. 5.3c**).[57]

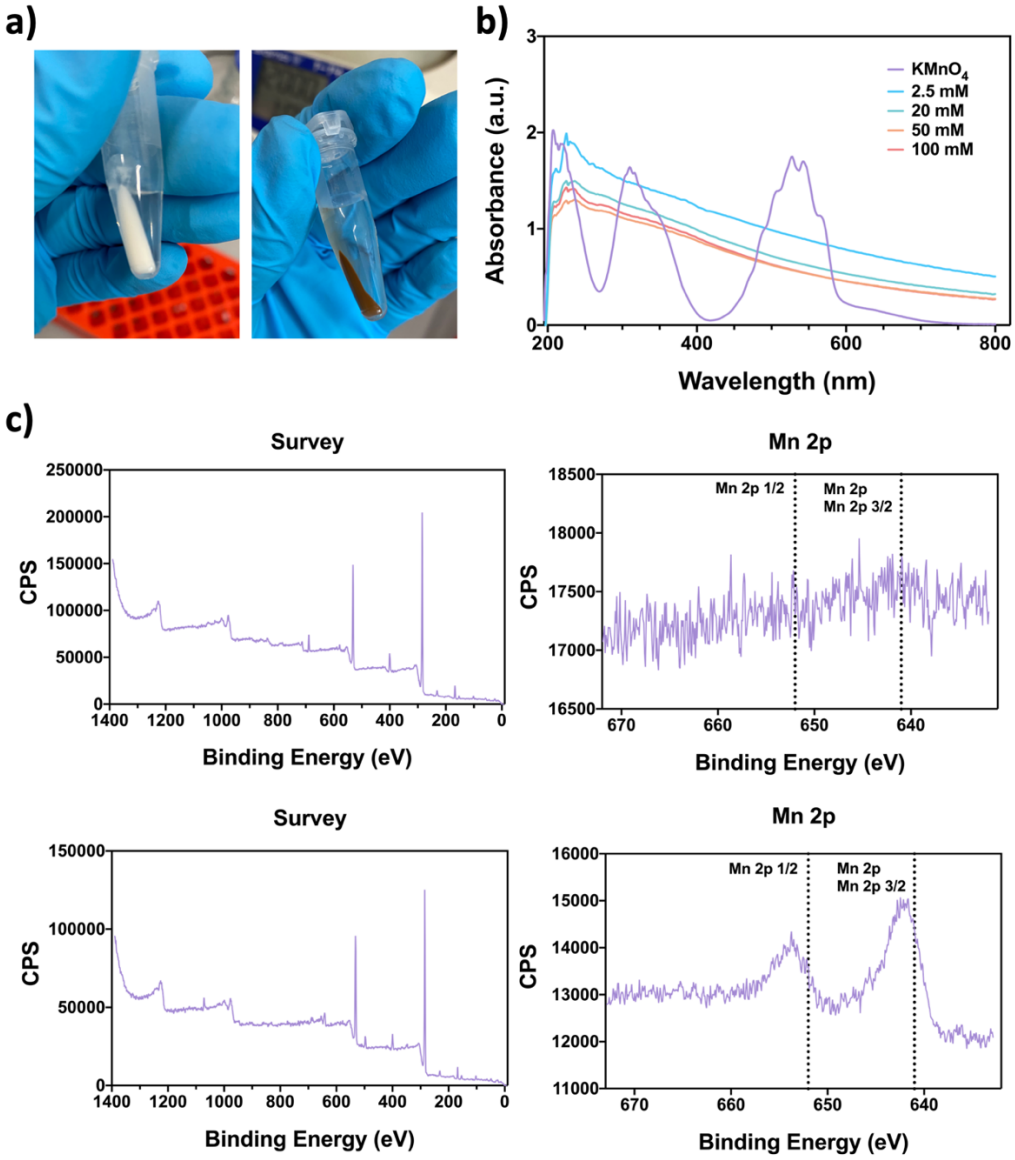

Fig. 5.3. *a) Polymer capsules before (left) and after (right) the in situ mineralization. b) UV-vis spectra of $KMnO_4$ in solution and polymer particles incubated with different $KMnO_4$ concentrations (e.g., 2.5, 20, 50 and 100 mM). c) XPS spectra of non-mineralized (upper row) and mineralized (lower row) polymer capsules ($KMnO_4$ concentration: 50 mM).*

In the case of the polymer capsules fabricated with the organic antioxidant outer layer of SENs, as the initial charge of the sacrificial template was negative too, these microparticles were also first incubated with PAH resulting in a surface charge shift from -13.8 ± 0.3 mV to 3.6 ± 0.7 mV (**Fig. 5.4a**). Thereafter, polyelectrolytes were assembled alternately obtaining a ζ-potential charge reversal after each deposition step which confirms the successful assembly of the deposited layers (**Fig. 5.4a**). After the addition of the SENs the change in the ζ-potential value was slightly appreciable. This could be due to the low SEN quantity and their non-uniform distribution around the outer layer.

To confirm the successful encapsulation of GOx and the adhesion of SENs onto the capsules, fluorescently labelled GOx (GOx-TRITC) and SEN encapsulating fluorescent CAT (CAT-FITC) at a concentration of 10 µg/mL were fabricated and analysed by means of confocal microscope. In this particular case, to obtain a uniform red signal in the core, provided by GOx-TRITC, an excess of non-fluorescently labelled GOx was added in the co-precipitation process of the sacrificial template together with GOx-TRITC. Since the enzyme is negatively charged and have a tendency to electrostatically interact with the positively charged inner membrane (i.e., the first PAH layer), the specific accumulation of the enzyme near the membrane was avoided by adding an excess of enzyme. In the obtained micrographs, a uniformly distributed red signal corresponding to the GOx and green fluorescence signals corresponding to the SENs were observed, accordingly confirming the successful incorporation of both enzymes in the fabricated polymer capsules (**Fig. 5.4b**). To further analyse the distribution of SENs transversal cuts of this capsules were taken with the confocal microscope and it was observed that the SENs were preferentially deposited on the outer layer of the capsule with an irregular distribution (**Fig. 5.4c**).

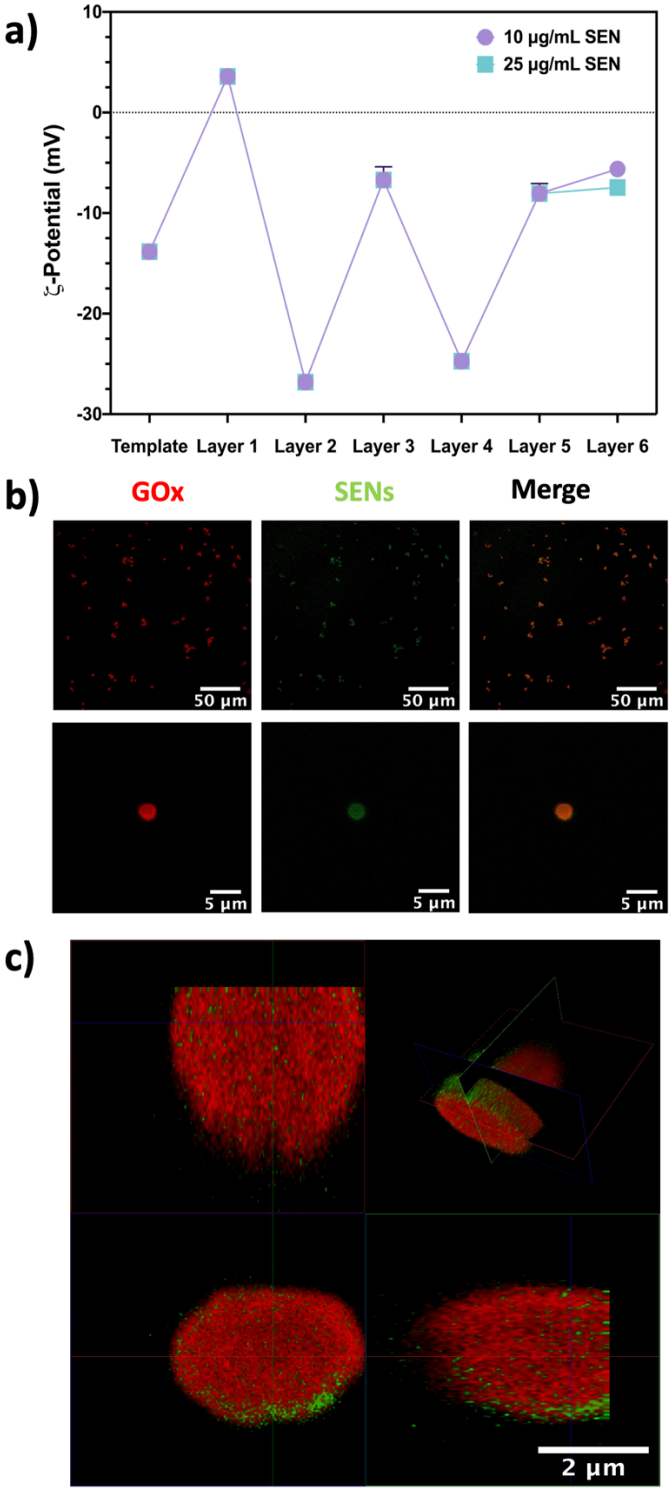

Fig. 5.4. a) *ζ-potential of $CaCO_3$-GOx microparticles after each layer deposition using for the fabrication of the final antioxidant layer two different SEN concentrations (10 and 25 µg/mL). b) Confocal micrographs of capsules fabricated with fluorescently labelled GOx and CAT encapsulating SENs (GOx-TRITC: Red /CAT-FITC: Green). c) Confocal microscope transversal section micrographs of capsules fabricated with fluorescently labelled GOx and CAT encapsulating SENs (GOx-TRITC: Red /CAT-FITC: Green).*

To further evaluate quantitatively the distribution of the stained microcapsules we analysed them using FACS. For this, we used three sample configurations: capsules only with GOx-TRITC inside, capsules only with FITC-stained SENs outside and capsules with the both stained enzymes. As control we used capsules without any of the stained enzymes in their architecture. To set the background values of fluorescence, raw capsules were first measured to obtain their size distribution and fluorescence background signal. In the obtained results, two main size groups were observed in which group A was the one with the larger capsules and a higher capsule quantity (i.e., 81. 2% of the total sample) (**Fig. 5.5a.1**). The fluorescence background signal of this group was clearly detectable while the smaller ones emitted a negligible signal, suggesting that they could be broken parts of microparticles as they are undetectable (**Fig. 5.5a.2, 5.5a.3**).

Once the setting values were obtained the rest of the samples were analysed under the same conditions. In the case of capsules with GOx-TRITC inside their cavity a significant decrease was observed in the amount of the group A capsules from 81.2% to 31.3% thus obtaining a larger amount of the smaller capsule parts (**Fig. 5.5b.1**). Group A capsules presented a significant shift in the red fluorescence signal confirming the presence of the stained enzyme in this group while the green fluorescence signal was similar to the background value (**Fig. 5.5b.2, 5.5b.3**). Analysing the particles only with the stained SENs, it was observed that the group A of the bigger particles here was larger (i.e., 70.2% of the total amount) (**Fig. 5.5c.1**). The change in the green signal was slightly detectable and as expected no changes were observed in the red fluorescence signal (**Fig. 5.5c.2, 5.5c.3**). The reason of this low green signal change could be the small size of the SENs and their irregular distribution around the capsules observed in the confocal microscope (**Fig. 5.4b, 5.4c**) which may limit their detectability by FACS. The last analysed capsules were the ones with the both stained enzymes. Here, the useful capsule quantity (i.e., group A) was again small, suggesting a loss of a high quantity of robust particles during the fabrication process and after the template removal consequence of the extra steps made for their obtention (**Fig. 5.5d.1**). However, despite this small quantity, the fluorescence signal change was clearly detectable in the red channel (**Fig. 5.5d.2**). In the

case of SENs, the green fluorescence signal change was slightly detectable due to their non-uniform distribution along the outer layer and their small size (**Fig. 5.5d.3**).

In view of these results, it could be concluded that the fabricated capsules were properly stained. The smaller signal change in the case of the green channel may be ascribed to the small size of the SENs and their irregular distribution in the polymeric shell. However, it should be taken into account the increasing population of small particles and artefacts (group B) consequence of the increasing number of steps in the procedure or the addition of several therapeutic agents, and a thorough optimization should be done to improve the obtained number of robust capsules for their following use.

5.3.2. Antioxidant capacity of polymer capsules with an outer antioxidant organic and inorganic layer

To assess the antioxidant capacity of the inorganic antioxidant system (i.e., polymer capsules with an outer MnO_2 layer), two biologically relevant H_2O_2 concentrations (10 and 50 µM) were used. Capsules at a final concentration of $1{\cdot}10^7$ and $1{\cdot}10^8$ polymer capsules/mL were incubated with H_2O_2 for 30 min. It was observed that, comparing to the control (i.e., 0 polymer capsules/mL), the fabricated capsules were capable of significantly ($p<0.05$) reducing the H_2O_2 from the solution (**Fig. 5.6a**). At the concentration of 10 µM H_2O_2 and $1{\cdot}10^7$ polymer capsules/mL, this reduction was significant for the concentrations of 20, 50 and 100 mM $KMnO_4$, where reduction values around 50% of the initial H_2O_2 concentration were observed. Although statistically significant, this reduction for the incubation concentrations of 2.5, 5 and 10 mM $KMnO_4$ was not so notorious and H_2O_2 reduction values below 20% were monitored. By increasing the polymer capsule concentration to $1{\cdot}10^8$ polymer capsules/mL, the reduction of H_2O_2 from the solution significantly increased and we obtained reduction values above 70% for all the studied concentrations.

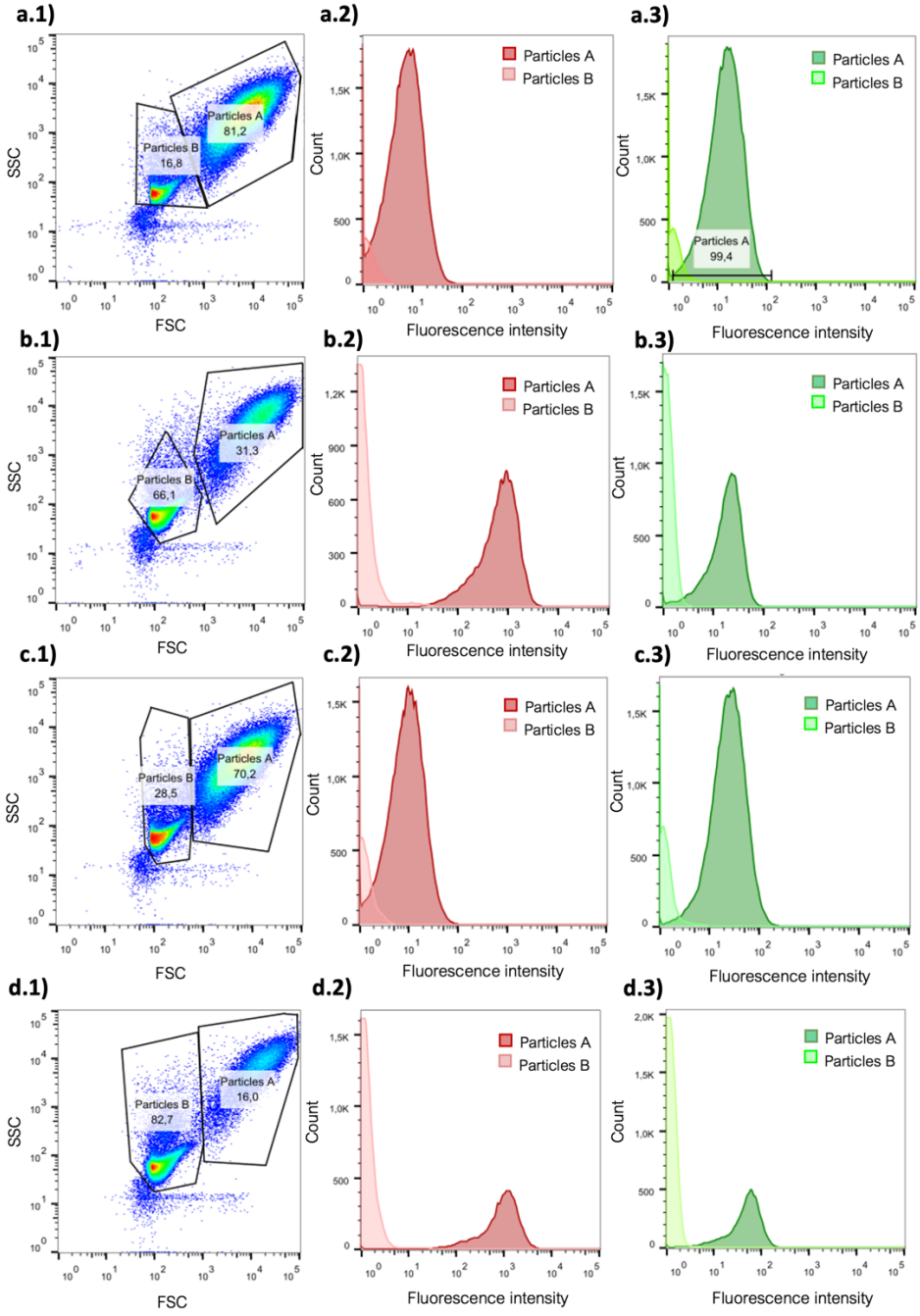

Fig. 5.5. *Sideward Scattering (SSC) and Forward Scattering (FSC) size distribution of the samples: control (a.1), capsules with GOx-TRITC inside (b.1), capsules with CAT-FITC outside (c.1) and capsules with both stained enzymes (d.1). Red fluorescence intensity of control (a.2), capsules with GOx-TRITC inside (b.2), capsules with CAT-FITC outside (c.2) and capsules with both stained enzymes (d.2). Green fluorescence intensity of control (a.3), capsules with GOx-TRITC inside (b.3), capsules with CAT-FITC outside (c.3) and capsules with both stained enzymes (d.3).*

In the case of 50 μM H_2O_2 the differences between the higher $KMnO_4$ concentrations (i.e., 20, 50, 100 mM) and the lower ones (i.e., 2.5, 5, 10 mM) were more evident (**Fig 5.6a**). Using the polymer capsule concentration of $1{\cdot}10^7$ polymer capsules/mL the H_2O_2 reduction capacity of all the systems was below 15%, suggesting that this capsule concentration is not enough for pathologies in which the H_2O_2 concentration exceeds the value of 50 μM. In this case, the group of capsules incubated with 20, 50 and 100 mM $KMnO_4$ for the production of the MnO_2 layer was capable of reducing 8.8 ± 1.4%, 13.3 ± 1.1% and 14.0 ± 1.0% of H_2O_2 respectively. However, as we reduced the $KMnO_4$ concentration in the incubation, the resulting capsules had no capacity to scavenge H_2O_2 from solution. However, by increasing the concentration of capsules to $1{\cdot}10^8$ polymer capsules/mL, H_2O_2 was almost completely reduced for 20, 50 and 100 mM $KMnO_4$. This reduction capacity significantly decreased when lower $KMnO_4$ concentrations were used, reducing in half the H_2O_2 scavenging capacity of the capsules fabricated with 5 and 10 mM and to values below 20% with 2.5 mM.

The obtained results demonstrate the capability of the fabricated capsules to efficiently scavenge H_2O_2 from solution specially using the capsules fabricated with the higher $KMnO_4$ concentrations (i.e., 20, 50 and 100 mM). In all the studied systems, a clear trend was observed: above 20 mM $KMnO_4$, the obtained H_2O_2 reduction values were almost similar regardless the $KMnO_4$ concentration, suggesting a saturation of the MnO_2 layer formation near this concentration. In view of these results, capsules fabricated with 50 mM $KMnO_4$ were chosen for the following experiments.

Regarding the organic antioxidant system (i.e., polymer capsules fabricated with an outer layer of catalase-loaded SENs), capsules were incubated only with 50 μM H_2O_2 as it is reported that this concentration is the minimum to induce deleterious responses on cells, eventually leading to oxidative stress.[58] Capsules with a SEN outer layer at a final concentration of $1{\cdot}10^7$ and $1{\cdot}10^8$ polymer capsules/mL were incubated for 30 min with H_2O_2. Using both SEN concentrations (i.e., 10 and 25 μg/mL), a complete reduction of the H_2O_2 of the solution was observed (**Fig. 5.6b**). This demonstrates that after the encapsulation of CAT in SENs and their assembly on the multilayer capsules, the antioxidant enzyme is capable of maintaining the specificity and reactivity towards H_2O_2. Consequently, the use of SENs as a part of the LbL polymeric membrane is envisioned as

a promising tool in the fabrication of antioxidant systems. Considering these results, for the following experiments, the concentration of 10 µg/mL of SENs was chosen to fabricate the outer antioxidant organic layer.

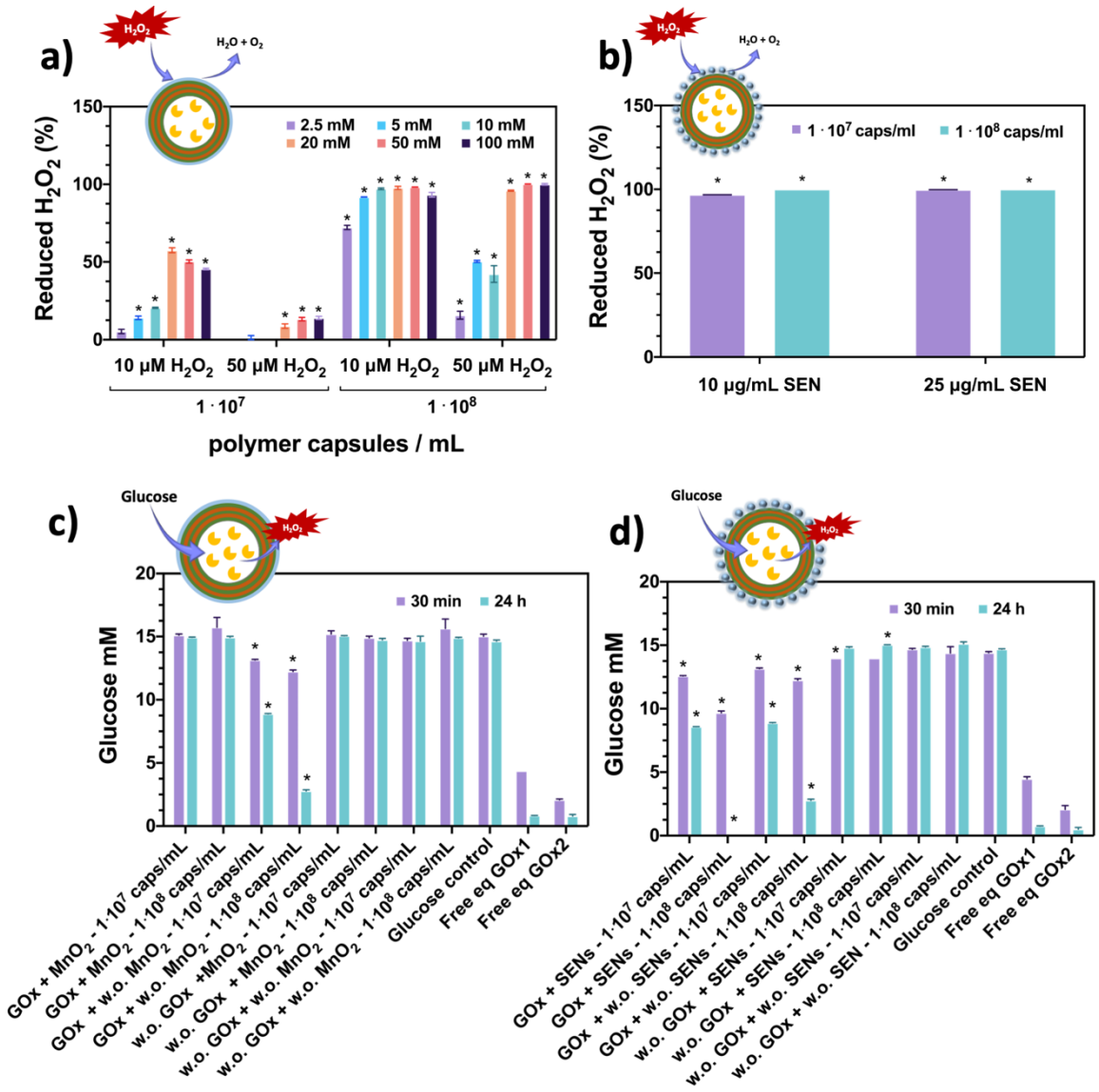

Fig. 5.6. *a) H_2O_2 scavenging capacity of polymer capsules at biologically relevant H_2O_2 concentrations (10 and 50 µM) using different $KMnO_4$ concentrations (2.5, 5, 10, 20, 50 and 100 mM) for the mineralization process. b) H_2O_2 scavenging capacity of polymer capsules with SENs at 50 µM H_2O_2 concentration. c) Glucose reduction capacity of the polymer capsules with an outer MnO_2 layer. d) Glucose reduction capacity of polymer capsules with an outer SEN layer. Asterisks (*) indicate significant differences ($p < 0.05$) with respect to each control (0 capsules/mL in (a) and (b), 15 mM glucose in (c) and (d)).*

5.3.3. Glucose reduction by polymer capsules with outer inorganic and organic antioxidant layer

To assess the capacity of the capsules to reduce glucose from the microenvironment, capsules at a final concentration of $1{\cdot}10^7$ and $1{\cdot}10^8$ polymer capsules/mL were incubated for 30 min and 24 h in a hyperglycaemic glucose solution (i.e., 15 mM).[23] For the cascade system analysed in this work, GOx was chosen as a model enzyme since it catalyses the reaction of the environmental glucose to yield gluconic acid and H_2O_2. Based on this reaction, a plethora of biomedical systems has been developed including insulin delivery capsules,[59] glucose sensors,[60] cancer cell targeting capsules[61] or antimicrobial capsules.[3] The last two applications exploit the enzymatic production of the cytotoxic H_2O_2 to combat cancerous cells and bacteria.[3,61] However, in other scenarios, the accumulation of ROS could have detrimental effects in surrounding cells and tissues, as well as in the catalytic activity of the enzyme. For this reason, scavenging the overproduced H_2O_2 will be of great interest.[59,60] Thus, to prove the capability of our LbL capsules to carry out cascade reactions, GOx was chosen to produce H_2O_2 that will be later scavenged by the outer antioxidant organic or inorganic layer.

In the particular case of MnO_2 containing capsules, four different systems were analysed: GOx + MnO_2-$1{\cdot}10^7$ polymer capsules/mL and -$1{\cdot}10^8$ polymer capsules/mL, GOx + w.o. MnO_2-$1{\cdot}10^7$ polymer capsules/mL and -$1{\cdot}10^8$ polymer capsules/mL, w.o. GOx + MnO_2-$1{\cdot}10^7$ polymer capsules/mL and -$1{\cdot}10^8$ polymer capsules/mL and w.o. GOx + w.o. MnO_2-$1{\cdot}10^7$ polymer capsules/mL and -$1{\cdot}10^8$ polymer capsules/mL. As controls, glucose at 15 mM and free equivalent GOx (i.e., GOx1 equivalent to the quantity of the encapsulated GOx in $1{\cdot}10^7$ polymer capsules/mL and GOx2 equivalent to the encapsulated GOx in $1{\cdot}10^8$ polymer capsules/mL) solutions were used. As expected, those capsules without the enzyme did not reduce the glucose from the solution (**Fig. 5.6c**). In contrast, those capsules bearing GOx in their core and without external MnO_2 layer significantly reduced glucose from the microenvironment after 24 h from 14.6 ± 0.1 mM to 8.6 ± 0.04 mM with $1{\cdot}10^7$ polymer capsules/mL and to 1.3 ± 0.2 mM with $1{\cdot}10^8$ polymer capsules/mL (**Fig. 5.6c)**. However, the capsules containing GOx and the outer MnO_2 layer were not capable of reducing glucose at any time point (**Fig. 5.6c)**. This

suggested that the MnO_2 layer formation affected the activity of the enzyme, hindering the capacity to reduce glucose from the microenvironment.

To gather more information about this behaviour, we acquired confocal images before and after $KMnO_4$ incubation from capsules fabricated using TRITC-GOx. As observed in the confocal images, the polymer capsules emitted signal in the red channel before permanganate incubation. Contrarily, this red fluorescent signal disappeared after permanganate incubation (**Fig. 5.7**). To explain this phenomenon two different hypothesis could be suggested: i) the enzyme may have escaped from the inner cavity during the incubation period and ii) the enzyme may have reacted with the permanganate, having a detrimental effect on its activity and fluorescent signal. Permanganate is a strong oxidant capable of degrading many compounds. As concluded from the incubation of free enzyme with permanganate (data not shown), the formation of precipitates was observed, that avoid the measurement of enzyme activity. We therefore suggest that the reason of the loss of the enzyme activity could be caused by the reaction between GOx and $KMnO_4$ during the formation of the MnO_2 external layer.

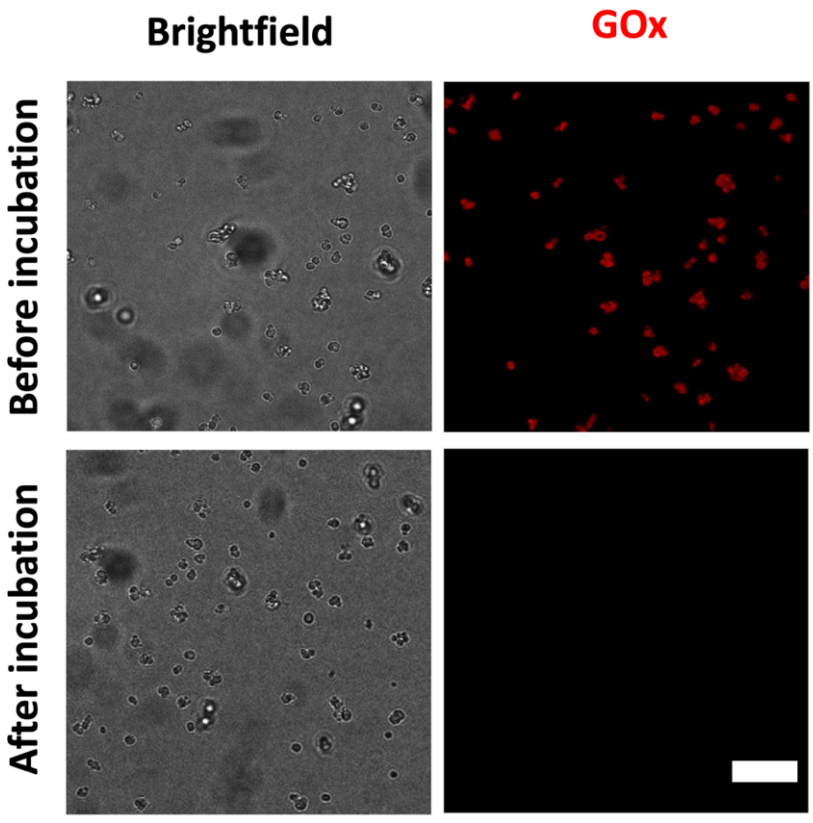

Fig. 5.7. *Confocal images of capsules before and after $KMnO_4$ incubation. Scalebar: 20 µm.*

Analysing the organic antioxidant system, four different polymer capsule configurations were similarly used: GOx + SENs-$1{\cdot}10^7$ polymer capsules/mL and -$1{\cdot}10^8$ polymer capsules/mL, GOx + w.o. SENs-$1{\cdot}10^7$ polymer capsules/mL and -$1{\cdot}10^8$ polymer capsules/mL, w.o. GOx + SENs-$1{\cdot}10^7$ polymer capsules/mL and -$1{\cdot}10^8$ polymer capsules/mL and w.o. GOx + w.o. SENs-$1{\cdot}10^7$ polymer capsules/mL and -$1{\cdot}10^8$ polymer capsules/mL. In the case of the capsules without GOx, the tendency was the same to the one observed for MnO_2 containing polymer capsules, and no reduction of the glucose was observed (**Fig 5.6d**). Capsules containing only GOx, presented a significant reduction of the glucose from the solution specifically at 24 h. Finally, those capsules with GOx and SENs showed a high capacity to reduce the glucose from the solution. After 30 min, the concentration was reduced from 14.4 ± 0.1 mM to 12.6 ± 0.04 mM in the case of $1{\cdot}10^7$ polymer capsule/mL and to 9.7 ± 0.1 mM using $1{\cdot}10^8$ polymer capsules/mL. After 24 h, this reduction was much higher obtaining almost a 50% percent reduction in the case of $1{\cdot}10^7$ polymer capsules/ mL and a complete reduction in the case $1{\cdot}10^8$ polymer capsules/ mL.

Based on these results, we can conclude that the *in situ* mineralization of MnO_2 needs further optimization to work with sensitive entities like enzymes. Due to its high oxidation capacity, $KMnO_4$ has a detrimental effect on the activity of the enzyme at the studied concentrations. However, on the other side, the organic system showed a high effectivity in reducing glucose from the solution being a promising candidate to carry out cascade reactions in LbL polymer capsules. Therefore, the organic alternative was only considered for further experiments trying to elucidate the capacity of the proposed system to perform cascade reactions.

5.3.4. Performing enzymatic cascade reactions within polymer capsules bearing and organic antioxidant outer layer.

To assess the capacity of the fabricated polymeric capsule to perform a cascade reaction consisting on the reduction of glucose and the subsequent scavenging of the produced H_2O_2, the fabricated capsules were incubated with three different glucose concentrations (i.e., 100, 250 and 500 μM). Higher glucose concentrations (hyperglycaemic values) were avoided for this experiment as glucose hindered the

effectivity of the Hydrogen Peroxide Fluorimetric Assay kit (data not shown). Capsules at a concentration of $1{\cdot}10^7$ and $1{\cdot}10^8$ polymer capsules/mL were incubated for 30 min with glucose solutions and after that the produced H_2O_2 was subsequently measured as a proof of the correct functioning of the cascade reaction. As control, capsules without SENs were used.

It was observed that capsules with the outer SEN layer produced significantly ($p<0.05$) lower H_2O_2 concentrations comparing to the control (**Fig. 5.8).** In the case of the capsules incubated with 500 µM glucose, at a concentration of capsules of $1{\cdot}10^8$ the production of H_2O_2 of the capsules without SENs exceeded the capacity of the kit to measure the concentration. However, those capsules with an outer SEN layer were capable of reducing efficiently the produced H_2O_2 to a concentration of 37 ± 0.2 µM. This difference was more evident using $1{\cdot}10^7$ capsules/mL. In those capsules without SENs, the production of H_2O_2 was 28.4 ± 0.4 µM, while it was reduced to 9.0 ± 0.1 µM with the incorporation of the antioxidant entities. Using the other two glucose concentrations, it was observed that the higher capsule concentrations (i.e., $1{\cdot}10^8$ polymer capsules/mL) were capable of significantly reducing the enzymatically produced H_2O_2 from values around 40 µM H_2O_2 to values near 10 µM H_2O_2. However, contrarily to 500 µM glucose, this difference was not so significant in the case of $1{\cdot}10^7$ capsules/mL.

Taken together, these results confirm the capability of the LbL polymer capsules decorated with antioxidant SENs to perform cascade reactions reducing both the glucose from the solution and the enzymatically produced H_2O_2, especially with a concentration of $1{\cdot}10^8$ capsules/mL.

5.3.5. Metabolic activity of MRC-5 cells in the presence of polymer capsules

The *in vitro* cytocompatibility of polymer capsules was tested with MRC-5 cells in the presence of various capsule concentrations ($1{\cdot}10^6$, $1{\cdot}10^7$ and $1{\cdot}10^8$ polymer capsules/mL) and the metabolic activity was measured after 24 and 72 h by means of AlamarBlue® assay. To do so, capsules without GOx in their inner cavity and with an outer *in situ* fabricated MnO_2 layer or SENs were used. In the particular case of SENs, an additional PSS negative layer was added after the SENs deposition to impart to the capsules a strong negative charge since it was demonstrated in Chapter 3 that external

positive charge causes a cytotoxic effect on cells. For the sterilization of the capsules with SENs, capsules were sterilized with ethanol before the SENs deposition and after this step the following procedures were performed under sterile conditions with the aim of preserving the integrity of the encapsulated enzyme (i.e., CAT). Cells in the absence of capsules were used as negative control, whereas capsules without an antioxidant outer layer at a concentration of $1{\cdot}10^7$ polymer capsules/mL were also considered.

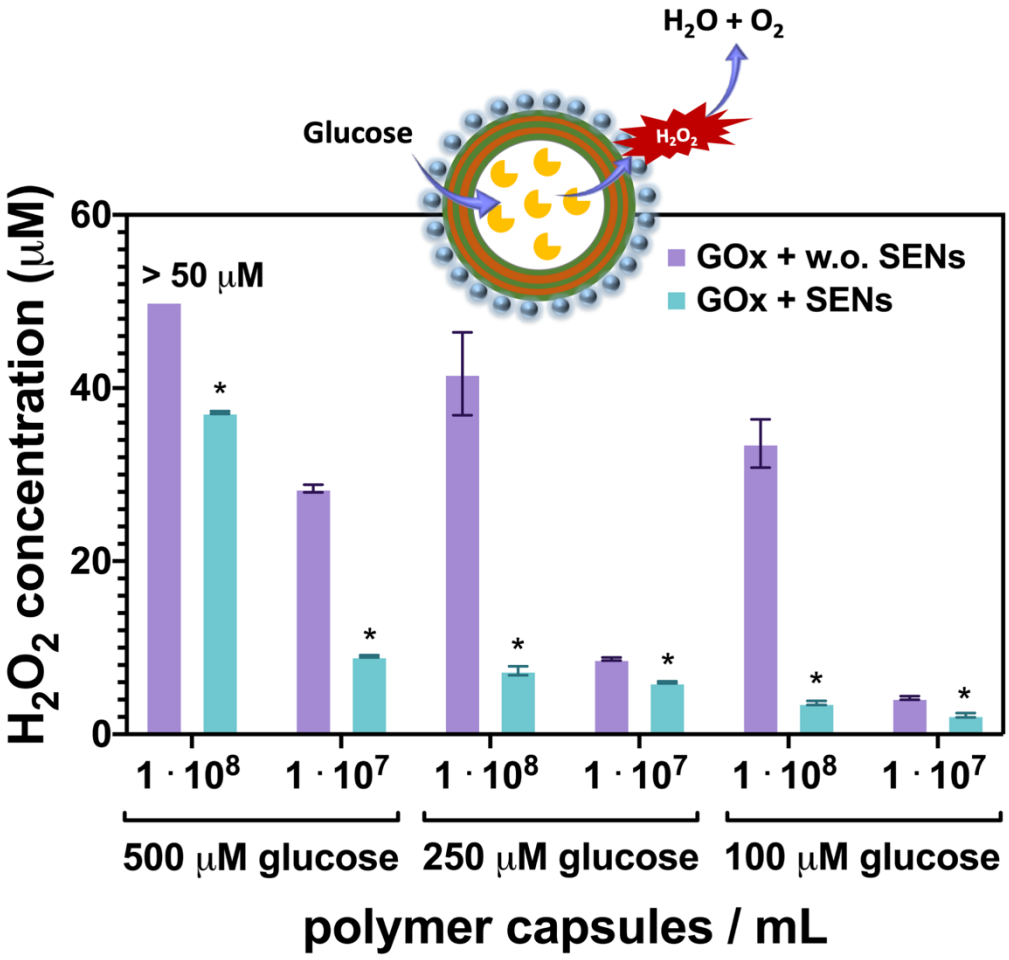

Fig. 5.8. *H_2O_2 production of the polymer capsules after their incubation with different glucose concentrations (e.g., 100, 250 and 500 μM). Asterisks (*) indicate significant differences ($p<0.05$) with respect to the control (capsules without SENs).*

In the case of capsules with MnO_2, cells were capable of maintaining a normal metabolic activity above the threshold value (i.e., 70%) after 72 h at the capsule concentrations of $1{\cdot}10^6$ and $1{\cdot}10^7$ polymer capsules/mL. In the case of $1{\cdot}10^8$ polymer capsules/mL, this

metabolic activity decreased significantly ($p<0.05$) probably due to the high capsule concentration (**Fig. 5.9**).

In the case of capsules containing SENs, after 24 h, cells were capable of maintaining metabolic activity values near or above the threshold value for all the studied concentrations (**Fig. 5.9**). After 72 h, cells in the presence of capsule concentrations of $1{\cdot}10^6$ polymer capsules/mL were capable of maintaining their metabolic activity near the control values (i.e., cells in absence of polymer capsules). In the case of $1{\cdot}10^7$ and $1{\cdot}10^8$ polymer capsules/mL, despite the metabolic activity was below the threshold value, cells were able to obtain metabolic activity values near 60%.

Altogether, the obtained cytotoxicity results suggest that the fabricated capsules were not cytotoxic specially using the capsule concentrations of $1{\cdot}10^6$ and $1{\cdot}10^7$ polymer capsules/mL.

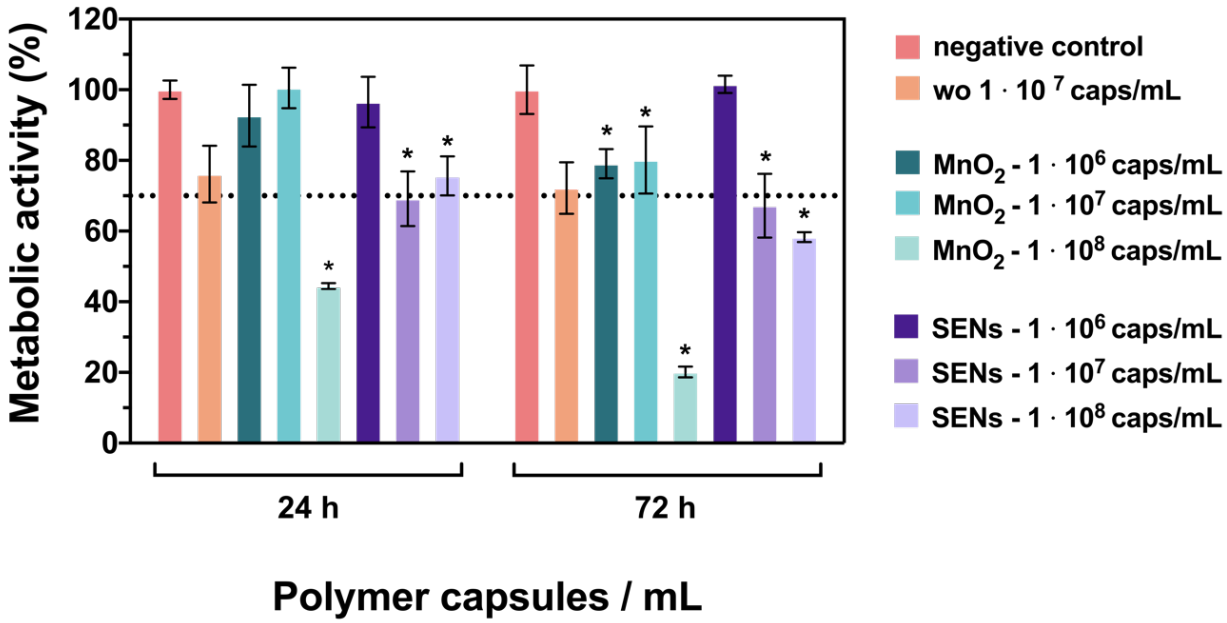

Fig. 5.9. *Metabolic activity of MRC-5 cells in the presence of polymer capsules. Asterisks (*) indicate significant differences ($p < 0.05$) with respect to the control (cells in absence of polymer capsules).*

5.4. Conclusions

In this chapter, we fabricated polymer capsules *via* the LbL approach and exploited the versatility of this method to create microreactors to perform cascade reactions. Polymer capsules encapsulating GOx within their core and with an outer antioxidant organic (i.e., SENs) and inorganic layer (i.e., MnO_2) were successfully fabricated and they showed promising results in terms of H_2O_2 scavenging. The glucose reduction of the fabricated capsules was measured after their incubation with a glucose solution at a hyperglycaemic concentration and the obtained results showed a significant reduction of the environmental glucose with those capsules bearing the external organic antioxidant layer. However, capsules with the outer inorganic antioxidant layer were not capable of reducing the glucose from the solution. The loss of fluorescence of the enzyme observed in the confocal images taken before and after the incubation of the capsules with $KMnO_4$, suggested that the enzyme reacts with permanganate and loses its activity. The capacity of capsules with the outer SENs layer and with GOx in their cavity to perform enzymatic cascade reaction was validated at different glucose concentrations. Accordingly, the combinatorial approach presented herein (i.e., positioning one enzyme in the inner cavity and another enzyme in the outer layer as SENs) could be considered in the future for the treatment and replacement of damaged cellular pathways.

References

(1) Belluati, A.; Craciun, I.; Palivan, C. G. Bioactive Catalytic Nanocompartments Integrated into Cell Physiology and Their Amplification of a Native Signaling Cascade. *ACS Nano* **2020**, *14* (9), 12101–12112. https://doi.org/10.1021/acsnano.0c05574.

(2) Van Dongen, S. F. M.; Nallani, M.; Cornelissen, J. J. L. M.; Nolte, R. J. M.; Van Hest, J. C. M. A Three-Enzyme Cascade Reaction through Positional Assembly of Enzymes in a Polymersome Nanoreactor. *Chem. - A Eur. J.* **2009**, *15* (5), 1107–1114. https://doi.org/10.1002/chem.200802114.

(3) Potter, M.; Najer, A.; Klöckner, A.; Zhang, S.; Holme, M. N.; Nele, V.; Che, J.; Massi, L.; Penders, J.; Saunders, C.; Doutch, J. J.; Edwards, A. M.; Ces, O.; Stevens, M. M. Controlled Dendrimersome Nanoreactor System for Localized Hypochlorite-Induced Killing of Bacteria. *ACS Nano* **2020**, *14* (12), 17333–17353. https://doi.org/10.1021/acsnano.0c07459.

(4) Donatan, S.; Yashchenok, A.; Khan, N.; Parakhonskiy, B.; Cocquyt, M.; Pinchasik, B. El; Khalenkow, D.; Möhwald, H.; Konrad, M.; Skirtach, A. Loading Capacity versus Enzyme Activity in Anisotropic and Spherical Calcium Carbonate Microparticles. *ACS Appl. Mater. Interfaces* **2016**, *8* (22), 14284–14292. https://doi.org/10.1021/acsami.6b03492.

(5) Ping, Y.; Guo, J.; Ejima, H.; Chen, X.; Richardson, J. J.; Sun, H.; Caruso, F. PH-Responsive Capsules Engineered from Metal-Phenolic Networks for Anticancer Drug Delivery. *Small* **2015**, *11* (17), 2032–2036. https://doi.org/10.1002/smll.201403343.

(6) Timin, A. S.; Muslimov, A. R.; Lepik, K. V.; Okilova, M. V.; Tcvetkov, N. Y.; Shakirova, A. I.; Afanasyev, B. V.; Gorin, D. A.; Sukhorukov, G. B. Intracellular Breakable and Ultrasound-Responsive Hybrid Microsized Containers for Selective Drug Release into Cancerous Cells. *Part. Part. Syst. Charact.* **2017**, *34* (5), 1–10. https://doi.org/10.1002/ppsc.201600417.

(7) Timin, A. S.; Muslimov, A. R.; Petrova, A. V.; Lepik, K. V.; Okilova, M. V.; Vasin, A.

V.; Afanasyev, B. V.; Sukhorukov, G. B. Hybrid Inorganic-Organic Capsules for Eficient Intracellular Delivery of Novel siRNAs against Influenza A (H1N1) Virus Infection. *Sci. Rep.* **2017**, *7* (1), 1–12. https://doi.org/10.1038/s41598-017-00200-0.

(8) She, Z.; Wang, C.; Li, J.; Sukhorukov, G. B.; Antipina, M. N. Encapsulation of Basic Fibroblast Growth Factor by Polyelectrolyte Multilayer Microcapsules and Its Controlled Release for Enhancing Cell Proliferation. *Biomacromolecules* **2012**, *13* (7), 2174–2180. https://doi.org/10.1021/bm3005879.

(9) Correa-Paz, C.; Navarro Poupard, M. F.; Polo, E.; Rodríguez-Pérez, M.; Taboada, P.; Iglesias-Rey, R.; Hervella, P.; Sobrino, T.; Vivien, D.; Castillo, J.; del Pino, P.; Campos, F.; Pelaz, B. *In Vivo* Ultrasound-Activated Delivery of Recombinant Tissue Plasminogen Activator from the Cavity of Sub-Micrometric Capsules. *J. Control. Release* **2019**, *308* (February), 162–171. https://doi.org/10.1016/j.jconrel.2019.07.017.

(10) Novoselova, M. V.; German, S. V.; Abakumova, T. O.; Perevoschikov, S. V.; Sergeeva, O. V.; Nesterchuk, M. V.; Efimova, O. I.; Petrov, K. S.; Chernyshev, V. S.; Zatsepin, T. S.; Gorin, D. A. Multifunctional Nanostructured Drug Delivery Carriers for Cancer Therapy: Multimodal Imaging and Ultrasound-Induced Drug Release. *Colloids Surfaces B Biointerfaces* **2021**, *200* (September 2020), 111576. https://doi.org/10.1016/j.colsurfb.2021.111576.

(11) German, S. V.; Bratashov, D. N.; Navolokin, N. A.; Kozlova, A. A.; Lomova, M. V.; Novoselova, M. V.; Burilova, E. A.; Zyev, V. V.; Khlebtsov, B. N.; Bucharskaya, A. B.; Terentyuk, G. S.; Amirov, R. R.; Maslyakova, G. N.; Sukhorukov, G. B.; Gorin, D. A. *In Vitro* and *in vivo* MRI Visualization of Nanocomposite Biodegradable Microcapsules with Tunable Contrast. *Phys. Chem. Chem. Phys.* **2016**, *18* (47), 32238–32246. https://doi.org/10.1039/C6CP03895F.

(12) Kozlovskaya, V.; Alford, A.; Dolmat, M.; Ducharme, M.; Caviedes, R.; Radford, L.; Lapi, S. E.; Kharlampieva, E. Multilayer Microcapsules with Shell-Chelated ^{89}Zr for PET Imaging and Controlled Delivery. *ACS Appl. Mater. Interfaces* **2020**, *12* (51), 56792–56804. https://doi.org/10.1021/acsami.0c17456.

(13) Chaudhary, Z.; Khan, G. M.; Abeer, M. M.; Pujara, N.; Wan-Chi Tse, B.; McGuckin, M. A.; Popat, A.; Kumeria, T. Efficient Photoacoustic Imaging Using Indocyanine Green (ICG) Loaded Functionalized Mesoporous Silica Nanoparticles. *Biomater. Sci.* **2019**, *7* (12), 5002–5015. https://doi.org/10.1039/c9bm00822e.

(14) Larrañaga, A.; Isa, I. L. M.; Patil, V.; Thamboo, S.; Lomora, M.; Fernández-Yague, M. A.; Sarasua, J. R.; Palivan, C. G.; Pandit, A. Antioxidant Functionalized Polymer Capsules to Prevent Oxidative Stress. *Acta Biomater.* **2018**, *67*, 21–31. https://doi.org/10.1016/j.actbio.2017.12.014.

(15) Popov, A. L.; Popova, N.; Gould, D. J.; Shcherbakov, A. B.; Sukhorukov, G. B.; Ivanov, V. K. Ceria Nanoparticles-Decorated Microcapsules as a Smart Drug Delivery/Protective System: Protection of Encapsulated P. Pyralis Luciferase. *ACS Appl. Mater. Interfaces* **2018**, *10* (17), 14367–14377. https://doi.org/10.1021/acsami.7b19658.

(16) Popov, A. L.; Popova, N. R.; Tarakina, N. V.; Ivanova, O. S.; Ermakov, A. M.; Ivanov, V. K.; Sukhorukov, G. B. Intracellular Delivery of Antioxidant CeO_2 Nanoparticles *via* Polyelectrolyte Microcapsules. *ACS Biomater. Sci. Eng.* **2018**, *4* (7), 2453–2462. https://doi.org/10.1021/acsbiomaterials.8b00489.

(17) Larrañaga, A.; Lomora, M.; Sarasua, J. R.; Palivan, C. G.; Pandit, A. Polymer Capsules as Micro-/Nanoreactors for Therapeutic Applications: Current Strategies to Control Membrane Permeability. *Prog. Mater. Sci.* **2017**, *90*, 325–357. https://doi.org/10.1016/j.pmatsci.2017.08.002.

(18) Marin, E.; Tiwari, N.; Calderón, M.; Sarasua, J. R.; Larrañaga, A. Smart Layer-by-Layer Polymeric Microreactors: PH-Triggered Drug Release and Attenuation of Cellular Oxidative Stress as Prospective Combination Therapy. *ACS Appl. Mater. Interfaces* **2021**, *13* (16), 18511–18524. https://doi.org/10.1021/acsami.1c01450.

(19) Zyuzin, M. V.; Timin, A. S.; Sukhorukov, G. B. Multilayer Capsules Inside Biological Systems: State-of-the-Art and Open Challenges. *Langmuir* **2019**, *35* (13), 4747–4762. https://doi.org/10.1021/acs.langmuir.8b04280.

(20) Fang, M.; Grant, P. S.; McShane, M. J.; Sukhorukov, G. B.; Golub, V. O.; Lvov, Y. M. Magnetic Bio/Nanoreactor with Multilayer Shells of Glucose Oxidase and

Inorganic Nanoparticles. *Langmuir* **2002**, *18* (16), 6338–6344. https://doi.org/10.1021/la025731m.

(21) Caruso, F.; Schüler, C. Enzyme Multilayers on Colloid Particles: Assembly, Stability, and Enzymatic Activity. *Langmuir* **2000**, *16* (24), 9595–9603. https://doi.org/10.1021/la000942h.

(22) Qi, W.; Yan, X.; Fei, J.; Wang, A.; Cui, Y.; Li, J. Triggered Release of Insulin from Glucose-Sensitive Enzyme Multilayer Shells. *Biomaterials* **2009**, *30* (14), 2799–2806. https://doi.org/10.1016/j.biomaterials.2009.01.027.

(23) Xu, C.; Lei, C.; Huang, L.; Zhang, J.; Zhang, H.; Song, H.; Yu, M.; Wu, Y.; Chen, C.; Yu, C. Glucose-Responsive Nanosystem Mimicking the Physiological Insulin Secretion *via* an Enzyme-Polymer Layer-by-Layer Coating Strategy. *Chem. Mater.* **2017**, *29* (18), 7725–7732. https://doi.org/10.1021/acs.chemmater.7b01804.

(24) Beloqui, A.; Baur, S.; Trouillet, V.; Welle, A.; Madsen, J.; Bastmeyer, M.; Delaittre, G. Single-Molecule Encapsulation: A Straightforward Route to Highly Stable and Printable Enzymes. *Small* **2016**, *12* (13), 1716–1722. https://doi.org/10.1002/smll.201503405.

(25) Beloqui, A.; Kobitski, A. Y.; Nienhaus, G. U.; Delaittre, G. A Simple Route to Highly Active Single-Enzyme Nanogels. *Chem. Sci.* **2018**, *9* (4), 1006–1013. https://doi.org/10.1039/c7sc04438k.

(26) Zhang, P.; Sun, F.; Tsao, C.; Liu, S.; Jain, P.; Sinclair, A.; Hung, H. C.; Bai, T.; Wu, K.; Jiang, S. Zwitterionic Gel Encapsulation Promotes Protein Stability, Enhances Pharmacokinetics, and Reduces Immunogenicity. *Proc. Natl. Acad. Sci. U. S. A.* **2015**, *112* (39), 12046–12051. https://doi.org/10.1073/pnas.1512465112.

(27) Yan, M.; Du, J.; Gu, Z.; Liang, M.; Hu, Y.; Zhang, W.; Priceman, S.; Wu, L.; Zhou, Z. H.; Liu, Z.; Segura, T.; Tang, Y.; Lu, Y. A Novel Intracellular Protein Delivery Platform Based on Single-Protein Nanocapsules. *Nat. Nanotechnol.* **2010**, *5* (1), 48–53. https://doi.org/10.1038/nnano.2009.341.

(28) Biswas, A.; Joo, K.; Liu, J.; Zhao, M.; Fan, G.; Wang, P.; Gu, Z.; Tang, Y. Endoprotease-Mediated Intracellular Protein Delivery Using Nanocapsules. **2011**, *5* (2), 1385–1394.

(29) Chen, G.; Abdeen, A. A.; Wang, Y.; Shahi, P. K.; Robertson, S.; Xie, R.; Suzuki, M.; Pattnaik, B. R.; Saha, K.; Gong, S. A Biodegradable Nanocapsule Delivers a Cas9 Ribonucleoprotein Complex for *in vivo* Genome Editing. *Nat. Nanotechnol.* **2019**, *14* (10), 974–980. https://doi.org/10.1038/s41565-019-0539-2.

(30) Gu, Z.; Yan, M.; Hu, B.; Joo, K. L.; Biswas, A.; Huang, Y.; Lu, Y.; Wang, P.; Tang, Y. Protein Nanocapsule Weaved with Enzymatically Degradable Polymerie Network. *Nano Lett.* **2009**, *9* (12), 4533–4538. https://doi.org/10.1021/nl902935b.

(31) Lin, Y.; Ren, J.; Qu, X. Catalytically Active Nanomaterials: A Promising Candidate for Artificial Enzymes. *Acc. Chem. Res.* **2014**, *47* (4), 1097–1105. https://doi.org/10.1021/ar400250z.

(32) Liang, M.; Yan, X. Nanozymes: From New Concepts, Mechanisms, and Standards to Applications. *Acc. Chem. Res.* **2019**, *52* (8), 2190–2200. https://doi.org/10.1021/acs.accounts.9b00140.

(33) Tapeinos, C.; Larrañaga, A.; Sarasua, J. R.; Pandit, A. Functionalised Collagen Spheres Reduce H_2O_2 Mediated Apoptosis by Scavenging Overexpressed ROS. *Nanomedicine Nanotechnology, Biol. Med.* **2018**, *14* (7), 2397–2405. https://doi.org/10.1016/j.nano.2017.03.022.

(34) Bao, Y.-W.; Hua, X.-W.; Zeng, J.; Wu, F.-G. Bacterial Template Synthesis of Multifunctional Nanospindles for Glutathione Detection and Enhanced Cancer-Specific Chemo-Chemodynamic Therapy. *Research* **2020**, *2020*, 9301215. https://doi.org/10.34133/2020/9301215.

(35) Xu, K. F.; Jia, H. R.; Zhu, Y. X.; Liu, X.; Gao, G.; Li, Y. H.; Wu, F. G. Cholesterol-Modified Dendrimers for Constructing a Tumor Microenvironment-Responsive Drug Delivery System. *ACS Biomater. Sci. Eng.* **2019**, *5* (11), 6072–6081. https://doi.org/10.1021/acsbiomaterials.9b01386.

(36) Marin, E.; Tapeinos, C.; Lauciello, S.; Ciofani, G.; Sarasua, J. R.; Larrañaga, A. Encapsulation of Manganese Dioxide Nanoparticles into Layer-by-Layer Polymer Capsules for the Fabrication of Antioxidant Microreactors. *Mater. Sci. Eng. C* **2020**, *117* (April), 111349. https://doi.org/10.1016/j.msec.2020.111349.

(37) Zhou, Y.; Liu, B.; Yang, R.; Liu, J. Filling in the Gaps between Nanozymes and

Enzymes: Challenges and Opportunities. *Bioconjug. Chem.* **2017**, *28* (12), 2903–2909. https://doi.org/10.1021/acs.bioconjchem.7b00673.

(38) Gordijo, C. R.; Abbasi, A. Z.; Amini, M. A.; Lip, H. Y.; Maeda, A.; Cai, P.; O'Brien, P. J.; Dacosta, R. S.; Rauth, A. M.; Wu, X. Y. Design of Hybrid MnO_2-Polymer-Lipid Nanoparticles with Tunable Oxygen Generation Rates and Tumor Accumulation for Cancer Treatment. *Adv. Funct. Mater.* **2015**, *25* (12), 1858–1872. https://doi.org/10.1002/adfm.201404511.

(39) Prasad, P.; Gordijo, C. R.; Abbasi, A. Z.; Maeda, A.; Ip, A.; Rauth, M.; Dacosta, R. S.; Wu, X. Y. Multifunctional Albumin - MnO_2 Nanoparticles Modulate Solid Tumor Microenvironment by Attenuating Enhance Radiation Response. *ACS Nano* **2014**, *8* (4), 3202–3212. https://doi.org/10.1021/nn405773r.

(40) Li, W.; Liu, Z.; Liu, C.; Guan, Y.; Ren, J.; Qu, X. Manganese Dioxide Nanozymes as Responsive Cytoprotective Shells for Individual Living Cell Encapsulation. *Angew. Chemie - Int. Ed.* **2017**, *56* (44), 13661–13665. https://doi.org/10.1002/anie.201706910.

(41) Luo, Y. Preparation of MnO_2 Nanoparticles by Directly Mixing Potassium Permanganate and Polyelectrolyte Aqueous Solutions. *Mater. Lett.* **2007**, *61* (8–9), 1893–1895. https://doi.org/10.1016/j.matlet.2006.07.165.

(42) Thermo Scientific. FITC and TRITC. *Meridian 0747* (46424).

(43) Dubowski, K. M. An O-Toluidine Method for Body-Fluid Glucose Determination. *Clin. Chem. 8* (3), 215–235.

(44) Feoktistova, N. A.; Vikulina, A. S.; Balabushevich, N. G.; Skirtach, A. G.; Volodkin, D. Bioactivity of Catalase Loaded into Vaterite $CaCO_3$ Crystals *via* Adsorption and Co-Synthesis. *Mater. Des.* **2019**, *185*, 108223. https://doi.org/10.1016/j.matdes.2019.108223.

(45) Petrov, A. I.; Volodkin, D. V.; Sukhorukov, G. B. Protein-Calcium Carbonate Coprecipitation: A Tool for Protein Encapsulation. *Biotechnol. Prog.* **2005**, *21* (3), 918–925. https://doi.org/10.1021/bp0495825.

(46) Sadasivan, S.; Sukhorukov, G. B. Fabrication of Hollow Multifunctional Spheres

Containing MCM-41 Nanoparticles and Magnetite Nanoparticles Using Layer-by-Layer Method. *J. Colloid Interface Sci.* **2006**, *304* (2), 437–441. https://doi.org/10.1016/j.jcis.2006.09.010.

(47) Gao, C.; Moya, S.; Lichtenfeld, H.; Casoli, A.; Fiedler, H.; Donath, E.; Möhwald, H. The Decomposition Process of Melamine Formaldehyde Cores: The Key Step in the Fabrication of Ultrathin Polyelectrolyte Multilayer Capsules. *Macromol. Mater. Eng.* **2001**, *286* (6), 355–361. https://doi.org/10.1002/1439-2054(20010601)286:6<355::AID-MAME355>3.0.CO;2-9.

(48) Antipov, A.; Shchukin, D.; Fedutik, Y.; Zanaveskina, I.; Klechkovskaya, V.; Sukhorukov, G.; Möhwald, H. Urease-Catalyzed Carbonate Precipitation inside the Restricted Volume of Polyelectrolyte Capsules. *Macromol. Rapid Commun.* **2003**, *24* (3), 274–277. https://doi.org/10.1002/marc.200390041.

(49) Sukhorukov, G. B.; Antipov, A. A.; Voigt, A.; Donath, E.; M̈hwald, H. PH-Controlled Macromolecule Encapsulation in and Release from Polyelectrolyte Multilayer Nanocapsules. *Macromol. Rapid Commun.* **2001**, *22* (1), 44–46. https://doi.org/10.1002/1521-3927(20010101)22:1<44::AID-MARC44>3.0.CO;2-U.

(50) Shi, J.; Wang, X.; Xu, S.; Wu, Q.; Cao, S. Reversible Thermal-Tunable Drug Delivery across Nano-Membranes of Hollow PUA/PSS Multilayer Microcapsules. *J. Memb. Sci.* **2016**, *499*, 307–316. https://doi.org/10.1016/j.memsci.2015.10.065.

(51) Guo, C.; Wang, J.; Dai, Z. Selective Content Release from Light-Responsive Microcapsules by Tuning the Surface Plasmon Resonance of Gold Nanorods. *Microchim. Acta* **2011**, *173* (3–4), 375–382. https://doi.org/10.1007/s00604-011-0570-y.

(52) Yashchenok, A. M.; Bratashov, D. N.; Gorin, D. A.; Lomova, M. V.; Pavlov, A. M.; Sapelkin, A. V.; Shim, B. S.; Khomutov, G. B.; Kotov, N. A.; Sukhorukov, G. B.; Möhwald, H.; Skirtach, A. G. Carbon Nanotubes on Polymeric Microcapsules: Freestanding Structures and Point-Wise Laser Openings. *Adv. Funct. Mater.* **2010**, *20* (18), 3136–3142. https://doi.org/10.1002/adfm.201000846.

(53) Tiourina, O. P.; Antipov, A. A.; Sukhorukov, G. B.; Larionova, N. I.; Lvov, Y.;

Möhwald, H. Entrapment of -Chymotrypsin into Hollow Polyelectrolyte Microcapsules. *Macromol. Biosci.* **2001**, *1* (5), 209–214. https://doi.org/10.1002/1616-5195(20010701)1:5<209::aid-mabi209>3.3.co;2-p.

(54) Valdepérez, D.; del Pino, P.; Sánchez, L.; Parak, W. J.; Pelaz, B. Highly Active Antibody-Modified Magnetic Polyelectrolyte Capsules. *J. Colloid Interface Sci.* **2016**, *474*, 1–8. https://doi.org/10.1016/j.jcis.2016.04.003.

(55) Wang, B.; Liu, P.; Jiang, W.; Pan, H.; Xu, X.; Tang, R. Yeast Cells with an Artificial Mineral Shell: Protection and Modification of Living Cells by Biomimetic Mineralization. *Angew. Chemie - Int. Ed.* **2008**, *47* (19), 3560–3564. https://doi.org/10.1002/anie.200704718.

(56) Bizeau, J.; Tapeinos, C.; Marella, C.; Larrañaga, A.; Pandit, A. Synthesis and Characterization of Hyaluronic Acid Coated Manganese Dioxide Microparticles That Act as ROS Scavengers. *Colloids Surfaces B Biointerfaces* **2017**, *159*, 30–38. https://doi.org/10.1016/j.colsurfb.2017.07.081.

(57) Briggs, D. *Handbook of X-Ray Phoelectron Spectroscopy*; 1992. https://doi.org/10.1002/0470014229.ch22.

(58) Sies, H. Hydrogen Peroxide as a Central Redox Signaling Molecule in Physiological Oxidative Stress: Oxidative Eustress. *Redox Biol.* **2017**, *11* (December 2016), 613–619. https://doi.org/10.1016/j.redox.2016.12.035.

(59) Zhang, C.; Hong, S.; Liu, M. D.; Yu, W. Y.; Zhang, M. K.; Zhang, L.; Zeng, X.; Zhang, X. Z. PH-Sensitive MOF Integrated with Glucose Oxidase for Glucose-Responsive Insulin Delivery. *J. Control. Release* **2020**, *320* (January), 159–167. https://doi.org/10.1016/j.jconrel.2020.01.038.

(60) Xu, S.; Zhang, Y.; Zhu, Y.; Wu, J.; Li, K.; Lin, G.; Li, X.; Liu, R.; Liu, X.; Wong, C. P. Facile One-Step Fabrication of Glucose Oxidase Loaded Polymeric Nanoparticles Decorating MWCNTs for Constructing Glucose Biosensing Platform: Structure Matters. *Biosens. Bioelectron.* **2019**, *135* (March), 153–159. https://doi.org/10.1016/j.bios.2019.04.017.

(61) Jo, S. M.; Wurm, F. R.; Landfester, K. Oncolytic Nanoreactors Producing Hydrogen

Peroxide for Oxidative Cancer Therapy. *Nano Lett.* **2020**, *20* (1), 526–533. https://doi.org/10.1021/acs.nanolett.9b04263.

CHAPTER 6.

General conclusions and future perspectives

CHAPTER 6. General conclusions and future perspectives

6.1. General conclusions

CHAPTER 3. Encapsulation of manganese dioxide nanoparticles into layer-by-layer polymer capsules for the fabrication of antioxidant microreactors.

1. **Encapsulation of MnO_2 within the cavity of LbL capsules is a valid strategy to create antioxidant polymer capsules based on nanozymes.** At 50 µM H_2O_2 concentration, a scavenging effect (from 100 ± 6% to 45 ± 3%) was only observed at a concentration of $1{\cdot}10^8$ polymer capsules/mL. However, at 10 µM H_2O_2 concentration, polymer capsules were able to efficiently scavenge H_2O_2 from solution at all the studied concentrations (i.e., $1{\cdot}10^6$, $1{\cdot}10^7$, $1{\cdot}10^8$ polymer capsules/mL).
2. **Polymer capsules bearing MnO_2 in their cavity are robust.** After continuous H_2O_2 scavenging cycles, polymer capsules lost part of their scavenging capacity but maintained their activity above 30%. After sterilization with ethanol, capsules were capable of maintaining their H_2O_2 scavenging capacity above 69 ± 6% for all the capsule concentrations.
3. **The surface charge of the polymer capsules determines their cytocompatibility.** Metabolic activity of the cells after 72 h of incubation with positively charged capsules decreased significantly (below the threshold value of 70%) at capsule to cell ratios of 100 and 1000 polymer capsules/cell. Metabolic activity of the cells after 72 h of incubation with negatively charged capsules was above 80% in all the ratios with the exception of 1000 polymer capsules/cell.
4. **The surface charge of the polymer capsules also plays an important role in the interaction with cells.** Negatively charged capsules were distributed uniformly in the cellular microenvironment, while positively charged capsules were accumulated around the cells.
5. **The developed polymer capsules protect cells from oxidative stress.** After 32 h of incubation, a beneficial response of the capsules was observed against 100 µM H_2O_2 stimuli for capsule concentrations of 10 polymer capsules/cell in positively charged capsules and concentrations of 10 and 100 polymer capsules/ cell in the negatively charged counterparts.

CHAPTER 4. Smart layer-by-layer polymeric microreactors: pH-triggered drug release and attenuation of cellular oxidative stress as prospective combination therapy

1. **The LbL approach can be successfully used for the incorporation of several active entities.** DOX was successfully incorporated on the multilayer membrane of the polymer capsules (1.9 μg per 10 mg of sacrificial template). Catalase was encapsulated in the cavity of the capsules and scavenged H_2O_2 from the solution. Accordingly, H_2O_2 decreased in a capsule concentration manner obtaining its complete scavenging with the capsule concentration of $1{\cdot}10^7$ polymer capsules/mL.
2. **The robustness of the capsules is compromised by the sterilization process.** After incubating the capsules with ethanol, the activity of the encapsulated enzyme decreased significantly. The reduced H_2O_2 at 50 μM drop from 97.3 ± 2.8% to 40.2 ± 4.1% using $1{\cdot}10^7$ polymer capsules/mL. An alternative fabrication process was considered for the following experiments.
3. **The developed capsules release the cargo in response to biologically relevant stimuli.** A pH-dependent release was obtained thanks to the incorporated pH-cleavable linker. The higher amount of DOX was released at lower pH (pH= 4.0) (8.5 μg) while the lower was release at the neutral pH (3.5 μg).
4. **The fabricated capsules are cytocompatible and protect cells from oxidative stress.** Cells maintained their metabolic activity after 72 h above the threshold value (i.e., 70%) for all the studied concentrations (10 polymer capsules/cell: 96.0 ± 8.1%, 100 polymer capsules/cell: 91.0 ± 9.1% and 1000 polymer capsules/cell: 94.9 ± 3.1%). Those capsules fabricated with dPG-DOX had a tendency to localize in the perinuclear region. At 100 and 1000 polymer capsule to cell ratios protected cells from continuous H_2O_2 stimuli after 48 h.

CHAPTER 5. Layer-by-layer polymer capsules with antioxidant outer inorganic and organic layer as microplatforms to perform cascade reactions.

1. **An antioxidant inorganic or organic layer can be incorporated on the surface of LbL polymer capsules.** MnO_2 antioxidant layer was successfully fabricated *in situ* onto the polymer capsules. As confirmed by confocal microscopy, SENs were efficiently attached to the polymer capsules. In spite of being distributed through all the membrane, they showed a preferential accumulation in the outer layer.
2. **Capsules with inorganic and organic antioxidant layer are capable of reducing H_2O_2 from the solution at biologically relevant concentrations (10 and 50 µM).**
3. **The fabricated polymer capsules bearing GOx in their cavity reduce glucose**. Glucose was reduced efficiently from the solution using capsules with SENs obtaining a complete reduction of the glucose after 24 h using a capsule concentration of $1 \cdot 10^8$ polymer capsules/mL. However, capsules with an outer MnO_2 layer were not capable of reducing glucose from the solution.
4. **Incubation of polymer capsules with permanganate has a detrimental effect on the activity of the encapsulated enzyme (GOx).** After $KMnO_4$ incubation, GOx lost the fluorescence intensity, suggesting a reaction between the permanganate and the enzyme, thus compromising its enzymatic activity.
5. **Polymer capsules fabricated *via* the LbL approach serve as potential microplatforms to perform enzymatic cascade reactions.** Capsules with an outer SEN layer and GOx within their cavity were capable of performing cascade reactions, efficiently reducing the enzymatically produced H_2O_2 after glucose reduction. The produced H_2O_2 at a concentration of 500 µM glucose using $1 \cdot 10^7$ polymer capsules/mL was 28.4 ± 0.4 µM for the capsules without SENs while for the capsules with SENs was 9.0 ± 0.1 µM.

6.2. Future perspectives

In the present thesis project, we explored the versatility of the layer-by-layer method, through the functionalization of different constituents of polymer capsules fabricated to work as microreactors. Accordingly, we developed three model systems functionalizing first the core in the Chapter 3 with MnO_2 nanoparticles to obtain capsules capable of reducing the H_2O_2 from the cellular microenvironment. In the following chapter (Chapter 4), we incorporated an extra functionality to the capsules to translate them from single functional microreactors to multifunctional. This was achieved by incorporating catalase within their core and a dendritic polyglycerol conjugated to a model drug (doxorubicin) with a pH-cleavable linker as part of the multilayer membrane. These capsules were capable of releasing the drug under acidic microenvironments while protecting cells form H_2O_2 insults. In Chapter 5, we explored also the functionalization of the outer layer fabricating an antioxidant organic (i.e., CAT containing SENs) or inorganic (i.e., *in situ* fabricated MnO_2 layer) layer together with the encapsulation of glucose oxidase. Thus, we were capable of fabricating polymer capsules to perform cascade reactions.

The results obtained in this thesis presented three different promising microplatforms for the treatment of several pathologies in which an overproduction of H_2O_2 is encountered. Furthermore, our results showed the versatility and the ease of functionalization provided by this fabrication method, thereby opening different ways to the fabrication of advanced systems to overcome the challenges present in complex pathologies. However, despite the versatility and the promising potential of this technology, this approach presents some limitations which are hindering the rapid translation of these systems to their clinical use.

As observed during this project, the production of these capsules remains at an artisanal level. In fact, the most commonly used fabrication protocols rely on the sequential immersion of a sacrificial template in different polyelectrolyte solutions, followed by repetitive washing steps. We observed that this protocol apart from being time-consuming, implies the continuous manual intervention leading to a lack of homogeneity in the capsule size distribution and reproducibility, together with low

efficiency of the process associated with the loss of a great amount of capsule during the washing steps. Thus, making a robust and reproducible production still represents a challenging objective. Within this context, many efforts have been made to enable the automatization and up-scaling of this method, suggesting methods based on microfluidics, tangential flow filtration or continuous flow reactors, which despite presenting some limitations can be promising strategies to achieve the above-mentioned translation.

Another issue observed related to this fabrication method is the long-term storage of the fabricated capsules, which is also a key factor to guarantee the safe translation of them to their clinical use. As in real clinical scenarios the fabrication of fresh polymer capsules is utopic, adequate storage conditions (e.g., temperature, pH) and states (e.g., in solution, dried, lyophilized) need to be further explored with the aim of preserving the integrity of the systems until their use. This analysis is beyond the scope of our research work and, despite several works have analysed the long-term storage of polymer capsule subjecting them to different conditions with promising results, all this works are only individual examples. Hence, a general evaluation specifying the proper storage conditions for each polyelectrolyte type and each encapsulated or functionalised entity should be done.

Furthermore, another key factor that should be thoroughly considered to enable the translation of these polymer capsules to the clinical use and that has received little attention in bibliography, is the sterilization. In the manufacturing of biomedical devices, the preservation of physical, chemical, mechanical and biocompatibility properties of the fabricated system should be guaranteed. The most commonly used methods include autoclaving, dry heating, chemical treatments (e.g., ethylene oxide and hydrogen peroxide), UV irradiation or ionizing radiations (e.g., gamma and beta radiation). However, it should be taken into account that some of these methods could irreversibly alter the original properties of the polymer used and also have a detrimental effect on the encapsulated active entity. For example, as observed in our particular case, as we use active entities like enzymes, we avoided the sterilization of our polymer capsules with ethanol due to the loss of activity of the enzyme. As a consequence, we worked in clean conditions and the employed solutions were sterile-filtered, limiting thus the

scalability and reliability of the fabricated system. Other systems, fabricated with thermal- or hydrolytic -sensitive biomaterials should avoid the use of autoclaving. For this reason, proper optimization and study should be done in the case of multilayer capsules and encapsulated therapeutic agents in order to ensure the preservation of the properties when translating to bigger production scales.

However, despite all these challenges, with this work we prove that polymer capsules fabricated *via* the layer-by-layer approach represent promising systems for accurate and personalized treatment. With a thorough optimization of the above mentioned up-scaling issues and with the help of emerging technologies the future use of polymer capsules in clinical applications may be much closer.